

# **Role of MicroRNAs in LPA-Induced Regulation of Stem Cell Differentiation Into Cardiomyocytes**

**Adem Nasraddin**

School of Life and Medical Sciences  
University of Hertfordshire

A thesis submitted to the University of Hertfordshire in  
partial fulfilment of the requirements of the degree of  
Doctor of Philosophy (PhD)

October 2018



# **ABSTRACT**

Lysophosphatidic acid (LPA) is known to exert a diverse range of effects in humans, specifically in the heart where it may cause apoptosis of cardiomyocytes at pathological concentrations. However, at physiological concentrations LPA may regulate cell migration, proliferation and even differentiation. The ability to drive stem cells down the cardiac lineage has, however not yet investigated and the potential underlying molecular mechanisms that could mediate this effect also remains to be determined. Since LPA is reported to accumulate in acute myocardial infarction and may rescue cardiac myocytes, we have hypothesised it may also be able to generate cardiac myocytes from stem cells. This hypothesis is based on observations that the signalling through which it exerts its biological effects are similar to those which have reported regulating stem cells regulation to various lineages. The aim of this thesis, therefore, was to study, firstly, the effectiveness of LPA in deriving cardiomyocytes and then to establish the molecular mechanisms involved focusing specifically on the expression profile of select miRNAs including mir-145, mir-1 and mir-133 which respectively linked to pluripotency and lineage commitments. All studies were carried out using the P19 stem cell line and were maintained and cultured in supplemented alpha-minimal essential medium ( $\alpha$ -MEM), comprised of antibiotics and foetal bovine serum (FBS). Embryoid bodies were formed from aggregates of the cells in a non-tissue culture grade plates with or without LPA for four days. These EBs are subsequently plated in an adherent 6-well plate and maintained in culture between 3 and 12 days, before being lysed for either western blotting or RNA analysis. When used pharmacological inhibitors of LPA receptors (Suramin (P2 purinergic/LPA receptor 4), H2L5765834 (LPA receptor 1, 3 & 5), H2L5186303 (LPA receptor 2 & 3) and TC-LPA5-4 (LPA receptor 5)), targeted protein kinases (PKC; by BIM I) and PI3-kinase (by LY294002), they were added to the cultures 1 hour before treatment with LPA. In parallel studies, cells were transfected with mir-145 and mir-1 using siRNAs for inhibitors or mimic for overexpression. The effect on MLC-1v and OCT4 protein expression then determined by western blotting. Successfully, the research revealed that LPA could achieve differentiation of P19 stem cells, and this was concentration and time-dependent. The maximum response was obtained with 20 $\mu$ M LPA and peaked on day 6. Subsequent experiments were carried out using 5 and/or 20 $\mu$ M LPA. Decreases paralleled the induction of MLC-1v in OCT4 expressions. The effects

of LPA were mediated through its receptors, specifically LPA receptors 4 and 5 and partially on LPA receptors 2 and 3. The effects were also mediated through the kinases like protein kinase C, although the involvements of PI3 kinase was only partial. Expressions of mir-145, mir-1 and mir-133 elevated following treatment with LPA. Suramin and BIM-I inhibited these changes but not affected by LY294002, H2L5186303, H2L5765834 and TC-LPA5-4. Transfection studies also suggested that mir-1 regulate differentiation through enhanced MLC-1v protein expression with and without LPA. In conclusion, the program of research conducted for this thesis has confirmed that LPA could be an endogenous modulator of stem cells differentiation to a cardiac lineage, more importantly this effect is mediated through its receptors 2, 3, 4 and 5 collectively, that may activate protein kinase PKC and PI3K and is under the influence of mir-145 and mir-1. Our work in this thesis suggests the active role of miRNAs specifically mir-145 and mir-1, which can indicate the need of further investigation to instigate the possible therapeutic targets and further prevent any fatal consequences of atherosclerosis or other heart-linked diseases.

# **ACKNOWLEDGMENT**

I would first like to thank my principal supervisor Dr Shori Thakur. Without her trust in me and words of motivation when I faced difficult situations I would not have reached this far. I also like to extend my gratitude to my second supervisor Professor Anwar Baydoun for his extensive guidance and support throughout my PhD research. The door to their offices were always open to resolve my trouble spots and answer my questions about my research. They consistently allowed this PhD study to be my own work but steered me in the right direction whenever they thought I needed it.

My PhD study journey was made easy with the assistance and help of the laboratory and technical staff who facilitated the access to run my research with ease. A warm-hearted thanks goes out to them.

I additionally, wish to express my sincere appreciation to my friends and colleagues for their continuous words of encouragement specially Anwar's lab group: Dr Ashish Patidar, Dr Hema Pramod, Dr Praveen Bingi, Dr Nimer Alsabeelah, Dr Mahdi Alsugoor and Dr Gaggan Maan.

Furthermore, my utmost gratitude is to Mr S. AlSulaiman for his continuous support to my family and myself. Without his generous backing, I would not have been able to fulfil my dream of achieving this prestigious state.

Finally, I must express my deepest gratefulness to my parents and to my partner for providing me with unfailing support and continuous love and encouragement throughout my journey of study and through the process of researching and writing this thesis. I would like to include my siblings in these special thanks for believing in me. This achievement would not have been attainable without them.

*THANK YOU.*

**DEDICATED TO MY 3 ANGELS  
SOUAD, SAUD & JENNA**

# **TABLE of CONTENT**

# Table of Contents

ABSTRACT.....	III
ACKNOWLEDGMENT .....	VI
TABLE of CONTENT.....	VIII
LIST of FIGURES .....	XI
LIST of TABLES .....	XV
ABBREVIATIONS.....	XVII
CHAPTER 1 INTRODUCTION.....	1
1.1. Heart development:.....	2
1.2. Stem cells.....	14
1.3. Lysophosphatidic acid (LPA).....	21
1.4. MicroRNA.....	26
1.5. Aims and objectives.....	32
CHAPTER 2 MATERIALS and METHODS.....	33
2.1. Routine cell culture .....	34
2.2. Cryopreservation.....	37
2.3. Embryoid body formation.....	37
2.4. The use of inhibitors and blockers of signalling and receptors .....	39
2.5. Transfection of miRNAs .....	39
2.6. Plating embryoid bodies for differentiation .....	40
2.7. Cell lysis and protein quantification.....	41
2.8. Cytotoxicity and cell viability assay.....	43
2.9. Western Blotting.....	44
2.10. Total RNA extraction and qRT-PCR: .....	47
2.11. Confocal microscopy and Immunofluorescence .....	53
2.12. Statistical data analysis .....	53
CHAPTER 3 RESULTS.....	54
3.1. Regulation of P19 stem cells (SCs) differentiation.....	55
3.2 Cell viability in the presence of various pharmacological inhibitors (MTT assay) .....	60
3.3 Establishment and development of cardiac cells model and examination of the effects of LPA on differentiation.....	65
3.4 PCR normalisation and quantification: .....	72

3.5	Concentration-dependent effects of LPA on the expression of transcription factors and key miRNAs targeted .....	79
3.6	Effects of pharmacological inhibitors of LPA receptors on the induction of differentiation: effects on protein and mRNA expression.....	86
3.7	Effects of kinase inhibition on the induction of differentiation: effects on protein and mRNA expression.....	102
3.8	Effects of knockdown and overexpression of mir-145 and mir-1 on differentiation ..	114
<b>CHAPTER 4 DISCUSSION .....</b>		<b>122</b>
4.1.	Primary cultures and model establishment .....	126
4.2.	Cardiac cells model and effects of LPA.....	126
4.3.	Concentration-dependent expression of transcription factors and key miRNAs induced by LPA .....	130
4.4.	Inhibition of LPA receptors .....	133
4.5.	Suppression of protein kinase-C inhibit differentiation .....	137
4.6.	Role of PI3K in LPA-induced regulation of MLC-1v and OCT4.....	138
4.7.	Effects of transfection of siRNA (inhibitors) and mimic (overexpression) with or without LPA.....	140
<b>CHAPTER 5 CONCLUSION and FUTURE WORK.....</b>		<b>143</b>
5.1	Conclusion.....	144
5.2	Future work .....	145
<b>References.....</b>		<b>146</b>

# **LIST of FIGURES**

# LIST of FIGURES

## Chapter 1

<b>Figure 1.1: The time course of the early embryonic cardiogenesis.....</b>	<b>3</b>
<b>Figure 1.2: Structural differences between the three non-coding RNA sequences.....</b>	<b>9</b>
<b>Figure 1.3: Source of different types of stem cells through the development stages from an embryo to the formation of organs (Jones, 2006).....</b>	<b>15</b>
<b>Figure 1.4: Embryonic stem cells lineages and stages (Keller, 2005). ....</b>	<b>16</b>
<b>Figure 1.5: Chemical structure of LPA.....</b>	<b>21</b>
<b>Figure 1.6: The synthesis process of LPA and the involvement of specific enzymes in the digestion: .....</b>	<b>22</b>
<b>Figure 1.8: Biogenesis and mechanism of miRNA in the inhibition process of the targeted mRNA (Tong &amp; Nemunaitis, 2008).....</b>	<b>28</b>
<b>Figure 1.9: Picture of wild-type C. elegans let-7 miRNA gene and a knocked-out let-7 miRNA gene which shows a developmental abnormality. ....</b>	<b>29</b>
<b>Figure 1.10: Role of specific miRNAs in the differentiation of human stem cells (Gangaraju &amp; Lin., 2009). ....</b>	<b>30</b>

## Chapter 2

<b>Figure 2.1: Illustration of the major cell culture steps. ....</b>	<b>35</b>
<b>Figure 2.2: Automated cell count trypsinised cultures using Countess® from Invitrogen Inc. ....</b>	<b>36</b>
<b>Figure 2.3: Cell count result and calculations.....</b>	<b>36</b>
<b>Figure 2.4: Setup of the plate for the transfection experiment.....</b>	<b>39</b>
<b>Figure 2.5: BCA protein standard curve. ....</b>	<b>43</b>
<b>Figure 2.6: The order of placing the items for transferring protein. ....</b>	<b>45</b>
<b>Figure 2.7: Steps for isolation of total RNA and small RNA (miRVana™) .....</b>	<b>48</b>

## Chapter 3

<b>Figure 3.1: Routine growth pattern of P19 stem cell line in culture.....</b>	<b>55</b>
<b>Figure 3.2: Formation of embryoid bodies in culture.....</b>	<b>56</b>
<b>Figure 3.3: Growth of plated EB in a monolayer. ....</b>	<b>57</b>
<b>Figure 3.4: Stained P19 cells treated with LPA and DMSO monolayers compared to control.....</b>	<b>58</b>
<b>Figure 3.5: Cellular viability of P19 cells when treated with different concentration of LPA by MTT assay. ....</b>	<b>61</b>
<b>Figure 3.6: Cellular viability of P19 cells when treated with different concentration of DMSO by MTT assay.....</b>	<b>61</b>
<b>Figure 3.7: Cellular viability of P19 cells when treated with different concentration of LY294002 by MTT assay. ....</b>	<b>62</b>
<b>Figure 3.8: Cellular viability of P19 cells when treated with different concentration of H2L5765834 by MTT assay. ....</b>	<b>62</b>
<b>Figure 3.9: Cellular viability of P19 cells when treated with different concentration of H2L5186303 by MTT assay.....</b>	<b>63</b>
<b>Figure 3.10: Cellular viability of P19 cells when treated with different concentration of TC-LPA5-4 by MTT assay. ....</b>	<b>63</b>
<b>Figure 3.11: Cellular viability of P19 cells when treated with different concentration of BIM-1 by MTT assay.....</b>	<b>64</b>

<b>Figure 3.12: Cellular viability of P19 cells when treated with different concentration of Suramin by MTT assay. ....</b>	<b>64</b>
<b>Figure 3.13: Protein expression of MLC-1v (%) induced by increasing concentrations of LPA. ....</b>	<b>65</b>
<b>Figure 3.14: Expression of OCT4 (%) induced by increasing concentrations of LPA. ....</b>	<b>66</b>
<b>Figure 3.15: Morphological structure of beating clusters of induced P19 stem cells. ....</b>	<b>66</b>
<b>Figure 3.16: Time-dependent induction of MLC-1v protein expression by LPA. ....</b>	<b>67</b>
<b>Figure 3.17: Protein expression of cardiac Troponin I in controls and LPA treated P19 cells.....</b>	<b>68</b>
<b>Figure 3.18: Protein expression of MLC-1v induced in Short time points by LPA on day 6.....</b>	<b>69</b>
<b>Figure 3.19: Protein expression of MLC-1v induced in Short time points by 5µM LPA.....</b>	<b>70</b>
<b>Figure 3.20: Protein expression of MLC-1v induced in Short time points by 20µM LPA. ....</b>	<b>70</b>
<b>Figure 3.21.: Protein expression of MLC-1v induced in Short time points by LPA at day 12.....</b>	<b>71</b>
<b>Figure 3.22: 1% denaturing agarose gel electrophoresis for total RNA samples. ....</b>	<b>73</b>
<b>Figure 3.23: 1.5% denaturing agarose gel electrophoresis for amplicon (Products of qPCR).....</b>	<b>73</b>
<b>Figure 3.24: Generating a standard curve to assess reaction optimisation for U6-housekeeping gene.....</b>	<b>75</b>
<b>Figure 3.25: Generating a standard curve to assess reaction optimisation for mir-15a. ....</b>	<b>75</b>
<b>Figure 3.26: Generating a standard curve to assess reaction optimisation for mir-145. ....</b>	<b>76</b>
<b>Figure 3.27: Generating a standard curve to assess reaction optimisation for mir-1. ....</b>	<b>76</b>
<b>Figure 3.28: Generating a standard curve to assess reaction optimisation for mir-133. ....</b>	<b>77</b>
<b>Figure 3.29: Generating a standard curve to assess reaction optimisation for OCT4.....</b>	<b>77</b>
<b>Figure 3.30: Generating a standard curve to assess reaction optimisation for NKX2.5.....</b>	<b>78</b>
<b>Figure 3.31: Generating a standard curve to assess reaction optimisation for GATA4. ....</b>	<b>78</b>
<b>Figure 3.32: Expression of OCT4 induced by LPA at different time points and concentrations. ....</b>	<b>79</b>
<b>Figure 3.33: Expression of OCT4 induced by 5µM of LPA at different time points.....</b>	<b>80</b>
<b>Figure 3.34: Expression of NKX2.5 induced by LPA at different time points and concentrations. ....</b>	<b>81</b>
<b>Figure 3.35: Expression of NKX2.5 induced by 5µM of LPA at different time points.....</b>	<b>81</b>
<b>Figure 3.36: Expression of mir-145 induced by LPA at different time points and concentrations. ....</b>	<b>82</b>
<b>Figure 3.37: Expression of mir-145 induced by 5µM of LPA at different time points.....</b>	<b>83</b>
<b>Figure 3.38: Expression of mir-1 induced by LPA at different time points and concentrations. ....</b>	<b>84</b>
<b>Figure 3.39: Expression of mir-1 induced by 5µM of LPA at different time points. ....</b>	<b>85</b>
<b>Figure 3.40: Effect of suramin on the expression of ventricular myosin light chain (MLC-1v). ....</b>	<b>87</b>
<b>Figure 3.41: Effect of LPA receptor inhibitors on the protein expression of MLC-1v.....</b>	<b>87</b>
<b>Figure 3.42: Effect of H2L5765834 on the protein expression of MLC-1v.....</b>	<b>88</b>
<b>Figure 3.43: Effect of H2L5186303 on the protein expression of MLC-1v.....</b>	<b>88</b>
<b>Figure 3.44: Effect of TC-LPA5-4 on the protein expression of ventricular myosin light chain. ....</b>	<b>89</b>
<b>Figure 3.45: Effect of LPAR inhibitors on the expression of OCT4.....</b>	<b>90</b>
<b>Figure 3.46: Effect of H2L5765834 on the protein expression of OCT4.....</b>	<b>90</b>
<b>Figure 3.47: Effect of H2L5186303 on the protein expression of OCT4.....</b>	<b>91</b>
<b>Figure 3.48: Effect of TC-LPA5-4 on the protein expression of OCT4. ....</b>	<b>91</b>
<b>Figure 3.49: Effect of LPAR inhibitors on the protein expression of GATA4. ....</b>	<b>92</b>

<b>Figure 3.50: Effect of H2L5765834 on the protein expression of GATA4.</b>	<b>93</b>
<b>Figure 3.51: Effect of H2L5186303 on the protein expression of GATA4.</b>	<b>93</b>
<b>Figure 3.52: Effect of TC-LPA5-4 on the Protein expression of GATA4.</b>	<b>94</b>
<b>Figure 3.53: Effect of H2L5186303 on the expression of mir-145 mRNA.</b>	<b>95</b>
<b>Figure 3.54: Effect of H2L5765834 on the expression of mir-145.</b>	<b>96</b>
<b>Figure 3.55: Effect of TC-LPA5-4 on the expression of mir-145.</b>	<b>96</b>
<b>Figure 3.56: Effect of LPA receptor antagonist on the expression of mir-1.</b>	<b>97</b>
<b>Figure 3.57: Effect of H2L5765834 on the</b>	<b>98</b>
<b>Figure 3.58: Effect of H2L5186303 on the expression of OCT4.</b>	<b>99</b>
<b>Figure 3.59: Effect of TC-LPA5-4 on the expression of OCT4.</b>	<b>99</b>
<b>Figure 3.60: Effect of LPA receptor antagonist on the expression of NKX2.5.</b>	<b>100</b>
<b>Figure 3.61: Effect of LPA receptor antagonist on the expression of mir-133.</b>	<b>101</b>
<b>Figure 3.62: Blots for the effect of BIM-1 inhibitor on protein expressions.</b>	<b>103</b>
<b>Figure 3.63: Effect of BIM-1 on the protein expression of ventricular myosin light chain.</b>	<b>103</b>
<b>Figure 3.64: Effect of BIM-1 on protein expression of OCT4.</b>	<b>104</b>
<b>Figure 3.65: Effect of BIM-1 on protein expression of GATA4.</b>	<b>104</b>
<b>Figure 3.66: Effect of BIM-1 on the expression of mir-145.</b>	<b>105</b>
<b>Figure 3.67: Effect of BIM-1 on the expression of mir-1.</b>	<b>106</b>
<b>Figure 3.68: Effect of BIM-1 on the expression of mir-133.</b>	<b>106</b>
<b>Figure 3.69: Effect of BIM-1 on the expression of OCT4.</b>	<b>107</b>
<b>Figure 3.70: Effect of BIM-1 on the expression of NKX2.5.</b>	<b>107</b>
<b>Figure 3.71: Effect of BIM-1 on the expression of GATA4.</b>	<b>108</b>
<b>Figure 3.72: Effect of LY294002 on the protein expression of MLC-1v.</b>	<b>109</b>
<b>Figure 3.73: Effect of LY294002 on the protein expression of OCT4.</b>	<b>110</b>
<b>Figure 3.74: Effect of LY294002 on the protein expression of GATA4.</b>	<b>110</b>
<b>Figure 3.75: Effect of LY294002 on the expression of mir-145.</b>	<b>111</b>
<b>Figure 3.76: Effect of LY294002 on the expression of mir-1.</b>	<b>112</b>
<b>Figure 3.77: Effect of LY294002 on the expression of mir-133.</b>	<b>112</b>
<b>Figure 3.78: Effect of LY294002 on the expression of OCT4.</b>	<b>113</b>
<b>Figure 3.79: Effect of LY294002 on the expression of NKX2.5.</b>	<b>113</b>
<b>Figure 3.80: Blots for the effect of knockdown and overexpression of mir-145 and mir-1 on MLC-1v.</b>	<b>116</b>
<b>Figure 3.81: Effect of knockdown and overexpression of mir-145 on MLC-1v.</b>	<b>116</b>
<b>Figure 3.82: Effect of knockdown and overexpression of mir-1 on MLC-1v.</b>	<b>117</b>
<b>Figure 3.83: Blot for the effect of knockdown and overexpression of mir-145 and mir-1 on OCT4.</b>	<b>119</b>
<b>Figure 3.84: Effect of knockdown and overexpression of mir-145 on OCT4.</b>	<b>119</b>
<b>Figure 3.85: Effect of knockdown and overexpression of mir-1 on OCT4.</b>	<b>120</b>

## Chapter 4

<b>Figure 4.1: LPA receptors and downstream signalling pathways.</b>	<b>134</b>
<b>Figure 4.2: The binding site of mir-143 Myosin light chain.</b>	<b>140</b>
<b>Figure 4.3: The binding site of mir-145 in OCT4 mRNA (Zhu et al., 2014).</b>	<b>141</b>

# **LIST of TABLES**

# **LIST of TABLES**

## **Chapter 1**

<i>Table 1.1: A comparison between sources of P19 embryonic carcinoma, embryonic stem cells, and embryonic germ cells (Boheler et al., 2002).</i>	17
<i>Table 1.2: Summary of main miRNAs playing a role in the differentiation into cardiomyocytes:</i>	31

## **Chapter 2**

<i>Table 2.1: Set up experiments for the determination of the effects of control, DMSO and LPA.</i>	38
<i>Table 2.2: Set up experiments for the determination of the concentration-dependent effect of LPA.</i>	38
<i>Table 2.3: Set up of steps and reagents for transfection experiments.</i>	40
<i>Table 2.4: Protein standard preparation</i>	42
<i>Table 2.5: Preparation recipe of 10X TBE buffer.</i>	49
<i>Table 2.6: Reverse transcription of samples from total RNA to cDNA using the miScript PCR system.</i>	49
<i>Table 2.7: miRNA primer sequence details.</i>	50
<i>Table 2.8: Primer binding details.</i>	51
<i>Table 2.9: Setup of qPCR reactions (mRNA)</i>	51
<i>Table 2.10: Setup of qPCR reactions (miRNA)</i>	52
<i>Table 2.11: Cycling conditions for qPCR.</i>	52

## **Chapter 3**

<i>Table 3.1: Concentration and purity for isolated total RNA using Nanodrop.</i>	72
<i>Table 3.2: One-way analysis of variance (ANOVA) table analysed for the antibodies MLC-1v and OCT4.</i>	115
<i>Table 3.3: One-way analysis of variance (ANOVA) table analysed for the antibodies MLC-1v and OCT4.</i>	121

## **Chapter 4**

<i>Table 4.1: Inhibitors and antagonists used and their targets.</i>	134
--	-----

# **ABBREVIATIONS**

ACE inhibitor	Angiotensin-converting enzyme inhibitor
ACTRIIA/B	Activin receptor type 2 A/B
Akt	Protein Kinase B
ALK	ALK Receptor Tyrosine Kinase
AP-1	Activator protein 1
APS	Ammonium persulfate
ARB	Angiotensin receptor blocker
ASCs	Adult stem cells
ATX	Autotaxin
BCA	Bicinchoninic Acid
BIM I	Bisindolylmaleimide I
BMP	Bone morphogenic protein
bp	Base-pair
BSA	Bovine serum albumin
BVHT	Braveheart
cAMP	Cyclic adenosine monophosphate
CAN	Cerberus and DAN family protein
CCB	Calcium channel blockers
CDC42	Cell Division Cycle 42
cDNA	Complementary Deoxyribo Nucleic Acid
CDX2	Caudal type homeobox2 transcription factor
CHD	Congenital heart defect
circRNA	Circular RNA
CM	Complete medium
CNS	Central nervous system
CO <sub>2</sub>	Carbon dioxide
Ct	Threshold cycle number
cTnC	Cardiac troponin C
cTnI	Cardiac troponin I
CYC A	Cyclophilin A
DAG	Di-acyl-glycerol
DCs	Dendritic cells
DDW	Double Distilled Water
Dkk	Dickkopf WNT Signaling Pathway Inhibitor
DMSO	Dimethyl sulfoxide
DNA	Deoxyribonucleic acid
DW	Distilled water
E	Efficiency of amplification
EBs	Embryoid bodies
ECC	Embryonic carcinoma cell

ECL	Enhanced chemiluminescence
ECM	Extracellular matrix
ECP	Eosinophil cationic protein
Edg	Endothelial differentiation gene
EDRF	Endothelial-derived relaxing factor
EDTA	Ethylene Diamine Tetra Acetic Acid
EGC	Embryonic germ cell
EGF	Epidermal growth factor
EIF2 $\alpha$	Eukaryotic initiation factor 2- $\alpha$
END-2	Visceral Endoderm like cells
ERKs	Extracellular signal Regulated Kinases
ESC-CM	Embryonic stem cells derived cardiomyocytes
ESCs	Embryonic stem cells
EtOH	ethanol
FBS	Foetal Bovine Serum
FENDRR	Foxf1 adjacent non-coding developmental regulatory RNA
FGF-4	Fibroblast growth factor
FHF	First Heart Field
FK506	Tacrolimus or Fujimysin
FKBP1A	FK506 binding site protein 1 A
Foxf1	Forkhead Box F1
Fz	Frizzled proteins
G3P	Glycerol-3-phosphate
G4s	G-quadruplex
GAPDH	Glyceraldehyde-3-Phosphate Dehydrogenase
GBP2	Growth factor binding protein 2
GDP	Guanosine diphosphate
GF	Growth factors
GPAT	Glycerophosphate acyltransferase
GPCRs	G protein-coupled receptors
GTP	Guanosine triphosphate
H3K27	Histone H3-lysine 27
H3K4me	Histone H3-lysine 4-trimethylation
H3K9ac	Histone H3-lysine 9-acetylation
HAND	Heart and neural crest derivatives expressed proteins
HCM	hypertrophic cardiomyopathy
hESC-CM	Human embryonic stem cells derived cardiomyocytes
HGF	Hepatocyte growth factor
HKG	Housekeeping gene
HRB	Horseradish peroxidase

HRCR	heart-related circRNA
IC50	Half maximal inhibitory concentration
ICM	Inner cell mass
IFN- $\gamma$	Interferon gamma
IGF	Insulin-like growth factor
IGF-IR	Insulin growth factor- receptor 1
IgG	Immunoglobulin
iNOS	Induced nitric oxide synthase
IP3	Inositol (1,4,5) tris-phosphate
iPSCs	Induced Pluripotent Stem cells
iPSCs-CM	Induced pluripotent stem cells derived cardiomyocytes
Isl1	Insulin gene enhancer protein1
ISO	Isoproterenol
JAK	Janus kinase signalling pathway
JNK	c-Jun N-terminal Kinases
kDa	Kilo daltons
KDR	Kinase Insert domain receptor
Klf-4	Kruppel-like factor-4
Km	Affinity constant (half maximal saturation constant)
LBP	Lipopolysaccharide-binding protein
LDL	Low Density Lipoprotein
LIF	Leukemic inhibitory factor
LIF	Leukaemia Inhibitory Factor
LPA	Lysophosphatidic acid
LPAAT	Lysophosphatidic acid acyltransferases
LPAR	Lysophosphatidic acid receptor
LPC	Lysophosphatidylcholine
LPL	Lysophospholipid
LPP	Lipid phosphate phospho- hydrolase
LPS	Lipopolysaccharide
LRP5/6	Low density lipoprotein receptor-related protein 5/6
LVEF	Left ventricular ejection fraction
mA	milliamp
MAG	Monoacyl glycerol
MAGT	Monoacyl glycerophosphate acyltransferase
MAPK	Mitogen Activated Protein Kinases
MEF	Mouse Embryonic Fibroblast
MEF2	Myocyte Enhancer Factor 2
MEK	Mitogen-activated ERK Kinase
mESCs	Mouse embryonic stem cells

MESP1	Mesoderm posterior 1
MHC	Myosin heavy chain
MI	Myocardial infarction
miRNA	micro RNA
MKP-1	Mitogen-activated protein kinase phosphatase 1
MLC	Myosin light chain
MLC-1v	Ventricular Myosin light chain
mRNA	Messenger Ribonucleic Acid
MSC-CM	Mesenchymal stem cells derived cardiomyocytes
MSCs	Mesenchymal stem cells
MTT	3-(4,5-Dimethylthiazol-2-yl)-2,5-diphenyltetrazolium bromide
ncRNA	Non-coding RNA
NFAT	Nuclear factor of activated T-cell
NF- $\kappa$ B	Nuclear transcription factor kappa B
NHE3	Na <sup>+</sup> /H <sup>+</sup> exchange isoform
NO	Nitric oxide
NOMO1	Nodal modulator 1
NP	Neuropathic pain
NPC	Neural progenitor cells
OC	Ovarian cancer
Oct 3/4	Octamer-binding protein-3/4
P/S	Penicillin/Streptomycin
P2Y	Purinergic receptor
p38 MAPK	p38 Mitogen activated protein kinase
PA	Phosphatidic Acid
PAP	Phosphatidic acid phosphatase
PBS	Phosphate-buffered saline
PcG	Polycomb group
PCI	Percutaneous coronary interventions
PCP	Planar cell polarity
PCR	Polymerase Chain Reaction
PDK 1/2	3-Phosphoinositide-Dependent Protein Kinase 1/2
PGCs	Primordial germ cells
PI3K	Phosphoinositide 3-kinase
PKA	Protein kinase A
PKB	Protein Kinase B
PKC	Protein Kinase C
PKR	Double-stranded RNA-dependent protein kinase
PL	Phospholipids

PLA	Phospholipase A
PLC	Phospho lipase C
PLD	Phospholipase D
PPAR $\gamma$	Peroxisome proliferator-activated receptor gamma
PTX	Pertussis toxin
PVDF	Polyvinylidene difluoride
q-PCR	Qualitative Real time Polymerase Chain Reaction
RA	Rheumatoid arthritis
RASMC	Rat aortic smooth muscle cell
RHO	Rhodopsin
RHOA	Ras homolog gene family A
RISC	RNA-induced silencing complex
RNA	Ribonucleic acid
RNA-G4s	RNA-G-quadruplex
ROCK	Rho associated kinase
RPM	Revolutions per minutes
RT	Reverse transcriptase
RTKs	Receptor tyrosine kinases
RT-PCR	Reverse Transcriptase Polymerase Chain Reaction
S.D.	Standard deviation
S.E.M.	Standard Error Mean
S1P	Sphingosine 1-phosphate
SCs	Stem cells
SD	Serum deprivation
SDS	Sodium Dodecyl Sulphate
SDS-PAGE	Sodium Dodecyl Sulphate Poly Acrylamide Gel Electrophoresis
SFRPs	Secreted frizzled-related proteins
SH-2	Src Homology Domain 2
SHF	Second Heart Field
siRNA	Small interfering RNA
Sox2	Sex determining region Y-box 2
TAK-1	Tat-associated kinase 1
Taq	Polymerase Thermus aquaticus Polymerase
TBE	Tris borate EDTA
TBS-T	Tris Buffer Saline-Tween
Tbx	T-box transcription factor
TEMED	Tetramethylethylenediamine
TGF	Transforming growth factor
TXA2	Thromboxane A2

UBC	Ubiquitin C
UTF1	Undifferentiated embryonic cell transcription factor 1
UTR	Untranslated region
VSM	Vascular smooth muscle cells
WDR77	WD Repeat Domain 77 gene
WHO	World health organisation
Wnt	Wingless/Integrated
$\alpha$ -MEM	Alpha Minimum Essential Medium

# **CHAPTER 1**

## **INTRODUCTION**

## **1.1. Heart development:**

The circulatory system is one of the first systems to develop in mammalian embryogenesis. The heart is one of the primary organs to form which is originally derived from the mesodermal germ layer. This system was extensively studied since 1920 on chick, mouse, and more recently on human embryos (Van Vliet *et al.*, 2012). The cardiac precursors are also found during pre-gastrulation, which is tested on cultured mouse explants by looking at the main cardiac transcription factors (Auda-Boucher *et al.*, 2000).

There are several transcription factors found to be involved in the formation of the cardiac mesoderm. Most of the early signalling pathways are studied and validated. Starting from the lateral plate mesoderm, the heart is understood to give rise to two distinct fields which develop into different parts of the heart explained as primary heart field (PHF) and secondary heart field (SHF) (Duelen & Sampaolesi, 2017). PHF is also called the first heart field (FHF) (Vincent & Buckingham, 2010; Van Vliet *et al.*, 2012). Both atrial valves and the left ventricles are products of the PHF or FHF, while the right ventricle and the outflow tract are developed from SHF (Duelen R & Sampaolesi M, 2017; Wu *et al.*, 2006). Although both fields share the same progenitors, some transcription factors and signalling pathways are explicitly regulated to serve each field.

### **1.1.1. Genetic factors involved**

One of the first genes to be activated is *Mesp1*, which encodes for the *Mesp1* protein and is predicted as a marker of the cardiac progenitor (Vincent & Buckingham, 2010). There are 150 reported mutations of genes involved in the development of cardiac lineage as reviewed by Brand in 2003. *NKX 2.5*, *eHAND*, *dHAND*, *GATA-4*, and other transcription factors are the leading key players to be targeted to evaluate cardiogenesis in transplanted or cultured cells (Figure 1.1).  $\alpha$ -cardiac actin mRNA and  $\beta$ -myosin heavy chain proteins were also tested by Auda-Boucher *et al.* (2000) using tissues from mouse embryo transplanted into a 2-day old chick. The author's work concluded that the presence of endoderm could stimulate the mesodermal cells to a cardiac lineage, unlike the ectoderm, which showed no influence on programming the mesoderm cells into cardiac fate.

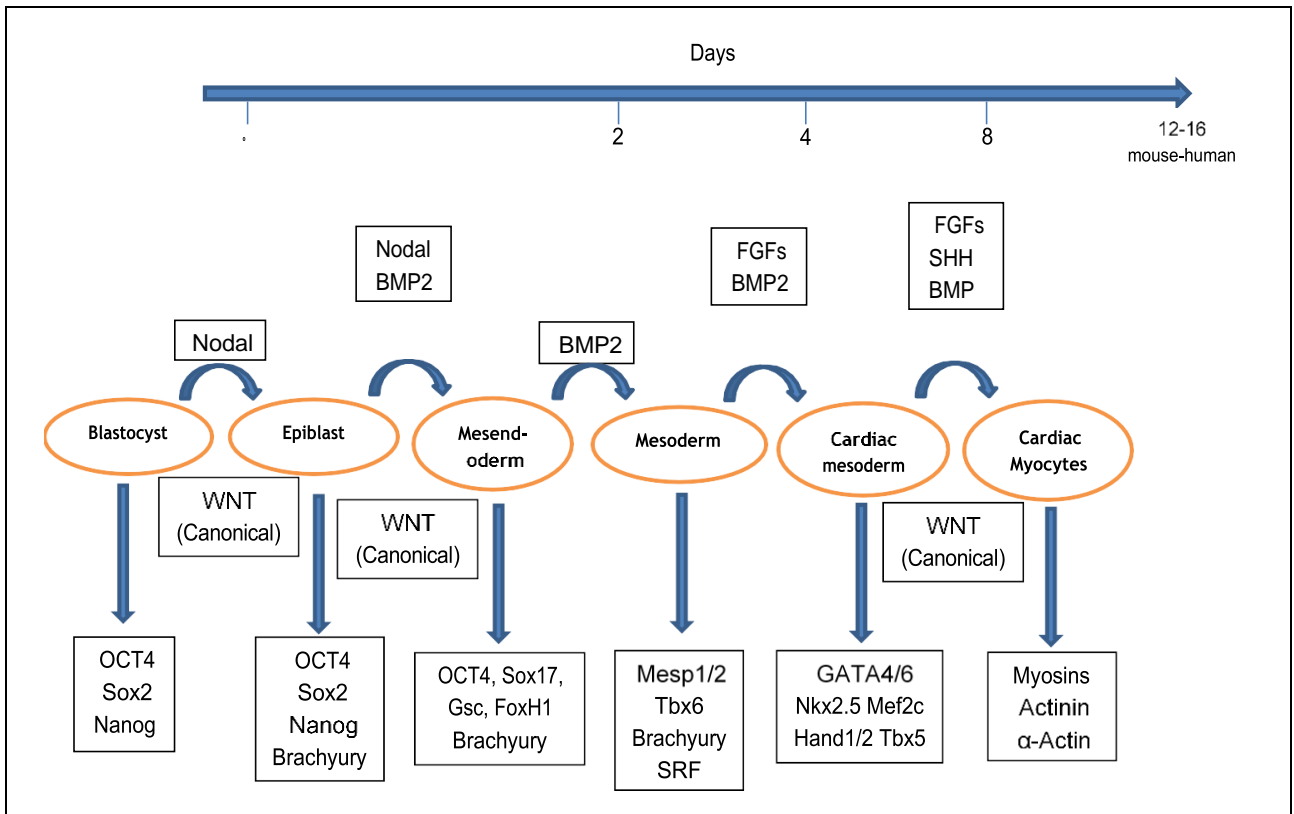


**Figure 1.1: The time course of the early embryonic cardiogenesis.**

Illustration from mouse embryonic stem cells (Blastocyst) main transcription factors and genes involved in the formation of the cardiac myocytes. This time course end on day 12 for the mouse and day 16 for humans. Signalling pathways involved: Nodal, BMP2 (Bone morphogenetic proteins 2), FGFs (Fibroblast growth factor) (Van Vliet *et al.*, 2012).

The downregulation of some of the key pluripotency transcription factors resulted in the enhancement of the differentiation of the cells into cardiac cells as well as the overexpression of Gata4, Tbx5, BAF60c (Van Vliet *et al.*, 2012) and Nkx2.5 (Wu *et al.*, 2006). Both PHF and SHF express KDR and Nkx 2.5, and selectively, ISL12 is expressed only by SHF (Wu *et al.*, 2006). Over-expression of some of the cardiac-specific markers like GATA4, Tbx5, and BAF60c were able to differentiate multipotent mesodermal stem cells (SCs) into cardiac myocytes (Takeuchi JK, Bruneau BG, 2009).

### 1.1.2. Cell signalling

It is widely agreed that the role of some of the signalling cues is critical in the regulation of cell fate during gastrulation (Duelen & Sampaolesi M., 2017). The activation and inhibition of some of these signalling pathways also is the tool used in directing the germ layer to be formed in the process. In some cases, more than one signalling pathway is involved, for instance, BMP4, Activin/Nodal and Wnt are involved in the formation of the different germ layers (Gadue *et al.*, 2005). TGF $\beta$ , BMP4, and Nodal are members of a family called Transforming Growth Factors (TGF) (Taha & Valojerdi, 2008). Wnt, Notch, and Hedgehog are other key signalling molecules which were extensively studied and linked to cardiogenesis (Marín- García, 2014; Liu, 2015; Fraineau *et al.*, 2017).

#### **BMP**

Bone morphogenetic proteins (BMPs) are growth factors which play a role in the development of neurological and ophthalmic system, adipose tissue, urinary system, musculoskeletal system, gastrointestinal system, and more importantly cardiovascular and pulmonary system (Wang *et al.*, 2014). Therefore, a lot of researchers have suggested that bone morphogenetic proteins should be called body morphogenetic proteins instead following the discovery of all its functions. Extracellularly it can act as an agonist or antagonist. BMPs generally crosstalk with other signalling pathways (Wang *et al.*, 2014). Hence why it is linked to many of the earliest processes including various regulatory roles in adult tissue homeostasis and organs formation (Zhang & Bradley, 1996, Bragdon *et al.*, 2011, Kobayashi *et al.*, 2005). Intracellularly BMP could be regulated by various factors like miRNAs, I-SMADs, Phosphatases and FKBP1A, and FKBP12. The last modulator is the membrane modulator of the BMP proteins (Wang *et al.*, 2014).

BMP acts through two types of signalling pathways, canonical and non-canonical (Yuan *et al.*, 2015; Cho *et al.*, 2010; Wang *et al.*, 2014). The SMAD canonical signal transduction is initiated by binding to the receptors on the cell surface. It is formed of two dimers type 1 (TGF- $\beta$  family ligands, ALK1-7) and type 2 serine/threonine kinase receptor. The non- canonical pathway is a SMAD-independent BMP signalling pathway activates the serine-threonine kinase of the MAPK family by the activation of TAK-1 by BMP-4 (Derynck & Zhang, 2003). Other BMPs can also affect different signalling pathways, including PI3k/AKT, PKC, Rho-GTPase (Zhang, 2009).

Currently, there are 20 expressed BMP family member identified, by which only 8 of these expressed in heart and linked to the cardiovascular system (Bragdon *et al.*, 2011). These are BMP-1, BMP-3, BMP-4, BMP-5, BMP-6, BMP-8a, BMP-8b, BMP-10. BMP-2 is not expressed

in the pharyngeal endoderm, where *Csx* is found to be expressed which along *Nkx2.5* has shown to be critical in mutant *Csx*. Likewise, a mutation in BMP-2 in mice caused abnormal development of the heart (Zhang & Bradley, 1996) which raise questions on the role both BMP-2 and *Csx/Nkx2.5* cluster plays and stress the need of extensive studies. BMP-2, according to Zhang & Bradley's conclusion (1996), is also involved in the relationship between the ectodermal cells and the mesodermal cells during the early embryonic development. In the amnion and chorion according to Jones *et al.* (1991), BMP-4 could not rescue the loss of BMP-2 despite the 92% homology shared between both in their amino acids (Zhang & Bradley, 1996). This results in the development of the heart in the exocoelomic cavity or arrest in the development of the heart due to the closure of the pro-amniotic canal.

## WNT

Wnt signalling pathway is one of the main pathways widely linked to several activities. It is established that WNT signalling is required for the induction of the mesodermal stage (Naito *et al.*, 2006) and primitive streak formation (Yamaguchi TP, 2001). WNT is understood to pursue its effect through two ways, canonical and non-canonical. The canonical is a  $\beta$ -catenin dependent pathway and is characterised better compared to the non-canonical (Gomez-Orte *et al.*, 2013). The canonical WNT ligands interact with the Frizzled (Fz) receptors and a lipoprotein receptor-related protein (LRP), specifically lipoprotein receptor-related protein 5 and 6 (LRP5 & LRP6) (Gay & Towler, 2017). This pathway is also known to be a stage-based regulator, especially in cardiomyogenesis and hematopoiesis (Naito *et al.*, 2006). Naito and his colleagues (2006) reported this developmental stage-specific (biphasic) by testing the expression of WNT genes in *Drosophila*, P19 cells, Chick, and *Xenopus* at different stages. In *Drosophila* cardiogenesis and the EB formation stage they found that WNT/Catenin activates the essential markers to induce the differentiation of ES into cardiomyocytes and at the same time act as an antagonist to the vascular marker genes (hematopoietic).

On the other hand, they found that the stage post-EB formation, it activates the hematopoietic/vascular genes and downregulates BMP, which, as a result, inhibits the cardiac genes. On the contrary, a negative role was reported in chick and *Xenopus* where WNT/catenin inhibited cardiomyogenesis at stages 5-6 and 8-9. However, the report discussed how the cells were already committed at this stage, and the fate was decided already in the gastrulation stage and SHF where the expression of WNT is high and activated (Gomez-Orte *et al.*, 2013; Naito *et al.*, 2006).

The non-canonical signal transduction is  $\beta$ -catenin independent, and the most popular pathways are the planar cell polarity (PCP) and the WNT/ $\text{Ca}^{2+}$  pathway (Gomez-Orte *et al.*, 2013). The canonical WNT/PCP acts through the c-Jun N-terminal kinases (JNK) (Meyer *et al.*, 2017). This pathway controls cytoskeletal activities and cellular orientation (Gay & Towler, 2017). Ras homolog A gene family (RHOA) and small GTPases RAC1 are also other downstream effectors of the Wnt/PCP signal transduction (Gomez-Orte *et al.*, 2013).

While the WNT/ $\text{Ca}^{2+}$  is predominantly linked with cardiovascular diseases due to its regulation of vascular smooth muscle cells (VSM) (Gay & Towler, 2017), it is also linked to inflammation (Kohn & Moon, 2005), cancer and neurodegenerative diseases (Gomez-Orte *et al.*, 2013). The G-protein coupled receptors family (GPCR) also releases calcium, which is mediated by Fz independently from the LRP5/LRP6 (Slusarski *et al.*, 1997; Kohn & Moon, 2005).

The role of Wnt and its functions specified in the cardiomyogenic stage is believed to be linked to BMP. WNT also promotes the development of PS cells by inducing the expression of brachyury from ES cells (Gadue *et al.*, 2005). The secreted frizzled-related proteins (SFRPs) inhibits the WNT pathway, and it inhibits both the canonical and the non-canonical sclerostin and Dickkopf (Dkk) proteins also inhibit the WNT pathway by binding to LRP5 and LRP6 proteins (Gay & Towler, 2017).

### **Nodal/Activin**

Nodal is a member of the TGF family and is one of the most critical growth factors in cardiogenesis (Gadue *et al.*, 2005) and organogenesis in general. Nodal is found to be mediated by several transcription factors and proteins like Crypto (Brand, 2003), FoxH1 (Lenhart *et al.*, 2013), Smad (Gahr *et al.*, 2012), Apelin (Deshwar *et al.*, 2016), Nodal modulator 1 (NOMO1) (Zhang *et al.*, 2015A) and other factors.

The signalling pathways of Nodal and Activin are very similar, and the effect is sometimes indistinguishable to which one is responsible, hence why it is widely referred to as Nodal/Activin or Activin/Nodal complex (Pauklin & Vallier, 2015).

It is understood that the Nodal/Activin ligands play an active role in the Inhibition of the neuroectoderm and the regulation of the pluripotent factors and most importantly drive the differentiation of the mesendoderm (Bertero *et al.*, 2015). In work presented by Bertero and his colleagues (2015), they demonstrated the link between Nodal-SMAD2/3 and the pluripotency transcription factor NANOG in maintaining self-renewal and differentiation. Nodal also plays a role in the mesodermal germ layers specification in the early stage (Kattman *et al.*, 2010). While in the later stage, Nodal is understood to inhibit and lower the expression of BMP on the left side of the cardiac field unilaterally (Veerkamp *et al.*, 2013). This action of Nodal results in cellular migration of the tissues and lower expression of non-muscular myosin which, overall, give rise to the cardiac left-right axis asymmetry of the heart (Veerkamp *et al.*, 2013; Brennanet., 2002).

The Nodal signal transduction binds to one of two Activin receptors through type I activin receptor through ALK4 or ALK7 and type II activin receptor ACTRIIA or ACTRIIB (Schier, 2003; Pauklin & Vallier, 2015). This action results in the phosphorylation of SMAD2 and SMAD3, which further initiates the downstream effects (Schier, 2003; Pauklin & Vallier, 2015).

### **1.1.3. Post-transcriptional factors involved by Non-coding RNA sequences and RNA G-quadruplexes:**

Recently, the post-transcriptional regulation has been investigated as one of the cues into solving the mechanisms in several biological activities. Regarding the cardiac development, there are two major groups of regulators; Non-coding sequences and G-quadruplex. Both share the same role in the regulation of mRNA and the translation of proteins (Nie *et al.*, 2015; Choong *et al.*, 2017). The non-coding sequences are of three types, a small non-coding RNAs sequence (SncRNAs), a long non-coding RNAs sequence (LncRNAs) and a circular non-coding sequence (CircRNAs) (Ottaviani & Martins, 2017). SncRNAs are the most researched group, the LncRNAs comes next, and finally the recently reported group CircRNAs. The structural differences are illustrated in figure 1.2.

## **RNA non-coding sequences**

The short non-coding RNA sequences (SncRNA) or in other words, the microRNAs (miRNAs) are an endogenous single-stranded sequence in the non-coding RNA sequence. It has been extensively studied, and some key miRNAs have been identified as regulators of precisely the cell fate, differentiation, development, proliferation, and regeneration, and repair of cardiomyocytes (Katz *et al.*, 2016; Choong *et al.*, 2017). miRNAs are introduced in detail in section 1.4.

LncRNAs similarly are another group of non-coding sequence which are longer than miRNAs (18-25 bp (Ying *et al.*, 2013)) with a size larger than 200 bp (Ottaviani & Martins, 2017). According to Nakagawa (2016), LncRNAs are key in the regulation of the epigenetic modifications as well as in genomic imprinting (allelic modulation) and the transcriptional and post-transcriptional genetic regulation. These set of regulators are found in both the nucleus and the cytoplasm, which explains the interaction with several molecules found in both either activated or inhibited (Ottaviani & Martins, 2017). LncRNAs Can perform RNA editing, polyadenylation, alternative splicing, and a 5' terminal methylguanosine capping post-transcriptionally. These activities take place when LncRNAs are activated when key transcriptional factors bind to the transcriptional start site (TSS) in the lncRNA (Choong *et al.*, 2017; Guttman *et al.*, 2009; Derrien *et al.*, 2012). These factors such as OCT4, SOX2, NANOG, NFκB, P53, and MYC regulates LncRNAs by binding to its TSS which is the place of the histone marks (Choong *et al.*, 2017; Guttman *et al.*, 2009; Derrien *et al.*, 2012). These histone marks, such as H3K27, H3K4me3, H3K9ac, and H3K4me2, are also associated with the expression of lncRNA (Derrien *et al.*, 2012).

In mice, there are two significant examples of the role of lncRNA in the differentiation and development of cardiac myocytes. Foxf1 adjacent non-coding developmental regulatory RNA (FENDRR) is proven to be critical and essential when silenced or inhibited; it can cause a severe defect in cardiac development (Grote *et al.*, 2013). FENDRR is also a vital regulator of some of the most important transcription factors in the development of cardiac fate (Grote *et al.*, 2013).

The other example is Braveheart (BVHT), which was identified by Klattenhoff and his colleagues (2013) to be crucial in initiating the cardiac lineage and in maintaining the cardiac fate during mammalian developments. They are linked to the progression of the mesodermal stage through the regulation of MesP1 and other cardiovascular gene networks.

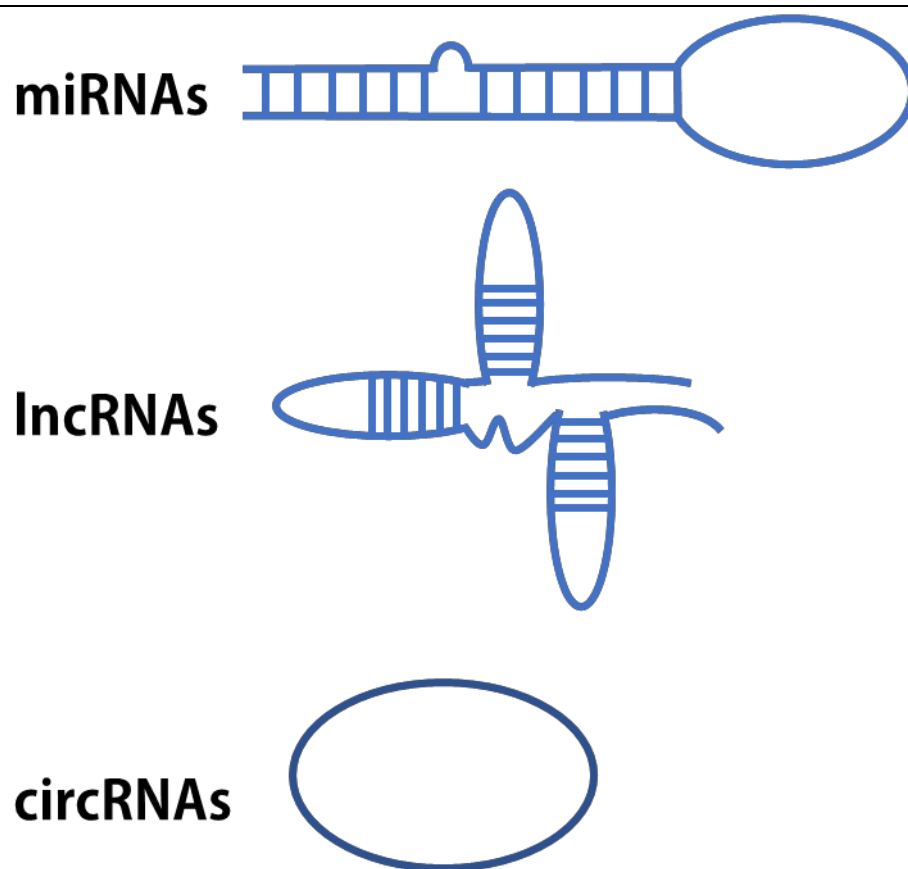


**Figure 1.2: Structural differences between the three non-coding RNA sequences.**

The last type of the non-coding sequences is circRNA. It is transcribed from intronic and exonic according to Hsiao *et al.* (2017), Qu *et al.* (2015) however, they could also originate from an anti-sense, intragenic and intergenic depending on the position of the gene and its adjacency. The role of circRNA and activities have been revealed and discussed (Qu *et al.*, 2015). Due to its circular configuration, circRNA contains no 5' and 3' ends, which concludes the reason for its stability (Hsiao *et al.*, 2017). However, in the biogenesis of the CircRNA it is back spliced when the 5' end moves towards the 3' end, hence how it leads to a circular RNA structure with covalently a closed loop (Siede *et al.*, 2017; Cheng & Joe, 2017).

Siede *et al.*, (2017) reported that a significant change in CircRNAs expression was found suggesting the critical role these set of non-coding sequences could possess. These were specifically regulated in the context of the cardiac  $\beta$ -adrenergic signalling and the cardiac myocyte differentiation state. They used a human induced pluripotent SCs derived from

cardiomyocytes. They also concluded that circRNAs are highly regulated in the case of the stress response as well as in the development of cardiac fate.

On the other hand, another group (Chen *et al.*, 2017) identified a circRNA which regulates vascular smooth muscle cells proliferation and migration. This finding elucidated by silencing the WDR77, which, as a result, suppressed VSMCs proliferation and migration by targeting its downstream regulators like FGF2 and mir-124. Another example of functions of circRNA in the heart is what is called heart-related circRNA (HRCR). It tends to play a role as an anti-hypertrophic agent by targeting mir-223 acting as a sequester of the RNA-binding protein (Wang *et al.*, 2016 B; Ottaviani & Martins, 2017).

From these previous examples, the critical role of circRNAs could be summarised as a miRNA sponge (decoy) which results in the termination of the post-transcriptional regulation by miRNA (Hansen *et al.*, 2013). They also manipulate and regulate mRNAs expression directly via imperfect base-pairing when attached to the mRNA (Hentze & Preiss, 2013). CircRNAs, moreover, could help in transporting miRNAs intracellularly to its targets as well as interacting with ribosomes and RNA-induced silencing complex (RISC) (Siede *et al.*, 2017). Altogether, suggest that circRNAs could be a key contributor into a lot of phenotypic diseases (Ottaviani & Martins, 2017) and other many processes like cancer, tissue developments and ageing (Qu *et al.*, 2015).

The importance of this non-coding sequences rest on the fact that they acquire almost 98% of the whole genome compared to 2% of the coding sequences (Carninci *et al.*, 2005) which explains the increasing interest on these ncRNAs and the possible roles as therapeutic targets or as disease markers.

## **RNA G-quadruplexes (G4s)**

G-quadruplex is formed of a tetrad-stranded structure rich in Guanine DNA and RNA sequence (Nie *et al.*, 2015; Cammas & Millevoi, 2017). In the non-coding sequence or the untranslated regions (UTRs) G4Ss are found in both the 5' and 3' end, according to Huppert and his colleagues (2008). While in the coding sequences (exons), it is found only in the 5' end (Eddy & Maizels, 2008).

RNA-G4S has recently been increasingly focused on compared to DNA-G4S. This is due to its regulatory roles in gene expression and translation (Agarwala *et al.*, 2015). Besides, RNA- G4s is also more stable and compact due to its single-stranded structure compared to the double-stranded deoxyribose sugar and the increased intramolecular bonds (Agarwala *et al.*, 2015).

RNA-G4S biologically function as a translational regulator, specifically repression and augmentation. It also features like a 3' end processing (alternative polyadenylation) as demonstrated within the downstream of P53s 3'end after a UV irradiation (Decorsière *et al.*, 2011). RNA-G4S has also been found to be like Rho in the mechanism of termination of transcriptions (Wanrooji *et al.*, 2010). The functions of RNA-G4s also includes mRNA-localisation and alternative splicing (Agarwala *et al.*, 2015).

These RNA-G4S motifs have recently been linked to other post-transcriptional regulators and ncRNAs. This is illustrated with lncRNAs (Jayaraj *et al.*, 2012) and miRNAs (Mirihana *et al.*, 2015) as well as the regulation of several gene expressions (Cammis & Millevoi, 2017) hence why this set of motifs attracted attention due to its competence in being a therapeutic target or markers.

#### **1.1.4. Cardiovascular diseases (CVDs)**

The cardiovascular system is one of the most studied systems in the body. Cardiovascular diseases (CVDs) are associated with high death rates (31%) in the world, according to the world health organisation (WHO). In 2015, 17.7 million were estimated to have died because of CVDs like coronary heart disease, strokes, atherosclerosis, and myocardial infarction (MI).

Congenital heart defect (CHD) malformation is one of the primary defects that occur during the development of babies before birth. Heart defects affect 1 in 100 babies, hypertrophic cardiomyopathy (HCM) is another form of the disease which is diagnosed at infancy and is the second most common form of heart muscle disease. Rheumatic heart disease and Kawasaki disease are all other forms of diseases linked to the heart. All these are affecting not only the health of the people of the world but also have a significant financial impact worldwide, especially in low and middle-income countries (WHO). Although research is ongoing and emerging, there are still several issues that remain unresolved and unanswered. In most of the European countries, CVD is the first death causing factor in premature babies

(De Backer *et al.*, 2003). Some risk factors that are involved in CVDs are high blood pressure (hypertension) (Forouzanfar *et al.*, 2017; Lim *et al.*, 2012), high cholesterol (Sinicato *et al.*, 2013), diabetes (Sinicato *et al.*, 2013), smoking (De Backer *et al.*, 2003), obesity (De Backer *et al.*, 2003) and genetic (a family history with a CVD) (Padmanabhan *et al.*, 2015; Kathiresan & Srivastava, 2012). All these factors, including others, could be interlinked and increase the susceptibility to a CVD which, as a result, could lead to mortality.

### **1.1.5. Pathophysiology of CVDs:**

In atherosclerosis, the dysfunction of endothelial cells results in the elevation of reactive oxygen species (ROS) which promotes foam cells or atherosclerotic lesions and increase oxidative stress in the heart (Ooi *et al.*, 2017). Oxidative stress joined with the inflammation developed as a result of the atherosclerotic lesions are also highly associated in causing CVDs (Sinicato *et al.*, 2013; Ooi *et al.*, 2017) and acute coronary syndromes (Ooi *et al.*, 2017). Similarly, MI is an outcome of cardiac cells death by ischaemic insult (Frangogiannis, 2015). This cell death is widely reported as either apoptosis of the cells or necrosis. The most robust difference is that with apoptosis the dead cells are cleared without the induction of inflammation, while in necrosis, it triggers the inflammatory factors justifiably due to the swelling that occurs to the cells (Frangogiannis, 2015). MI is also mainly caused by coronary atherosclerotic disease in the heart, specifically by the rupture of the plaques, which also leads to thrombosis pathophysiologically (DeWood *et al.*, 1980; Frangogiannis, 2015). The severe loss of these myocardial cells post-infarction could lead to hypertrophy and fibrosis because of the exhaustion of the non-infarcted cardiomyocytes (Frangogiannis, 2015; Tham *et al.*, 2015).

Cardiac hypertrophy, however, pathologically is associated with factors like epigenetic changes, cellular dysfunctions, over-production of pro-inflammatory cytokines, and fibrosis. These changes, also, are induced because of either hypertension or MI and further would cause prolonged and abnormal hemodynamic stress (Tham *et al.*, 2015; Shimizu & Minamino, 2016).

### **1.1.6. Recent therapies linked to cardiovascular diseases**

Despite promising pre-clinical studies, some clinical trials on cardiovascular diseases have been less conclusive with slightly conflicting findings. However, currently, there are several pharmaceutical drugs and therapies used, like  $\beta$ -receptor blockers like acebutolol, angiotensin receptor blocker (ARB), angiotensin-converting enzyme inhibitor (ACE inhibitor) like enalapril and renin inhibitor and calcium channel blockers (CCB).

There is also a lot of promising results and reports pre-clinically either on animal models or at the cellular level. This includes using non-coding regulators which have been shown to be able to contribute to the transcriptional changes in disease models as well as in clinical samples. Yang and his colleagues (2017) discussed how the CircRNA\_081881 regulates miR-548, which is also a peroxisome proliferator-activated receptor gamma (PPAR $\gamma$ ) regulator, which acts as a heart-protective factor. Several miRNAs are linked to many CVDs; this includes but not limited to mir-133, mir-21, mir-132, mir-208a, and mir-1 (Roma-Rodrigues *et al.*, 2015). Oligonucleotides modification is used to decrease the expression of these miRNAs (AntagomiRs) as well as using RNA mimics for overexpression (Roma-Rodrigues *et al.*, 2015).

One of the most highly promising therapies is exploiting cell therapy or SCs therapy (Malliaras & Marban, 2011). This therapy includes the transplantation of SCs to the infarcted heart for the regeneration and repair of the damaged tissue. Induced pluripotent stem cell (iPSC)-derived cardiomyocytes are specifically under the spotlight. A group led by Shiba (2016) reached a conclusion based on their experiments on Monkeys. The Monkeys with matching MHC iPSC- derived cardiomyocytes showed no immune rejection up to week 12 and showed no signs of tumours besides other downsides that were found soon after transplantation, however, this is a promising step in tackling two of the biggest problems that face cell therapies in the heart. Some of the limitations in using pluripotent embryonic SCs clinically are the risk of tumours, immunogenicity, and genetic instability, including ethical matters (Robertson 2001). In 2014, a damaged heart tissue in a primate myocardial infarction model was grafted and repaired using embryonic SCs (Chong *et al.*, 2014). This finding and others have given some hope to the possibility of using in vitro programmed cells without risks. Prof Mummery who is one of the first people to inject ESC to animal heart suggests that these findings and contributions will move this therapy forward to the clinical field sooner if future studies address the effect of larger grafts with longer follow up and

address any possible complications (Fernandez-Ruiz, 2016).

SCs are essential in developing effective treatment strategies for most of these diseases by either repairing or regenerating the cells and tissues or using them as a mimic to the actual organ in-vitro by using a specific differentiation inducer to the cells using cell culture techniques. New novel opportunities are needed and to this end stem cell therapy is emerging as a potential therapy for regenerating the infarcted or failing myocardium especially with the little reported changes in the impaired cardiac functions from the clinical trials.

## 1.2. Stem cells

SCs are the foundation for all the different cells and tissues. These cells can self-renew by continuously dividing and growing through mitosis. SCs can be driven to differentiate into another specific kind of cells with a specialised function which, as a result, can form the different lineages and tissues in the body.

This differentiation can be monitored by a set of genes which can be expressed or repressed in the cells (Potten & Loeffler, 1990) through any differentiation or specialisation inducer. In vivo, this can happen by the interaction of SCs with neighbouring specialised or differentiated cells, by chemicals secreted, or by signalling through growth factors. While in vitro, scientists can drive the SCs to specialise in the petri dish by inducing with growth factors (signalling pathways activation). Cell substrates are used as an extracellular matrix (ECM) constituent in plates, by which the SCs would be grown on top of this ECM, which will give rise to a specific lineage. A published example of these ECM with cell substrates is a matrigel which contained pancreatic cells. Pluripotent SCs were grown on top of the ECM in a plate, and the cells developed into an actual pancreatic cell (Zhang *et al.*, 2009). Other ECM substrates include fibronectin, collagen, laminin, and hyaluronic acid (Cell and Molecular Biology and Imaging of SCs “book,” 2014). This co-culturing of existing differentiated and undifferentiated cells in the same culture would allow specific proteins to be secreted on the ECM and the three-dimensional structures of the cells form a spherical aggregate known as embryoid bodies (EB), which mimics the natural process of differentiation and the development of new cells.

### 1.2.1. Types of Stem cells

There are different types and classifications of SCs according to the potential of each to be differentiated. Totipotent, pluripotent, and multipotent stem cells are the major types which can differentiate into various lineages. Other kinds of SCs are oligopotent or unipotent. These cells can only differentiate into limited cell types (Gülçin, and Erdal, 2012). Totipotent is the earliest stage of stem cell in the organism by which it can give rise to a whole living species with the identical specification to the mother cell. Pluripotent SCs are cells which can be differentiated into any other cell type unlimitedly by which after this stage, the cells cannot have the same specificity as pluripotent and the lineages of these cells will be limited.

Multipotent cells are mainly found within organs, and they are limited to cells linked to their tissue type. For example, a multipotent blood stem cell can be differentiated into the different kinds of blood in the body, while the multipotent cardiac SCs can be driven to produce endothelial cells, myocytes, and smooth muscle cells (Beltrami *et al.*, 2003). Unipotent SCs are cells which have the potential to be developed into one single cell type. Figure 1.3 illustrates the different stages of SCs from an embryo to the differentiated cells.

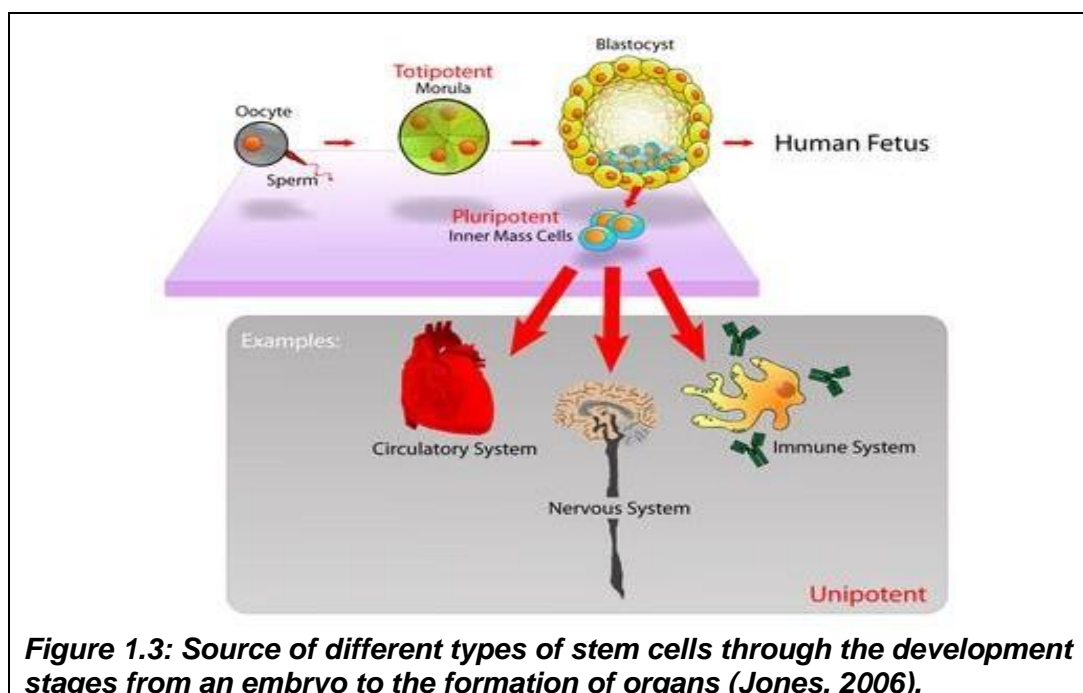
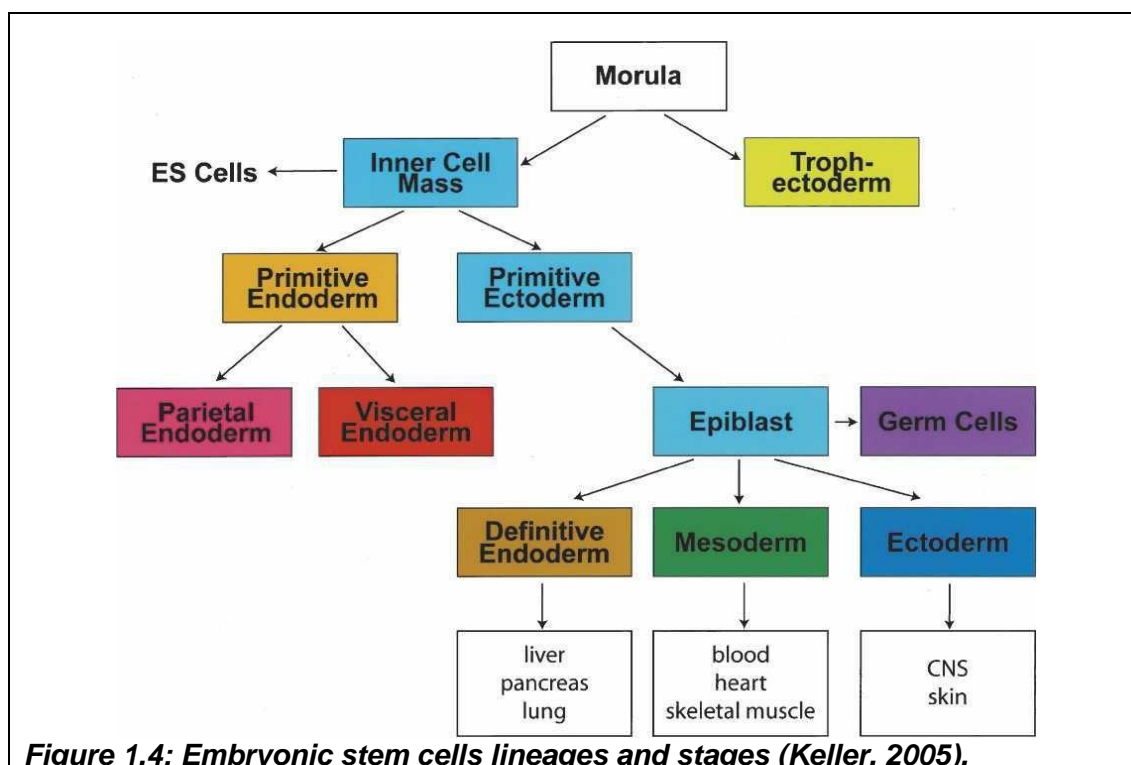


**Figure 1.3: Source of different types of stem cells through the development stages from an embryo to the formation of organs (Jones, 2006).**

There are two classes of SCs; embryonic stem cell and adult stem cell (somatic). This classification depends on the source of these cells and the capability they hold to be differentiated into more varied kind of cells or the ability to self-renew. Embryonic stem (ES) cells are pluripotent cells which are found in the inner cell mass (ICM) of the blastocyst (Evans and Kaufman, 1981; Martin, 1981; Keller, 2005). ES can self-renew, and it serves as building blocks for the body. Adult SCs are multipotent cells and have limited ability to self- renew or to differentiate into various kinds of cells. This limitation is because these cells are produced in a specific tissue environment, which limits their differentiation into other cell types linked to other tissues.

### 1.2.2. Embryonic Stem cells (ES)

According to Smith (2001), ES cells give rise to three different germ layers, endoderm, mesoderm, and ectoderm-derived lineages. Each layer gives rise to distinct lineage and tissues (Figure 1.4). The endoderm gives rise to the liver, pancreas, and lung, while mesoderm develops into blood, heart and skeletal muscles and ectoderm develop into the central nervous system (CNS) and skin (Keller, 2005).



### 1.2.3. Types of the embryonic pluripotent stem cells

Embryonic SCs can be sub-grouped into embryonic carcinoma cells (EC) or embryonic germ cells (EGC) (Boheler *et al.*, 2002). The difference is that ES cells are derived from the ICM and epiblast in the blastocyst stage in the embryo. However, EC is a tetracarcoma isolated from the extra-uterine sites in mice which have been transferred initially from the (ES) cells in the epiblast in the ICM (Table 1.1). EG cell line is isolated from the genital ridge of 9.5-12.5dpc embryos of a mouse by the ES transferred from the ICM and derived from primordial germ cells (PGCs). EC in comparison to ES and EG does not require feeder cells to be cultivated, while the other two groups (ES & EG) are feeder cell layers dependent (e.g., mouse embryonic fibroblast). A lack of this feeder layer, which contains differentiation inhibitors would result in the cells to lose the stability of the chromosomes karyotype and the function of being self-renewing cells (Boheler *et al.*, 2002).

**Table 1.1: A comparison between sources of P19 embryonic carcinoma, embryonic stem cells, and embryonic germ cells (Boheler *et al.*, 2002).**

Type of Stem cells	Origin	Feeder Layer	Karyotype	Development into lineages
<b>Embryonic stem cells (ES)</b>	Inner cell mass (ICM)	Yes	Euploid	Multiple
<b>Embryonic carcinoma cells (EC-P19 cells)</b>	Extra uterine sites	No	Heteroploid	Limited
<b>Embryonic germ cells (EG)</b>	Primordial germ cells	Yes	Euploid	Limited

#### **1.2.4. Induced Pluripotent Stem cells (iPSCs)**

iPSCs hold a potential source of a self-renewing and spontaneously growing cells with the ability to be derived from different cell types in the body. iPSCs were recently discovered by re-programming to pluripotent SCs from an adult differentiated cell. It was reported by Takahashi & Yamanaka, in 2006 and was examined on somatic cells by inducing four different transcription factors, which are Oct3/4, SOX2, c-Myc, and KLF4. These four transcription factors share the same objective, which is keeping the cells in their undifferentiated state and keeps the cells regenerated and renewed. Other successful combinations of the transcription factors which could generate iPS cells include Sox2, Oct4, Lin28, and Nanog (Yu *et al.*, 2007). The process of producing these cells includes overexpressing several endogenous pluripotency inducers in the cells. These inducers have been recently found to help maintain and induce transcription factors like Oct3/4, SOX2, and KLF4. Xu *et al.* (2009) reported that mir-145 is at its lowest expression level in ESCs, which means the pluripotency transcription factors were at their highest level of expression as a result. On the other hand, they found that mir-145 was highly overexpressed during differentiation, which correlates with the decrease of the pluripotency markers of the transcription factors (Xu *et al.*, 2009). What makes iPSC unique is that they are remarkably like ES cells in their morphology, proliferation, and gene expression (Yamanaka *et al.*, 2012).

#### **1.2.5. Induction of embryonic stem cells differentiation**

One of the most popular ways of inducing differentiation of SCs is by forming embryoid bodies (EBs) in a suspension culture plate. The fate of these embryoid bodies could be monitored by either adding specific growth factors (GF), transcription factors, and drugs. Recently, another endogenous factor is being highlighted by researchers, and these are the non-translated sequences (i.e., miRNAs), which proved to play a significant role in regulating the factors which keep the cells in their original undifferentiated state by renewing and regenerating those cells (Xu *et al.*, 2009). Embryoid bodies could be formed in a 3-dimensional culture using a technique called hanging drop technique. 3D cell culture is a technique which creates scaffold-free cells in three dimensional instead of the usual 2-dimensional embryoid culture. Recent results showed that 3D spheroid cell culture formed *in vitro* mimics the *in vivo* development and growth of cells more than the 2D cell culture. Differentiation can be induced by using GF in the medium to drive the SCs to be differentiated

into their fate. An example of a successful growth factor transcription factors/signalling showing a significant difference in the expression between the control and the GF induced stem cell in a research done by Ayatollahi from Iran in a published paper in 2011. This paper illustrated that insulin-like growth factor (IGF) induced differentiation of mesenchymal SCs. Moreover, another research carried out by a group in 2000 led by Schuldiner demonstrated that eight different GFs could develop in cells derived from human embryonic SCs (hESCs). Besides these papers, many other research papers showed that using GF for inducing differentiation of SCs is a successful way of driving ESCs to develop into another type of cells.

Another example of differentiation inducer is transcription factors or signalling molecules like BMPs, leukemic inhibitory factor (LIF), GATA family, and Nkx-2.5. All are linked to the process of the differentiation either positively or negatively. According to Monzen *et al.* (1999), BMPs exert their effect on the cells by inducing an antagonist which inhibits the differentiation of the cells into cardiomyocytes by stopping the transcription factors associated in their development into cardiac cells. This BMP antagonist is called Noggin. However, the differentiation could be reactivated either by overexpressing BMP-2 or adding the BMP protein to the culture. In the same research paper, GATA-4 and Nkx-2.5 were shown to be highly expressed during the differentiation process of SCs into a cardiomyocyte. This reaction to the differentiation has been confirmed by Grepin *et al.* (1997) who examined this zinc finger cardiac transcription factors and concluded that GATA-4 could cause embryonic stem cell markers to be down-regulated, while the cardiac transcription factors to be activated or over-expressed (Grepin *et al.*, 1997; Boheler *et al.*, 2002). LIF is understood to play a negative role in blocking the differentiation of the cells as well as the development of mesoderm cells (Boheler *et al.*, 2002).

Emerging models of organs *in vitro* that mimic naturally formed tissues or organs are one of the highly focused areas by scientists using ES cells in the last 20 years (Keller, 2005). Various ways of deriving the lineages of ES cells have been discovered and applied for the same reason for the best tissue model. These contribute in understanding the nature of the development of these tissues, and the kind of the disorders in the tissues by identifying defect markers or targeting the main reason behind the problem or using these in-vitro tissues for transplantation as replacement or regeneration to the defected organs.

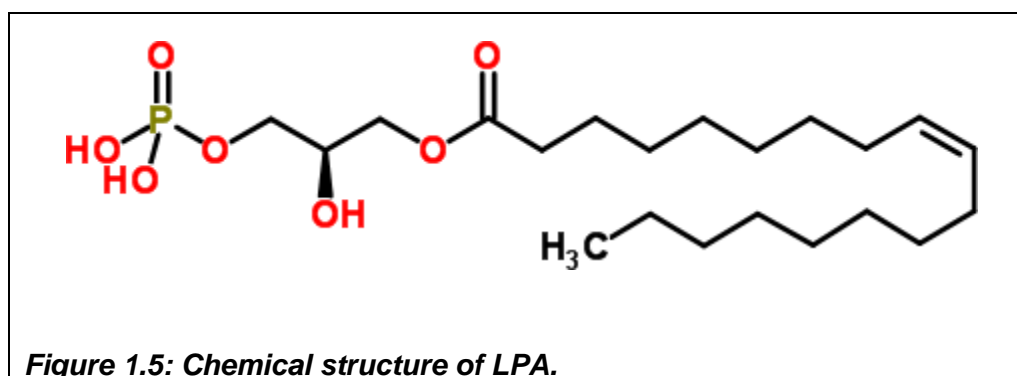
The key player in this process could be the identification of a clinically relevant molecule for inducing the differentiation of SCs. One of the favourites used agents for the differentiation of the tetracarcoma stem cell-like P19 cell line into cardiomyocytes is dimethyl sulfoxide (DMSO) (Abilez *et al.*, 2006; Angello *et al.*, 2006; Van der Heyden *et al.*, 2003A; Boheler *et al.*, 2002; Jasmin *et al.*, 2010; Edwards *et al.*, 1983; Arreola *et al.*, 1993; Skerjanc, 1994). In this thesis, the agent that will be focused on is Lysophosphatidic acid (LPA) which is of more physiological relevance but has not been thoroughly investigated about the differentiation of SCs into cardiomyocytes nor has its potential underlying mechanisms been fully investigated.

### **1.2.6. Induction of the differentiation of P19 cells into cardiomyocytes:**

P19 cells are pluripotent teratocarcinoma cells induced in the C3H/HeHa mouse (Jasmin *et al.*, 2010). The uniqueness of the P19 cell line lies on that it can grow undifferentiated rapidly without the need of feeder layers like ES cells (Choi *et al.*, 2004). They also have proven to be one of the excellent models to mimic the early stages of cardiogenesis and beyond (Paquin *et al.*, 2002). These pluripotent like EC, P19 cells are established to being able to induce differentiation into multiple cell types that represent the three germ layers (McBurney, 1993). The differentiation of P19 cells into the neuroectoderm derivatives like neurons, microglia, and astroglia has been shown by retinoic acid (RA) as one of the main lineages. Skeletal muscles, as well as cardiac, has also been widely developed to represent the endodermal and mesodermal stages by using DMSO in aggregates of P19 cells (McBurney, 1993). The induction of differentiation into cardiomyocytes by DMSO is the most studied kind of induction using P19 cells (Angello *et al.*, 2006; Jasmin *et al.*, 2010). Comparing the efficiency of the differentiation of P19 cells showed that using a non-toxic or a physiological relevant agent to drive the differentiation is more effective than using other chemical agents like DMSO (McBurney, 1993; Skerjanc *et al.*, 1999; Paquin *et al.*, 2002). There are several reported agents for being able to induce the cardiac differentiation using P19 cells, oxytocin (Paquin *et al.*, 2002), 5-azacytidine (Choi *et al.*, 2004), cardiogenol C (Wu *et al.*, 2004), and finally DMSO as mentioned earlier. Moreover, Lysophosphatidic acid has recently emerged as one of the cardiac lineage inducers in our group using P19 cells (Pramod, 2017).

### 1.3. Lysophosphatidic acid (LPA)

Lysophosphatidic acid is a product of a blood clotting process and a serum-constituent that activates a G-protein coupled receptors found in different cell types to initiate the various processes (Moolenaar *et al.*, 1997). It is revealed that LPA plays a similar role to hormones and growth factors (Eichholtz, 1993; Moolenaar *et al.*, 1997). Some papers suggest that the purpose of LPA is stimulating platelet aggregation, smooth muscle contraction, neuronal cell rounding, and neurite retraction and initiate proliferation in fibroblasts (Eichholtz, 1993). Ishii *et al.*, (2004) suggest, that LPA is involved in cellular processes, proliferation, apoptosis, inhibition, cell migration, secretion of chemokine and cytokines in addition to other roles not yet revealed (Figure 1.5).

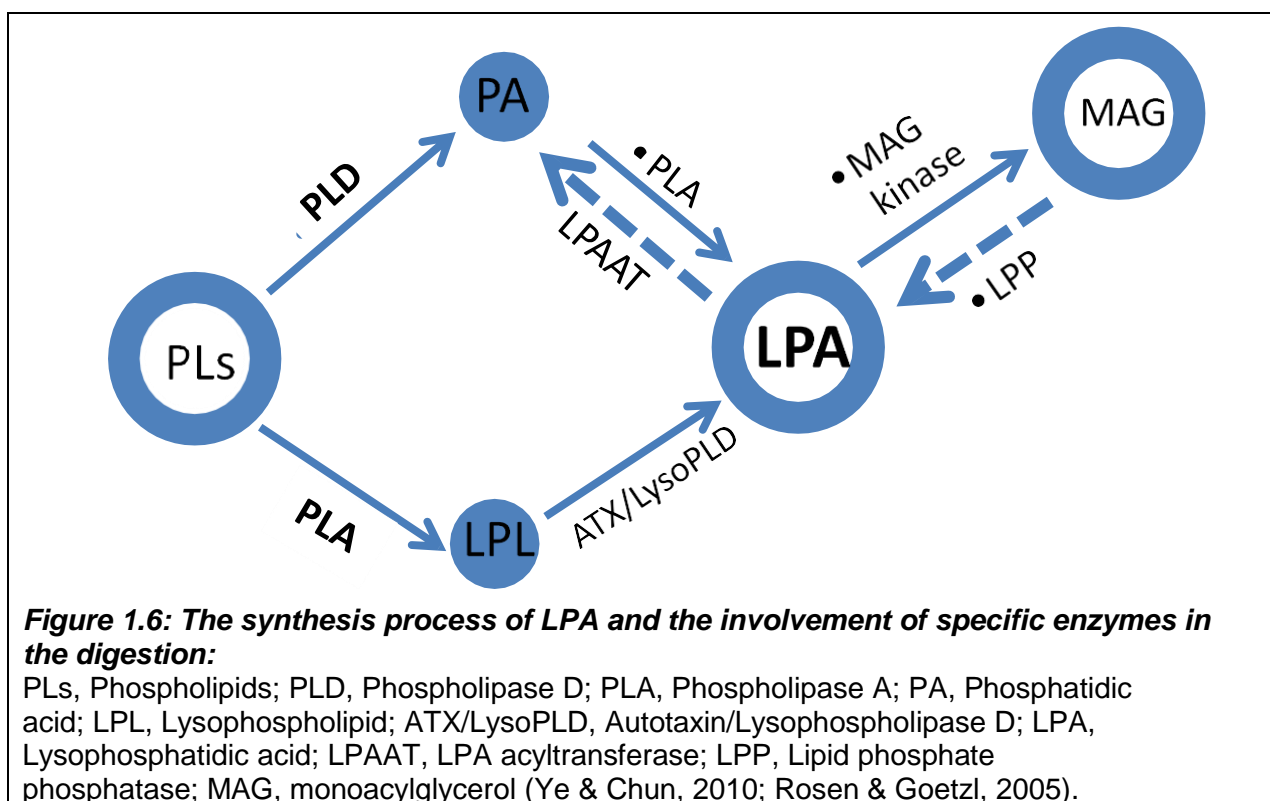


Previously, phospholipids were understood to be as building blocks for the cell membranes and tissues but, this hypothesis is no more recognised and recent publications have reported phospholipids could play a critical role in cell signalling and in mediating vascular physiology and pathophysiology due to their circulation in the blood (Moolenaar *et al.*, 1999). LPA was first identified in 1978, then in 1989, the growth factor-like roles were discovered, and in 1996, the LPA receptors were identified (Tigyi, 2001).

#### 1.3.1 Production and release of LPA

LPA is a glycerophospholipid which consists of three different parts in its chemical structure: head group, linker group, and lipophilic tail which explains why LPA is one of the easily soluble phospholipids in water (Xu *et al.*, 2001). LPA is mainly produced from phosphatidic acid (PA) processed into phospholipids (PLs) then hydrolysed by autotaxin (ATX), an enzyme secreted by phospholipase D (PLD) which is an ectonucleotide

pyrophosphatase/phosphodiesterase-2 (ENPP2) (Perrakis & Moolenaar, 2014) and could be produced in the external cellular membrane by the hydrolysis of lysophosphatidylcholine (LPC) (van Dijk *et al.*, 1998). Other mechanisms and production pathways have been reported depending on the site of release of LPA and the cell type. According to Pages *et al.* (2001), LPA could be produced intracellularly in mitochondria and the endoplasmic reticulum by the acylation of glycerol-3-phosphate by the glycerol-3-phosphate-acyltransferase. Moreover, the active circulating LPA molecules are transformed by dephosphorylation to monoacylglycerol (MAG) (Figure 1.6).



Ongoing research in our group has made significant progress in recognising LPA as an endogenous bio-lipid inducer of stem cell differentiation into cardiomyocytes, and from other reports, can also regulate proliferation, adhesion, migration, survival, and morphogenesis (P´ebay *et al.*, 2007). LPA regulates the immune activation response by activating T cells and dendritic cells (DCs) (Chen R *et al.*, 2006). As to its role in the immune system, LPA is increasingly found to play significant roles in the cardiovascular system, nervous system, reproductive system, respiratory system and in cancer (P´ebay *et al.*, 2007).

This shows that LPA is involved in many biological processes by signal transduction and signalling molecules through the G protein-coupled receptors (GPCRs) primarily through LPA receptors 1, 2, 3, 4 and 5 (LPA1-LPA5) (P´ebay *et al.*, 2007) and LPA6 which may be a new member of the GPCRs activated by LPS (Pasternack *et al.*, 2008). Several papers now suggest that LPA regulate the differentiation of SCs, protect different types of cells, including cardiac myocytes from apoptosis, and enhance myocytes contractility (Lin *et al.*, 2010).

### **1.3.2 Lysophosphatidic acid receptors (GPCRs)**

As indicated above, LPA acts on potentially six different G-protein (Gi, Gq, G12/13 alpha subunits) coupled receptors (LPA1-LPA6). One more receptor is recently reported as an addition to the family (reviewed by Ye & Chun, 2010) and two other potential receptors are being validated. Each receptor mediates different and multiple roles and responses at the cellular level (Lin *et al.*, 2010). Some of the roles of each receptor are not yet clearly established, but the downstream targets are suggested to be as follows in figure 1.7.

LPA1 and LPA2 seem to be similar in their targets, and both have a high affinity towards 1-acyl- and 2-acyl-LPA, while LPA3 has a higher affinity for 2-acyl-LPA (reviewed by Ye & Chun, 2010). LPA1, LPA2, and LPA3 receptors are mainly found in the testis, according to Ye *et al.* (2008). LPA1 and LPA2 are two highly expressed receptors in human prostate cancer cells (Xie *et al.*, 2002). While, LPA4, LPA5, and LPA6 are shown relatively less compared to LPA1-3. The LPA4 receptor is expressed in the ovary (Noguchi *et al.*, 2003) and LPA5 expressed in ESCs, spleen, dorsal root ganglion, and small intestine (Kotarsky *et al.*, 2006). Additionally, Pasternack *et al.* (2008) suggested that P2Y5 receptor (LPA6) is essential for hair growth and maintenance. They claim to be the first to indicate the link and the importance of a G-protein coupled receptor to human hair. Several LPA receptors are also found in the heart and involved in the overall mammalian development. LPA1 is expressed in tissues like the heart (Contos *et al.*, 2000). LPA3 and S1p1, however, are found to be highly expressed in the developing heart specifically (Ohuchi *et al.*, 2008). Although, LPA2, LPA4, and LPA5 are found to be expressed in the heart at a lower level compared to their presence in other tissues (as reviewed by Yung *et al.*, 2014).

### 1.3.3 Role of LPA in diseases:

LPA is understood to function pathologically and physiologically and tend to influence cellularly apoptosis, proliferation, and other processes (Sengupta *et al.*, 2004). Hence, LPA is linked to several abnormalities and defects in human, animal, and cell lines.

Neuropathic pain (NP) develop as a consequence of multiple sclerosis, cancers, diabetes, as well as other chronic diseases (Velasco *et al.*, 2017). It occurs once lesions to the central nerve fibres advances or in the case of acute nerve injuries (Velasco *et al.*, 2017). LPA expression was found to be over-expressed, which suggested a role in demyelination of the neurons as one of the core causes of NP (Yung *et al.*, 2014). Also, Inoue's group (2004) elaborated on the role of LPA in NP through Rho-kinase, ROCK, and Ras pathways via  $G\alpha_{12/13}$  and LPA could trigger and maintain NP.

LPA could be one of the challenges in cancer patients treated with chemotherapy, as it activates AKT, which protects cells from induced apoptosis potentially caused by chemotherapy (Baudhuin *et al.*, 2002). LPA is also linked to ovarian, prostate, breast, pancreatic, colon, lung, melanoma, and hepatoma cancers. It is, however, most extensively studied in ovarian cancer (OC) (Sengupta *et al.*, 2004). LPA plays a crucial role in migration, invasion, and metastatic activities. Sengupta *et al.* (2004) reviewed that for successful metastasis, cells should: a) detach from the original area of cancer, b) be able to survive under adverse situations, c) migrate to any distant locations, d) adhere to and invade the basement membrane of new loci, and e) grow as secondary metastatic foci.

In OC, LPA act as a growth factor (Xu *et al.*, 1995). It is also highly elevated in OC patients compared to other cancers and control (disease-free patients) (Xu *et al.*, 1998). Yu and his colleagues (2016) also showed that LPA is highly correlated to the metastatic capabilities in OC. LPA1, LPA2, and LPA3 were significantly higher in a patient with metastatic OC. Besides, the OC cell lines, which responded well to the LPA induced invasion, showed higher metastasis colonisation capabilities. Mitogen-activated protein kinase 1 (MEKK1) is one of the essential agents in the OC-linked migration of the cells, activated by G(i)-Ras-dependent manner (Bian *et al.*, 2004). The G(i)-Ras-MEKK1 pathway mediates LPA-stimulated OC's cell migration by facilitating focal adhesion kinase redistribution to focal contact (Bian *et al.*, 2004). The heavy focus in OC is because it is the deadliest disease among the gynaecological types of cancers (Yu *et al.*, 2016).

In prostate cancer, part of the roles played by LPA is activation of NFκB, which enhances the survival of prostate cancer (Kue *et al.*, 2002). It also activates extracellular signal-regulated kinase 1 & 2 (ERK) pathway and transactivates EGFR which induces the proliferation of androgen, which also stimulates prostate cancer (Kue *et al.*, 2002; Sengupta *et al.*, 2004).

In CVDs, LPA could influence platelets, cardiomyocytes, blood cells, SMC, endothelial cells, and fibroblasts (Sengupta *et al.*, 2004). Calcium is also, modulated by LPA receptors which in conjunction with WNT could regulate vascular smooth muscle cells and it is predominantly linked to diseases in the heart (An *et al.*, 1998; Hunter *et al.*, 1999; Dubin *et al.*, 2010). LPA similarly regulate cell migration and vascular maturation in the cardiovascular system (Teo *et al.*, 2009).

Human CD34 in MI were rescued and survived better when treated with LPA in a concentration and time-dependent manner (Kostic *et al.*, 2015). This group also confirmed experimentally the capability of LPA to induce cell proliferation and inhibit apoptosis. LPA is also reported to directly activate PPAR $\gamma$ , a known heart-protective factor (McIntyre *et al.*, 2003; Yang *et al.*, 2017). This action may indicate that any defect linked to the PPAR $\gamma$  pathway could be because of lack of activation or the over-activation by LPA.

Some GPCRs are shown to regulate other receptors indirectly through miRNA. In this regard, LPA3 mediated heart hypertrophy has been suggested to involve blockade of the expression of LPA1 using miRNA23a which was overexpressed after the signal transduction of LPA3 was activated (Ye *et al.*, 2005; Yang *et al.*, 2013). The involvement of miRNA in the broad activities of LPA within some of the complex mechanisms is yet to be fully established.

## 1.4. MicroRNA

MicroRNAs are a tiny regulatory non-coding sequence in RNA; they range from 18-25 nucleotides in length (Huang, 2010; Ying *et al.*, 2013) and are first described and discussed by two research groups, Pasquinelli *et al.* (2000) and Reinhart *et al.* (2000). Both addressed the link between miRNA and let-7 and the regulation of cell functions. miRNAs are now widely known in terms of their structure, involved mechanisms, and roles. They are found in the 3' untranslated region (3' UTR) and may regulate 60% of mammalian and human genes (Friedman, 2009). These miRNAs were discovered when a group of researchers were studying a gene called lin-14 in *C. elegans* development in 1993 and found that a small non-coding sequence regulated this gene. They found two sets of RNA of different sizes, the first one with 61nt and the other one was 22nt. The 61nt RNA was found to be the precursor of the 22nt, now referred to as microRNA (miRNA) (Bartel, 2004). miRNA can regulate targeted mRNA by either the cleavage of the mRNA if the miRNA perfectly complements the sequence on the mRNA or by repression, which is activated if the sequence does not complement perfectly. In this case, the mRNA is post-transcriptionally silenced (Bartel, 2009) (Figure 1.9).

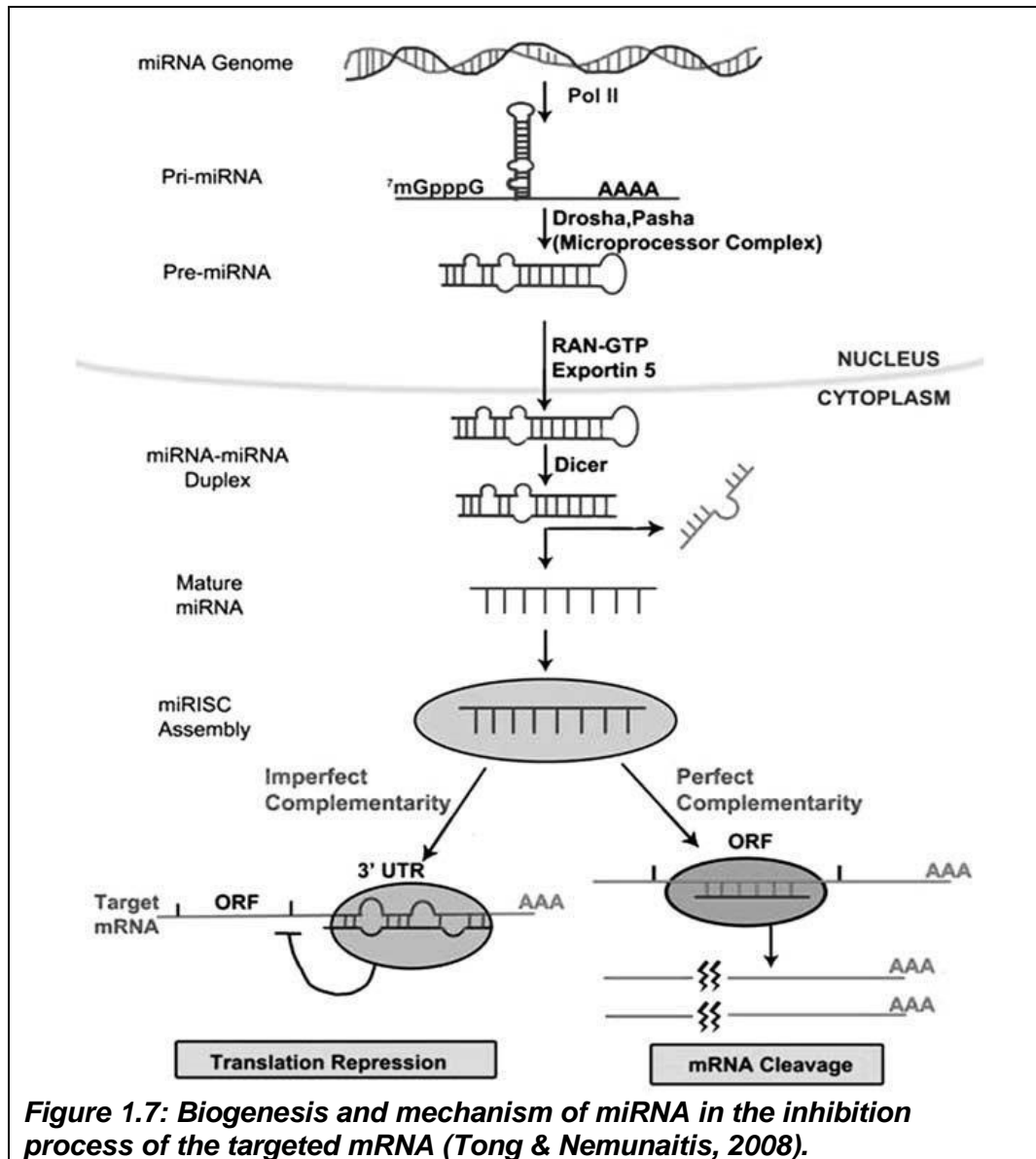
miRNAs can be quantified either by qRT-PCR (Wilson *et al.*, 2010, Pratt *et al.*, 2013) or by using specific primers which can be studied by northern blot gel electrophoresis. Flow cytometry is another specific miRNA detection process that uses the beads-based technique. One of the differences between this technique and other is that it is analysed in a solution, unlike the different techniques examined in glass plates. Digital counting, Micro-Arrays, and sequencing are different techniques that un-specifically detect all miRNAs in any sample, and they are ideal techniques for miRNA profiling. Northern blot is said to be a standard in the detection of miRNA with limitations which make it unfavourable because of its low sensitivity and is time-consuming (Cissell & Deo, 2009). However, qPCR is one of the most convenient techniques in quantifying miRNAs and is less costly compared to the mentioned techniques. The only downside is that the number of targets is limited and could be less specific depending on the primers and the sensitivity.

Many investigators are discovering the significance of miRNAs in most of the diseases influenced by this small single-stranded RNA. However, it is not clear exactly how miRNAs influence and target critical proteins production. Potential targets could be predicted through a database website Called "TargetScan" (<http://targetscan.org>).

According to the latest version of update of the discovered miRNAs database, “miRBase” (<http://mirbase.org>) there are currently 3,5828 mature miRNAs identified (21), an increase of 5,441 mature miRNAs since last release (20). “HMDD” (the Human microRNA Disease Database) is a database website which reports all diseases which are validated to be regulated by miRNAs. Last released update suggests that the number reached 378 diseases linked to 572 miRNAs.

### **1.4.1 Biogenesis of microRNA**

MicroRNAs are a non-coding RNAs that act at the post-transcriptional level to regulate gene expression (Tong & Nemunaitis, 2008). In the mature form, they exist as short (22 nucleotides) single-stranded RNA molecules. These originate from a primary large 70 nucleotides transcript called pri-microRNAs (Figure 1.8) (Broderick & Zamore, 2011). This pri-miRNA contains a multiple stem-loop known as a hairpin structure. RNase II enzyme Drosha initially processes it in the nucleus which changes it into pre-miRNA and then transported to the cytoplasm by an enzyme called exportin where they are converted to the mature form by a second RNase III enzyme called, DICER (Broderick & Zamore, 2011). Once produced, the mature microRNA subsequently incorporates into a ribonucleic particle, forming the RNA-induced silencing complex (RISC). The latter induce gene silencing, targeting mRNA for degradation to prevent protein expression (Tong & Nemunaitis, 2008). In doing so, microRNAs regulate a multitude of physiological processes and have also been implicated in several diseases.



### 1.4.2 The role of microRNA in development

MicroRNAs control and regulate development in almost all mammals, plants, and insects by controlling the genes responsible for producing proteins, including growth factors which help in the development of the organisms. Lin-4, let-7, and mir-10 genes are found in the HOX cluster are examples of miRNAs that control development in the body of *C. elegans* and mammals in general (Bartel, 2004). miRNAs are also found to be involved in the development of cancers in cells highlighting the effect of miRNAs and their link to diseases in humans. The role for some miRNAs has been acknowledged. For instance, miRNAs-1 and -133 are known to regulate the differentiation and the development of cardiac cells and the cardiovascular system (Wilson KD *et al.*, 2010).

### 1.4.3 The role of microRNA in diseases:

There are more than 378 different diseases linked to 572 miRNAs (HMDD) including cancer (metastatic and non-metastatic), cardiovascular diseases, nervous system diseases, diabetes and all its complications including insulin dependent and non-insulin dependent. All these make miRNAs important to understand and to prioritise as they may be potential therapeutic targets in the treatment of most of the diseases (Figure 1.9). In addition, miRNAs could be targeted as markers to identify diseases in any organ or tissue, where the miRNAs may be linked to the disease or found to be upregulated.

Insulin production intra-cellularly is regulated by miRNA by blocking two of the inhibitors of insulin (Tattikota & Poy, 2011). Mir-24, mir-26 and mir-148 are reported to share the same mRNA targets, Bhlhe22 and Sox6, which in their active state inhibits the production of insulin. This inhibition was confirmed after the up-regulation of Bhlhe22 and Sox6 after the enzyme Dicer was knocked out (Tattikota & Poy, 2011). This outcome shows how a deficiency in a miRNA could develop into a life-threatening problem. Another form of miRNA mutation with a consequence is that associated with let-7 miRNA in *C. elegans* which caused a developmental, physical abnormality as shown on the figure below (Reinhart *et al.*, 2000; Rougvie, 2001). Majority of animals with the loss of let-7 by mutation or knockout would result in ruptured vulvas, which, as a result, cause their death.

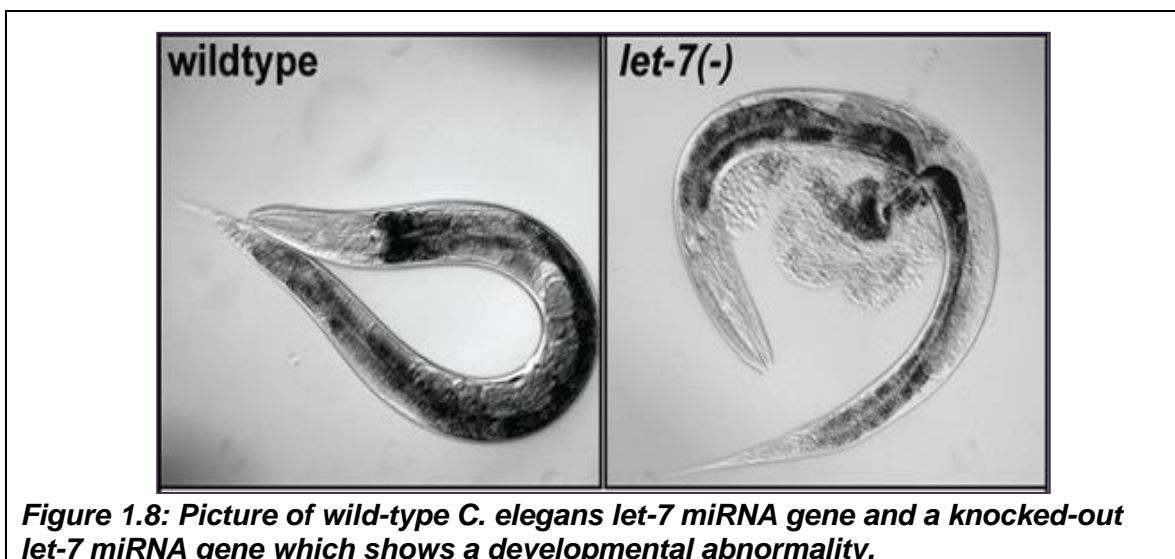


**Figure 1.8: Picture of wild-type *C. elegans* let-7 miRNA gene and a knocked-out let-7 miRNA gene which shows a developmental abnormality.**

Depending on the organism, organ, tissue, and cell, miRNAs could vary in their functions and regulatory roles in all linked diseases. Various miRNAs play a role in heart diseases like miRNA-21, -195, and -208 which cause hypertrophy (Rooij *et al.*, 2007), heart failure, and response to stress, while miRNAs-1 and miRNA-133 are found to regulate some aspects of cardiac diseases as well as monitoring the development and the differentiation of the cardiovascular system (Wilson KD *et al.*, 2010).

### 1.4.4 MicroRNA and Stem cells

Recently miRNAs have been found to be able to re-program differentiated SCs and play a role in differentiating pluripotent cells (reviewed in Trevor *et al.*, 2010) and de-differentiate somatic cells into induced pluripotent cells (Nakagawa *et al.*, 2008). Other research suggests that miRNAs can repress pluripotency of human embryonic SCs (hESCs) (Xu *et al.*, 2009). Overall, researchers agreed that miRNAs are a vital regulator of differentiating cells and development of cells (Figure 1.10). Thus, miRNAs play a role in de-differentiating programmed cells by inducing pluripotency and reprogramming the cells. Some of the functions that are reported and published are illustrated in table 1.2.

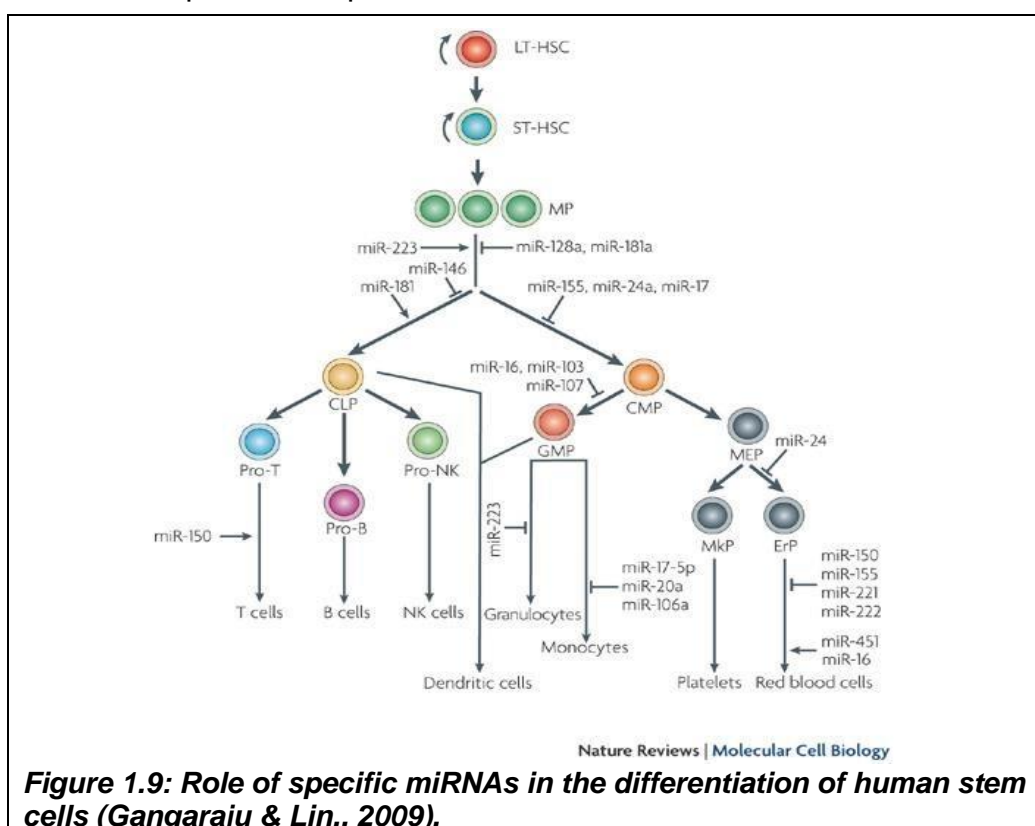


**Table 1.2: Summary of main miRNAs playing a role in the differentiation into cardiomyocytes:**

#	miRNA	Reference	Effect	Main targets
1	1	(Rajala <i>et al.</i> , 2011) (Callis & Wang., 2008) (Rooij <i>et al.</i> , 2007) (Wilson <i>et al.</i> , 2010)	Overexpression increased the proportion of beating aggregates.	Cdk9 (Ghanbarian <i>et al.</i> , 2011)
		(Care` <i>et al.</i> , 2007)	Decreased expression induced hypertrophy, while overexpression inhibited hypertrophy.	RhoA, Cdc42, & Nelf-A/WHSC2
		(Thum <i>et al.</i> , 2007)	Expansion of cardiac and muscle progenitor cells & proliferation of the ventricular myocytes.	Notch ligand delta
2	133	(Rajala <i>et al.</i> , 2011)	Differentiation into cardiac cells	
		(Care` <i>et al.</i> , 2007) (Yang <i>et al.</i> , 2013)	Decreased expression induces hypertrophy, while overexpression inhibits hypertrophy in the heart.	RhoA, Cdc42, & Nelf-A/WHSC2
3	208	(Rooij <i>et al.</i> , 2007) (Rajala <i>et al.</i> , 2011) (Yang <i>et al.</i> , 2013)	Heart-specific and required for cardiac growth under stress. Highly up-regulated in cardiac- differentiated ESCs	
4	499	(Wilson <i>et al.</i> , 2010) (Sluijter <i>et al.</i> , 2010)	Expression would Induce cardiac differentiation	SOX6 & Wnt/ $\beta$
5	145	(Rajala <i>et al.</i> , 2010) (Xu <i>et al.</i> , 2009)	Decreased in ESC, upregulated during EBs and differentiation	Oct4, SOX2, KLF4 and pluripotency
6	23a	(Yang <i>et al.</i> , 2013) (Wang <i>et al.</i> , 2012)	-Involved in the modulation of cardiac function. -Regulate (inhibit) hypertrophy in the heart when activated by LPA3 through LPA ligands.	-LPA1 receptor -Foxo3a
7	206	(Rajala <i>et al.</i> , 2011)	Associated with cardiac remodelling	

### **1.4.5 MicroRNA and differentiation of Stem cells (P19) into cardiomyocytes regulated by LPA**

Unpublished observations from our group (Pramod 2017) have shown that LPA can induce cardiac cells differentiation from P19 SCs. Other researchers confirmed the role of LPA in the differentiation of SCs into cardiac cells (Pébay *et al.*, 2007). The differentiation of p19 cells can be assessed by observing the presence of the protein markers for cardiac lineage and by observing beating cell (Pébay *et al.*, 2007, reviewed in Humphrey, 2009). Wilson and his team (2010) suggested using Flow cytometry for a cardiac marker called  $\alpha$ -sarcomeric to confirm the differentiation of the hESCs and observing a pluripotency marker like OCT4 which is believed to be significantly decreased in the case of the differentiation of the stem cells. miRNAs have been recently linked to the process of differentiation as well as reprogramming of cells (Ivey *et al.*, 2008). Assessing the reciprocal role these post-transcriptional regulators play is critical and vital to grasp the mechanism of this differentiation fully. The main miRNAs to be targeted are mir-1, mir-133 as cardiac markers, and mir-145 as pluripotency marker using qPCR.

## **1.5. Aims and objectives**

This thesis aims to examine and possibly establish the role of miRNAs in the regulation of P19 SCs in the LPA induced stem cell differentiation into cardiomyocytes. Further to this, to investigate the involvement of the various LPA receptors and signalling pathways and study the relationship with these miRNAs.

The achievement of this aim is to be accomplished through confirming the ability of LPA to induce the regulation of stem cell differentiation into cardiac cells regulation of LPA induced effects through specific transcription factors and markers. The first stage of the studies involves looking at the effect of LPA and establishing whether it is concentration and time-dependent (long and short course). After which select LPA receptors and kinase inhibitors will be investigated to determine their role in differentiation. The involvement of miRNAs and the identification of the primary key miRNAs that are critical for differentiation will also be inspected. Furthermore, the inhibition and over-expression of these miRNAs will be evaluated in the presence and absence of LPA.

# **CHAPTER 2**

## **MATERIALS and METHODS**

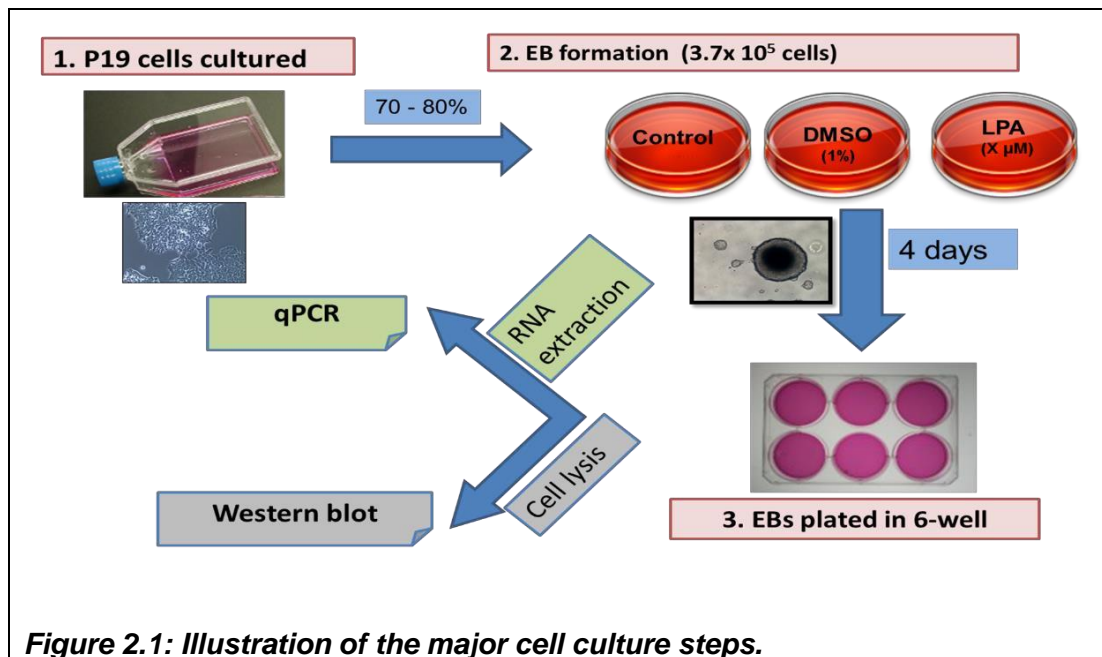
## 2.1. Routine cell culture

The P19 stem cell line derived from a C3H/He strain mouse was ordered from the European Collection of Cell Cultures (ECACC; Salisbury, UK).

The vial was thawed and then cultured in a T25 tissue culture flask containing complete medium (CM) which was  $\alpha$ -minimal essential medium ( $\alpha$ -MEM) consisting of 10% foetal bovine serum (FBS) and 1% of penicillin/streptomycin. When the cultures reached a confluency of around 70-80%, the cells were trypsinised and a density of  $3.7 \times 10^5$  cells/ml was plated into non-tissue culture grade Petri dish for four days. During this period, the cells were treated with or without LPA (5-20 $\mu$ M) in the absence and presence of select drugs. Other experiments require following different steps. Inhibitor experiments require pre-treatment for 30-60 minutes before adding LPA to the cells. Regarding the transfection experiments, cells were transfected prior to forming EBs, and these cells were then formed into EBs for four days and plated to be lysed at specified time points.

All the P19 cells studies were performed in a cell culture lab to avoid contaminations, and all techniques were performed inside the biosafety cabinet following aseptic techniques and strict cell culture regulations. A brief of the routine cell culture process is illustrated in figure 2.1.

Cells were placed into a 25ml flask containing 6ml of CM. The media was changed the next day after washing with 5 ml of 1X phosphate buffer saline (PBS) twice. The media was changed every other day until the cells reached a confluency of 70-80% then they were trypsinised to be passaged and cultured in a new 75 ml flask with 13 ml of CM. Cells are routinely incubated in 5% CO<sup>2</sup> incubator at 37°C and 95% air.



### 2.1.1 Trypsinisation

Confluent cells at T75 flask were trypsinised to be sub-cultured or form embryoid bodies. First, the medium in the flask was removed and cells rinsed with 1X PBS twice each with 10 ml, then 4 ml of 1X trypsin incubated for 2-5 minutes with a gentle tapping on the side of the flask to make sure all cells were detached. The cells were re-suspended with 8-9 ml of CM and transferred into a 15 ml falcon tube to be centrifuged at 13,000 rpm for 5 minutes. After centrifugation, the supernatant was discarded, and the pellet was resuspended with 3-4 ml of CM and mixed thoroughly to be ready for forming embryoid bodies after performing cell and viability count.

### 2.1.2 Cell count

Cell counting was performed using a Countess® (Figure 2.2) from Invitrogen, Life technologies. This machine is an automated cell counter which counts the total number of cells (live and dead cell; Figure 2.3) allowing for the viability to be determined.



**Figure 2.2: Automated cell count trypsinised cultures using Countess® from Invitrogen Inc.**

(A) Countess® machine includes glass slides and trypan blue. (B) The user interface of the Countess® machine shows a sample picture of cells on the slide and a total number of cells, live and dead cell count and the viability percentage.

A 10 µl aliquot from the sample of resuspended cells was transferred into an Eppendorf tube and mixed with 10µl of 0.08% of trypan blue. 10µl from the mix was added to the counting chamber of the slide, cells counted, and the numbers determined as follows (Figure 2.3):

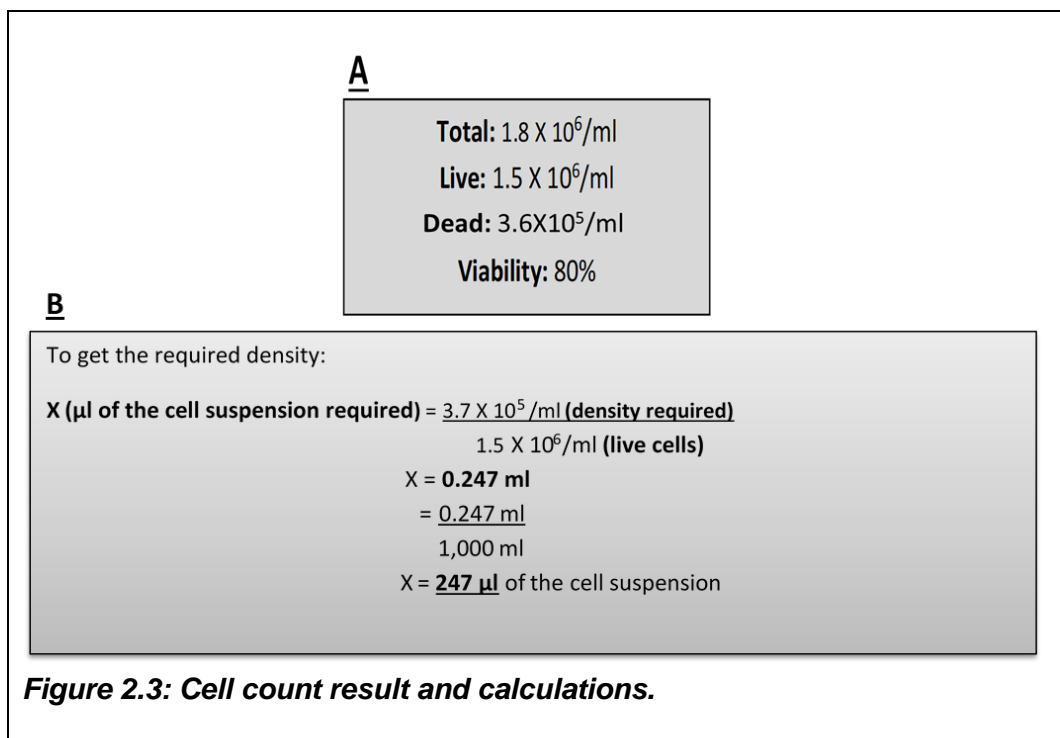


**Figure 2.3: Cell count result and calculations.**

After this step, cells were ready to be transferred into a suspension culture to form embryoid bodies (EBs).

## **2.2. Cryopreservation**

The freezing medium was prepared by mixing 10% of glycerol with 90% of FBS. Following washing and trypsinisation, cells were spun at 1000 RPM at 4°C for 5mins. The supernatant was discarded gently, and the cells re-suspended with 1ml of the freezing medium. This suspension was split into two cryovials (1:2 ratio) and left in a Mr Frosty container in a -80°C freezer overnight before being transferred into liquid nitrogen tank for long term storage, properly labelled with the type of cells, date and passage number.

## **2.3. Embryoid body formation**

Embryoid bodies were formed in a non-adherent petri dish (6ml). The seeding density was  $3.5 \times 10^5$  to avoid the cells being overcrowded and to allow the EBs to have space to grow to the required size.

### **2.3.1 Induction of stem cell differentiation using LPA**

Lyophilised LPA was ordered from Sigma Aldrich and dissolved in 0.1 (w/v) fatty acid-free bovine serum albumin mixed with 1X PBS (pH 7.2) with a final concentration of 5mM stock. 5µM of LPA was used in the studies as this had previously been determined to induce significant differentiation without adverse effects on the cells (Pramod, 2015). 1% DMSO was also used as a positive control. The cells were left to grow over four days once treated with LPA or DMSO (Table 2.1).

**Table 2.1: Set up experiments for the determination of the effects of control, DMSO and LPA.**

		Control	DMSO (1%)	LPA (5 $\mu$ M)
1	Volume of cell suspension (3.5X10 <sup>5</sup> cells/ml)	247 $\mu$ l	247 $\mu$ l	247 $\mu$ l
2	Volume of condition	0	60 $\mu$ l	6 $\mu$ l
3	Volume of media	5,753 $\mu$ l	5,693 $\mu$ l	5,747 $\mu$ l
4	Total volume	6000 $\mu$ l	6000 $\mu$ l	6000 $\mu$ l

### 2.3.2 Embryoid body formation and treatment with different concentrations of LPA

In these experiments, the concentration-dependent effect of LPA (0 $\mu$ M – 20 $\mu$ M) on the differentiation of P19 cells into cardiomyocytes was investigated. An example of the calculation is illustrated in the table below (Table 2.2).

**Table 2.2: Set up experiments for the determination of the concentration-dependent effect of LPA.**

NO.		LPA (0.5 $\mu$ M)	LPA (2 $\mu$ M)	LPA (5 $\mu$ M)	LPA (10 $\mu$ M)	LPA (20 $\mu$ M)
1	Volume of cell suspension (3.5X10 <sup>5</sup> cells/ml)	247 $\mu$ l	247 $\mu$ l	247 $\mu$ l	247 $\mu$ l	247 $\mu$ l
2	Volume of LPA stock (5mM)	0.6 $\mu$ l	2.5 $\mu$ l	6 $\mu$ l	12 $\mu$ l	24 $\mu$ l
3	Volume of media	5,753 $\mu$ l	5,750 $\mu$ l	5,747 $\mu$ l	5,741 $\mu$ l	5,729 $\mu$ l
4	Total volume	6000 $\mu$ l	6000 $\mu$ l	6000 $\mu$ l	6000 $\mu$ l	6000 $\mu$ l

## 2.4. The use of inhibitors and blockers of signalling and receptors

EBs were formed prior to adding LPA following the collection of the pellet and the resuspension with fresh media. The EBs are treated with the selected inhibitor for 1 hour before being treated with LPA (5uM) and then left to incubate for four days without changing the medium. This EBs were collected and plated for a defined time of period (Section 2.6).

The inhibitors used are Suramin (Sigma Aldrich, UK), LY294002 (Tocris, UK), H2L5765834 (Tocris, UK), H2L5186303 (Tocris, UK), TC LPA5 4 (Tocris, UK), and bisindolylmaleimide I (BIM I) (Merck Chemicals Ltd, UK). Most of the inhibitors were diluted or dissolved in DMSO but with no more than 0.08% of DMSO as a final concentration.

## 2.5. Transfection of miRNAs

Once a T75 flask reaches a confluence of around 70-80% it was trypsinised and plated in a 6-well plate for transfection.  $0.25 \times 10^6$  cells/ml were seeded in each well and left for 24 hours in a CO<sub>2</sub> incubator. Wells were labelled as 1- control, 2- negative (Lipofectamine® RNAiMAX only), 3- (target A) inhibitor, 4- (target A) mimic, 5- (target B) inhibitor and 6- (target B) mimic (Figure 2.4). After 24 hours, cells were then treated with each condition mixed with FBS and free of P/S antibiotics medium following the protocol supplied by the company (Table 2.3). Plates are then incubated for another 24-48 hours and cells allowed to form EBs in the absence and presence of LPA for four days before being transferred into tissue culture grade 6-well plates. Protein lysates and RNA were extracted on day 6.

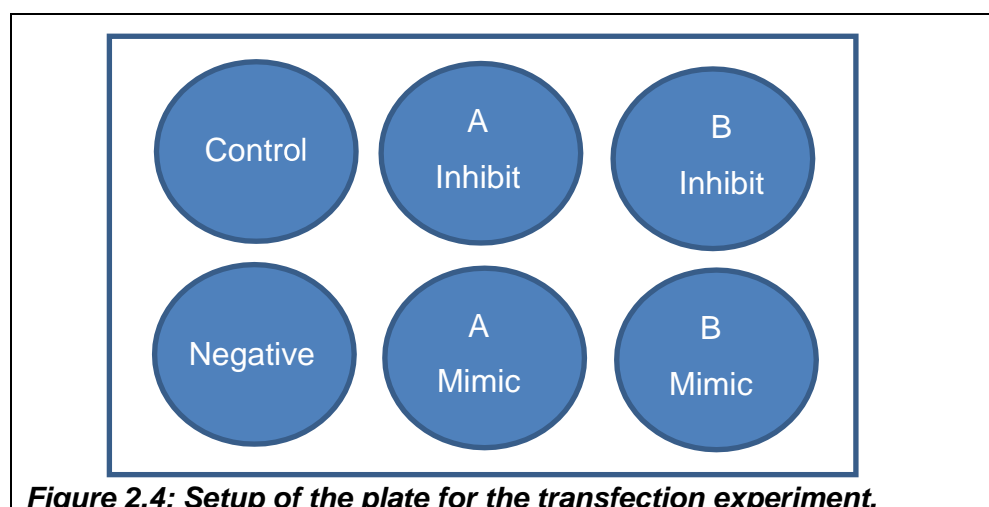


**Figure 2.4: Setup of the plate for the transfection experiment.**

**Table 2.3: Set up of steps and reagents for transfection experiments.**

Steps		6-well
1	Seeded cells	0.25X10 <sup>6</sup> cells/ml
2	Incubation	24 hours
3	Dilute Lipofectamine RNA + $\alpha$ Medium	150 $\mu$ L + 9 $\mu$ L
4	Dilute siRNA + $\alpha$ Medium	150 $\mu$ L + 3 $\mu$ L (30pmol)
5	Mix diluted siRNA + diluted Lipofectamine RNAiMAX (1:1)	150 $\mu$ L + 150 $\mu$ L
6	Incubation	5 minutes
7	Add siRNA-lipofect.mix to cells	250 $\mu$ L (25pmol)
8	Incubation	24-48 hours

The siRNAs for the inhibitor and mimic of mir-1 and mir-145 were used to study any possible effect on several proteins and mRNA targets using the suggested protocol by the supplier.

## 2.6. Plating embryoid bodies for differentiation

On the fourth day after forming the 3D aggregates of EBs, the EBs were transferred into a tissue culture grade plate. Plating started by transferring all the contents of the dish into a new falcon tube and left inside the safety cabinet until a clear aggregate of pellets collected at the bottom of the tube. The supernatant was discarded gently, and then resuspended with fresh CM and mixed before starting the process of plating. Based on the experimental design, EBs are then plated in 6 or 12 well plate or even in a single tissue culture plate according to the time point required. The plates were then incubated in a CO<sup>2</sup> incubator at 37°C for 3-12 days, and the media was changed every second day. Day 0 was the only exception which was not plated because cells were lysed on the same day, and the samples kept for analysis.

## **2.6.1 Short time course experiment**

For Short time course experiments, cells were treated with LPA after the cells reach 60% confluency in a T25 flask on a monolayer. The time range from 5, 15, 30 minutes, and then 1, 3, 6, 9, and 24 hours. Complete medium was mixed with 5 $\mu$ M or 20 $\mu$ M LPA and incubated with the cells for the time specified. Cells were then washed with PBS twice, trypsinised and set up to form EBs for four days. The EBs were subsequently plated in tissue culture grade plates and allowed to grow into monolayers, lysing cells at day 6 and day 12.

## **2.7. Cell lysis and protein quantification**

The media in each plate was discarded, the wells washed with 1ml of 1X PBS twice. Following this, the cells were lysed with 1X of ice-cold lysis buffer (2mM of Tris-HCl (pH 7.4), 1% Sodium dodecyl sulphate (SDS). The cells were scraped using the back of a yellow pipette tip and collected in an Eppendorf tube which was heated (95°C) for 5 minutes and sonicated in an ultrasound water bath three times for 30 seconds each and then was centrifuged for 25 minutes. The upper phase was separated from the lower and used for the protein assay and western blotting.

### **2.7.1 Protein quantification assay (BCA)**

The bicinchoninic acid assay (BCA assay) was used to determine the quantity of cell protein concentration. Standards were prepared by mixing 50 mg of bovine serum albumin (BSA) dissolved in 5ml of double distilled water (DDW), and a set of concentrations from 0-3 $\mu$ g/ $\mu$ l were prepared as follows (table 2.4):

**Table 2.4: Protein standard preparation**

No.	Protein/well ( $\mu\text{g}$ )	BSA ( $\mu\text{l}$ )	DDW ( $\mu\text{l}$ )	Protein concentration ( $\mu\text{g}/\mu\text{l}$ )
1	0	0	1000	0
2	1	20	980	0.2
3	2	40	960	0.4
4	3	60	940	0.6
5	5	100	900	1
6	10	200	800	2
7	20	300	700	3

Subsequently, 5 $\mu\text{l}$  of the standard concentrations were pipetted into 96-well plate, 5 $\mu\text{l}$  of 1X lysis buffer was added to each standard. Sample wells were prepared by adding 5 $\mu\text{l}$  of lysed sample proteins together with 5 $\mu\text{l}$  of DDW. Finally, 100 $\mu\text{l}$  of BCA reagent (Reagent A + reagent B, 1:50) was added to all wells. Each standard and sample were done in a triplet. The plate was left to incubate on a plate shaker for 45 minutes at room temperature before analysing the absorbance at 620nm wavelength. The quantity of protein in each well was determined from the standard curve (Figure 2.5).

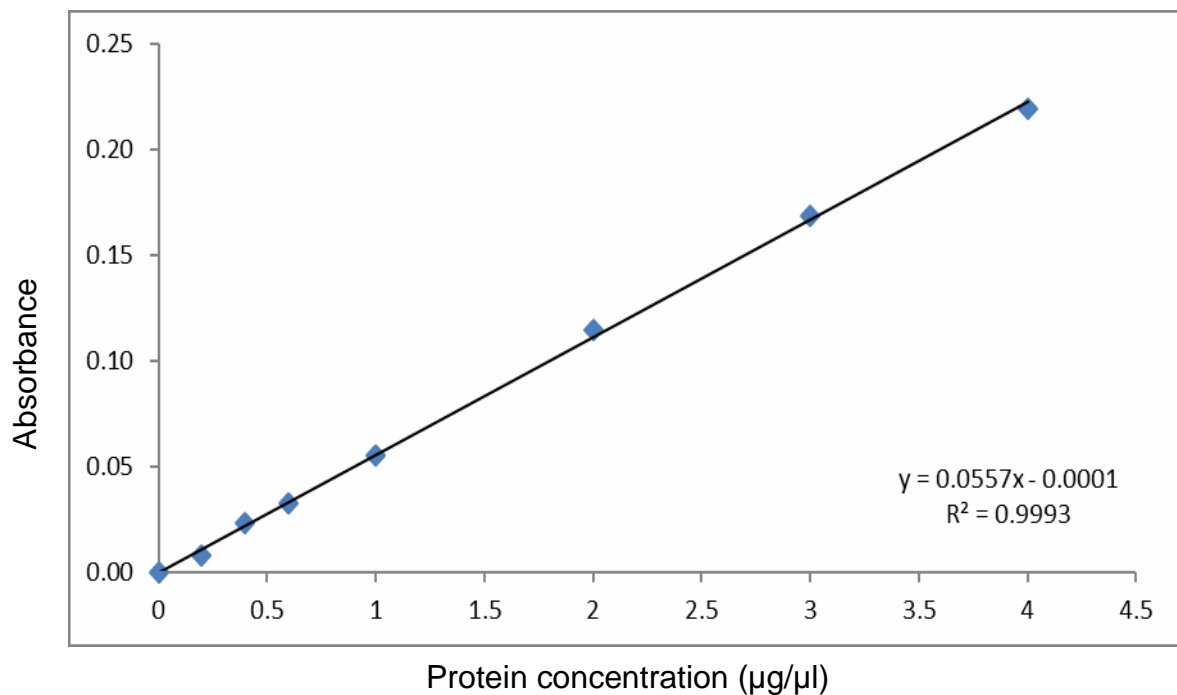


**Figure 2.5: BCA protein standard curve.**

## 2.8. Cytotoxicity and cell viability assay

The MTT (3-(4, 5-dimethyl-2-thiazolyl)-2, 5-diphenyl-2H-tetrazolium bromide) assay was used to determine the cytotoxicity that could be detected following treatment under different conditions. MTT (Sigma) is a yellow tetrazole which is enzymatically transformed into a crystallised purple formazan by metabolically active live cells.

Cells were initially seeded in a 96-well plate and treated with drugs or conditions (in replicates) mixed with complete medium for 24 hours. Afterward, 200µl of a 5mg/ml stock of the MTT solution was added to each well for 4 hours with a final concentration of 0.5mg/ml per well. The medium was then discarded, formazan crystals were dissolved in 200µl of isopropanol. Absorbance was finally taken at 540nm on a Multiskan® plate reader (Ascent). Changes in cell viability were calculated relative to the 100% of controls.

## 2.9. Western Blotting

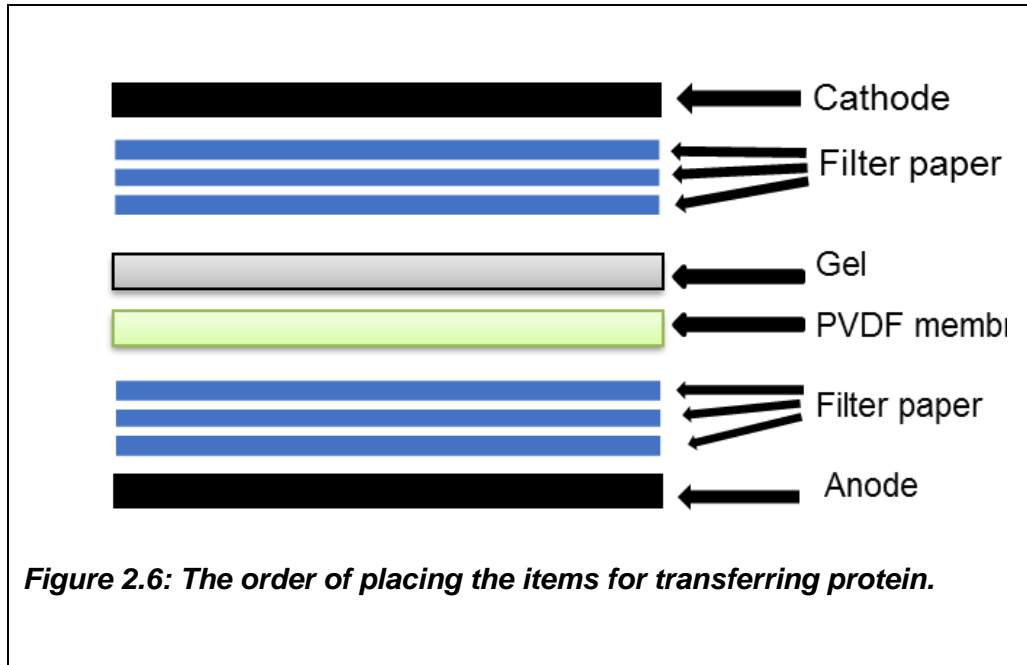
Western blot was carried out using a polyacrylamide gel or SDS-PAGE on a Mini-PROTEAN® Tetra Cell from BIO-RAD.

First, the casting frame and the glass plate sandwich were set on the casting stand and filled with DDW to check for any leakage. While observing the sandwich glass for any possible leakage resolving and stacking gels for two gels were prepared. 10ml of resolving gel (12%) was prepared by mixing 3.31ml of DW and 3.99ml of 30% acrylamide/bisacrylamide mixture beside 2.5ml of cold 1.5M of Tris-HCl (pH8.8) and 100µl of 10% SDS. 100µl of 10% ammonium persulphate (APS) and 60 µl of tetra-methyl-ethylene-diamine (TEMED) were added right before filling the glass plate sandwich with the resolving gel. Bubbles were removed using isobutanol layered on the top of the resolving gel.

Next, 4ml of stacking buffer gel was prepared by adding 2.44ml of DW, 0.52ml (520µl) of 30% acrylamide/bisacrylamide mixture along with 1ml of cold 0.5M Tris-HCl (pH6.8) and 40µl of 10% SDS. Again, 20 µl of APS and 4 µl TEMED were added right before pouring the mixture on top of the resolving gel followed by placing the comp (for wells formation) in the stacking gel. The glass plate sandwich was separated from the casting frame and attached to the clamping frame (electrode assembly) face to face and placed in the electrophoresis tank which was filled with 1X tank buffer prepared by mixing 1X 0.025 M of Tris base, 0.192 M glycine and 0.1% of SDS. Lysates were prepared by mixing a sample buffer (bromophenol blue) at a ratio of 1:5 for 5X loading buffer or 1:1 for the 2X loading buffer. These samples were prepared to be loaded on the gel by heating for 5 minutes alongside the biotinylated protein molecular ladder. The loaded concentration of each sample was calculated to give 20µg/µl per well. The gel was run at 220V at 40mA (20mA/gel) and increased up to 50mA (25mA/gel) after the samples passed the stacking region of the gel.

### 2.9.1 Protein transfer from the gel to polyvinylidene difluoride membrane (PVDF):

PVDF membrane and six filter papers were cut into the gel size. Three filter papers were placed below the gel and the other three on top of the gel once placed on the membrane. The membrane was soaked for 5 minutes in methanol then washed with distilled water (DW) before placing it in the sandwich (Figure 2.6).



1X Transfer buffer (48mM Tris base pH7.5 + 39mM glycine + 0.0375% SDS and a 20% methanol) was poured to the sandwich on the semi-dry transfer cell that enclosed the gel and bubbles removed. The transfer was carried out at 50mA (25 mA/gel) for 15-20 minutes.

### 2.9.2 Membrane blocking:

After the transfer, the membrane was transferred into a plastic plate contained a blocking buffer which was a mixture of 200µl of tween20, 10g of fat-free milk and 90ml of DDW and membranes were blocked for at least 1 hour or more.

### 2.9.3 Incubations with primary and secondary antibodies:

5ml of the blocking buffer was used for the primary antibody, myosin light chain-1v (MLC-1v; diluted 1:100) or the other antibodies diluted according to supplier's instructions. Each membrane was placed in a plastic hybridisation bag together with the relevant antibody, ensuring air bubbles were eliminated. The bag was sealed and stuck tightly on a shaker at

4°C (cold room) overnight. The next day the membrane was removed from the hybridisation bag and washed with 1X washing buffer for 30 minutes on an orbital shaker, changing the wash buffer every 10 minutes. The process was repeated with the secondary antibody ( $\beta$ -actin; diluted 1:5000) and with the anti-biotin antibody (diluted 1:1000) which were incubated with the membrane on a shaker for 1 hour at room temperature. After 1 hour the membrane was again transferred for washing using 1X washing buffer but this time washed 5 times, each for 10 minutes.

#### **2.9.4 Stripping and re-probing membranes:**

Western blot stripping buffer (Restore™) supplied by Thermo Scientific was used to strip membranes to allow re-probing a different target with a different antibody following the manufacturer's protocol. First, the chemiluminescent substrate was discarded, and the membrane washed with PBS until the substrate was washed away. Following the previous step, the membrane was soaked in the Restore™ stripping buffer for 5 to 15 mins at room temperature then washed with TBST and blocked for 1 hour. The protocol for primary and secondary antibodies was next followed (as previously illustrated). The membrane is finally exposed for analysis and either stored for future re-probing or discarded.

#### **2.9.5 Protein bands visualisation:**

ECL western blotting substrate solution from Thermo Fisher was used and was prepared as described in the manufacturer's protocol by mixing the two solutions before pouring on the membrane and incubated for 5 minutes. The membranes were imaged on my ECL Imager, which determines the most suitable exposure time and saves it to be analysed. Membranes post this step were kept for possible future re-probing for other targets.

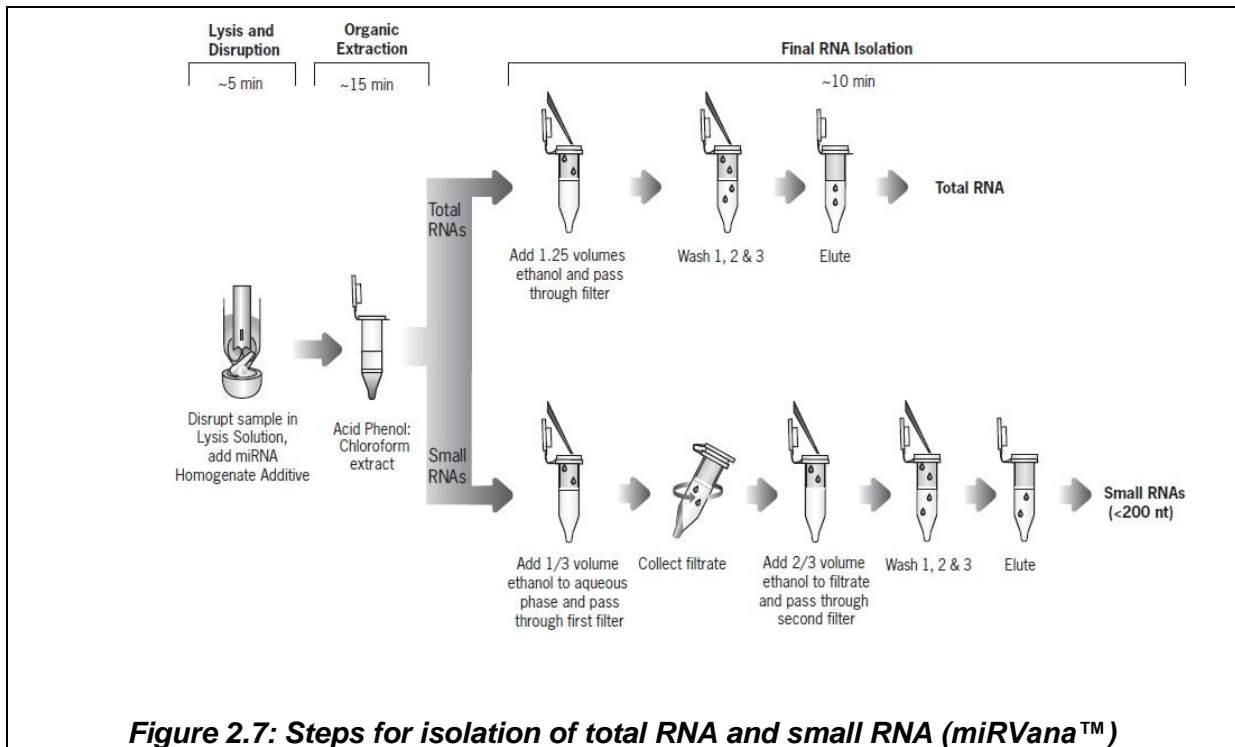
## **2.10. Total RNA extraction and qRT-PCR:**

Cells were analysed either on day 6 or 12 after the EBs were plated in a six-well plate. Media was removed, and the plate was placed on an ice bucket to preserve cells from the degradation of the proteins. Washed with 1X PBS twice and then 300-600µl (according to the rate of the growth) of lysis/binding solution from the miRNA isolation kit from Ambion (miRVana™; Invitrogen™) was added. The lysates were then collected and mixed by pipetting and transferred into an Eppendorf tube and vortexed vigorously to completely lyse all the cells (Figure 2.8).

The next step was adding a volume of 1/10 of the miRNA homogenate additive solution (included in the kit) to the lysate. The mixture was incubated for 10 minutes at 4°C in an ice bucket. Acid-phenol: chloroform equal to the volume of the lysate solution was then added. Acid-phenol: chloroform was not supplied with the kit, so was prepared using a dilution of 125µl:25µl. The mixture was vortexed for 30-60 seconds and centrifuged at the highest speed. The aqueous layer (top phase) was carefully collected, and the volume was noted for the following steps. This kit gives the option of isolating a total RNA and small RNA (Fig. 2.7).

### **2.10.1 Total RNA isolation using the miRVana™ kit**

For the isolation of total RNA, a 1:25 volume of absolute ethanol was added to the recovered aqueous phase, and the mixture was passed through a capillary tube provided in the kit with a filter and centrifuged at 10,000 rpm for 15 seconds. The liquid which passed through the filter was then discarded, washed with washing solution 1 (700µl) and centrifuged as in the previous step. The washing solution 2/3 was used twice (500µl) and centrifuged each time, and the liquid was removed. The empty tube with the filter was then centrifuged for 1 minute just to remove traces of fluid. The last step was applying a pre-heated (95°C) 100 µl of elute solution (Supplied in the kit) to a fresh collecting tube and spun for 20-30 seconds. All the steps were following the suggestion of the supplier illustrated in figure 2.8 suggested by the supplier.



## 2.10.2 Determination of RNA quality and quantity

After extracting RNA from each sample, concentrations were determined by absorbance at 260nm, and the purity was established by the absorbance ratio of 260/280 and 260/230 nm. NanoDrop™ ND-1000 UV-Vis Spectrophotometer was used to analyse samples.

## 2.10.3 Agarose gel electrophoresis

Two types of gel analysis were performed due to the two different kind of RNA. Total RNA was examined on a 1% denaturing agarose gel, while the product of the qPCR (Amplicon) on 1.5% denaturing agarose gel. 1µg per sample per lane was used. Agarose was mixed with 1x Tris- Boric acid-EDTA (TBE buffer or TE) to prepare the gels (Table 2.5).

**Table 2.5: Preparation recipe of 10X TBE buffer.**

Concentration	Component	For 1L (dissolved and adjusted to 1L)
0.9M	Tris base	109g
0.9M	Boric acid	55g
20mM	0.5M EDTA	40ml

The mixture of agarose and TBE was heated in a microwave for 1-2 minutes until the agarose powder was dissolved. Gel Red stain was added to the beaker, left to cool down and then poured into the gel casting tray with the comb placed prior to pouring the agarose. The agarose gel was finally analysed using the MyECL™ imager machine.

A miScript Reverse Transcriptase kit (Qiagen) was used to convert the total RNA to cDNA. Total volume per reaction was 20µl, and 2µg of total RNA per reaction was used and was calculated using the data from the spectrophotometer (table 2.6.). Samples were kept at -80°C to avoid any degradations.

**Table 2.6: Reverse transcription of samples from total RNA to cDNA using the miScript PCR system.**

Component	RT sample
miScript Reverse Transcriptase Mix	2µl
10x miScript Nucleics Mix	2µl
RNA sample (Template)	Up to 9µl
5x miScript HiFlex Buffer*	4µl
Nuclease-free water	To make up to 20µl
<b>Total per reaction</b>	<b>20µl</b>

## 2.10.4 Primers design and dilution

Custom primer assays for SYBR green were supplied by Qiagen. miScript Primer Assay for miRNAs and QuantiTect Primer Assay for the other genes were used. Primers used are illustrated in table 2.7. All miRNAs primers share a single universal reverse primer and were supplied as a lyophilised forward primer. Other mRNA targets are provided with a mix of lyophilised forward and reverse primers. 550µl for the miscript and 1.1ml of the QuantiTect primers were reconstituted according to the manufacturer’s protocol delivered with the assays. All miScript assays derived from mature sequences in the miRBase database (<http://microrna.sanger.ac.uk>). QuantiTect assays were also derived from gene sequences in the NCBI database (Table 2.7 & 2.8). ([www.ncbi.nlm.nih.gov/RefSeq](http://www.ncbi.nlm.nih.gov/RefSeq)). Both groups were validated and showed to be highly efficient and sensitive by Qiagen ([www.qiagen.com](http://www.qiagen.com)).

<b>Table 2.7: miRNA primer sequence details</b>		
<b>miRNA</b>	<b>Primer ID</b>	<b>miRNA sequence (5'-3')</b>
<b>miR-145</b>	mmu-miR-145a-5p	5'GUCCAGUUUUC CAGGAAUCCCU
<b>miR-1</b>	mmu-miR-1a-3p	5'UGGAAUGUAAAGAAGUAUGUAU
<b>miR133</b>	mmu-miR133a-3p	5'UUUGGUCCCCUUCAACCAGCUG
<b>U6</b>	Hs_RNU6	Forward: CGC TTC GGC AGC ACA TAT AC Reverse: AAA ATA TGG AAC GCT TCA CGA
<b>Universal Reverse Primer</b>		ATCC AGT GCA GGG TCC GAG G

**Table 2.8: Primer binding details**

miRNA	Primer ID	Detected transcript
OCT4	Pou5f1	NM_013633
Gata4	GATA binding protein 4	NM_008092
NKx2.5	NK2 homeobox 5	NM_008700

U6, a commonly used control house-keeping gene, was ordered with the primers and was included in the miScript PCR starter kit.

## 2.10.5 Samples set up for qPCR

The SYBR green dye was used to amplify and quantify the targets. The kit used was the miScript PCR starter kit. A reaction mix was first prepared according to the numbers of samples and repeats (as shown in table 2.9 and 2.10). The total reaction mix was 20-25µL perwell.

**Table 2.9: Setup of qPCR reactions (mRNA)**

Component	Volume/reaction (20µL)	Volume/reaction (25µL)
QuantiTect SYBR green PCR master mix	10µL	12.5µl
QuantiTect Primer Assay	2µL	2.5µl
RNase-free water	Makeup to 20 µL	Makeup to 25µL
Template cDNA	≤2µl	≤2.5µl
Total volume	20µL	25µL

<b>Component</b>	<b>Volume/reaction (20µL)</b>	<b>Volume/reaction (25µL)</b>
<b>QuantiTect SYBR green PCR master mix</b>	10µL	12.5µl
<b>miScript Primer (Universal Reverse Primer)</b>	2µL	2.5 µl
<b>miScript Primer Assay</b>	2µL	2.5µl
<b>RNase-free water</b>	Makeup to 20µL	Makeup to 25µL
<b>Template cDNA</b>	≤2µl	≤2.5µl
<b>Total volume</b>	20µL	25µL

Once all master mixes were prepared, plates were sealed with an adhesive seal and centrifuged briefly for 1 minute. The machine used was the QuantStudio™ 7 Flex Real-Time PCR System (96-well). And the cycling conditions are set as per the supplier's instructions for 40 cycles (Table 2.11). Normalisation for some house-keeping genes and the primers took place first, and a standard curve was acquired to compare stability and efficiency of each primer. Samples were set up in duplicates with negative control (No template) and positive control genes (U6).

<b>Step</b>	<b>Time</b>	<b>Temperature</b>	<b>Comment</b>
<b>Activation step</b>	15 min	95°C	HotStarTaq DNA Polymerase gets activated in this step.
<b>3-step cycling:</b>			
<b>1- Denaturation</b>	15 sec	94°C	
<b>2- Annealing</b>	30 sec	55°C	
<b>3- Extension</b>	30 sec	70°C	Perform fluorescence data collection
<b>Cycle number</b>	40 Cycles		

Normalisation for some house-keeping genes and the primers took place first, and a standard curve was acquired to compare stability and efficiency of each primer. Samples were set up in duplicates with negative control (No template) and positive control genes (U6).

### **2.10.6 Analysis of relative gene expression:**

Experiments were performed following the Comparative  $C_T$  ( $\Delta\Delta C_T$ ) method. In this method, the  $C_T$  for control and the other conditions were noted for targeted genes and the housekeeping gene. The fold difference was then calculated based on the data produced.

## **2.11. Confocal microscopy and Immunofluorescence**

Adherent cultures of P19 cells were grown to reach up to 50-60% of confluence under the regular conditions mentioned earlier. Cells are then fixed and stained by removing the media from the plate and washed with PBS twice. The following step was to fix the cells with Ice-cold methanol for 20 minutes prior to rinsing the plates briefly with PBS after the excess fixative is discarded. The cells were then incubated in a blocking buffer containing 5% of BSA dissolved in PBS for 30 minutes to block any non-specific bindings. Next, the primary antibodies OCT4 (Abcam®; ab19857) and Troponin I (Abcam®; ab47003) were then diluted in the used blocking buffer at 1µg/ml for an hour. The cells are then rinsed with PBS for 3 times considering a 5 minutes gap in between. The incubation with a secondary antibody using a mixture of a green goat anti-rabbit IgG called Alexa fluor® 488 (2µg/ml), and a drop of a blue DAPI as a nuclear stain was used for an hour in 5% BSA. The plate from this step was covered with aluminium foil to protect it from light. Finally, the cells are again rinsed briefly three times with five minutes of the gap before the visualisation with Nikon Confocal Microscope (TE-2000U) at a magnification of 100x immersion oil.

## **2.12. Statistical data analysis**

Statistics and calculation were performed with GraphPad Prism software. All the results are the mean SEM of at least 3 separate experiments. Statistical difference was calculated by ANOVA (one and two way) and T-test with post hoc studies based on the need of each independent experiments. The software used for all statistical analysis studies was GraphPad Prism version 5.

# **CHAPTER 3**

## **RESULTS**

### 3.1. Regulation of P19 stem cells (SCs) differentiation

P19 cells were seeded and maintained undifferentiated. Furthermore, its fate was driven with different concentrations and different inducers following the routine cell culture techniques.

#### 3.1.1 Maintenance of monolayers of semi-confluent P19 cells

Figure 3.1 shows a primary culture of P19 cells growing normally with no unexpected differentiation or changes in confluence. The cells from day 4 were ready to be resuspended to form embryoid bodies (EBs) for further experimentation and analysis. Inverted microscopes were routinely used to examine any morphological or growth pattern changes.

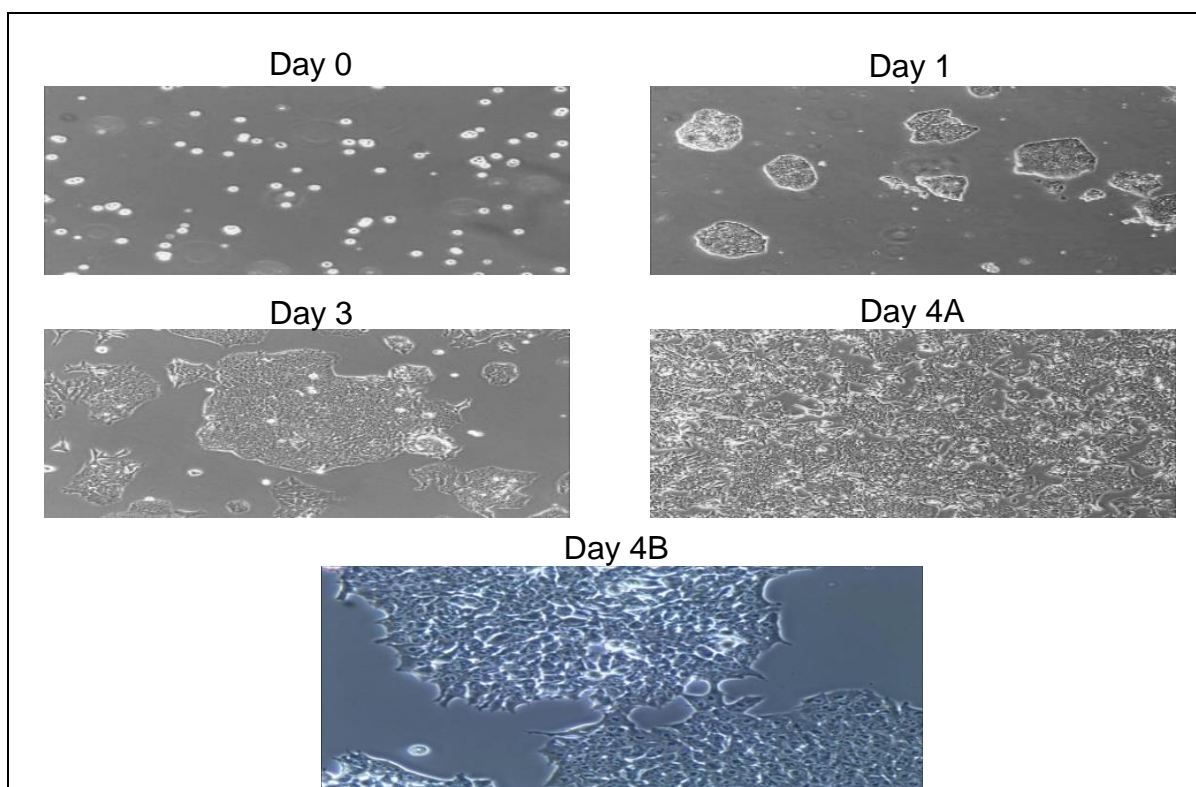
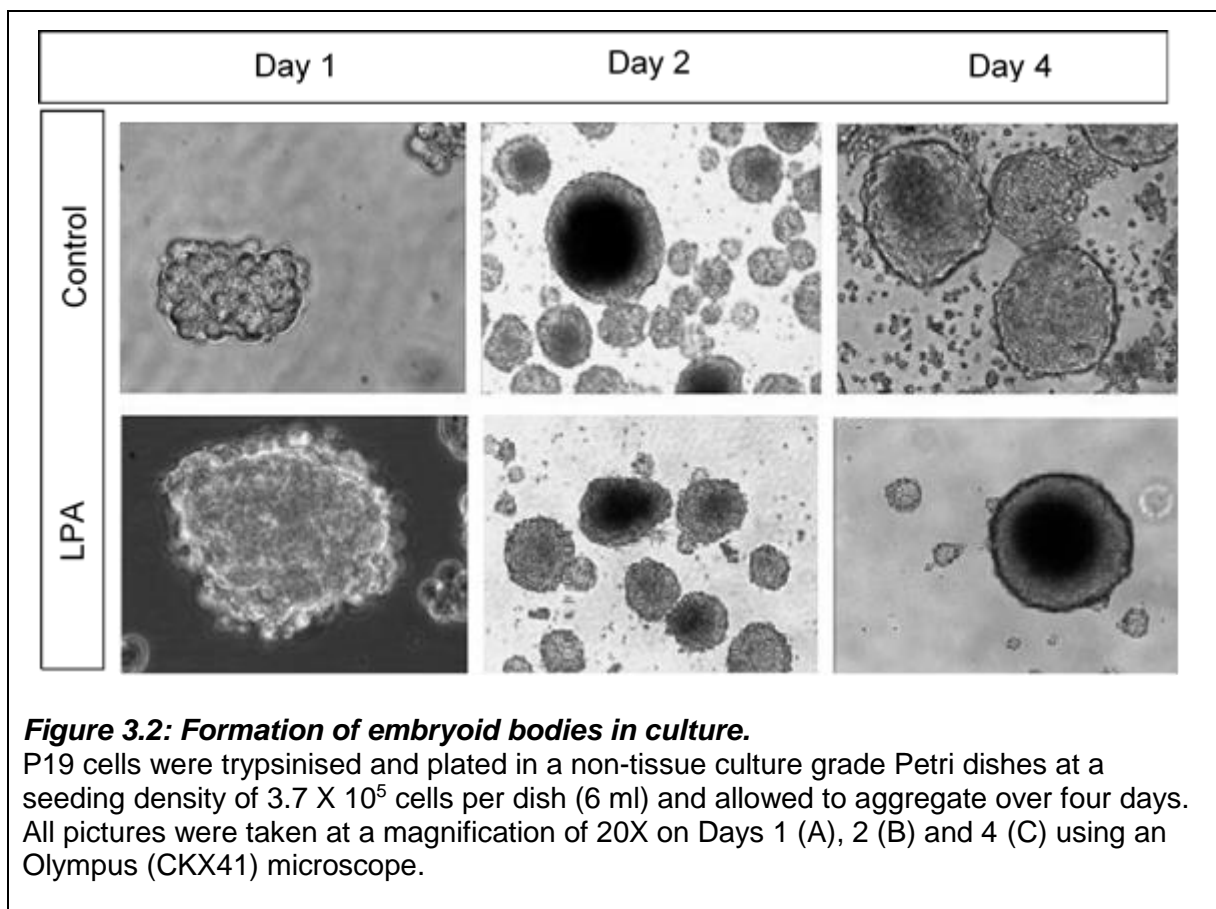


**Figure 3.1: Routine growth pattern of P19 stem cell line in culture.**

Cells maintained under routine culture as monolayers in a T75 flask with complete media. The figures are representative of the growth on days 0, 1, 3 and 4 (A and B at 10X and 20x Magnification, respectively). Photographs were taken at 10X and 20X magnification under an inverted Microscope (Olympus microscope CKX41).

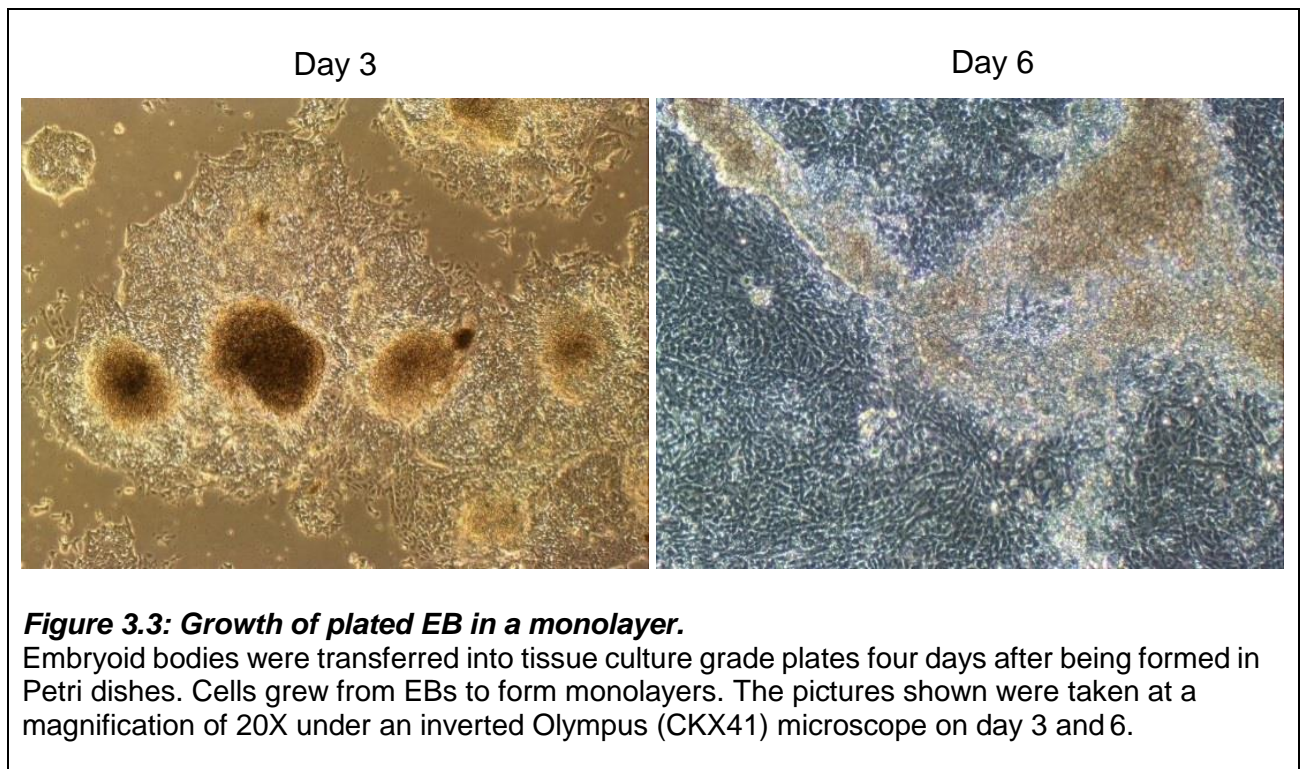
### 3.1.2 Formation of embryoid bodies

P19 cells formed an aggregation of a three-dimensional structure of cells or EBs. The EBs were non-adherent, appeared spherical, and ultimately big, depending on the cells mass. The formation of EBs was not altered in the presence of Lysophosphatidic acid (LPA). Plated cells still aggregated, forming spherical 3D EBs, which was similar both in size and structure to the controls (Figure 3.2).



### 3.1.3 Growth of plated embryoid bodies into monolayers

Embryoid bodies were plated in a 6-well tissue culture grade plates on the fourth day. As shown in Figure 3.3, EBs attached as soon as they were plated, and cells grew into monolayers from the mass of EBs. This growth pattern was also consistent and established when treated with LPA.



### 3.1.4 Confocal microscopy

Isolated P19 cells were cultured and immune-stained with protein markers like octamer-binding transcription factor 4 (POU5F1 (OCT4)) as a pluripotency marker to assess differentiation. The second antibody that was used is Troponin I, which is a cardiac lineage marker. Cells were either Control (untreated or undifferentiated) or LPA and DMSO pre-treated (Figure 3.4). This experiment aimed to give an insight into the possible behaviours of the cells in response to the treatment with any of the mentioned inducers compared to control.

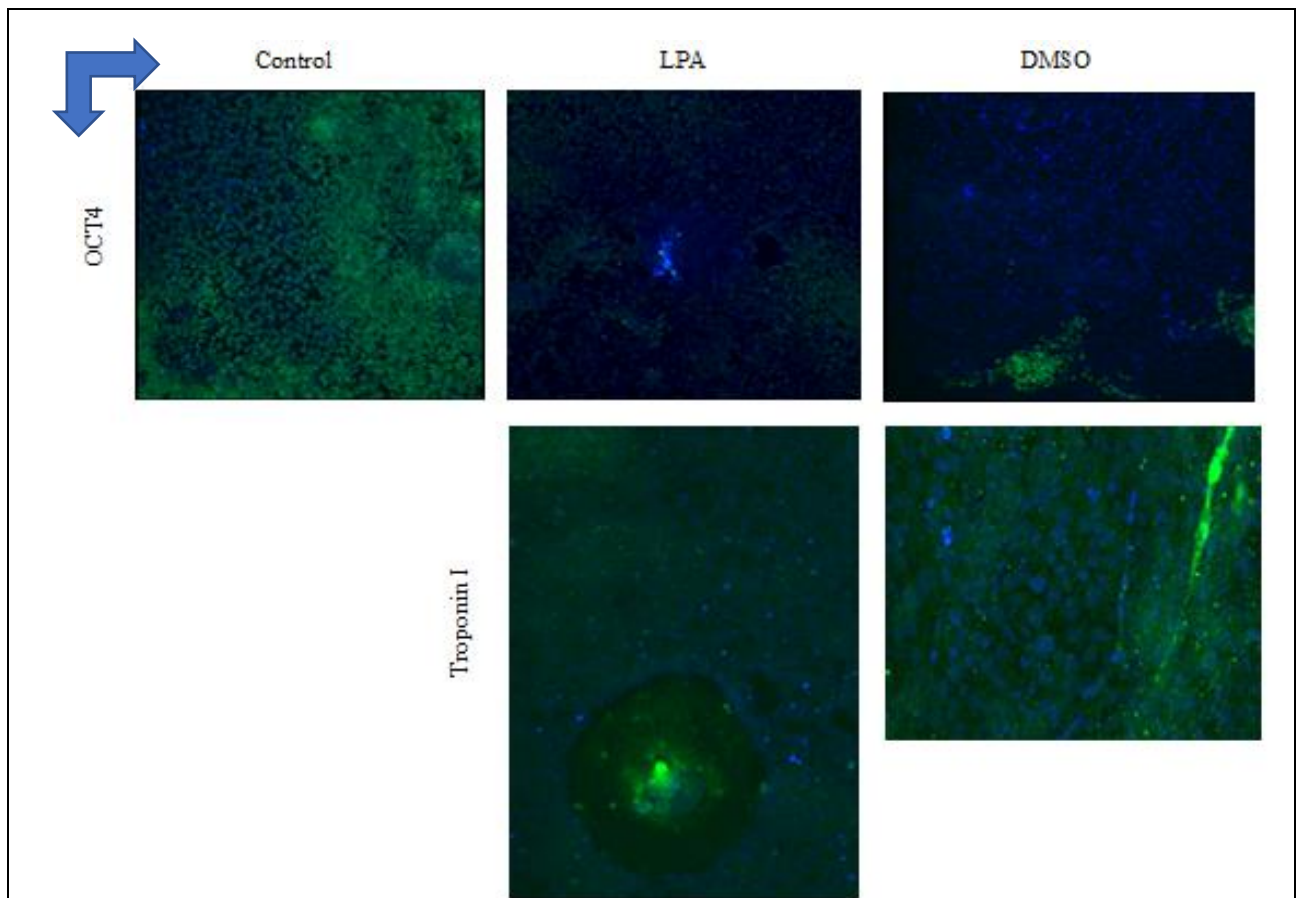


**Figure 3.4: Stained P19 cells treated with LPA and DMSO monolayers compared to control.**

P19 cells were plated in 6-well plates and allowed to grow for two days, then incubated with a primary antibody (OCT4 and Troponin I antibodies (Green)) for one hour. This was followed by incubation with the goat anti-rabbit IgG secondary antibody (Alexa Fluor 488) for an hour beside a DAPI dye (Blue) to stain the nucleus. Nikon Confocal Microscope (TE-2000U) was used at a magnification of 100x immersion oil. The photograph is representative and suggest an effect of treatment with different conditions on the expression of OCT4 and Troponin I, compared to control (untreated).

OCT4 is more intensely stained in control cells. This also contrasts with LPA and DMSO treated cells, which shows a decreased stain and expression of OCT4. On the other hand, the green stain of troponin I show a high intensity and expression in LPA and DMSO incubated cells (Figure 3.4). Although the control is missed for cells stained by troponin I, however, it still gives a hint on the high expression of the Troponin I in comparison to the expression of OCT4 in both cells.

### **3.2 Cell viability in the presence of various pharmacological inhibitors (MTT assay)**

To confirm whether responses to various drugs were specific and indeed related to their pharmacological actions, the MTT cytotoxicity assay was carried out to establish cell viability under the different experimental conditions. Effect of DMSO, BIM-1, LY294002, Suramin, H2L5765834, H2L5186303, and TC-LPA5-4 was assessed. Bisindolylmaleimide 1 (BIM-1) a chemical compound with a selective and potent with inhibitory roles for PKC isoforms, PKA, PKG and myosin-light-chain-kinase (MLCK) with an  $IC_{50}$  of 10nM. LY294002 also, which is a PI3-kinase inhibitor (PI3-K $\beta$ , PI3-K $\alpha$ , PI3-K $\sigma$ , and PI3-K $\gamma$ ) have an  $IC_{50}$  for PI3-K $\beta$ , PI3-K $\alpha$ , PI3-K $\sigma$  and PI3-K $\gamma$  respectively at 0.31, 0.73, 1.06 and 6.60 $\mu$ M. Suramin on the other side blocks binding sites of GPCRs specifically LPA receptor 4 and calmodulin including acting as an antagonist for the P2 purinergic with an  $IC_{50}$  of 43 $\mu$ M. H2L5765834 binds to LPA receptor 1, 5, and 3 with  $IC_{50}$  of 94, 463, and 752nM. With H2L5186303, LPA receptor 2, 3, and 1 are targeted with  $IC_{50}$  of 8.9, 1230, and 27354nM. TC-LPA5-4 is a selective antagonist of LPA receptor 5 with an  $IC_{50}$  of 0.8 $\mu$ M

The toxicity of LPA was tested by incubating cells 24 hours with 1- 80 $\mu$ M of LPA and conducting the MTT assay at the end of the relevant incubation period. The results show a significant change in cell viability as measured by MTT. Turkey test showed that only cells treated with 40 $\mu$ M are significantly less viable than the control (Figure 3.5).

With DMSO, used as a positive control for induction, the cytotoxic effect was statistically significant and started to show at 5% and was significant at 10 and 20% (Figure 3.6). Well above the 1% used for inducing differentiation. In parallel studies, LY294002 was investigated at 0.5, 1, 10, 20, and 40 $\mu$ M and was also statistically significant, but was found to only be cytotoxic at 40 $\mu$ M which again was much higher than the actual concentrations to be used in the following studies (Figure 3.7).

H2L5765834 (0.5-30 $\mu$ M; Figure 3.8), H2L5186303 (0.5-30 $\mu$ M; Figure 3.9), TC-LPA5-4 (0.5-40 $\mu$ M; Figure 3.10), and Suramin (5-500 $\mu$ M; Figure 3.12) showed no statistically significant change in cell viability. BIM-1, on the other hand, was statistically significant, although it was well tolerated up to 10 $\mu$ M, showing some degree of reduced cell viability at 20 $\mu$ M but this was not significant until 40 $\mu$ M (Figure 3.11).

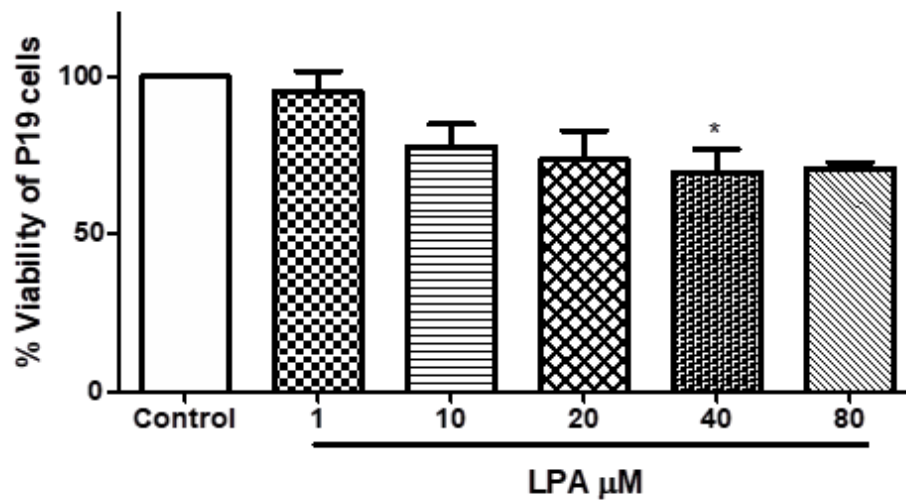


**Figure 3.5: Cellular viability of P19 cells when treated with different concentration of LPA by MTT assay.**

Cells were incubated with LPA concentration 1-80 $\mu\text{M}$ , for 24 hours followed by incubation for 4 hours with MTT as illustrated in the previous chapter. The data represents a % change in cell viability with the control taken as 100%. The bars represent the densitometric mean  $\pm$  SEM from 5 independent experiments. One-way analysis of variance (ANOVA) followed by Turkey comparison method was used to determine statistical significance. \* denotes  $p < 0.05$  compared to control.

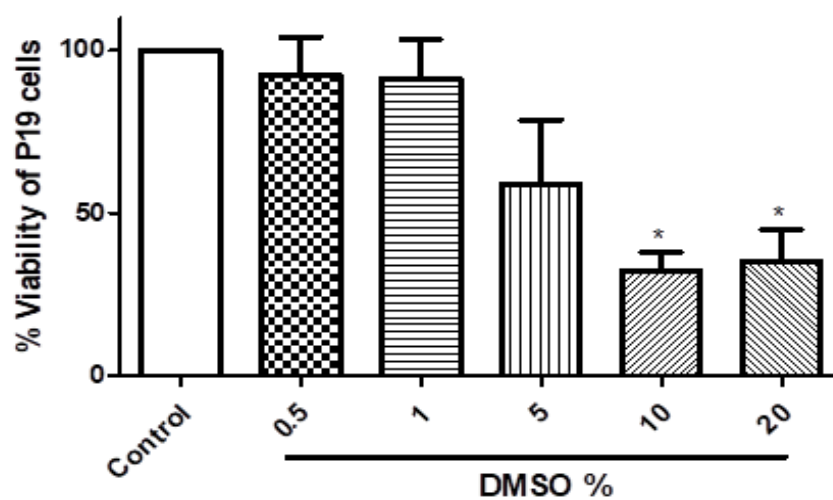


**Figure 3.6: Cellular viability of P19 cells when treated with different concentration of DMSO by MTT assay.**

Cells were incubated with DMSO 0.5-20 $\mu\text{M}$ , for 24 hours followed by incubation for 4 hours with MTT as illustrated in the previous chapter. The data represents a % change in cell viability with the control taken as 100%. The data represent the means  $\pm$  S.E.M from 3 individual experiments. One-way analysis of variance (ANOVA) was used to determine statistical significance. \* denotes  $p < 0.05$  compared to control cells.

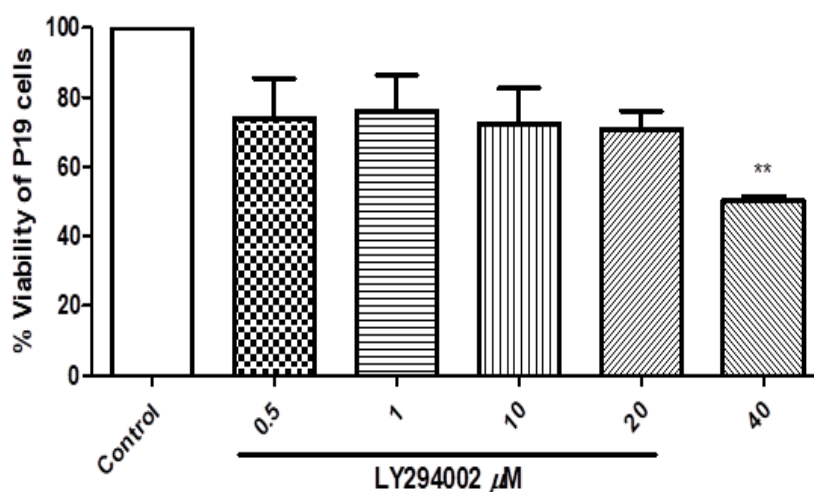


**Figure 3.7: Cellular viability of P19 cells when treated with different concentration of LY294002 by MTT assay.**

Cells were incubated with LY294002 0.5-40 $\mu\text{M}$ , for 24 hours followed by incubation for 4 hours with MTT as illustrated in the previous chapter. The data represents a % change in cell viability with the control taken as 100%. The data represent the means  $\pm$  S.E.M from 3 individual experiments. One-way analysis of variance (ANOVA) was used to determine statistical significance. \*\* denotes  $p < 0.01$  compared to control cells.

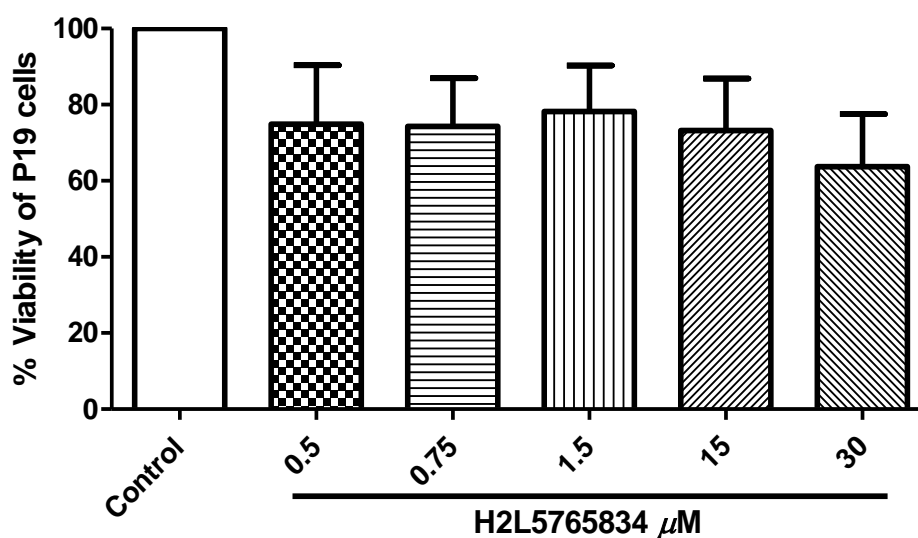


**Figure 3.8: Cellular viability of P19 cells when treated with different concentration of H2L5765834 by MTT assay.**

Cells were incubated with H2L5765834 0.5-30 $\mu\text{M}$ , for 24 hours followed by incubation for 4 hours with MTT as illustrated in the previous chapter. The data represents a % change in cell viability with the control taken as 100%. The data represent the means  $\pm$  S.E.M from 3 individual experiments.

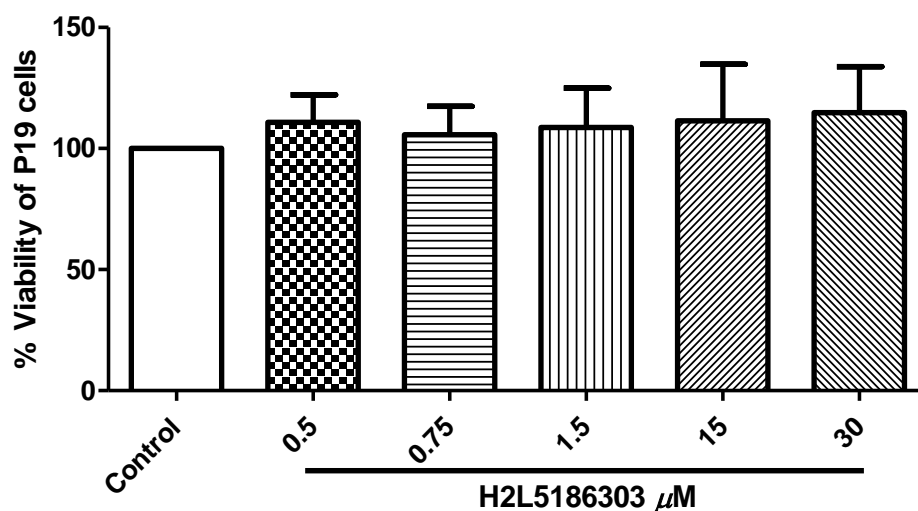


**Figure 3.9: Cellular viability of P19 cells when treated with different concentration of H2L5186303 by MTT assay.**

Cells were incubated with H2L5186303 0.5-30 $\mu\text{M}$ , for 24 hours followed by incubation for 4 hours with MTT as illustrated in the previous chapter. The data represents a % change in cell viability with the control taken as 100%. The data represent the means  $\pm$  S.E.M from 3 individual experiments.

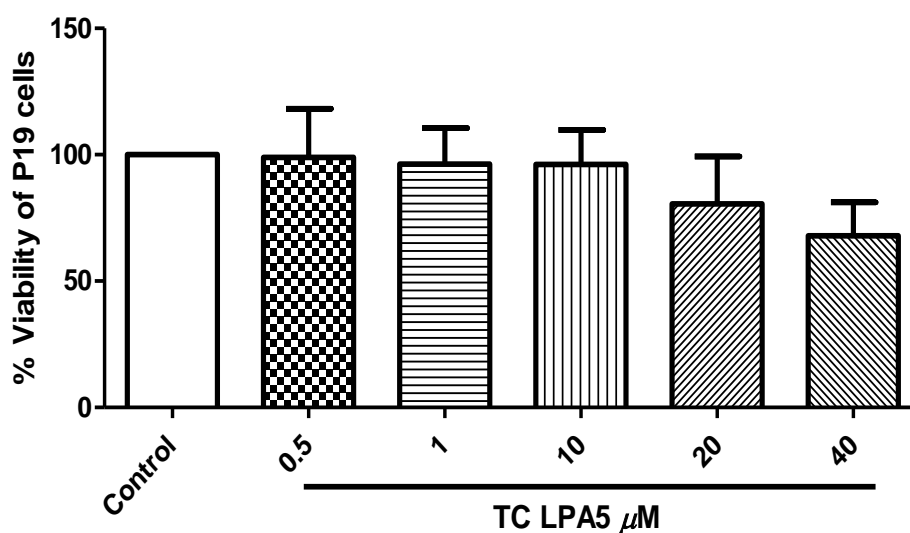


**Figure 3.10: Cellular viability of P19 cells when treated with different concentration of TC-LPA5-4 by MTT assay.**

Cells were incubated with TC-LPA5-4 0.5-40 $\mu\text{M}$ , for 24 hours followed by incubation for 4 hours with MTT as illustrated in the previous chapter. The data represents a % change in cell viability with the control taken as 100%. The data represent the means  $\pm$  S.E.M from 3 individual experiments.

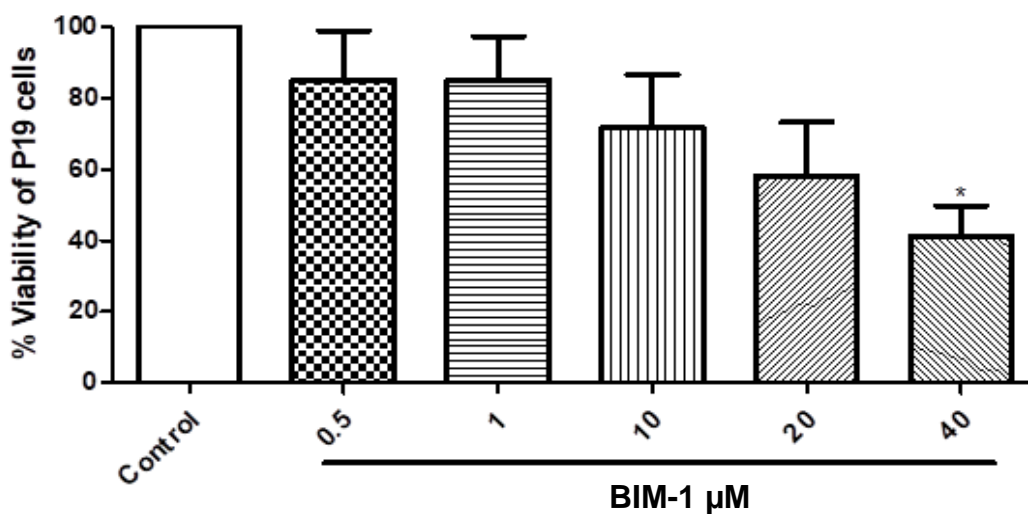


**Figure 3.11: Cellular viability of P19 cells when treated with different concentration of BIM-1 by MTT assay.**

Cells were incubated with BIM-1 0.5-40 $\mu\text{M}$ , for 24 hours followed by incubation for 4 hours with MTT as illustrated in the previous chapter. The data represents a % change in cell viability with the control taken as 100%. The data represent the means  $\pm$  S.E.M from 3 individual experiments. One-way analysis of variance (ANOVA) was used to determine statistical significance. \* denotes  $p < 0.05$  compared to control cells

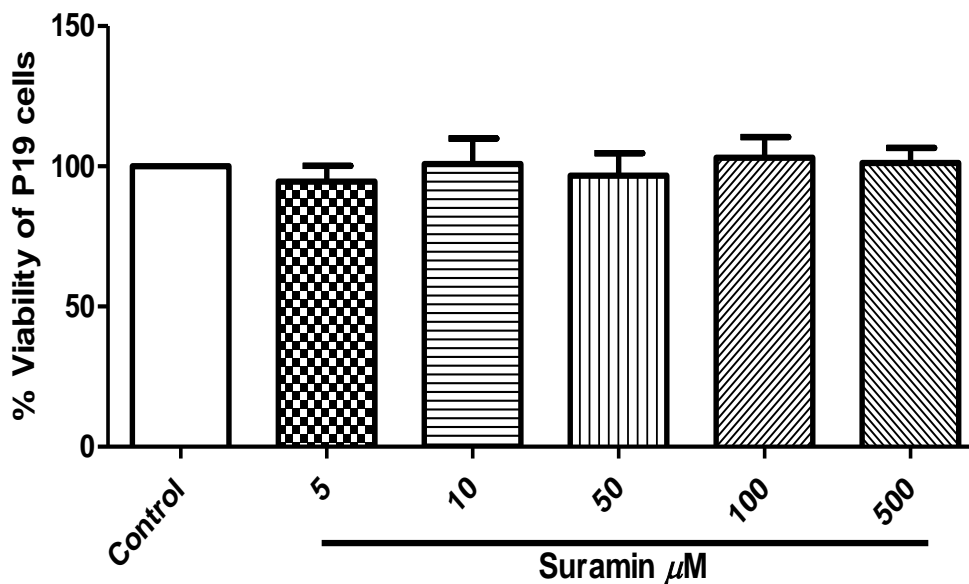


**Figure 3.12: Cellular viability of P19 cells when treated with different concentration of Suramin by MTT assay.**

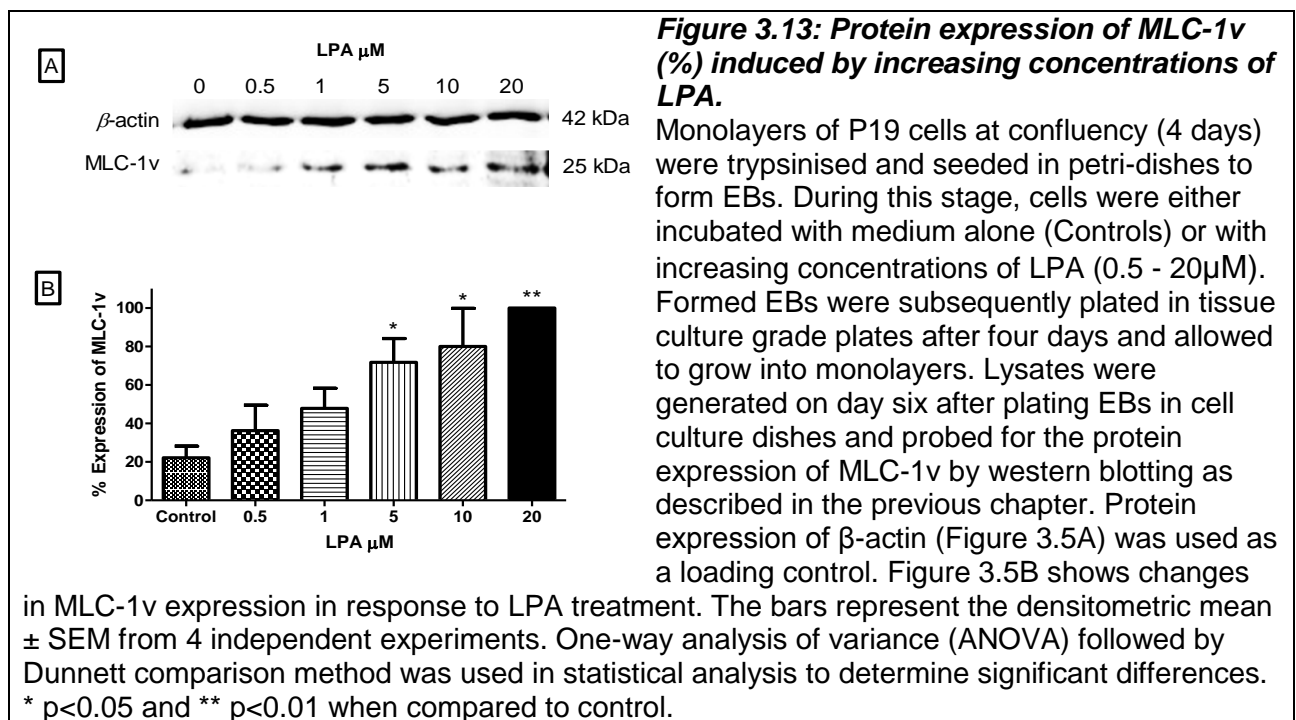
Cells were incubated with Suramin 5-500 $\mu\text{M}$ , for 24 hours followed by incubation for 4 hours with MTT as illustrated in the previous chapter. The data represents a % change in cell viability with the control taken as 100%. The data represent the means  $\pm$  S.E.M from 3 individual experiments.

### 3.3 Establishment and development of cardiac cells model and examination of the effects of LPA on differentiation

In this section, establishing the capability of LPA to regulate the differentiation P19 SCs into cardiomyocytes was crucial to confirm previous data from our group. It was also essential to understand this regulation in terms of sensitivity to concentration and time course of the induction of effects, especially immediately after exposure to LPA. Currently, it is not clear how early SCs commit to a cardiac lineage when exposed to LPA, and this has been investigated in this thesis.

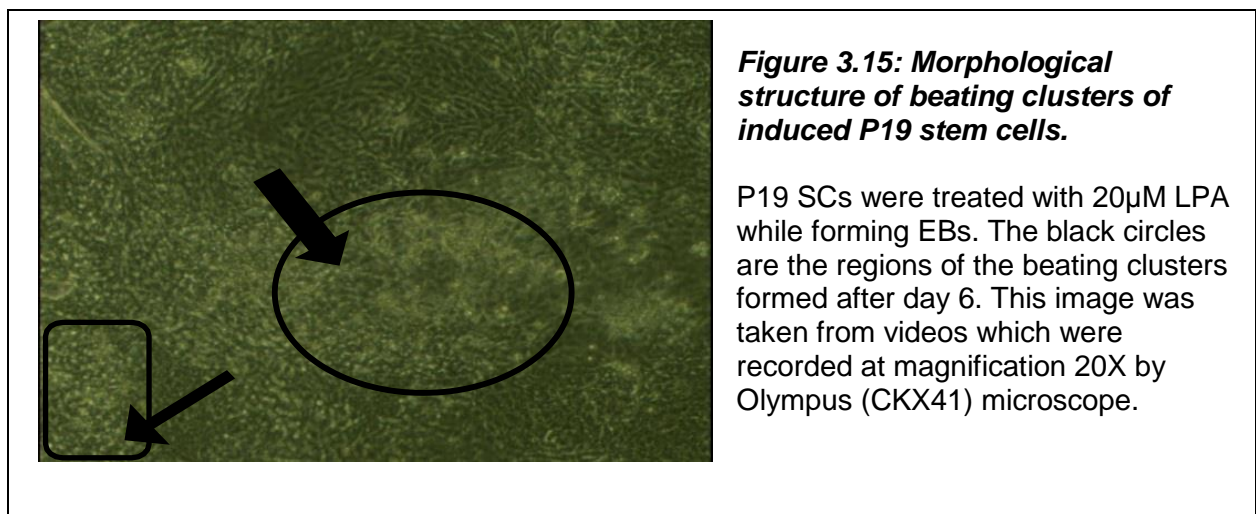
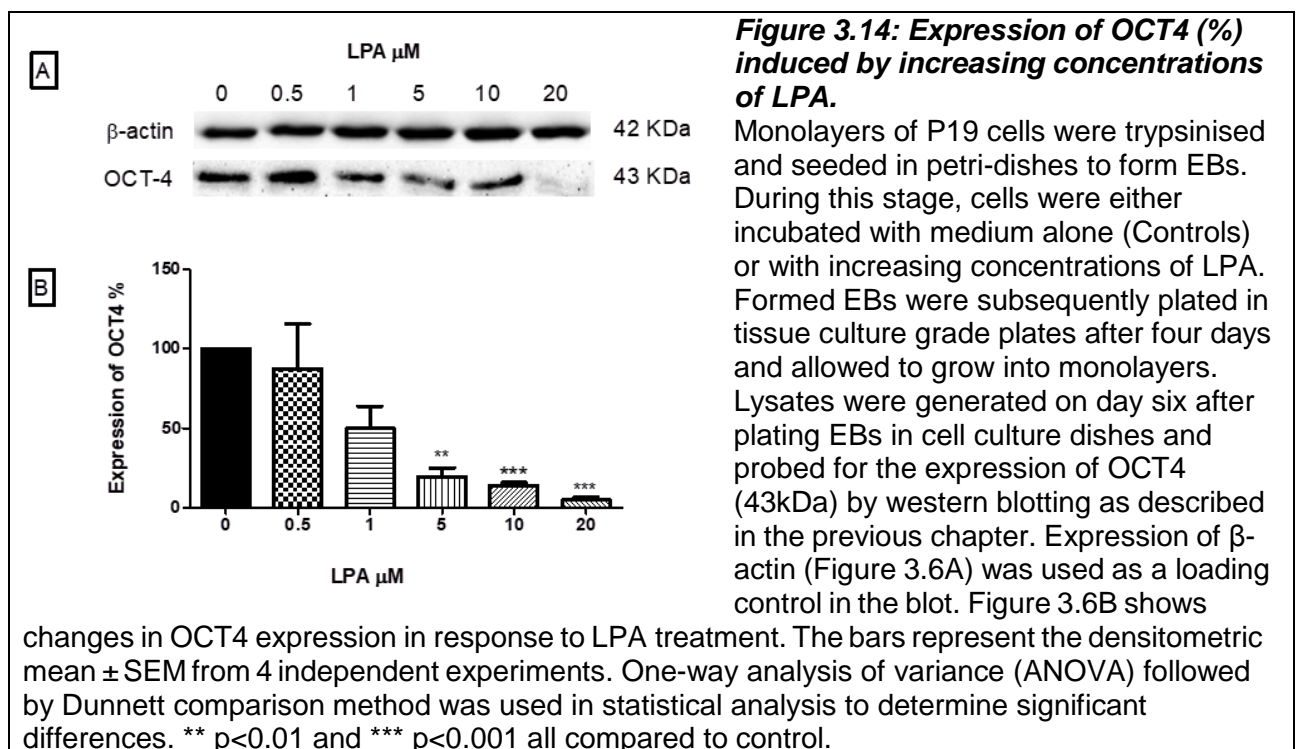
#### 3.3.1 Expression of MLC-1V protein induced by different LPA Concentrations

Differentiation into cardiomyocytes was determined by monitoring changes in ventricular myosin light chain (MLC-1v) protein expression. In these studies, MLC-1v has increased in response to the increasing concentrations of LPA ( $\mu\text{M}$ ). The increase to the latter was statistically significant at 5 $\mu\text{M}$  10 $\mu\text{M}$  as well as at 20 $\mu\text{M}$ , which induced the maximum expression of MLC-1v as shown by western blotting (Figure 3.13B). This concentration also induced spontaneously beating clusters of the cells, which is one of the characteristics of the presence of cardiomyocytes (Figure 3.15).



### 3.3.2 Expression of OCT4 protein induced by different LPA Concentrations

In parallel with MLC-1v, changes in OCT4 were also investigated in lysates generated from P19 SCs treated with increasing concentrations of LPA. Figure 3.14 shows a decrease in the expression of OCT4 as the concentration of LPA increased. At LPA 20 $\mu$ M, the expression of OCT4 was the lowest, which parallels with the increase in the number of beating clusters found after observing the monolayer from day three onwards (Figure 3.14). OCT4 expression was significantly different compared to the control at 5 $\mu$ M (and this was more evident in 10 $\mu$ M and 20 $\mu$ M



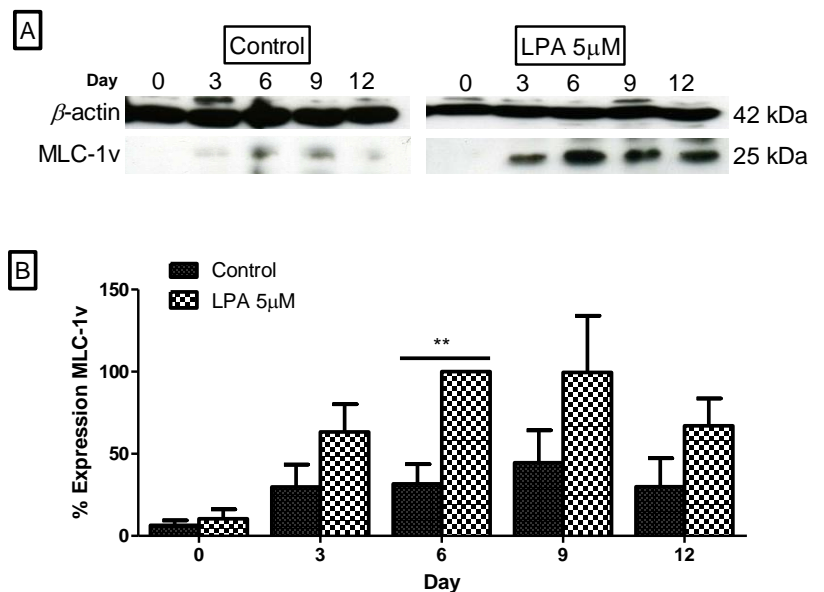
### 3.3.3 Time-dependent induction of MLC-1v protein expression by LPA

Treatment of cells with LPA (5 $\mu$ M) caused a time-dependent increase in MLC-1v expression, which was at a maximum in lysates generated at day 6 and maintained up to day 9 but declining by day 12. Levels of MLC even at day 12 were, however, still higher than controls where MLC expression remained relatively unaltered throughout the 12 days incubation period (Figure 3.16).

**Figure 3.16: Time-dependent induction of MLC-1v protein expression by LPA.**

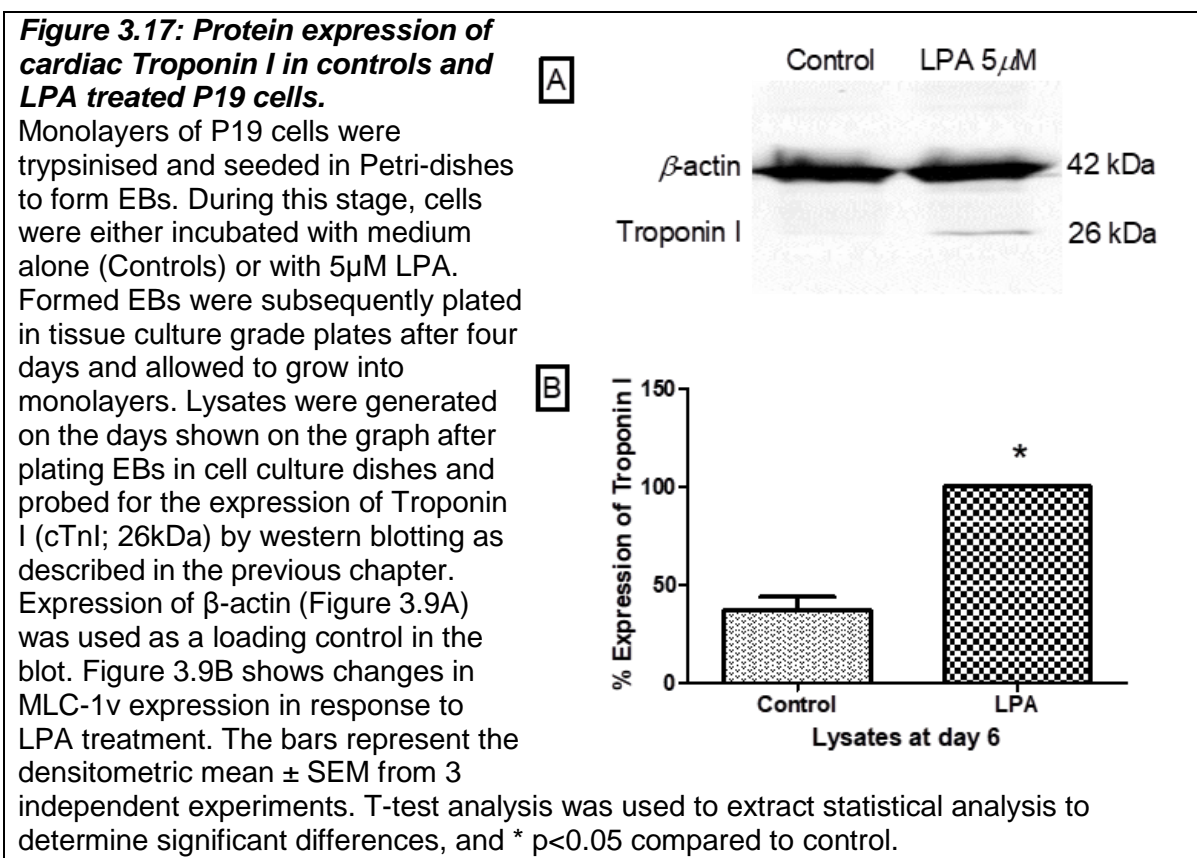
Monolayers of P19 cells were trypsinised and seeded in Petri-dishes to form EBs. During this stage, cells were either incubated with medium alone (Controls) or with 5 $\mu$ M LPA. Formed EBs were subsequently plated in tissue culture grade plates after four days and allowed to grow into monolayers. Lysates were generated on the days shown on the graph after plating EBs in cell culture dishes and probed for the protein expression of MLC-1v (25kDa)

by western blotting as described in the previous chapter. Protein expression of  $\beta$ -actin (Figure 3.8A) was used as a loading control in the blot. Figure 3.8B shows changes in MLC-1v expression in response to LPA treatment. The bars represent the densitometric mean  $\pm$  SEM from 5 independent experiments. T-test analysis was used to extract statistical analysis to determine significant differences and \*\*  $p < 0.01$  compared to control.



### 3.3.4 Protein expression of Troponin I in controls and LPA treated P19 cells

To further confirm that LPA induced differentiation of P19 SCs into cardiomyocytes, lysates were also analysed for another cardiac specific marker, Troponin I. As shown in Figure 3.17, the controls had less induction or expression of Troponin I than the LPA treated cells which illustrated a significant induction (Figure 3.17).



### 3.3.5 Expression of MLC-1v following short incubations with LPA

In these studies, the aim was to determine whether MLC-1v expression can be induced by LPA when incubated for shorter time points, ranging from 5 min to 24 hours. This was done to determine whether LPA induces the expression of MLC-1v at an early time-point. DMSO was used in parallel studies for comparison. LPA was used at two different concentrations, 5 $\mu$ M and 20 $\mu$ M. Lysates were generated on day 6 and day 12 for analysis of MLC-1v expression by western blotting.

Earlier time points up to 9 hours did not appear to be enough for significant induction of MLC-1v in lysates generated six days after plating EBs in cell culture dishes. There was, however, an increase in MLC-1v expression following 24h incubation with LPA before plating EBs in the cell culture plates (Figures 3.18., 3.19. and 3.20.).

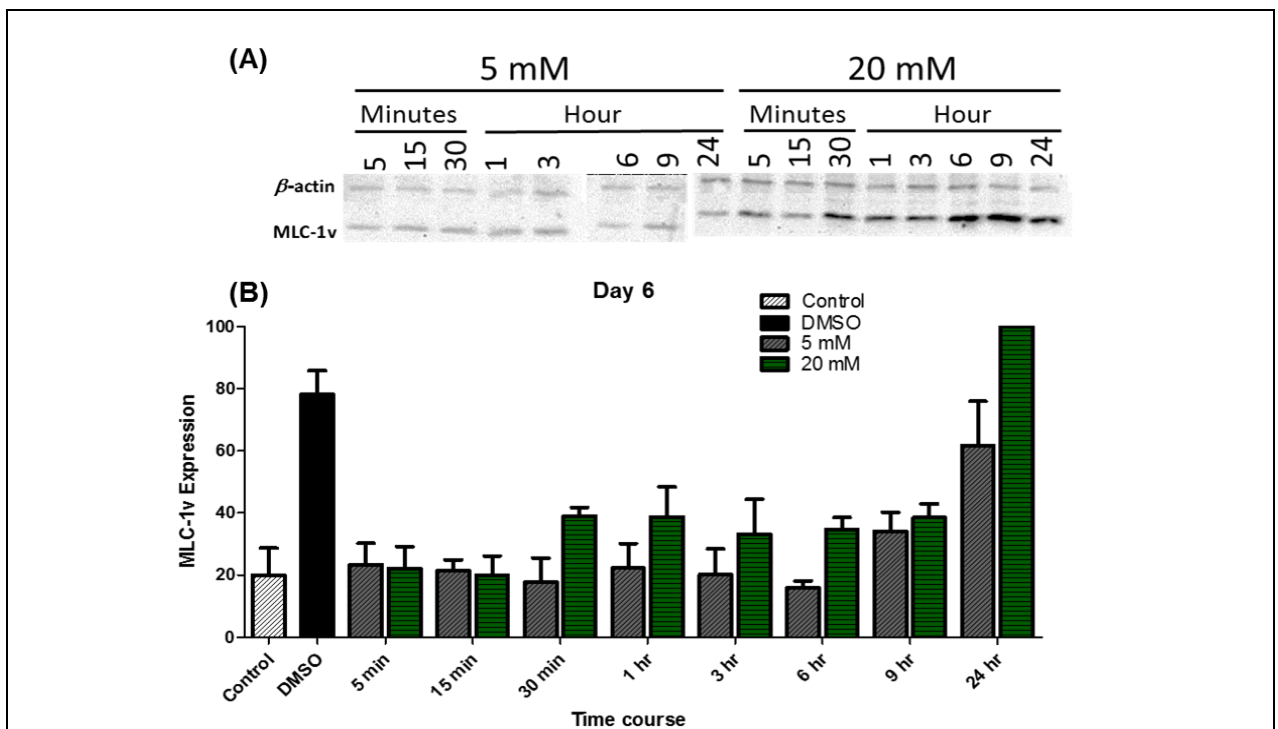


**Figure 3.18: Protein expression of MLC-1v induced in short time points by LPA on day 6.**

Monolayers of P19 cells were trypsinised and seeded in petri-dishes to form EB. During this stage, cells were treated medium alone (Controls) or with LPA (5 $\mu$ M & 20 $\mu$ M) for 5 min to 24 hours. P19 cells were also treated with DMSO in a monolayer (as a positive control). Formed EBs were subsequently plated in tissue culture grade plates after four days and allowed to grow into monolayers. Lysates were generated on day six after plating EBs in cell culture dishes and probed for the expression of MLC-1v by western blotting as described in the previous chapter. Expression of  $\beta$ -actin was used as a loading control in the blot, and the bars represent the densitometric mean  $\pm$  SEM from 3 independent experiments (B).

**Figure 3.19: Protein expression of MLC-1v induced in Short time points by 5µM LPA**

Short time-dependent (5 min to 24 hours) protein expression of MLC-1v at 5µM lysates collected at day six compared with % of LPA 5µM treated for four days. The densitometric represents mean ± SEM from 3 independent experiments. One-way analysis of variance (ANOVA) method was used to extract statistical information. The P value \* p<0.5 and \*\*\*p<0.001 compared to LPA 5µM.

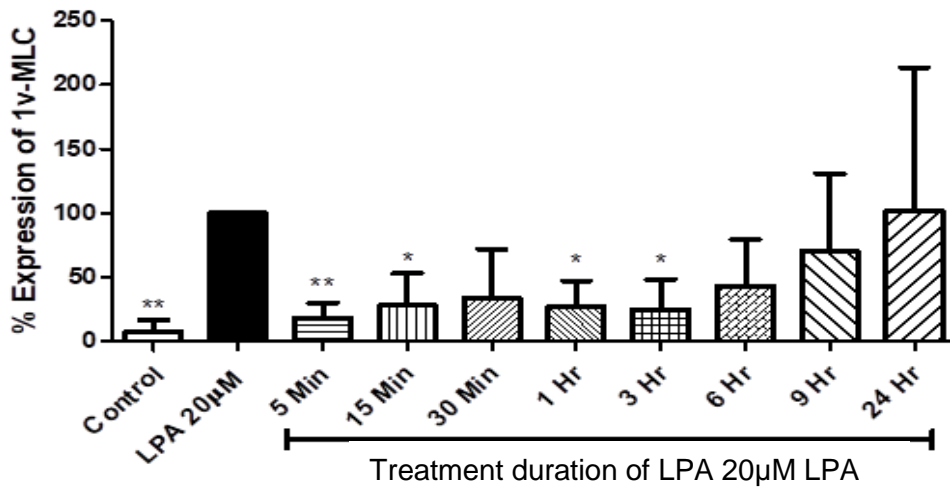
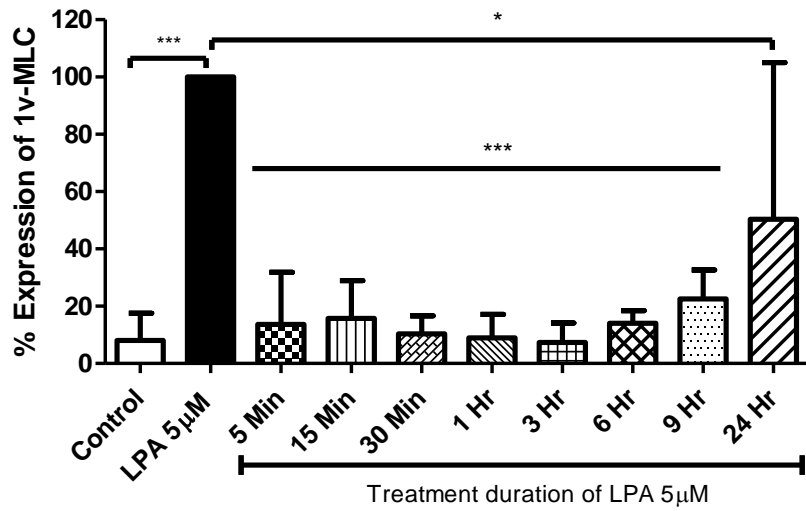
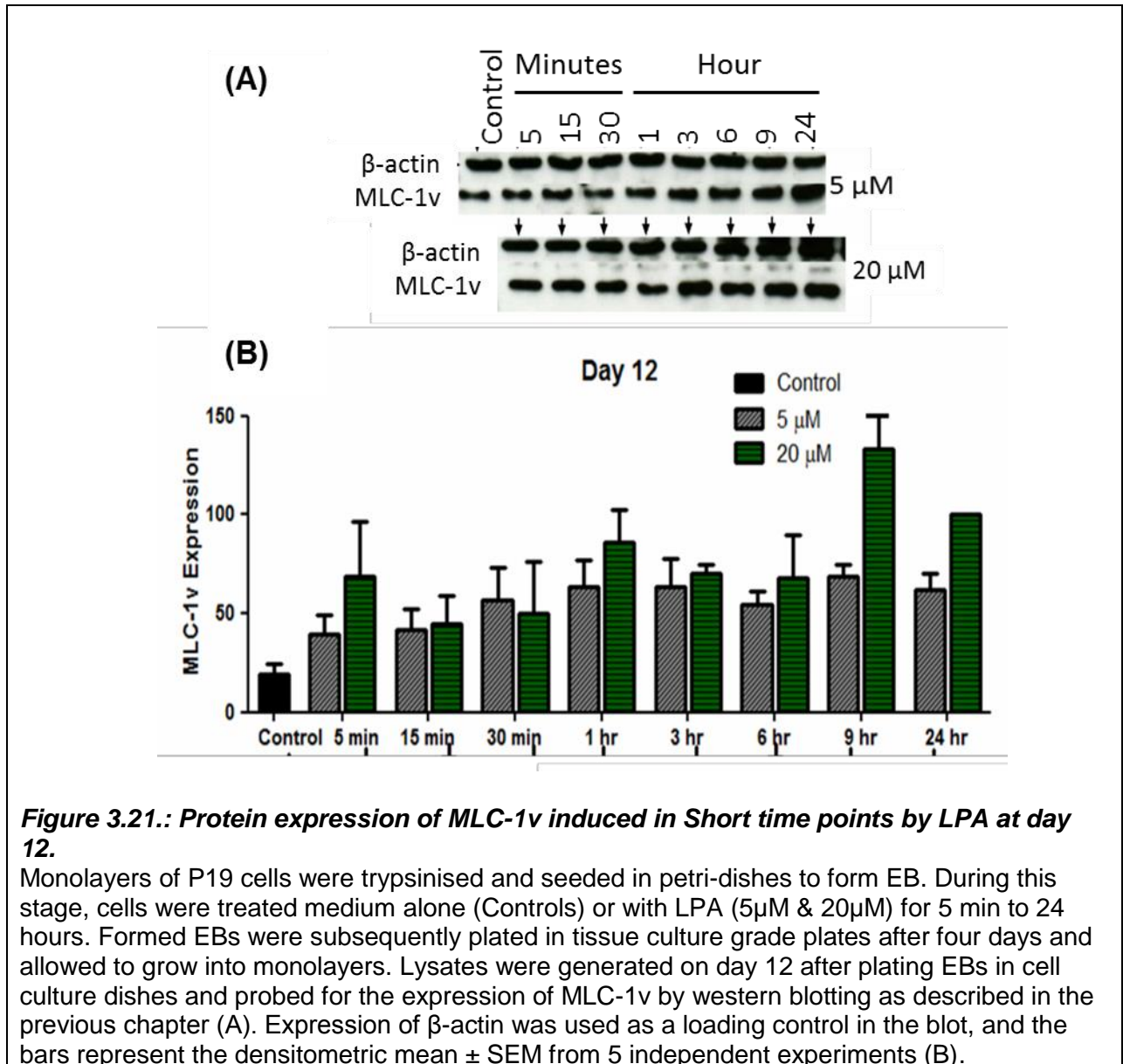


**Figure 3.20: Protein expression of MLC-1v induced in Short time points by 20µM LPA.**

Short time-dependent expression (5 min to 24 hours) of MLC-1v at 20µM lysates collected at day 6 compared with % of LPA 5µM treated for four days. The densitometric represents mean ± SEM from 3 independent experiments. One-way analysis of variance (ANOVA) method was used to extract statistical information. The P value \* p<0.5 and \*\* p<0.01 compared to LPA 20µM.

By comparison, in lysates generated on day 12, MLC-1v expression was significantly higher at all time points from 5 min to 24 hours (Figure 3.21). However, the expressions trend was higher, specifically at 9 and 24 hours treated cells with 20 $\mu$ M of LPA.



## 3.4 PCR normalisation and quantification:

### 3.4.1 The purity of isolated RNA

Table 3.1 shows the purity and concentration of RNA in the samples generated from P19 cells from BIM-1 inhibitor experiment. The absorbance at 260/280 was between 1.99-2.04 with an average of 2.01, while, the 260/230 was 2.05. The concentrations of RNA isolated was high and averaged 616 ng/ $\mu$ l.

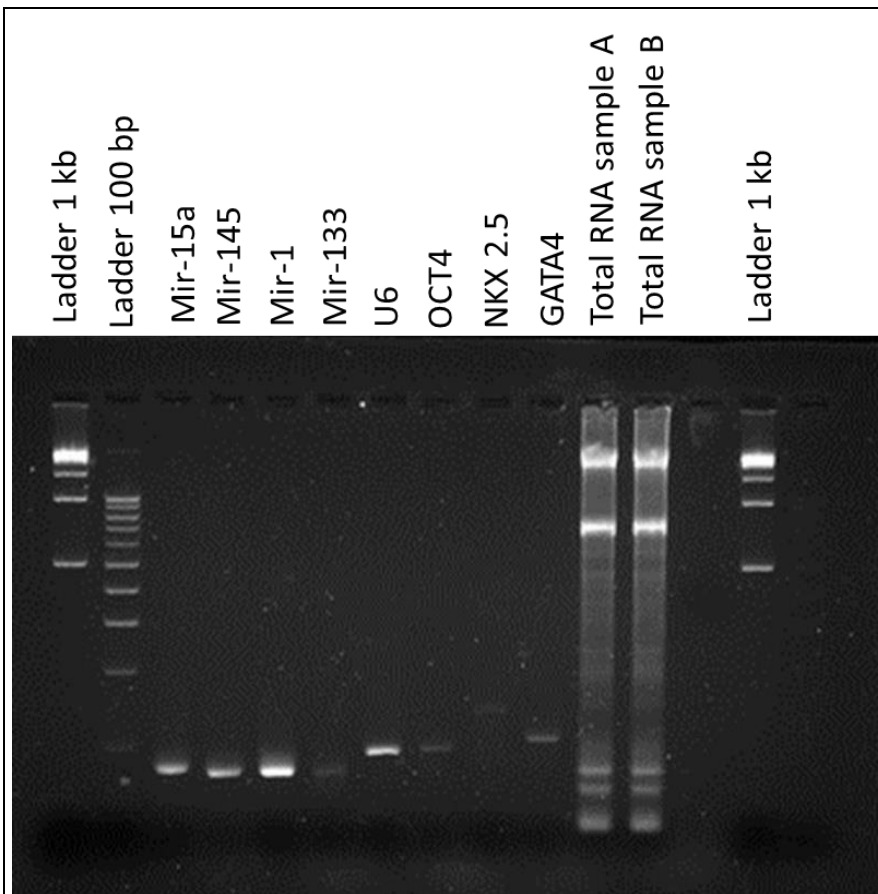
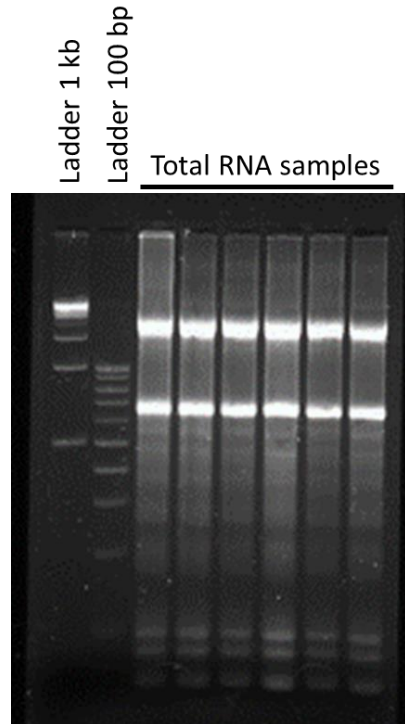
**Table 3.1: Concentration and purity for isolated total RNA using Nanodrop.**

Experiment	Condition	Concentration (ng/ $\mu$ l)	260/280	260/230
N1	Control	720	2	2.15
	LPA	648	2.04	2.16
	BIM-1	551	2.03	2.12
	BIM-1+LPA	600	2.04	2
N2	Control	623	2.04	2.15
	LPA	624	2.01	1.85
	BIM-1	611	2.02	2.10
	BIM-1+LPA	715	2.02	2.11
N3	Control	718	2.02	1.92
	LPA	598	2	2.05
	BIM-1	466	1.99	1.95
	BIM-1+LPA	518	2.02	1.92

In addition to the spectrophotometric analysis, the purity of the RNA isolated was also established by gel electrophoresis. Figure 3.22 below illustrates how pure the RNA samples isolated were. 28s and 18s rRNA are seen with no smears that may indicate genomic DNA, other contaminants or RNA degradation. Figure 3.23 also shows identified single band which represents the primer amplified in qPCR with no smears or multiple amplification of non-specific mRNAs.

**Figure 3.22: 1% denaturing agarose gel electrophoresis for total RNA samples.**

Lysates were collected on day six from EBs plated in cell culture dishes for total RNA extraction using the miRVana™ kit from Ambion. 1µg/ml of each sample obtained was used in each well. This agarose gel was pre-stained with GelRed. Lanes represent, L1= ladder 1 kb, L2= ladder 100 bp, L3= Control P19 cells, L4-L8= LPA treated P19 cells. This gel was visualised using the MyECL imager.



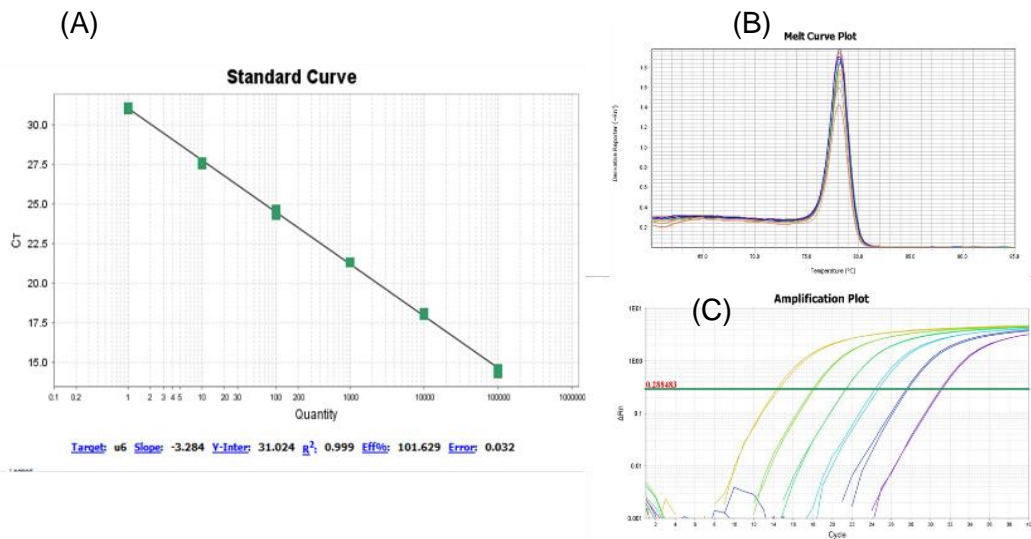
RNA sample B, L14= ladder 1 kb. This gel was visualised using the MyECL imager.

**Figure 3.23: 1.5% denaturing agarose gel electrophoresis for amplicon (Products of qPCR).**

Lysates collected on day 6 EBs were plated in cell culture dishes for total RNA extraction using the miRVana™ kit from Ambion. Samples were reverse transcribed to get cDNA samples, probed for the targets, and amplified using real-time PCR. 1µg/ml of each sample was used in each well. Agarose gel was pre-stained with GelRed. Lanes represents, L1= ladder 1 kb, L2= ladder 100 bp, L3= mir-15a, L4= mir-145, L5=mir-1, L6= mir-133, L7= U6, L8= OCT4, L9= NKX2.5, L10= GATA4, L11= Total RNA sample A, L12= Total

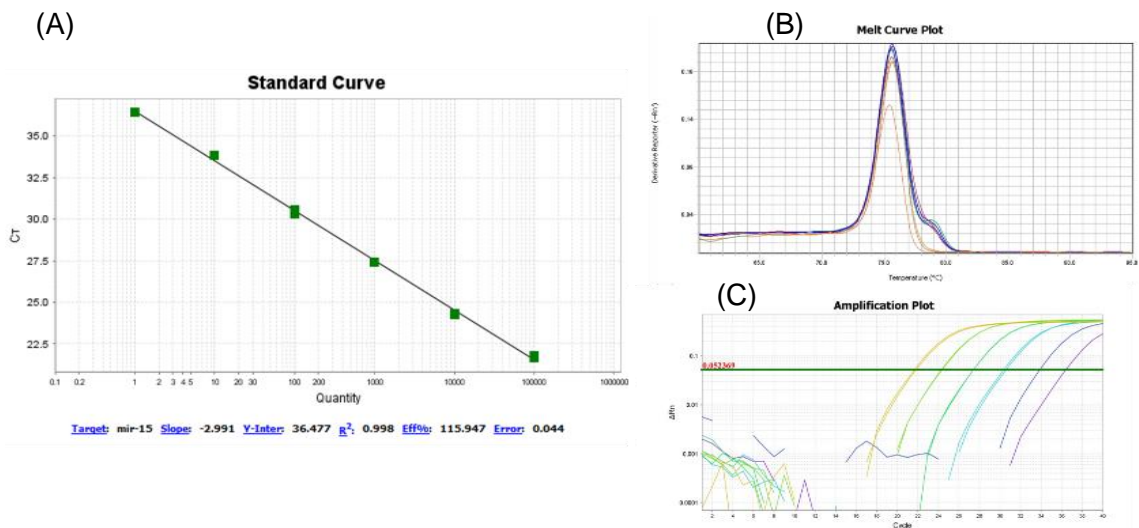
### **3.4.2 Real-time/Reverse-transcription polymerase chain reaction (qRT-PCR).**

Two genes were tested for their stability and efficiency to be used as a control with the samples, U6 and mir-15a. In addition to these, mir-145, mir-1, mir-133, OCT4, Nkx2.5, and GATA4 were also screened. A standard curve using 10-fold serial dilutions was prepared for 6 points. Each dilution was repeated in duplicate. Some of the points were flagged (excluded) to get a better slope and efficiency (Figures 3.24- 3.31). For normalisation of any gene or primer, it is essential to get a single unique peak temperature in the melting curve plot (Figures 3.24B-3.31B) as this suggests that the primer is specific. Secondly, it gives information about the amplification blot relative fluorescence against the cycle number for each dilution (Figures 3.24C-3.31C). Lowest dilution in which the cycle threshold ( $C_T$ ) range between 20-30 cycles is an ideal concentration to be used in further qRT-PCR reactions for the same primer detected by SYBR-green. Efficiency and the slope equation help in getting reproducible and validated data (Figures 3.24A-3.31A). The  $R^2$  value represents the linearity of the data or how well the experimental data fit the regression line. In addition, this can suggest how good the pipetting techniques were and how reproducible the results are. The ideal linear standard curve should be  $R^2 > 0.980$  and efficiency % closer to 100%. Figures 3.24-3.31 show the standard curves melting curves and amplification plots for U6-housekeeping gene, mir-15a, mir145, mir-1, mir-133, OCT4, Nkx2.5, and GATA4, respectively.



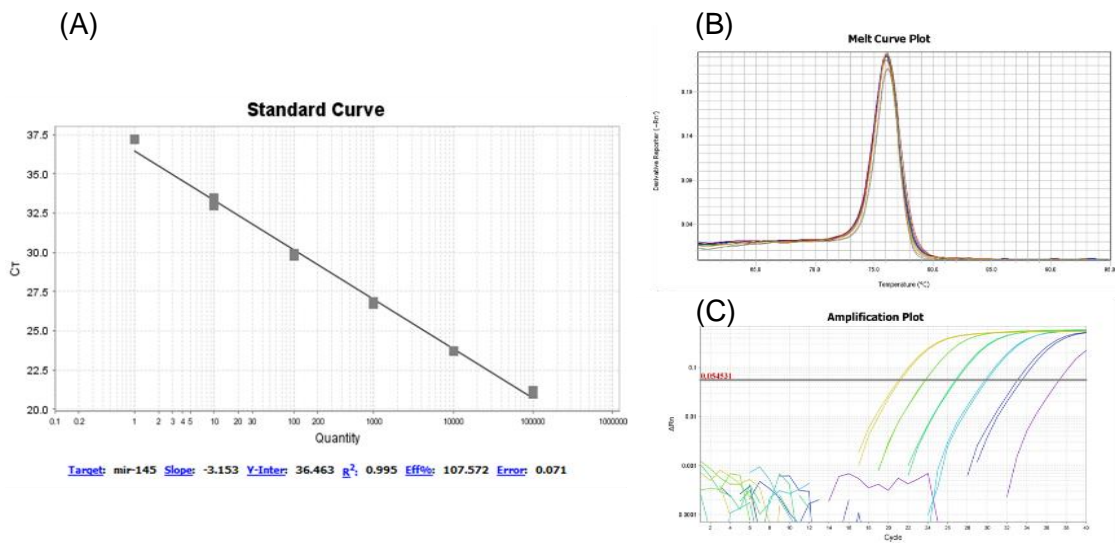
**Figure 3.24: Generating a standard curve to assess reaction optimisation for U6-housekeeping gene.**

A standard curve was generated using a 10-fold dilution of the U6 gene using SYBR-green analysed by QuantStudio™ 7 Flex Real-Time PCR System (Qiagen). Each dilution was assayed in duplicates in three separate times. (A) A standard curve with the CT plotted against the log of the starting copy numbers. The regression line, R<sup>2</sup> value, and efficiency are at the bottom of the graph. (B) The melting curve which shows how specific the primer is by looking at the number of peaks. (C) Amplification plot, relative fluorescence against cycle number.



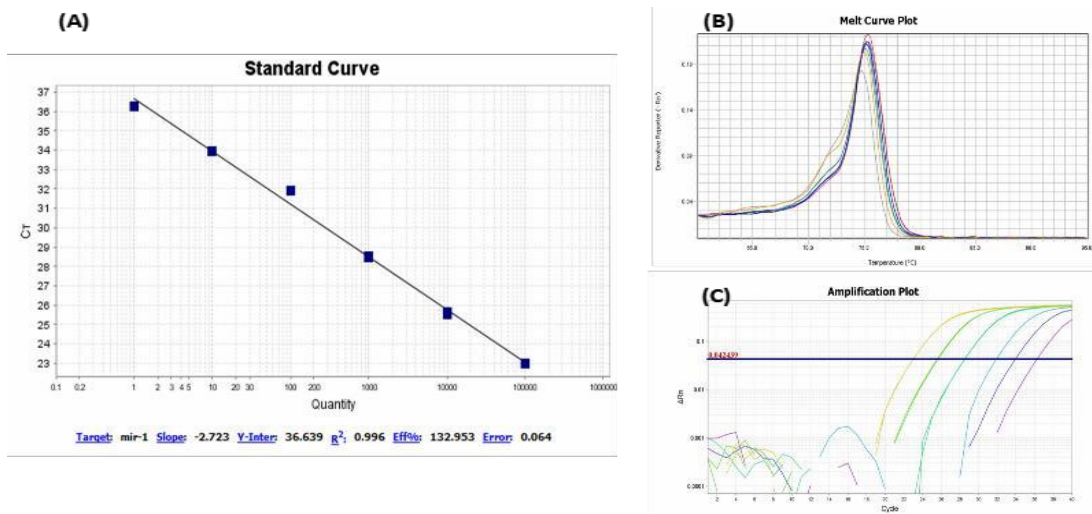
**Figure 3.25: Generating a standard curve to assess reaction optimisation for mir-15a.**

A standard curve was generated using a 10-fold dilution of mir-15a using SYBR-green dye analysed by QuantStudio™ 7 Flex Real-Time PCR System (Qiagen). Each dilution was assayed in duplicates in three separate times. (A) A standard curve with the CT plotted against the log of the starting copy numbers. The regression line, R<sup>2</sup> value, and efficiency are at the bottom of the graph. (B) The melting curve which shows how specific the primer is by looking at the number of peaks. (C) Amplification plot, relative fluorescence against cycle number.



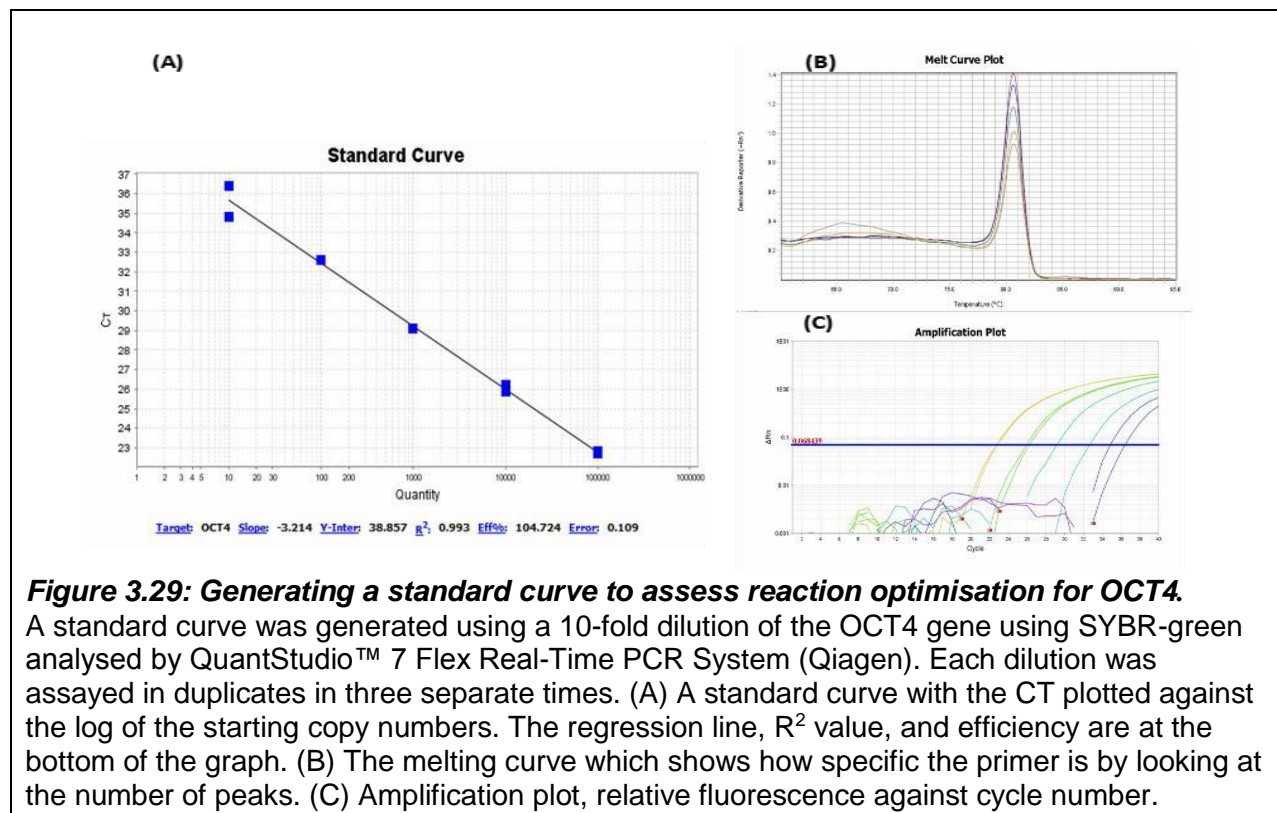
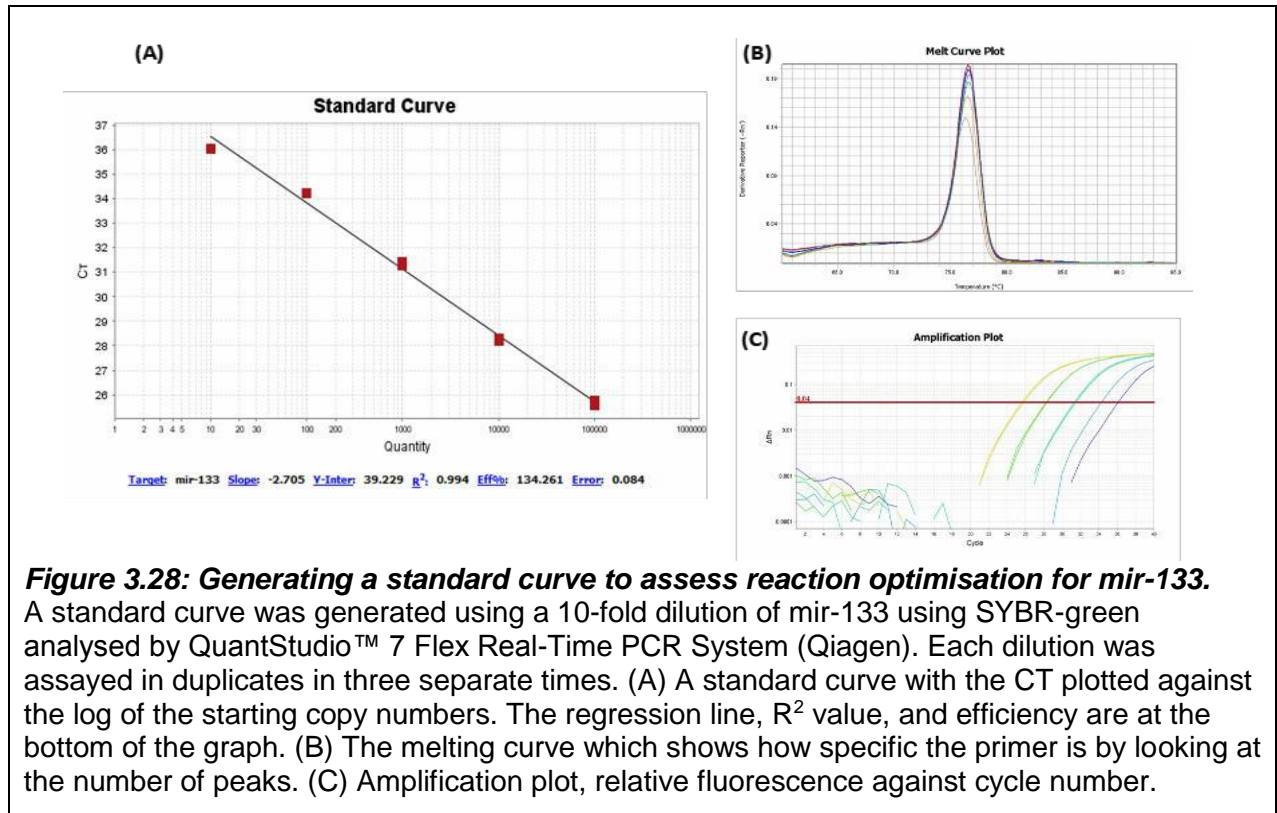
**Figure 3.26: Generating a standard curve to assess reaction optimisation for mir-145.**

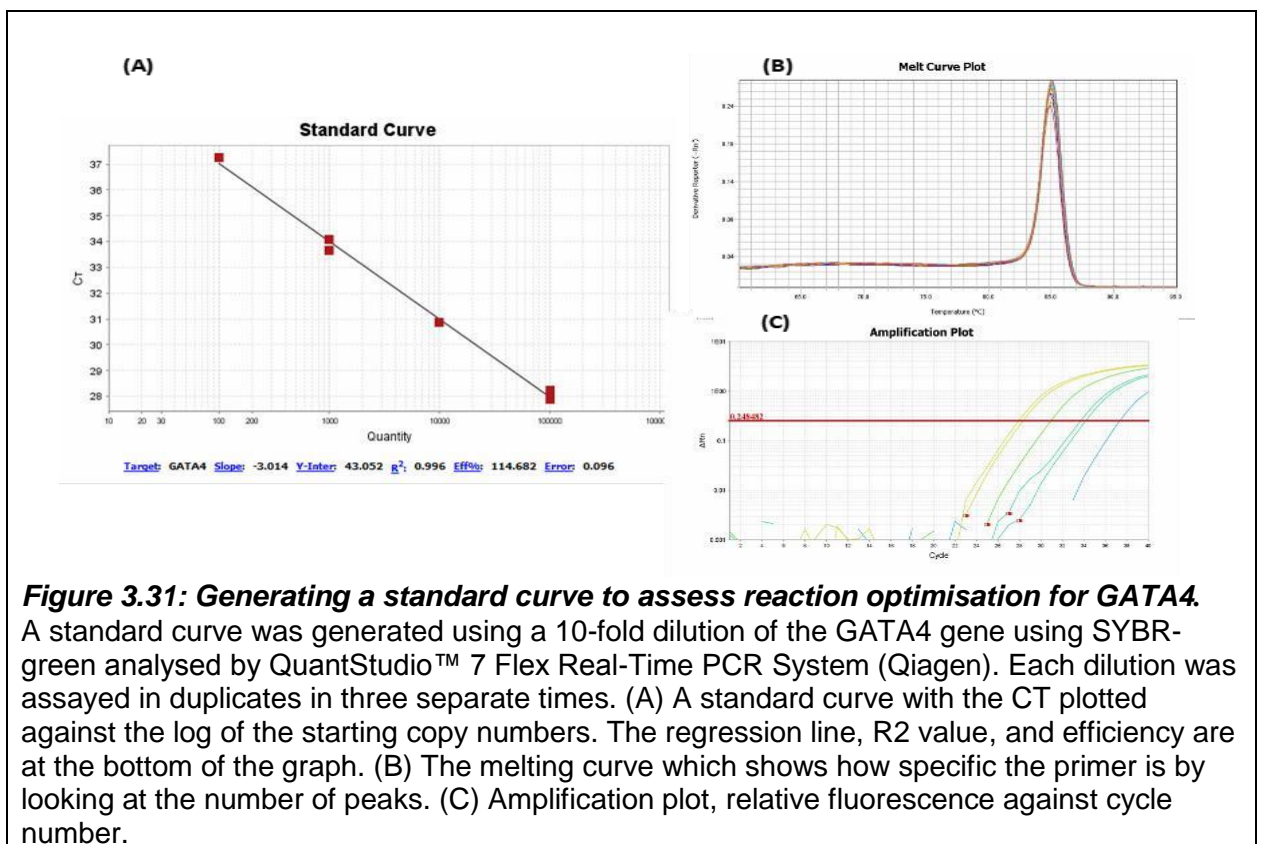
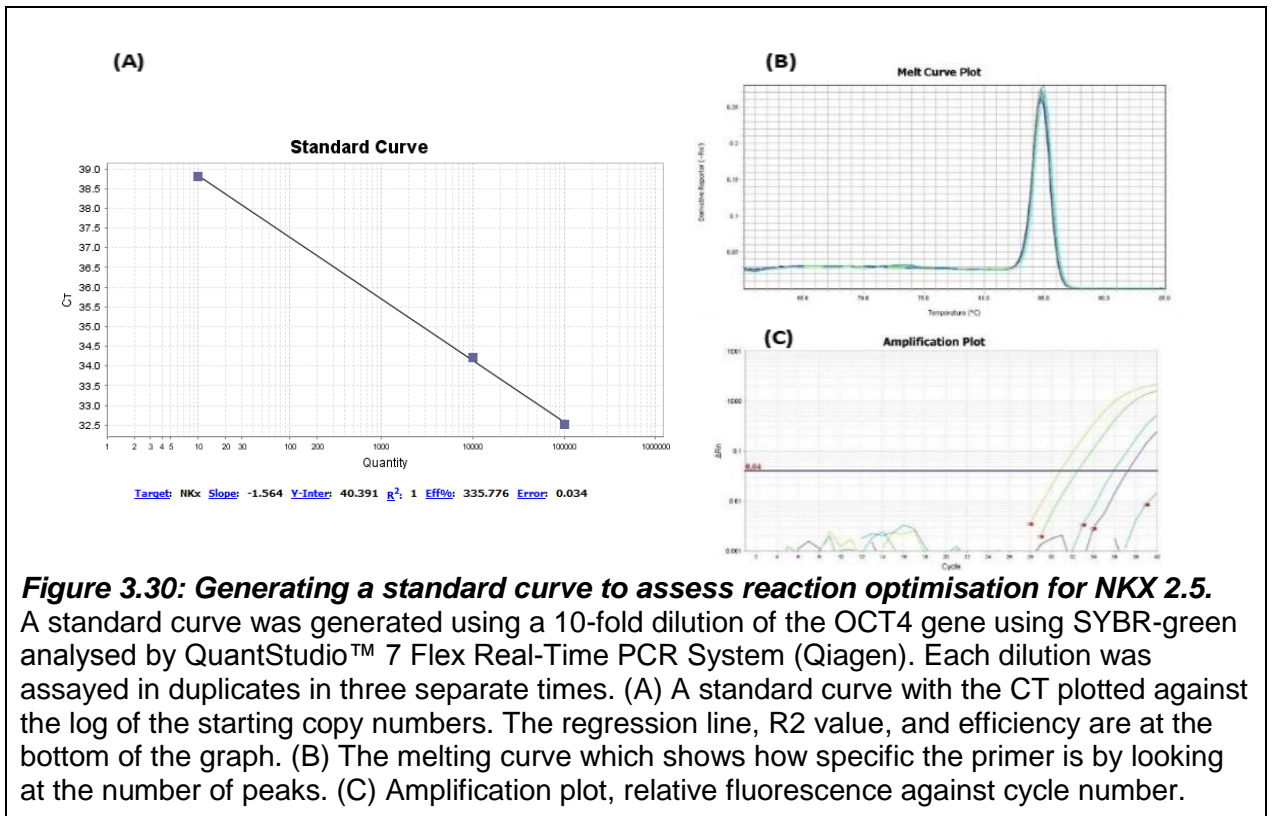
A standard curve was generated using a 10-fold dilution of mir-145 using SYBR-green analysed by QuantStudio™ 7 Flex Real-Time PCR System (Qiagen). Each dilution was assayed in duplicates in three separate times. (A) A standard curve with the CT plotted against the log of the starting copy numbers. The regression line,  $R^2$  value, and efficiency are at the bottom of the graph. (B) The melting curve which shows how specific the primer is by looking at the number of peaks. (C) Amplification plot, relative fluorescence against cycle number.



**Figure 3.27: Generating a standard curve to assess reaction optimisation for mir-1.**

A standard curve was generated using a 10-fold dilution of mir-1 using SYBR-green analysed by QuantStudio™ 7 Flex Real-Time PCR System (Qiagen). Each dilution was assayed in duplicates in three separate times. (A) A standard curve with the CT plotted against the log of the starting copy numbers. The regression line,  $R^2$  value, and efficiency are at the bottom of the graph. (B) The melting curve which shows how specific the primer is by looking at the number of peaks. (C) Amplification plot, relative fluorescence against cycle number.





### 3.5 Concentration-dependent effects of LPA on the expression of transcription factors and key miRNAs targeted

In this section, the focus is on the results obtained by qPCR targeting several genes and miRNAs over 3, 6, & 12 days using varying concentrations of LPA (0.5-20 $\mu$ M).

#### 3.5.1 OCT4

The expression of OCT4 at days 3, 6, and 12 showed no statistically significant changes when compared to controls. Although OCT4 expression appeared to increase at day 3 ( $1.461 \pm 1.053$  to  $1.705 \pm 0.9930$  folds) in cells treated with LPA (5 $\mu$ M to 20 $\mu$ M) the increases were not significant compared to control (Figure 3.32). Figure 3.33 is a summary of the data obtained for LPA at 5 $\mu$ M over three days ( $1.461 \pm 1.05$  folds), six days ( $0.799 \pm 0.147$  folds) and 12 days ( $0.8077 \pm 0.244$  folds).

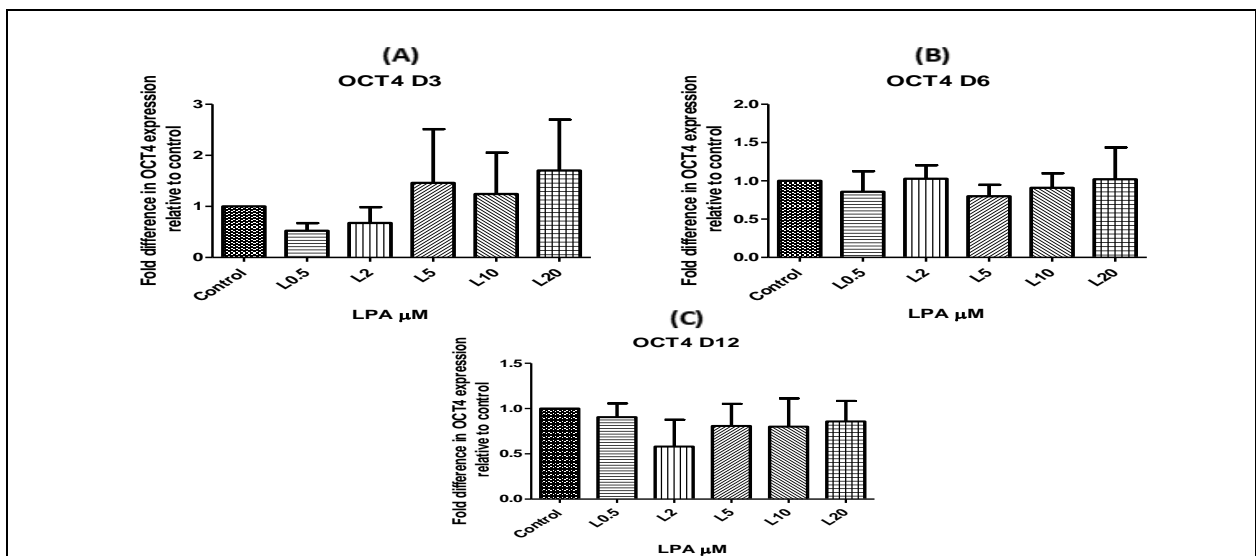
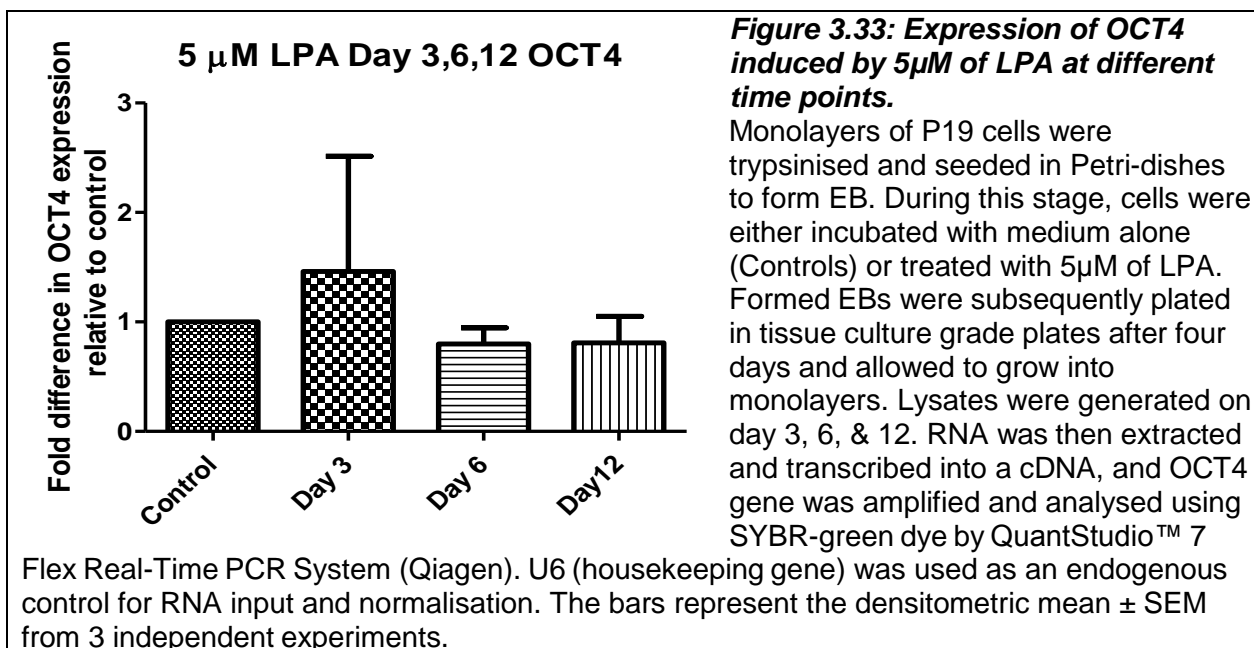


**Figure 3.32: Expression of OCT4 induced by LPA at different time points and concentrations.**

Monolayers of P19 cells were trypsinised and seeded in Petri-dishes to form EBs. During this stage, cells were either incubated with medium alone (Controls) or treated with LPA at 0.5-20 $\mu$ M. Formed EBs were subsequently plated in tissue culture grade plates after four days and allowed to grow into monolayers. Lysates were generated on day 3 (A), 6 (B), 12 (C). RNA was then extracted and transcribed into a cDNA, and OCT4 gene was amplified and analysed using SYBR-green dye by QuantStudio™ 7 Flex Real-Time PCR System (Qiagen). U6 (housekeeping gene) was used as an endogenous control for RNA input and normalisation. The bars represent the densitometric mean  $\pm$  SEM from 3 independent experiments.



### 3.5.2 NKX2.5

An increasing trend in the expression of the NKX2.5 gene was clear at days 3 (Figure 3.34A) and 12 (Figure 3.34C). The lowest expression was in cells treated with 0.5μM ( $0.56 \pm 0.21$ -fold change on day 3 and  $1.3 \pm 0.41$ -fold change on day 12) and highest at 20μM ( $2.33 \pm 1.45$ -fold change on day 3 and  $4.09 \pm 2.67$ -fold change on day 12). These differences did not show statistical significance partly because of the limited n values and to variations in the expression levels. In contrast to the data from days 3 and 12, there was no obvious trend in NKX2.5 expression on day six at any of the concentrations of LPA used (figure 3.34B). These observations, although preliminary, suggest a potential biphasic response in NKX 2.5 expression following LPA treatment. Expression of NKX 2.5 in LPA 5μM treated cells over the days 3, 6, and 12 were compared, and it was highest at day 12 with  $2.77 \pm 1.65$  (Figure 3.35).

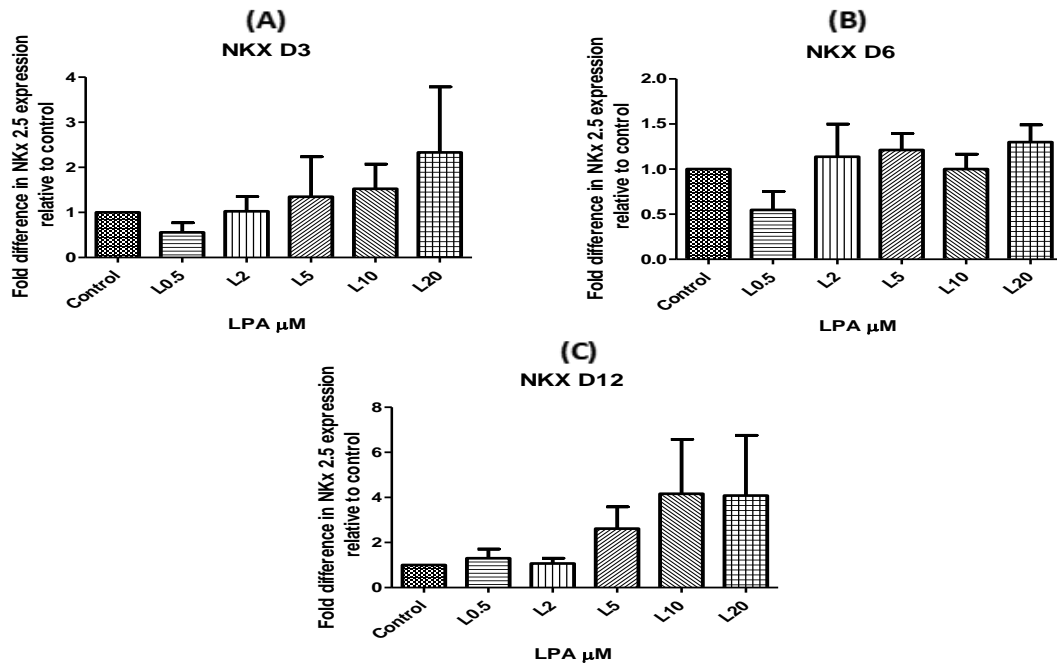


**Figure 3.34: Expression of NKX2.5 induced by LPA at different time points and concentrations.** Monolayers of P19 cells were trypsinised and seeded in Petri-dishes to form EBs. During this stage, cells were either incubated with medium alone (Controls) or treated with LPA at 0.5μM - 20μM. Formed EBs were subsequently plated in tissue culture grade plates after four days and allowed to grow into monolayers. Lysates were generated on day 3 (A), 6 (B), 12 (C). RNA was then extracted and transcribed into a cDNA and gene was amplified and analysed using SYBR-green dye by QuantStudio™ 7 Flex Real-Time PCR System (Qiagen). U6 (housekeeping gene) was used as an endogenous control for RNA input and normalisation. The bars represent the densitometric mean ± SEM from 3 independent experiments.

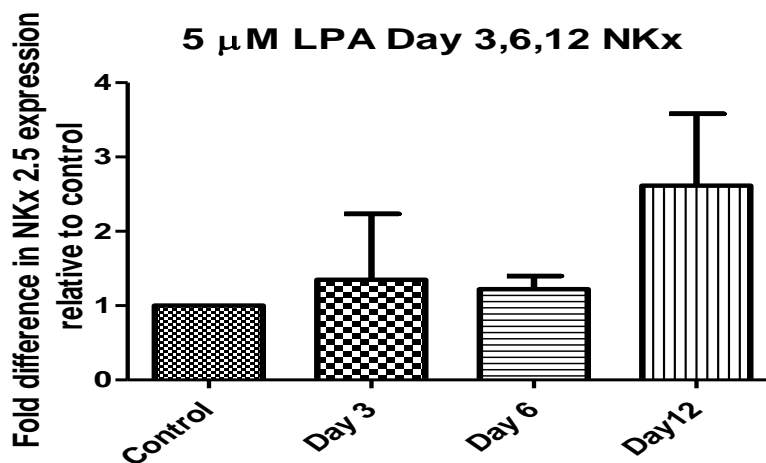


**Figure 3.35: Expression of NKX2.5 induced by 5μM of LPA at different time points.**

Monolayers of P19 cells were trypsinised and seeded in Petri-dishes to form EB. During this stage, cells were either incubated with medium alone (Controls) or treated with 5μM of LPA. Formed EBs were subsequently plated in tissue culture grade plates after four days and allowed to grow into monolayers. Lysates were generated on day 3, 6, & 12. RNA was then extracted and transcribed into a cDNA, and NKX2.5 gene was amplified and analysed using

SYBR-green dye by QuantStudio™ 7 Flex Real-Time PCR System (Qiagen). U6 (housekeeping gene) was used as an endogenous control for RNA input and normalisation. The bars represent the densitometric mean ± SEM from 3 independent experiments.

### 3.5.3 mir-145

Lysates collected at day three from cells treated with increasing concentration of LPA showed an increase in mir-145 expression, which was highest at 20µM (1.96 ± 0.91 folds; Figure 3.36A). At day 6, mir-145 expression was maximal with 5µM LPA (P<0.5) but declined back to near basal levels at 10µM and 20µM (Figure 3.36B). There was also a significant variation between 2 and 5µM of LPA (P<0.01) (Figure 3.36B). The trend at day 12 (Figure 3.36C) reflect a decrease in mir-145 with concentrations of LPA up to 10µM. There were, however, variations in the data as reflected by the standard errors and there was, therefore, no statistical difference when compared to controls. Expression of mir-145 in LPA 5µM treated cells over the days 3, 6, and 12 were compared, and it was the highest at day 6 with statistical significance (Figure 3.37).

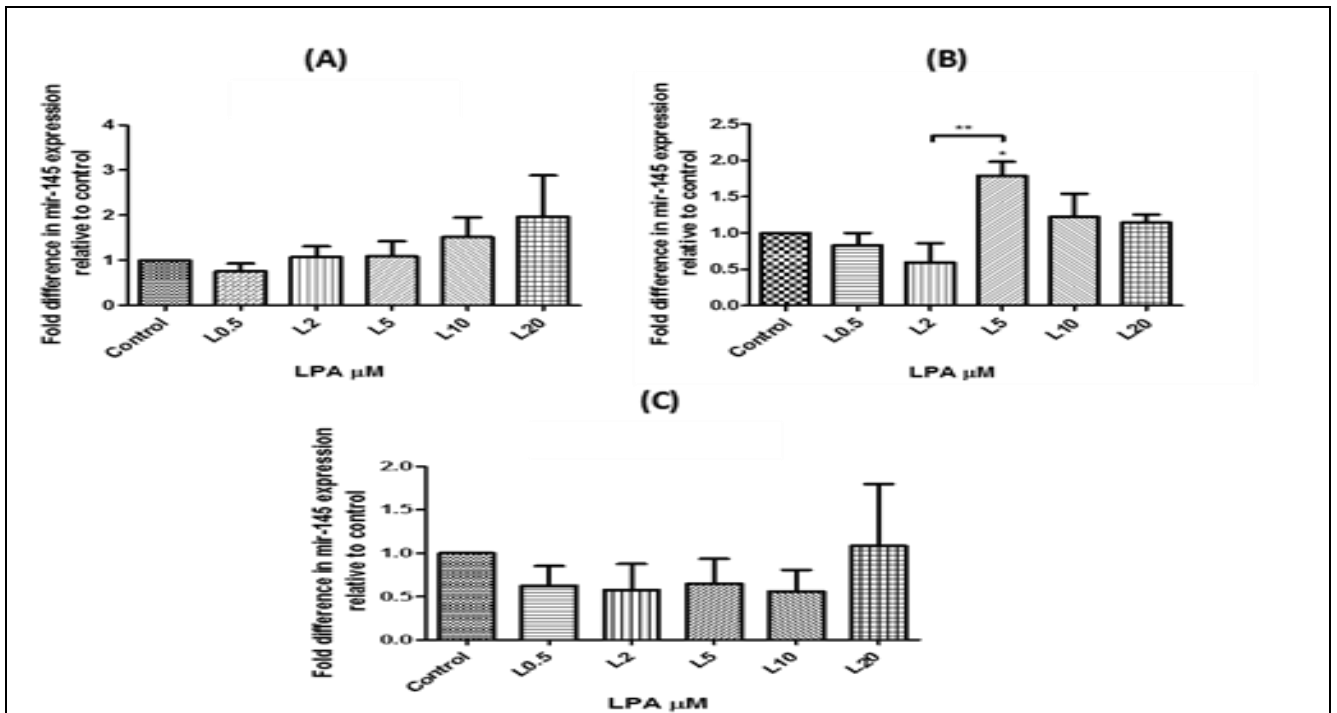


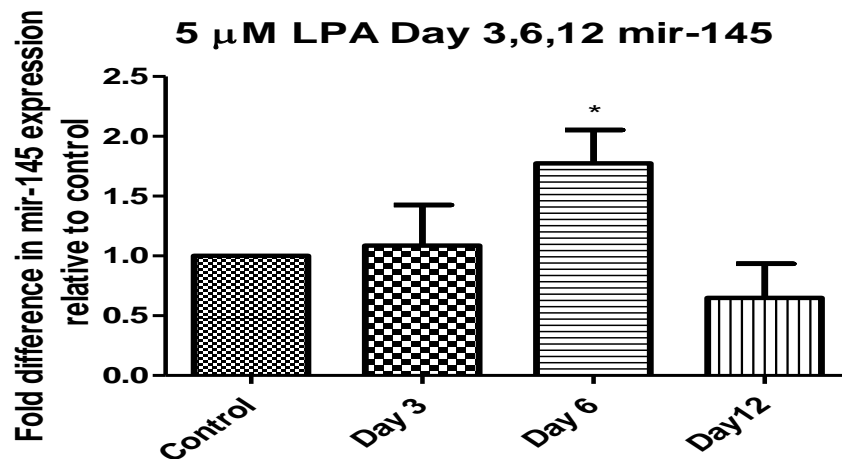
**Figure 3.36: Expression of mir-145 induced by LPA at different time points and concentrations.**

Monolayers of P19 cells were trypsinised and seeded in Petri-dishes to form EB. During this stage, cells were either incubated with medium alone (Controls) or treated with LPA at 0.5µM - 20µM. Formed EBs were subsequently plated in tissue culture grade plates after four days and allowed to grow into monolayers. Lysates were generated on day 3 (A), 6 (B), 12 (C). RNA was then extracted and transcribed into a cDNA, and mir-145 gene was amplified and analysed using SYBR-green dye by QuantStudio™ 7 Flex Real-Time PCR System (Qiagen). U6 (housekeeping gene) was used as an endogenous control for RNA input and normalisation. The densitometric represents mean ± SEM from 3 independent experiments. One-way analysis of variance (ANOVA) method was used to extract statistical information. \* P value of <0.5 and \*\* p<0.01.

**Figure 3.37:**  
**Expression of mir-145 induced by 5 $\mu$ M of LPA at different time points.**

Monolayers of P19 cells were trypsinised and seeded in Petri-dishes to form EBs. During this stage, cells were either incubated with medium alone (Controls) or treated with 5 $\mu$ M of LPA.

Formed EBs were subsequently plated in tissue culture grade plates after four days and allowed to grow into monolayers. Lysates were generated on day 3, 6, & 12. RNA was then extracted and transcribed into a cDNA, and mir-145 gene was amplified and analysed using SYBR-green dye by QuantStudio™ 7 Flex Real-Time PCR System (Qiagen). U6 (housekeeping gene) was used as an endogenous control for RNA input and normalisation. The bars represent the densitometric mean  $\pm$  SEM from 3 independent experiments. One-way analysis of variance (ANOVA) method was used to extract statistical information. The \* denotes a P value of  $p < 0.5$  compared to control.



### 3.5.4 mir-1

mir-1 gene was found to increase in response to increasing concentrations of LPA at days three and six but not at day 12 where levels of mir-1 gene were not significantly different to controls. The increases at day 3 were evident with 2-10 $\mu$ M LPA ( $p < 0.5$ ) (Figure 3.38A). At day six, the increase with 20 $\mu$ M was just below statistical significance while responses to 5 $\mu$ M appeared to be significant when compared to controls and the latter was statistically variant between 2 and 20 $\mu$ M of LPA treated cells (Figure 3.38B). At day 12, mir-1 showed no variation in comparison to control contrary to day 3 and 6 (Figure 3.38C). Additionally, expression of mir-1 in LPA 5 $\mu$ M treated cells over the days 3, 6, and 12 were compared, and it was the highest at day 6 with statistical significance (Figure 3.39).

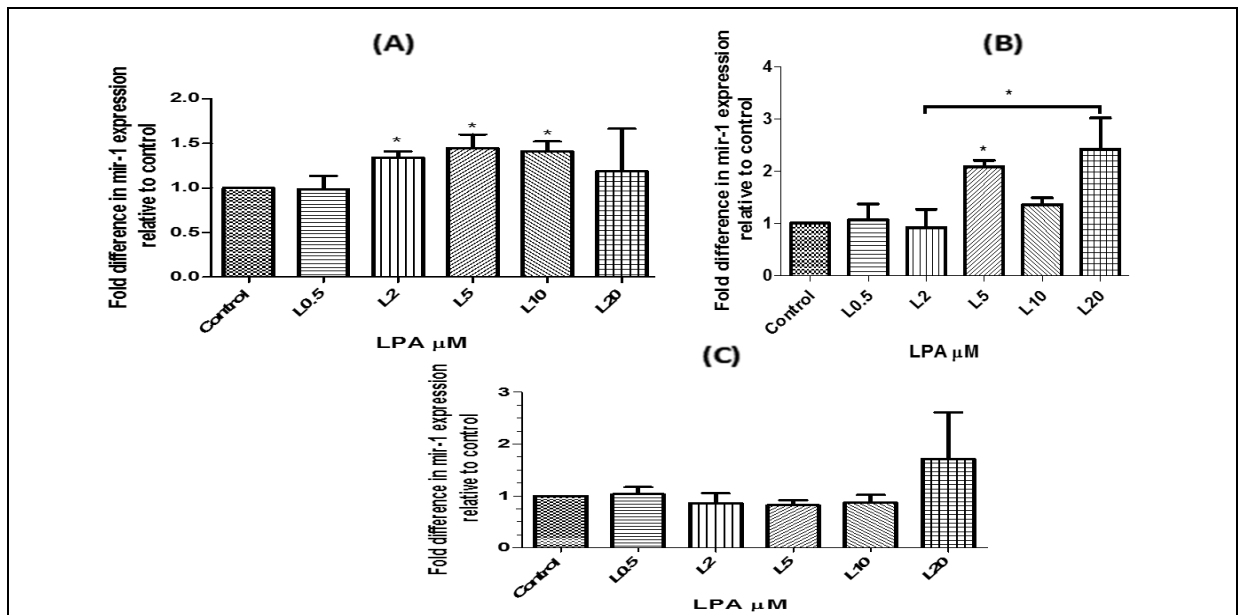


**Figure 3.38: Expression of mir-1 induced by LPA at different time points and concentrations.**

Monolayers of P19 cells were trypsinised and seeded in Petri-dishes to form EBs. During this stage, cells were either incubated with medium alone (Controls) or treated with LPA at 0.5 $\mu$ M- 20 $\mu$ M. Formed EBs were subsequently plated in tissue culture grade plates after four days and allowed to grow into monolayers. Lysates were generated on day 3 (A), 6 (B), 12 (C). RNA was then extracted and transcribed into a cDNA, and mir-1 gene was amplified and analysed using SYBR-green dye by QuantStudio™ 7 Flex Real-Time PCR System (Qiagen). U6 (housekeeping gene) was used as an endogenous control for RNA input and normalisation. The bars represent the densitometric mean  $\pm$  SEM from 3 independent experiments. One-way analysis of variance (ANOVA) method was used to extract statistical information. The \* denotes a P value of  $p < 0.5$  compared to control.

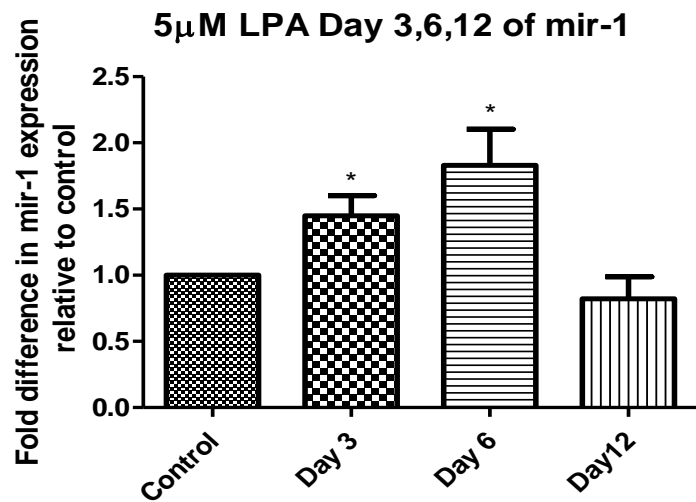
**Figure 3.39: Expression of mir-1 induced by 5 $\mu$ M of LPA at different time points.**

Monolayers of P19 cells were trypsinised and seeded in Petri-dishes to form EBs. During this stage, cells were either incubated with medium alone (Controls) or treated with LPA at 0.5 $\mu$ M- 20 $\mu$ M. Formed EBs were subsequently plated in tissue culture grade plates after four days and allowed to grow into monolayers.

Lysates were generated on day 3 (A), 6 (B), 12 (C). RNA was then extracted and transcribed into a cDNA, and mir-1 gene was amplified and analysed using SYBR-green dye by

QuantStudio™ 7 Flex Real-Time PCR System (Qiagen). U6 (housekeeping gene) was used as an endogenous control for RNA input and normalisation.

The bars represent the densitometric mean  $\pm$  SEM from 3 independent experiments. One-way analysis of variance (ANOVA) method was used to extract statistical information. The \* denotes a P value of  $p < 0.5$  compared to control.



## **3.6 Effects of pharmacological inhibitors of LPA receptors on the induction of differentiation: effects on protein and mRNA expression**

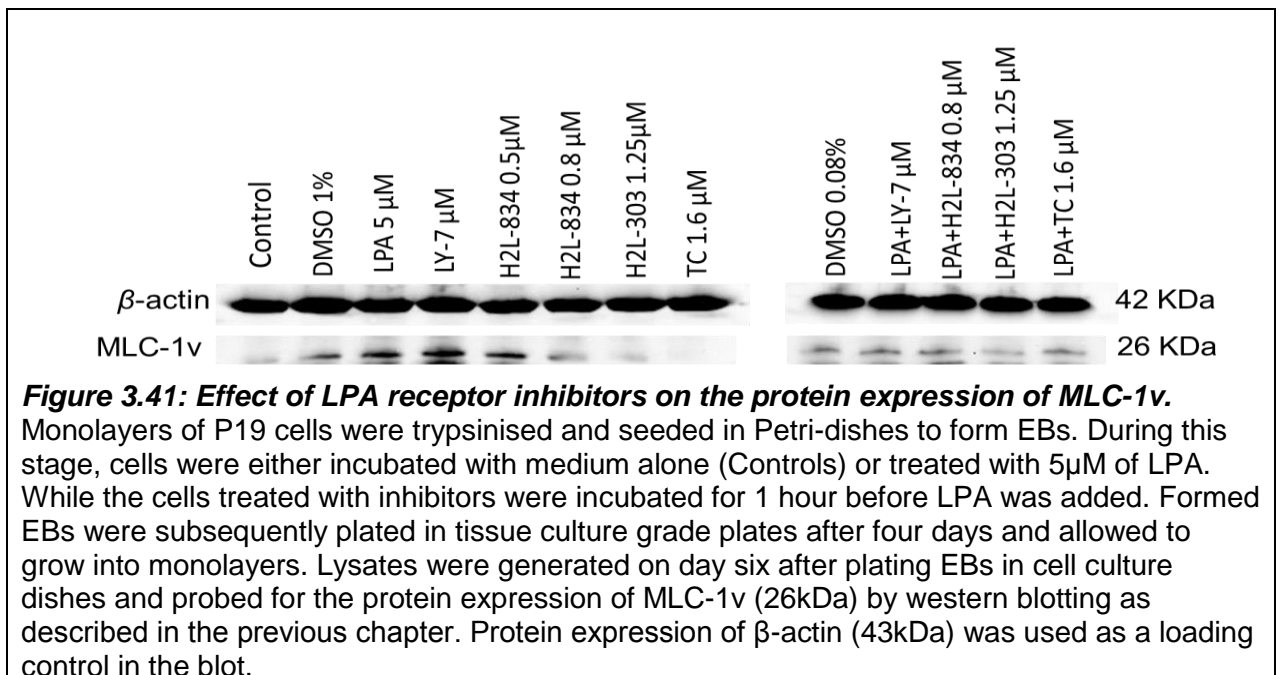
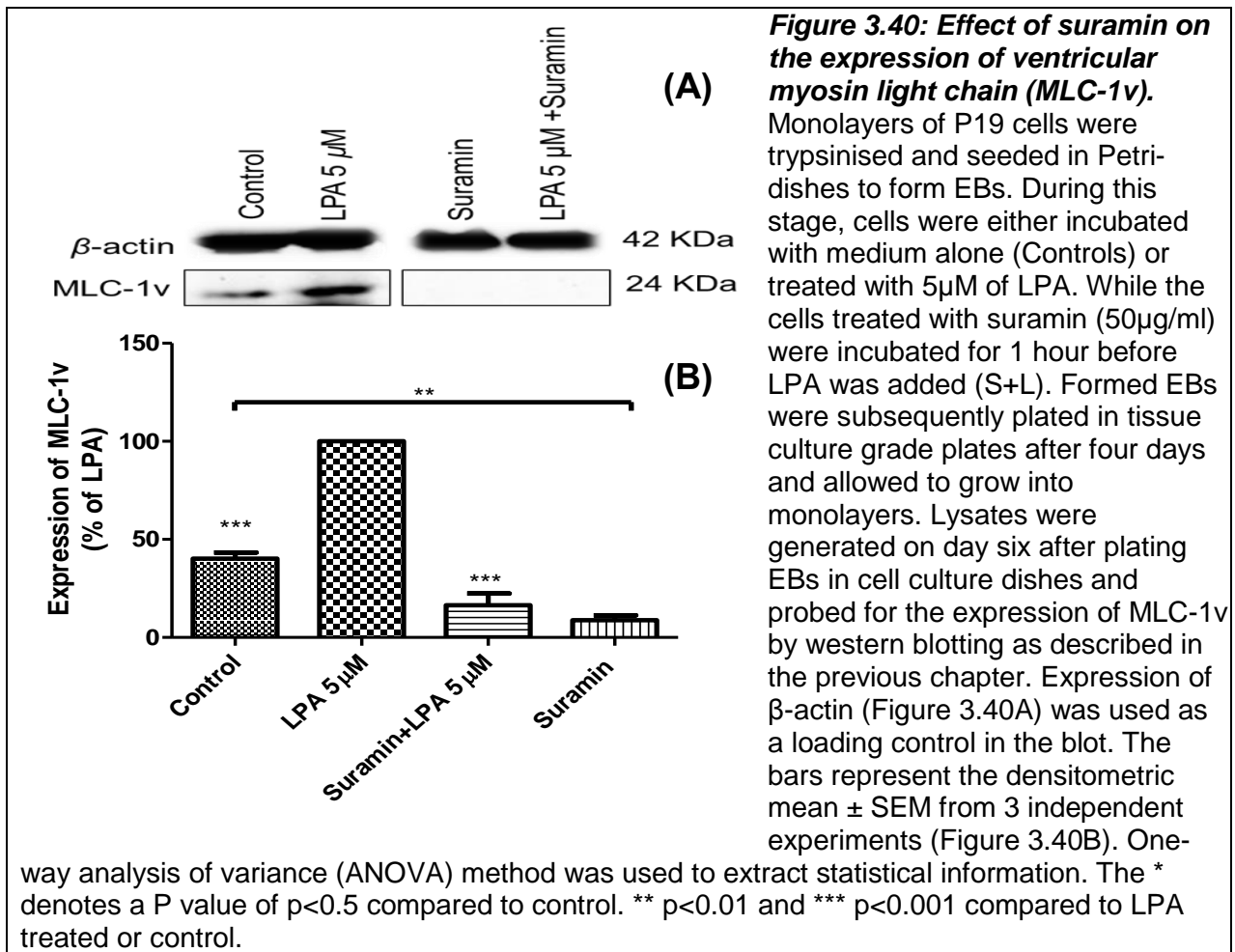
In this section, results are focused on the impact of Suramin, H2L5765834, H2L5186303, and TC-LPA5-4 to target specific binding sites of LPA receptors to block activation of differentiation induced by 5µM. Suramin using 50µg/ml to target LPA receptor 4, H2L5765834 using 0.5µM to target LPA receptor 1 & 5, 0.8µM to target LPA receptor 3 in addition to LPA receptors 2 & 3 to be antagonised by H2L5186303 with a concentration of 1.25µM. Finally, a 1.6µM of TC-LPA5-4 was to antagonise LPA receptor 5. The effects of these compounds on the yield of specific antibodies and mRNA/miRNA were determined by either western blotting or qPCR, followed by a statistical analysis via a one-way analysis of variance (ANOVA).

### **3.6.1 Effects of LPA receptors antagonists on protein expression**

Experiments were carried out to investigate whether the LPA receptor antagonists altered the protein expression of MLC-1v, OCT4, and GATA4. This was assessed by western blot analysis and compared qualitatively and quantitatively in graphs and statistical analysis.

#### **Effect of LPA receptors inhibitors on MLC-1v expression**

Suramin significantly inhibited the expression of MLC-1v in cells treated with LPA (5µM). Interestingly suramin also appeared to suppress the basal expression of MLC-1v in controls (Figure 3.40). In contrast to suramin, Cells treated with H2L5765834 by itself showed a slight increase in expression of MLC-1v compared to control but had no significant effect on LPA induced MLC-1v protein expression (Figures 3.41 and 3.42). Similarly, H2L5186303 (1.25µM) did not affect either the basal nor LPA induced MLC-1v expression (Figures 3.41 and 3.43). TC-LPA5-4 (1.6µM) on the other hand, did not affect basal levels of MLC-1v but suppressed LPA-induced expression of MLC. Thus, it was marginal but significant when compared to the LPA response (Figures 3.41 and 3.44).



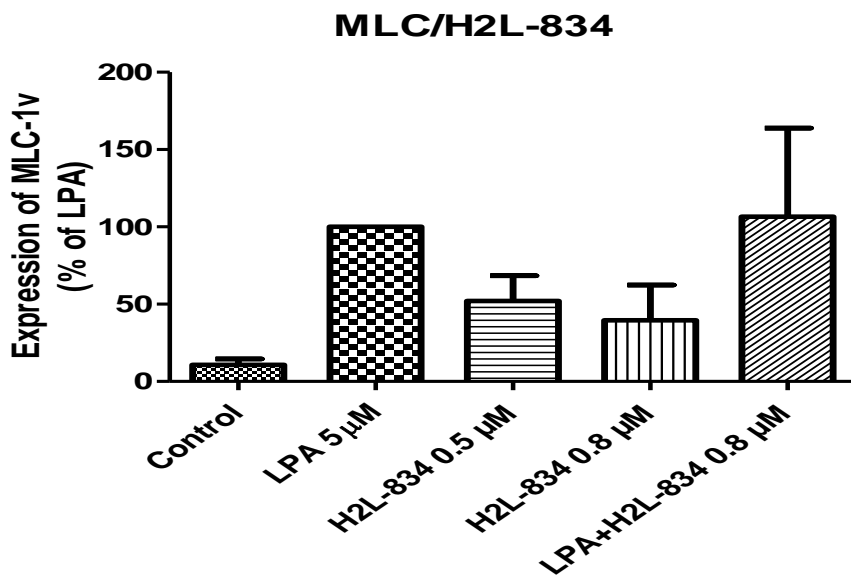


**Figure 3.42: Effect of H2L5765834 on the protein expression of MLC-1v.**

Monolayers of P19 cells were trypsinised and seeded in Petri-dishes to form EBs. During this stage, cells were either incubated with medium alone (Controls) or treated with 5 $\mu$ M of LPA. While the cells treated with H2L5765834 (0.5 & 0.8 $\mu$ M) were incubated for 1 hour before LPA was added. Formed EBs were subsequently

plated in tissue culture grade plates after four days and allowed to grow into monolayers. Lysates were generated on day six after plating EBs in cell culture dishes and probed for the expression of MLC-1v by western blotting as described in the previous chapter. Expression of  $\beta$ -actin (Figure 3.41) was used as a loading control in the blot. The bars represent the densitometric mean  $\pm$  SEM from 3 independent experiments.

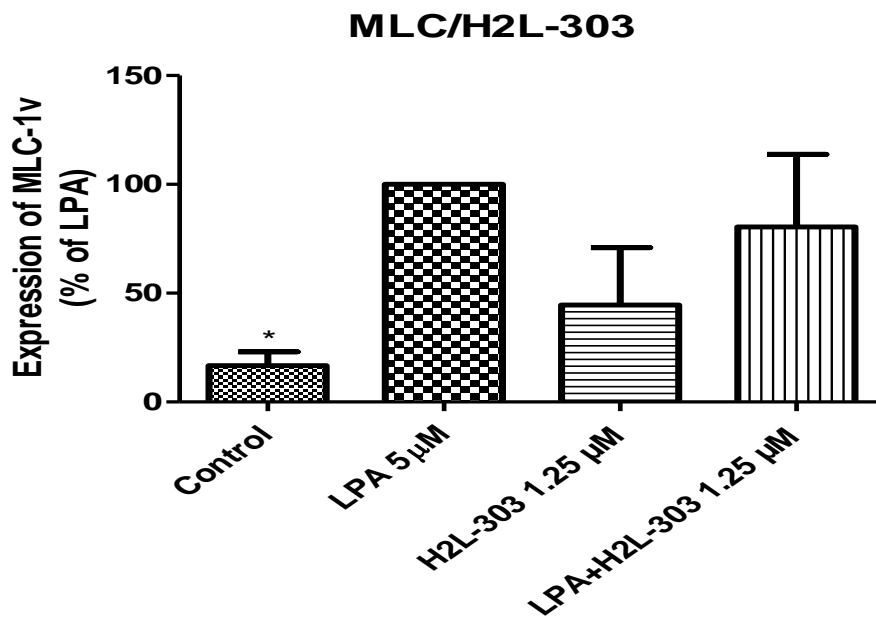
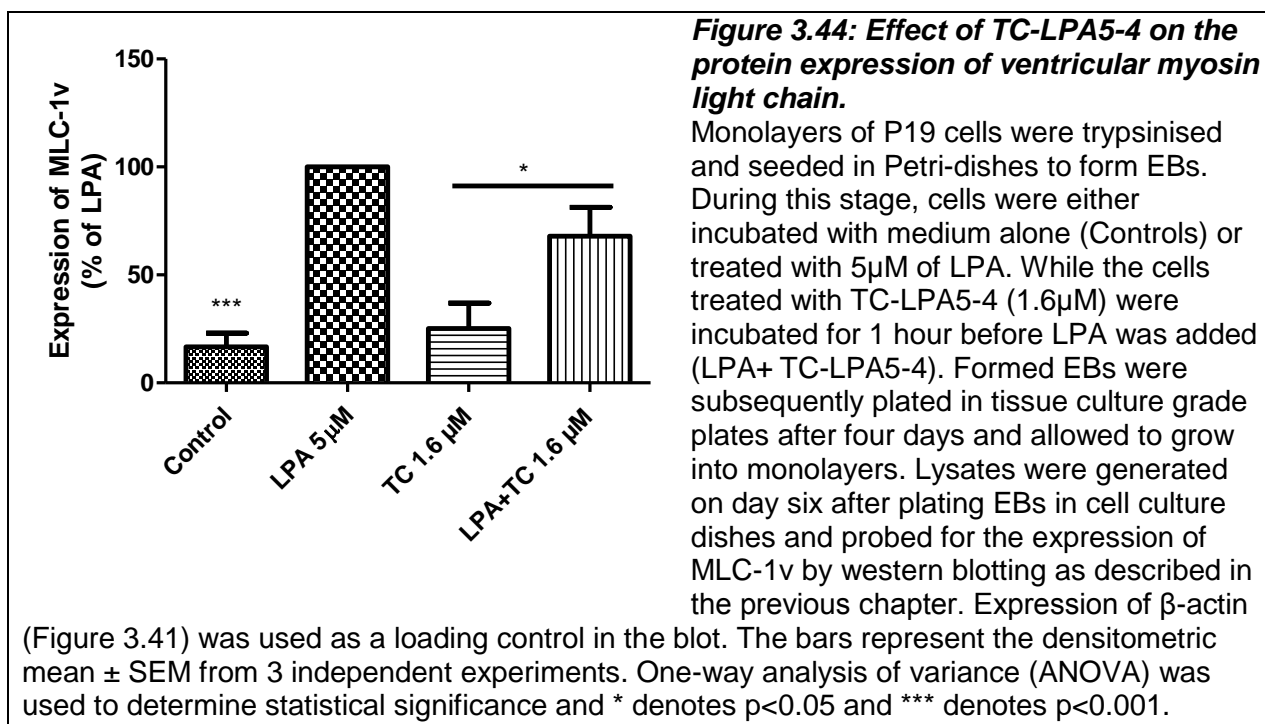


**Figure 3.43: Effect of H2L5186303 on the protein expression of MLC-1v.**

Monolayers of P19 cells were trypsinised and seeded in Petri-dishes to form EBs. During this stage, cells were either incubated with medium alone (Controls) or treated with 5 $\mu$ M of LPA. While the cells treated with H2L5186303 (1.25 $\mu$ M) were incubated for 1 hour before LPA was added. Formed EBs were subsequently

plated in tissue culture grade plates after four days and allowed to grow into monolayers. Lysates were generated on day six after plating EBs in cell culture dishes and probed for the expression of MLC-1v by western blotting as described in the previous chapter. Expression of  $\beta$ -actin (Figure 3.41) was used as a loading control in the blot. The bars represent the densitometric mean  $\pm$  SEM from 3 independent experiments. One-way analysis of variance (ANOVA) method was used to extract statistical information, and the \* denotes  $p < 0.05$  compared to LPA treated bar.



### Effect of LPA receptors inhibitors on OCT4 expression

In these studies, changes in OCT4 expression was investigated. The data in Figure 3.45 shows that OCT4 expression was enhanced in controls and suppressed following LPA treatment. The next sets of results are from cells treated with or without H2L5765834, H2L5186303, or TC-LPA5-4. Of these three compounds, H2L5765834 partially reversed the suppression of OCT4 caused by LPA (Figures 3.45 and 3.46), but this was not statistically significant due to some degree of variability in the mean data except for LPA, presumably due to the small n numbers. H2L5186303 (Figures 3.45 and 3.47) and TC-LPA5-4 (Figures 3.45 and 3.48) on the other hand reversed the suppression of OCT4 caused by LPA, bringing levels back to those seen in controls, and this was statistically significant. Neither inhibitor had any effect on control OCT4 levels when applied on their own.

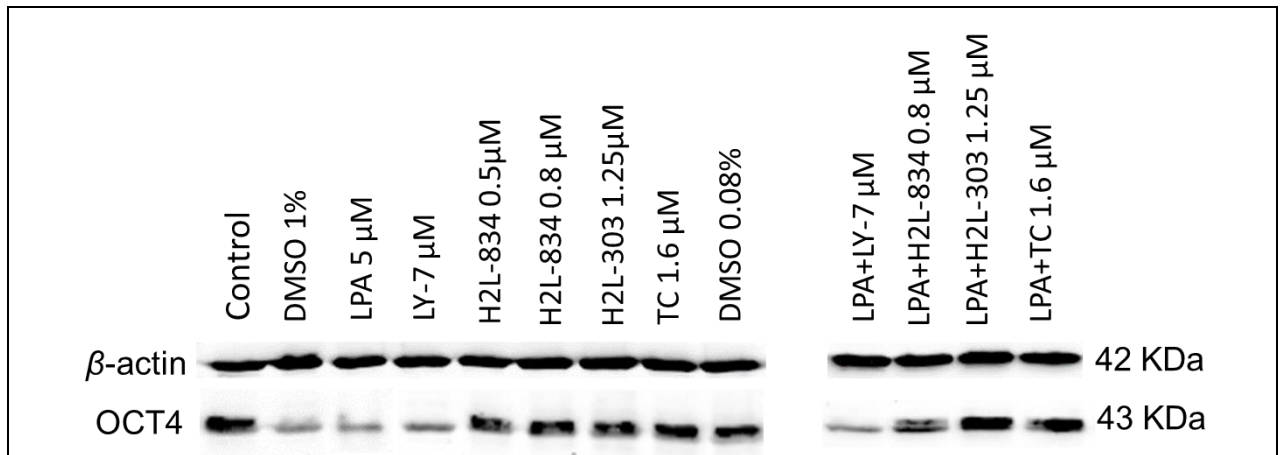


**Figure 3.45: Effect of LPAR inhibitors on the expression of OCT4.**

Monolayers of P19 cells were trypsinised and seeded in Petri-dishes to form EBs. During this stage, cells were either incubated with medium alone (Controls) or treated with 5 $\mu$ M of LPA. While the cells treated with inhibitors were incubated for 1 hour before LPA was added. Formed EBs were subsequently plated in tissue culture grade plates after four days and allowed to grow into monolayers. Lysates were generated on day six after plating EBs in cell culture dishes and probed for the protein expression of OCT4 (43kDa) by western blotting as described in the previous chapter. Protein expression of  $\beta$ -actin (43kDa) was used as a loading control in the blot.

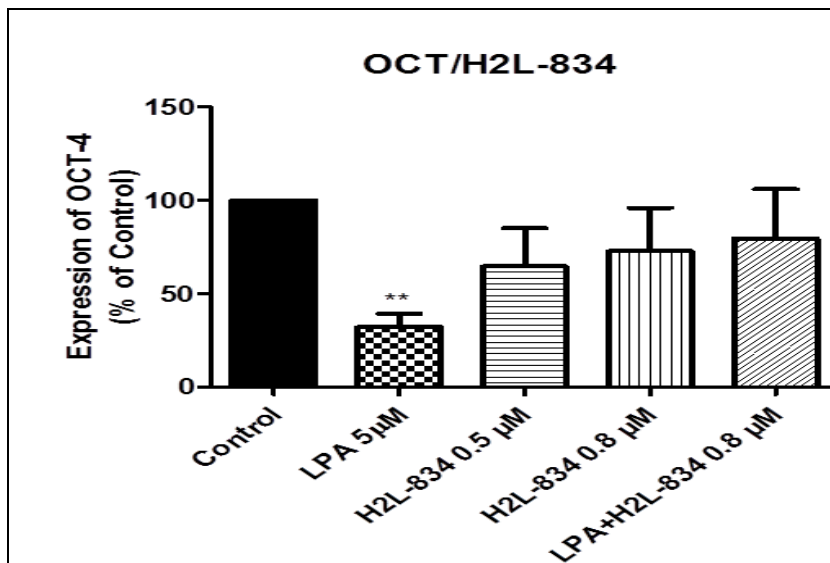


**Figure 3.46: Effect of H2L5765834 on the protein expression of OCT4.**

Monolayers of P19 cells were trypsinised and seeded in Petri-dishes to form EBs. During this stage, cells were either incubated with medium alone (Controls) or treated with 5 $\mu$ M of LPA. While the cells treated with H2L5765834 (0.5 & 0.8 $\mu$ M) were incubated for 1 hour before LPA was added. Formed EBs were subsequently plated in tissue culture grade plates after

four days and allowed to grow into monolayers. Lysates were generated on day six after plating EBs in cell culture dishes and probed for the protein expression of OCT4 (43kDa) by western blotting as described in the previous chapter. Protein expression of  $\beta$ -actin (Figure 3.45) was used as a loading control in the blot. The bars represent the densitometric mean  $\pm$  SEM from 3 independent experiments. One-way analysis of variance (ANOVA) was used to determine statistical significance, and \*\* denotes  $p < 0.01$  compared to control.

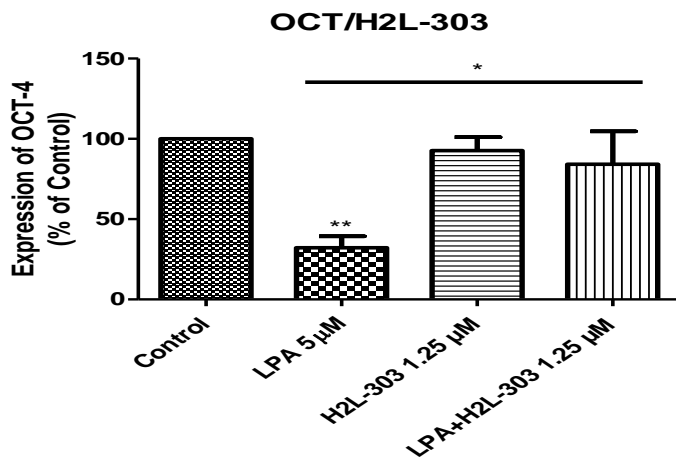


**Figure 3.47: Effect of H2L5186303 on the protein expression of OCT4.**

Monolayers of P19 cells were trypsinised and seeded in Petri-dishes to form EBs. During this stage, cells were either incubated with medium alone (Controls) or treated with 5 $\mu$ M of LPA. While the cells treated with H2L5186303 (1.25 $\mu$ M) were incubated for 1 hour before LPA was added. Formed EBs were subsequently plated in tissue culture grade plates after four days and allowed to grow into

monolayers. Lysates were generated on day six after plating EBs in cell culture dishes and probed for the protein expression of OCT4 (43kDa) by western blotting as described in the previous chapter. Expression of  $\beta$ -actin (Figure 3.45) was used as a loading control in the blot. The bars represent the densitometric mean  $\pm$  SEM from 3 independent experiments. One-way analysis of variance (ANOVA) was used to determine statistical significance and \* denotes  $p < 0.05$  and \*\* denote  $p < 0.01$  compared to control.

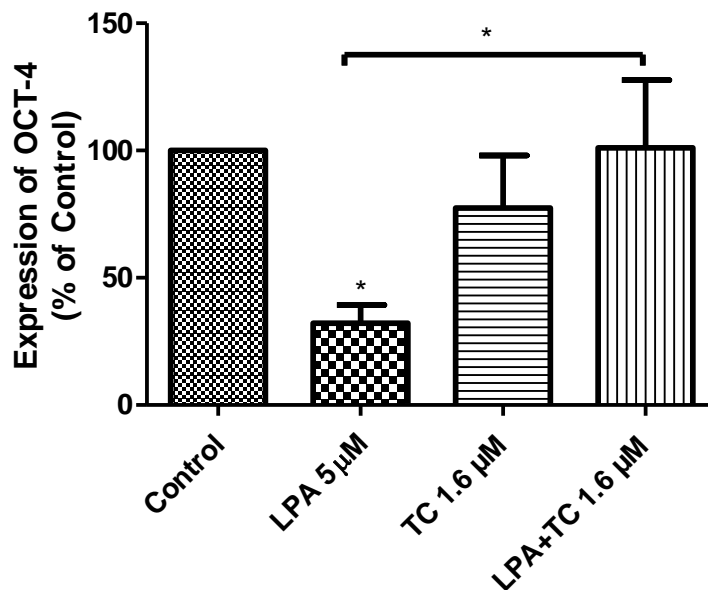


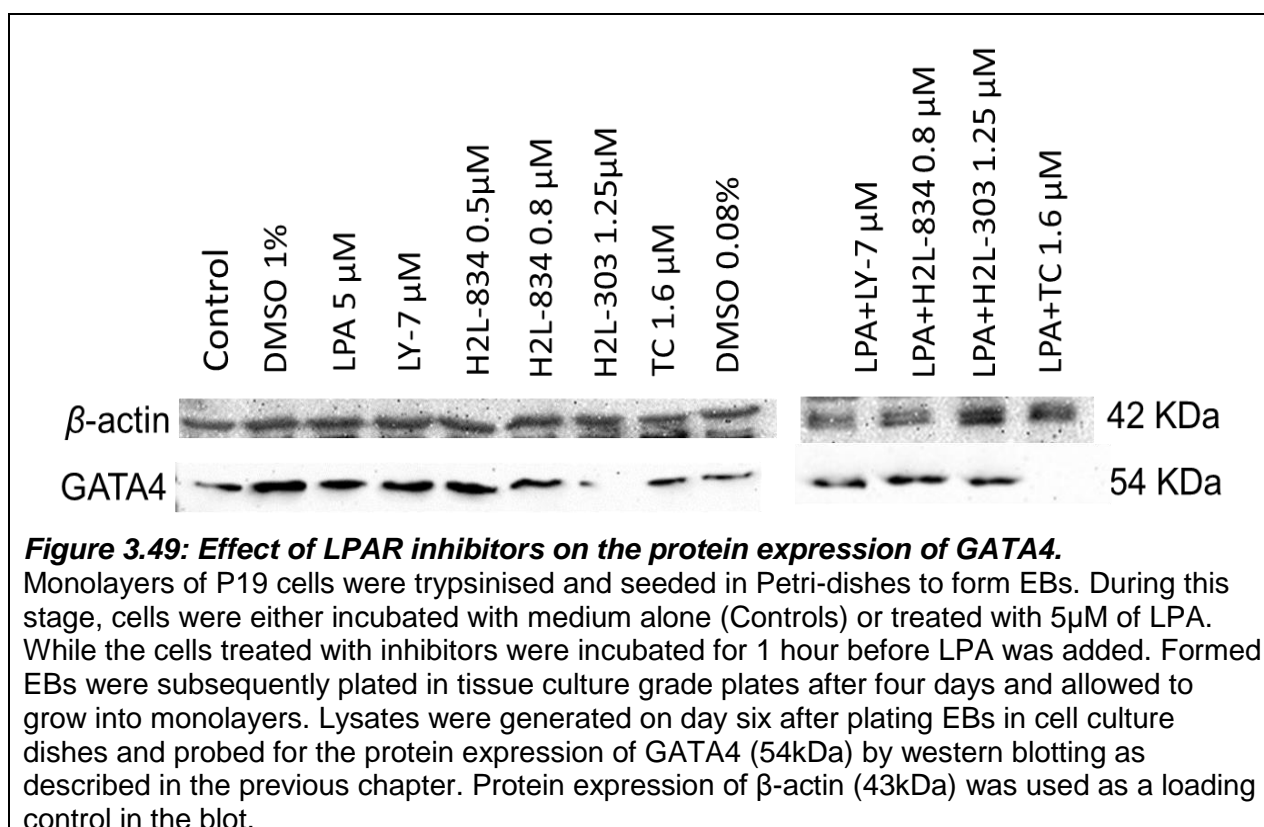
**Figure 3.48: Effect of TC-LPA5-4 on the protein expression of OCT4.**

Monolayers of P19 cells were trypsinised and seeded in Petri-dishes to form EBs. During this stage, cells were either incubated with medium alone (Controls) or treated with 5 $\mu$ M of LPA. While the cells treated with TC-LPA5-4 (1.6 $\mu$ M) were incubated for 1 hour before LPA was added. Formed EBs were subsequently plated in tissue culture grade plates after four days and allowed to grow into monolayers. Lysates were generated on day six after plating EBs in cell culture dishes and probed for the protein expression

of OCT4 (43kDa) by western blotting as described in the previous chapter. Protein expression of  $\beta$ -actin (Figure 3.45) was used as a loading control in the blot. The bars represent the densitometric mean  $\pm$  SEM from 3 independent experiments. One-way analysis of variance (ANOVA) was used to determine statistical significance, and \* denotes  $p < 0.05$  compared to control.

## Effect of LPA receptors inhibitors on GATA4 expression

In parallel with the studies above, changes in GATA4 expression was also investigated. In contrast to OCT4, GATA4 expression was relatively low under control conditions but enhanced in the presence of LPA (5 $\mu$ M) as demonstrated on the blot (Figure 3.49). Similar trends were also observed with H2L5765834 (Figure 3.50), H2L5186303 (Figure 3.51) and TC-LPA5-4 (Figure 3.52) which on their own appeared to enhance GATA4 expression but also suppressed that induced by LPA, with a statistical significance only for TC-LPA5-4 respectively. There was, however, significant variability in the data for each compound when applied alone, making it necessary to increase the n values in future studies to confirm statistical significance.



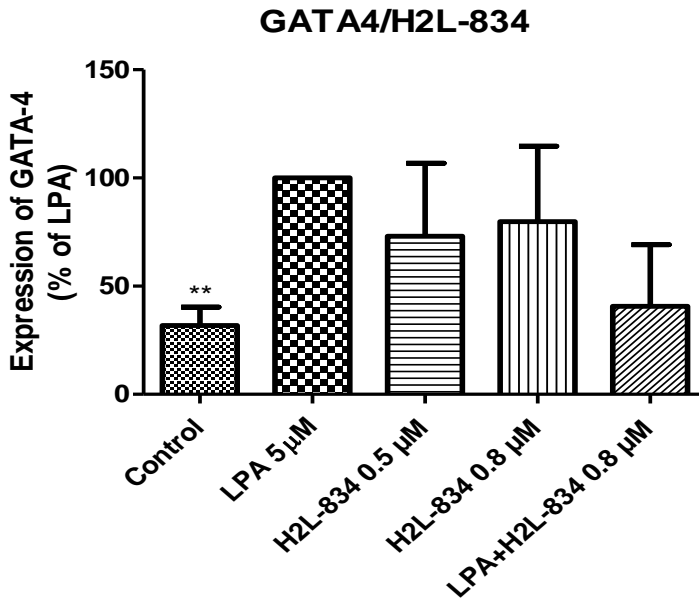


**Figure 3.50: Effect of H2L5765834 on the protein expression of GATA4.**

Monolayers of P19 cells were trypsinised and seeded in Petri-dishes to form EBs. During this stage, cells were either incubated with medium alone (Controls) or treated with 5μM of LPA. While the cells treated with H2L5765834 (0.5 & 0.8μM) were incubated for 1 hour before LPA was added. Formed EBs were subsequently plated in tissue culture grade plates after four days and allowed to grow into monolayers. Lysates were generated on day six after plating EBs in cell culture dishes and probed for the protein expression of GATA4 by western blotting as described in the previous chapter.

Protein expression of β-actin (Figure 3.49) was used as a loading control in the blot. The bars represent the densitometric mean ± SEM from 3 independent experiments. One-way analysis of variance (ANOVA) was used to determine statistical significance, and \*\* denote p<0.01 compared to LPA treated bar.

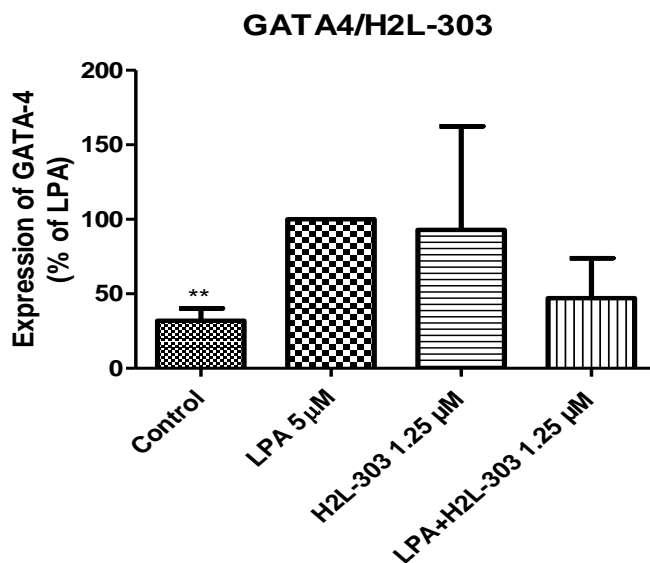


**Figure 3.51: Effect of H2L5186303 on the protein expression of GATA4.**

Monolayers of P19 cells were trypsinised and seeded in Petri-dishes to form EBs. During this stage, cells were either incubated with medium alone (Controls) or treated with 5μM of LPA. While the cells treated with H2L5186303 (1.25μM) were incubated for 1 hour before LPA was added. Formed EBs were subsequently plated in tissue culture grade plates after four days and allowed to grow into monolayers. Lysates were generated on day six after plating EBs in cell culture dishes and probed for the protein expression of GATA4 by western blotting as described in the previous chapter.

Protein expression of β-actin (Figure 3.49) was used as a loading control in the blot. The bars represent the densitometric mean ± SEM from 3 independent experiments. One-way analysis of variance (ANOVA) was used to determine statistical significance, and \*\* denote p<0.01 compared to LPA treated bar.

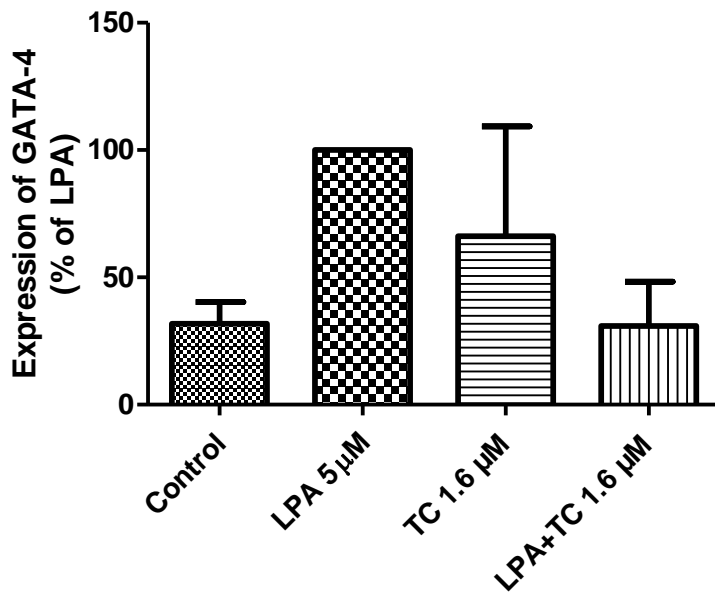


**Figure 3.52: Effect of TC-LPA5-4 on the Protein expression of GATA4.**

Monolayers of P19 cells were trypsinised and seeded in Petri-dishes to form EBs. During this stage, cells were either incubated with medium alone (Controls) or treated with 5µM of LPA. While the cells treated TC-LPA5-4 (1.6µM) were incubated for 1 hour before LPA was added. Formed EBs were subsequently plated in tissue culture grade plates after four days and allowed to grow into monolayers. Lysates were generated on day six after plating EBs in cell culture dishes and probed for the protein expression of GATA4 by western blotting as described in the previous chapter.

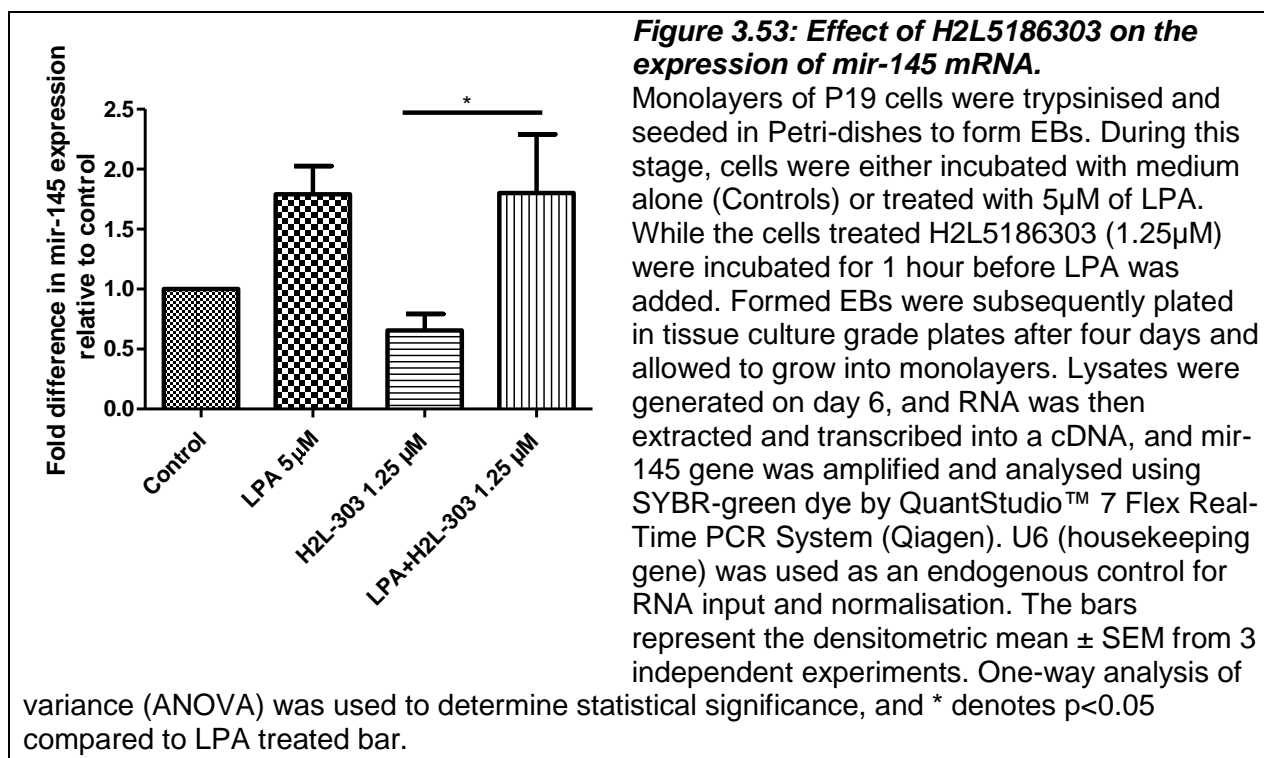
Protein expression of  $\beta$ -actin (Figure 3.49) was used as a loading control in the blot. The bars represent the densitometric mean  $\pm$  SEM from 3 independent experiments.

### 3.6.2 Effects of LPA receptors antagonists on mRNA expression:

Additional to the studies above, parallel experiments were carried out to investigate whether the LPA receptor antagonists altered the expression of miR-145, miR-1, miR-133, OCT4, and NKX2.5 at the mRNA level. Mir-145 and OCT4 were targeted due to their roles in stemness and pluripotency. While mir-1, mir-133, and NKX2.5 were targeted for their reported activities in cardiomyocytes.

#### Effect of LPA receptor antagonist on the mir-145 expression

As shown previously, the expression of mir-145 is statistically significantly higher in LPA-treated cells when compared to controls (Section 3.5.3.). Treatment with 1.25 $\mu$ M of H2L5186303 caused a marginal decrease in mir-145 expression, which was not statistically significant and had no obvious effect on the induction caused by LPA (Figure 3.53). This was also the case for H2L5765834 (0.5 & 0.8 $\mu$ M; Figure 3.54) and for TC LPA5 4 (1.6 $\mu$ M; Figure 3.55) which had little or no effect on basal and LPA-induced expression of mir-145 suggesting that this effect of LPA is independent of LPA receptors 1, 3 and 5.



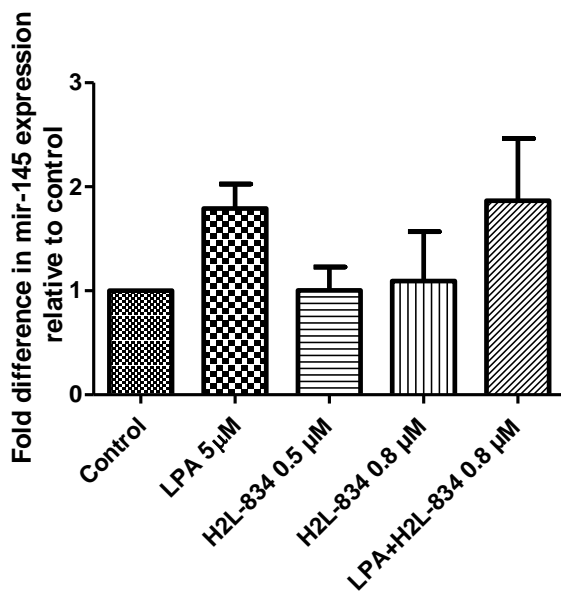


**Figure 3.54: Effect of H2L5765834 on the expression of mir-145.**

Monolayers of P19 cells were trypsinised and seeded in Petri-dishes to form EBs. During this stage, cells were either incubated with medium alone (Controls) or treated with 5µM of LPA. While the cells treated H2L5765834 (0.5 & 0.8µM) were incubated for 1 hour before LPA was added. Formed EBs were subsequently plated in tissue culture grade plates after four days and allowed to grow into monolayers. Lysates were generated on day 6 and RNA was then extracted and transcribed into a cDNA, and mir-145 gene was amplified and analysed using SYBR-green dye by QuantStudio™ 7 Flex Real-Time PCR System (Qiagen). U6 (housekeeping gene) was used as an endogenous control for RNA input and normalisation. The bars represent the densitometric mean ± SEM from 3 independent experiments.

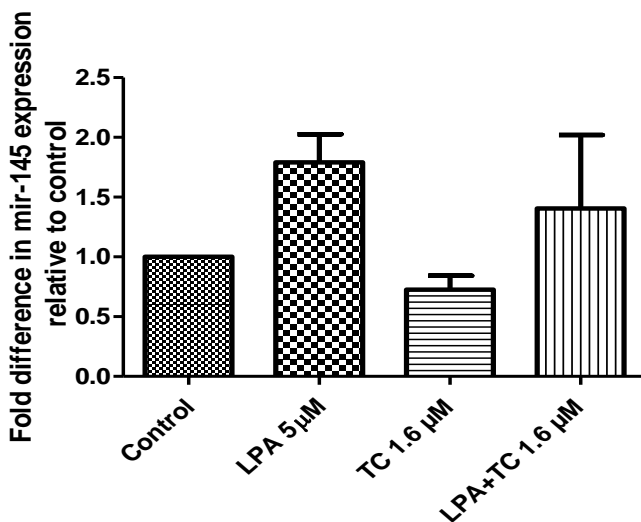


**Figure 3.55: Effect of TC-LPA5-4 on the expression of mir-145.**

Monolayers of P19 cells were trypsinised and seeded in Petri-dishes to form EBs. During this stage, cells were either incubated with medium alone (Controls) or treated with 5µM of LPA. While the cells treated TC-LPA5-4 (1.6µM) were incubated for 1 hour before LPA was added. Formed EBs were subsequently plated in tissue culture grade plates after four days and allowed to grow into monolayers. Lysates were generated on day 6 and RNA was then extracted and transcribed into a cDNA and mir-145 was amplified and analysed using SYBR-green dye by QuantStudio™ 7

Flex Real-Time PCR System (Qiagen). U6 (housekeeping gene) was used as an endogenous control for RNA input and normalisation. The bars represent the densitometric mean ± SEM from 3 independent experiments.

## Effect of LPA receptor antagonist on the mir-1 expression

Consistent with the data presented earlier (Section 3.5.4), the expression mir-1 was also higher compared to control, induced by LPA (5 $\mu$ M), but, with the exception that in the current experiment it was not significant (Figure 3.56). Additionally, all the inhibitors including H2L5186303 (1.25 $\mu$ M; Figure 3.56A), H2L5765834 (0.5 & 0.8 $\mu$ M; Figure 3.56B) and TC-LPA5-4 (1.6 $\mu$ M; Figure 3.56C) did not significantly alter or affect the basal levels of mir-1 but shows a partial decrease compared to LPA with the inhibitor

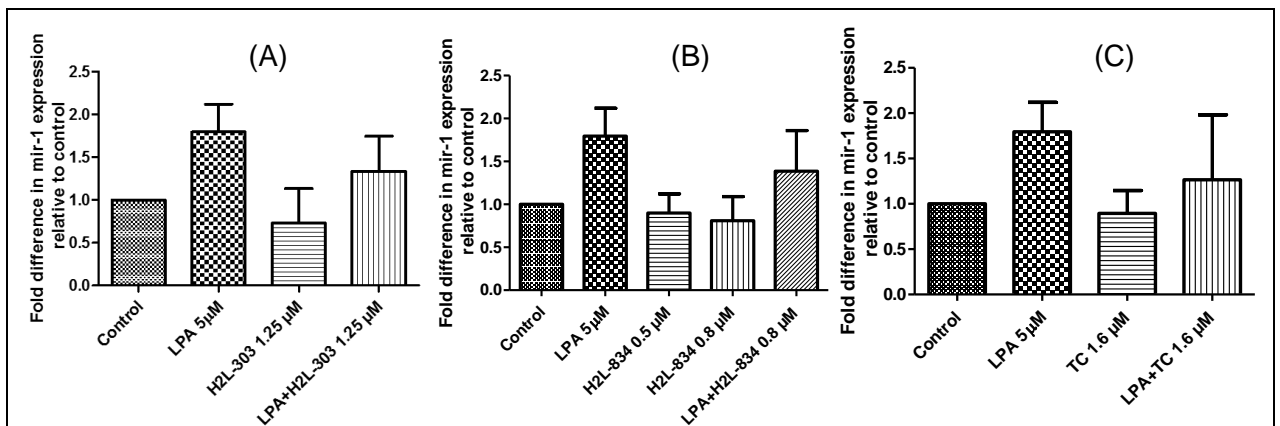
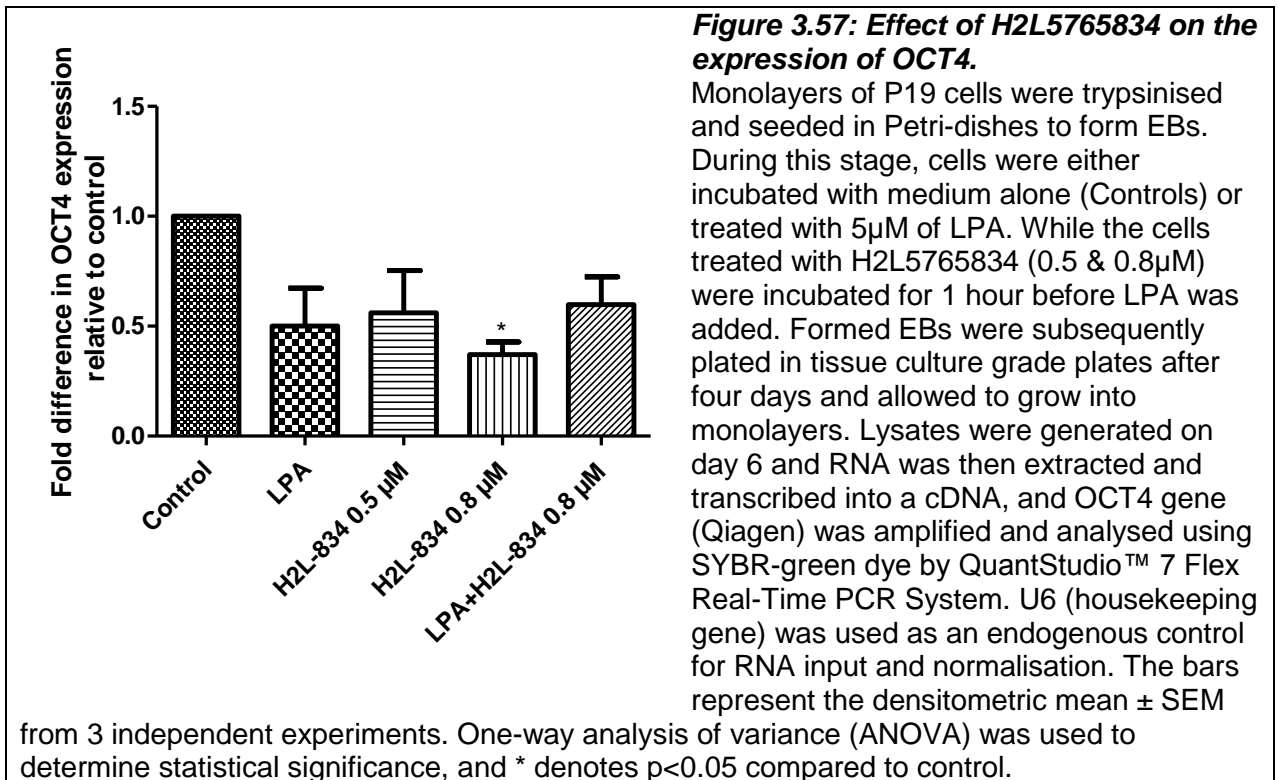


**Figure 3.56: Effect of LPA receptor antagonist on the expression of mir-1.**

Monolayers of P19 cells were trypsinised and seeded in Petri-dishes to form EBs. During this stage, cells were either incubated with medium alone (Controls) or treated with 5 $\mu$ M of LPA. While the cells treated H2L5186303 (1.25 $\mu$ M) (A), H2L5765834 (0.5 & 0.8 $\mu$ M) (B) and TC-LPA5-4 (1.6 $\mu$ M) (C) were incubated for 1 hour before LPA was added. Formed EBs were subsequently plated in tissue culture grade plates after four days and allowed to grow into monolayers. Lysates were generated on day 6 and RNA was then extracted and transcribed into a cDNA, and mir-1 gene was amplified and analysed using SYBR-green dye by QuantStudio™ 7 Flex Real-Time PCR System (Qiagen). U6 (housekeeping gene) was used as an endogenous control for RNA input and normalisation. The bars represent the densitometric mean  $\pm$  SEM from 3 independent experiments.

## Effect of LPA receptor antagonist on OCT4 expression

The basal expression of OCT4 was marginally significantly downregulated when P19 cells were treated with LPA (5 $\mu$ M) in this experiment. This expression of OCT4 was also suppressed by H2L5765834 (0.8 $\mu$ M) when added in the absence of LPA, but, the antagonist did not change or further enhance the inhibition caused by LPA (Figure 3.57). Similarly, H2L5186303 (1.25 $\mu$ M; Figure 3.58) and TC-LPA5-4 (1.6 $\mu$ M; Figure 3.59) slightly suppressed basal OCT4 protein expression, respectively but not statistically. Furthermore, H2L5186303 and TC-LPA5-4 did reverse the inhibition of OCT4 expression caused by LPA, but evidently by TC-LPA5-4 only compared to LPA treated cells. This reaction of the antagonist on the LPA receptor was not observed with H2L5765834.



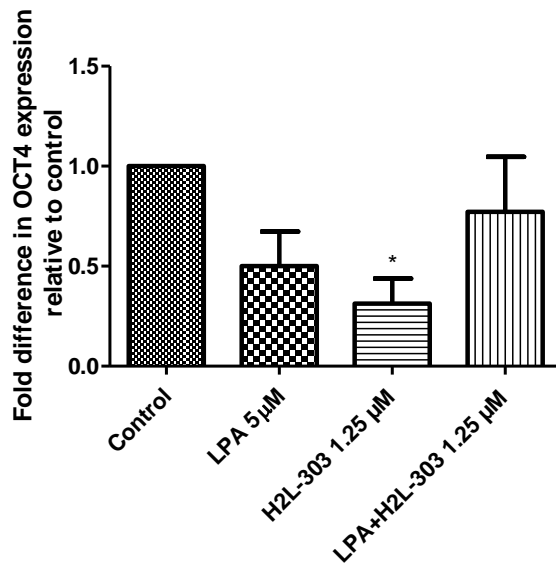


**Figure 3.58: Effect of H2L5186303 on the expression of OCT4.**

Monolayers of P19 cells were trypsinised and seeded in Petri-dishes to form EBs. During this stage, cells were either incubated with medium alone (Controls) or treated with 5 $\mu$ M of LPA. While the cells treated H2L5186303 (1.25 $\mu$ M) were incubated for 1 hour before LPA was added. Formed EBs were subsequently plated in tissue culture grade plates after four days and allowed to grow into monolayers. Lysates were generated on day 6 and RNA was then extracted and transcribed into a cDNA, and OCT4 gene was amplified and analysed using SYBR-green dye by QuantStudio™ 7 Flex Real-Time PCR System (Qiagen). U6 (housekeeping gene) was used as an endogenous control for RNA input and normalisation. The bars represent the

densitometric mean  $\pm$  SEM from 3 independent experiments. One-way analysis of variance (ANOVA) was used to determine statistical significance, and \* denotes  $p < 0.05$  compared to control.

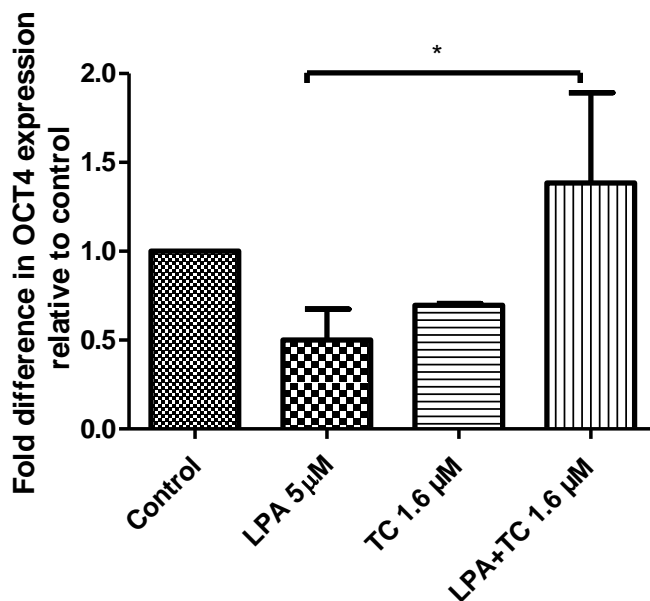


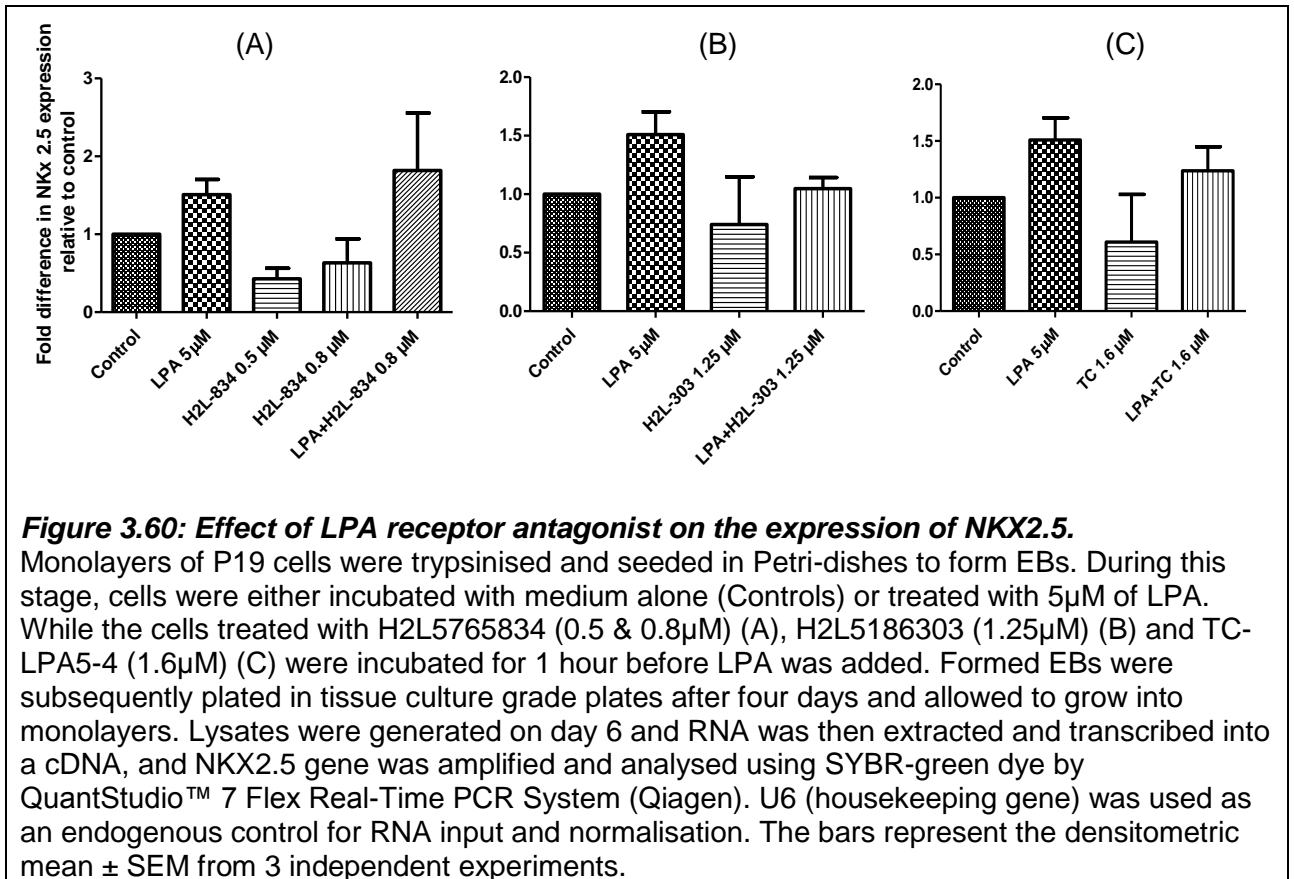
**Figure 3.59: Effect of TC-LPA5-4 on the expression of OCT4.**

Monolayers of P19 cells were trypsinised and seeded in Petri-dishes to form EBs. During this stage, cells were either incubated with medium alone (Controls) or treated with 5 $\mu$ M of LPA. While the cells treated with TC-LPA5-4 (1.6 $\mu$ M) were incubated for 1 hour before LPA was added. Formed EBs were subsequently plated in tissue culture grade plates after four days and allowed to grow into monolayers. Lysates were generated on day 6 and RNA was then extracted and transcribed into a cDNA, and OCT4 gene was amplified and analysed using SYBR-green dye by QuantStudio™ 7 Flex Real-Time PCR System (Qiagen). U6 (housekeeping gene) was used as

an endogenous control for RNA input and normalisation. The bars represent the densitometric mean  $\pm$  SEM from 3 independent experiments. One-way analysis of variance (ANOVA) was used to determine statistical significance, and \* denotes  $p < 0.05$  compared to LPA treated bar.

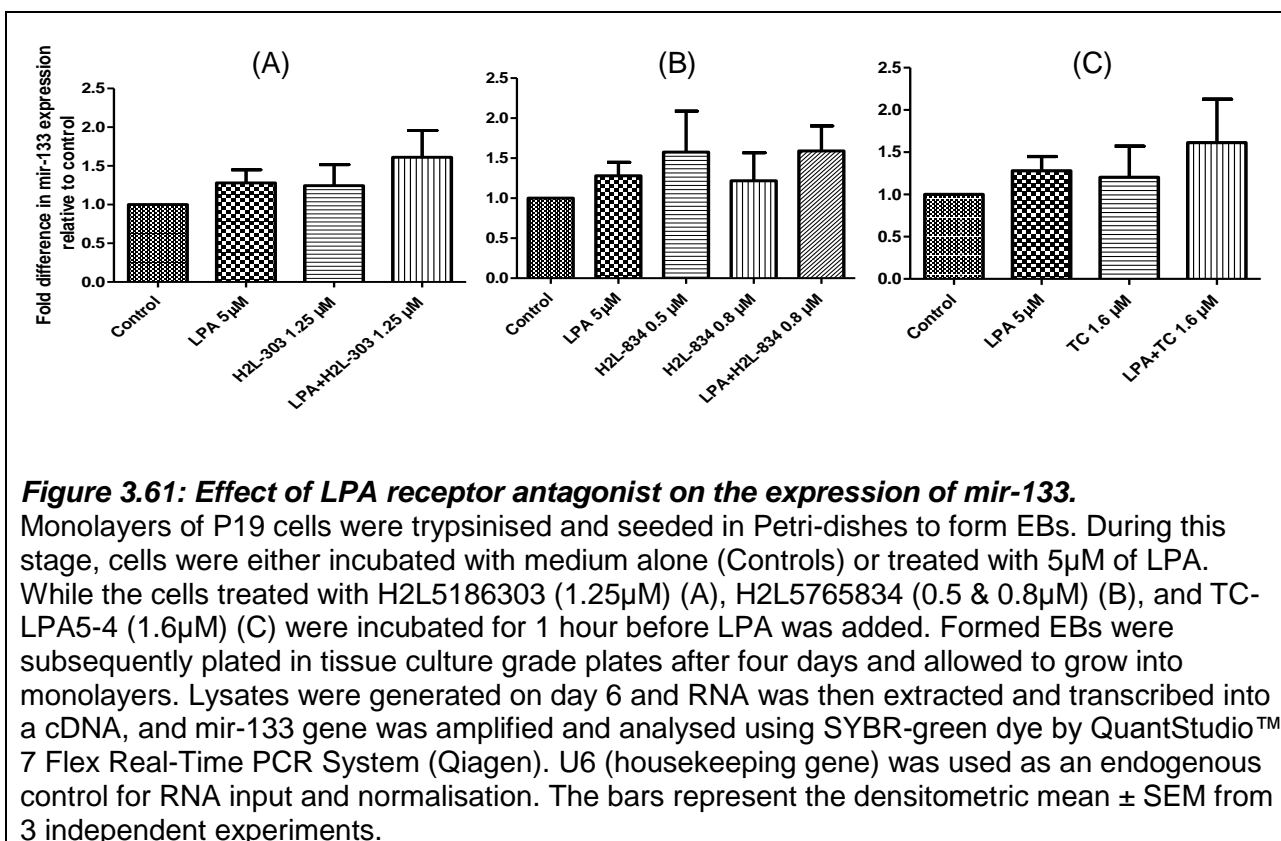
## Effect of LPA receptor antagonist on NKX 2.5 expression

LPA-treatment marginally enhanced the expression of NKX2.5 when compared to control (Figure 3.60). Treatment with H2L5765834 (0.5 & 0.8 $\mu$ M; Figure 3.60A) downregulated basal NKX2.5 expression, but this appeared to be statistically non-significant and marginal. H2L5765834 also had no significant effect on the LPA induced response (Figure 3.60A). H2L5186303 (1.25 $\mu$ M) on the other hand, seems to be decreasing the elevation in NKX 2.5 caused by LPA but did not affect basal levels when applied on its own (Figure 3.60B). When used, TC-LPA5-4 (1.6 $\mu$ M) had little or no effect on either basal or LPA-induced changes in NKX2.5 expression (Figure 3.60C).



## Effect of LPA receptor antagonist on the mir-133 expression

The basal expression of mir-133 was not as significantly enhanced by LPA when compared to the others investigated above (Section 3.5.5). Although the trend, in this case, showed an increase, it was not found to be statistically significant when compared to control levels. Furthermore, neither basal nor changes induced by LPA were altered by either H2L5186303 (1.25 $\mu$ M; Figure 3.61A), H2L5765834 (0.5 $\mu$ M; Figure 3.61B) or TC-LPA5-4 (1.6 $\mu$ M; Figure 3.61C).



## **3.7 Effects of kinase inhibition on the induction of differentiation: effects on protein and mRNA expression**

The Inhibitors in these studies focused on the inhibition of specific kinases which previous studies in our group had indicated may be associated with the induction of differentiation by LPA. The inhibitors used includes BIM-1 (bisindolylmaleimide 1) a selective and potent inhibitor of PKC isoforms, PKA, PKG and myosin-light-chain-kinase (MLCK), and LY294002 which is a PI3-kinase inhibitor (PI3-K $\beta$ , PI3-K $\alpha$ , PI3-K $\sigma$  and PI3-K $\gamma$ ). The IC<sub>50</sub> for PI3-K $\beta$ , PI3-K $\alpha$ , PI3-K $\sigma$  and PI3-K $\gamma$  is respectively 0.31, 0.73, 1.06 and 6.60 $\mu$ M. These effects of these compounds on targeted antibodies and mRNA/miRNA expression were also analysed and investigated.

### **3.7.1 Effects of BIM-1 inhibition on protein expression**

The impacts of BIM-1 (10 $\mu$ M) on MLC (24kDa), OCT4 (43kDa) and GATA4 (54kDa) were investigated at the protein level using western blotting (Figure 3.62). Consistent with data shown earlier on the development of the model, expression of MLC was significantly enhanced following treatment of P19 cells with LPA (5 $\mu$ M). This induction of MLC was inhibited back to control levels in cells pre-treated with BIM-1 (10 $\mu$ M; Figure 3.63). Interestingly, basal OCT4 expression was not significantly altered by LPA, which contrasts with the inhibitions reported above (Figure 3.64). The reason for this discrepancy is unclear and could potentially reflect a lack of response of cells to LPA. BIM-1 appears to enhance OCT4s protein expression, but this was not significant when compared to control and may, therefore, be due to experimental variation rather than an actual change in expression levels. BIM-1, however, suppressed LPA induced GATA4s protein expression but on its own did not affect basal expression levels (Figure 3.65).

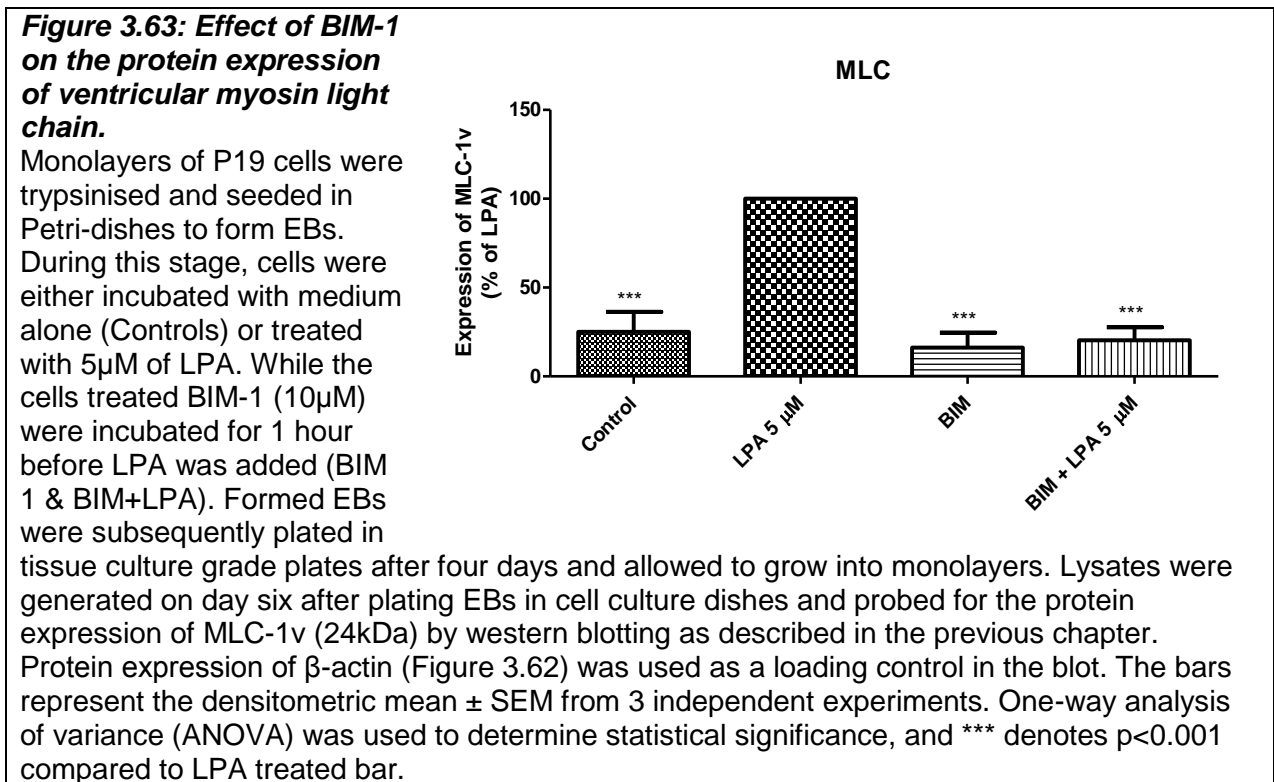
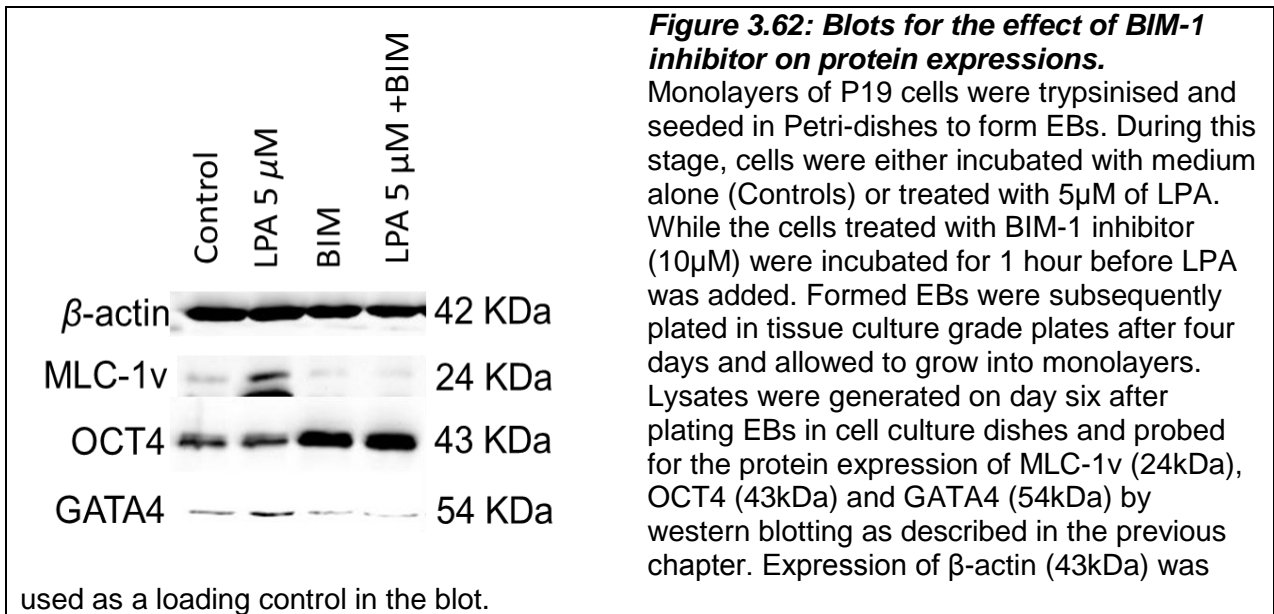


**Figure 3.64: Effect of BIM-1 on protein expression of OCT4.**

Monolayers of P19 cells were trypsinised and seeded in Petri-dishes to form EBs. During this stage, cells were either incubated with medium alone (Controls) or treated with 5 $\mu$ M of LPA. While the cells treated BIM-1 (10 $\mu$ M) were incubated for 1 hour before LPA was added (BIM 1 & BIM+LPA). Formed EBs were subsequently plated in tissue culture grade plates

after four days and allowed to grow into monolayers. Lysates were generated on day six after plating EBs in cell culture dishes and probed for the protein expression of OCT4 (43kDa) by western blotting as described in the previous chapter. Protein expression of  $\beta$ -actin (Figure 3.62) was used as a loading control in the blot. The bars represent the densitometric mean  $\pm$  SEM from 3 independent experiments.

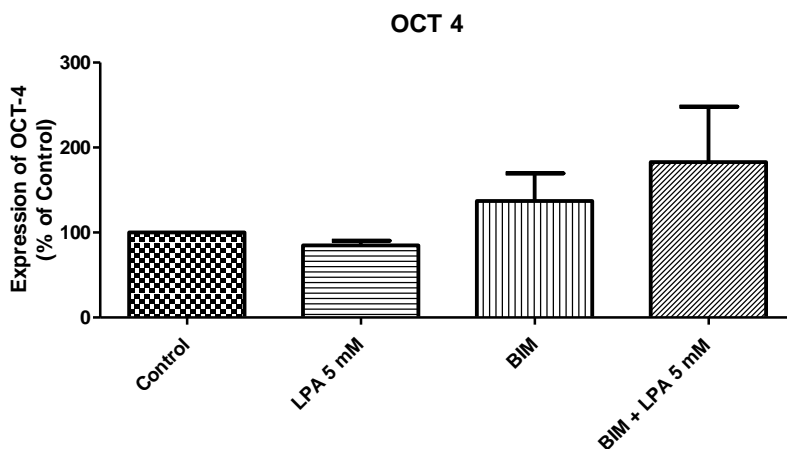
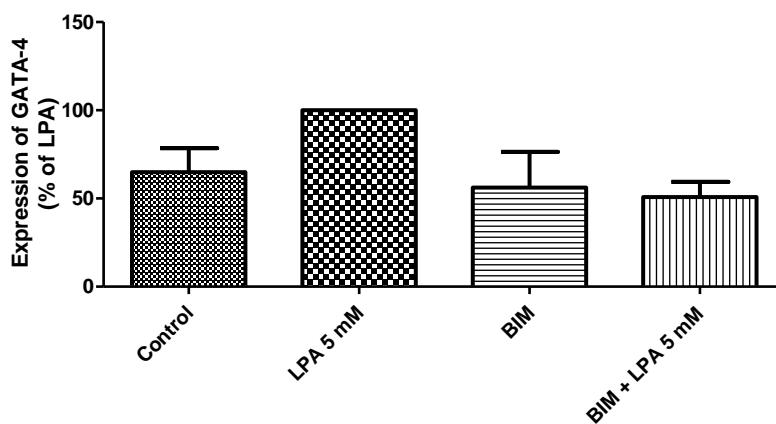


**Figure 3.65: Effect of BIM-1 on protein expression of GATA4.**

Monolayers of P19 cells were trypsinised and seeded in Petri-dishes to form EBs. During this stage, cells were either incubated with medium alone (Controls) or treated with 5 $\mu$ M of LPA. While the cells treated BIM-1 (10 $\mu$ M) were incubated for 1 hour before LPA was added (BIM 1 & BIM+LPA). Formed EBs were subsequently plated in

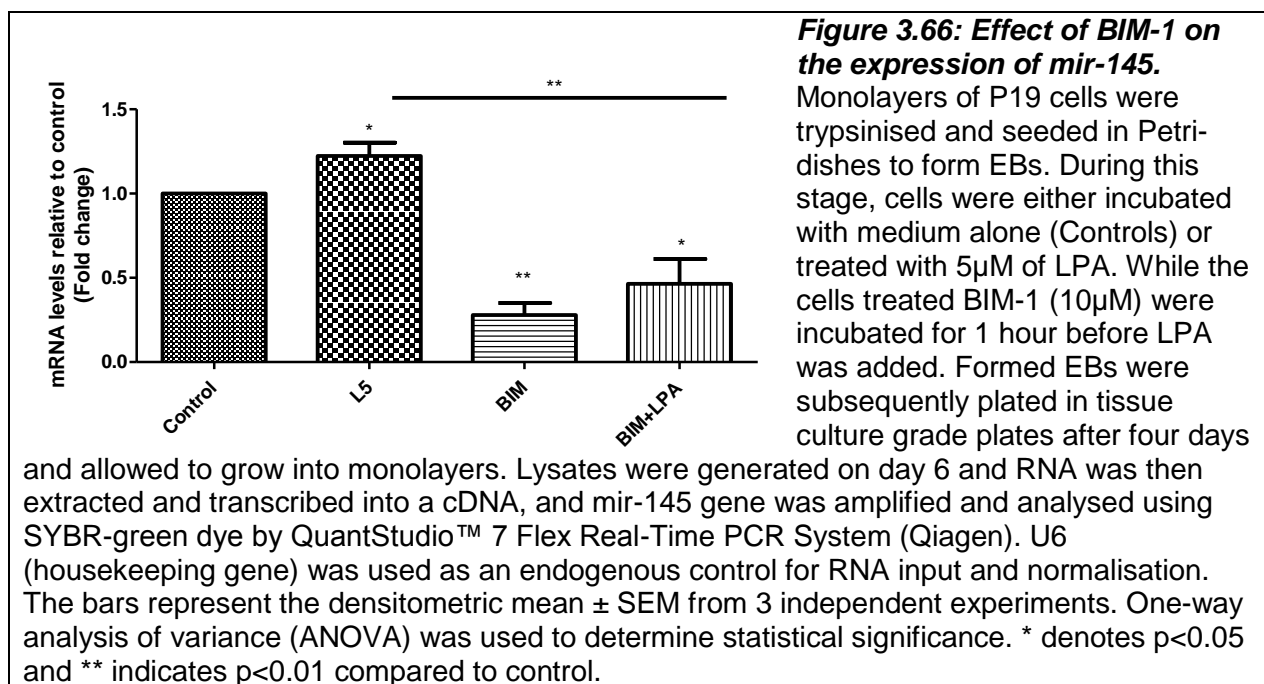
tissue culture grade plates after four days and allowed to grow into monolayers. Lysates were generated on day six after plating EBs in cell culture dishes and probed for the protein expression of GATA4 (54kDa) by western blotting as described in the previous chapter. Protein expression of  $\beta$ -actin (Figure 3.62) was used as a loading control in the blot. The bars represent the densitometric mean  $\pm$  SEM from 3 independent experiments.

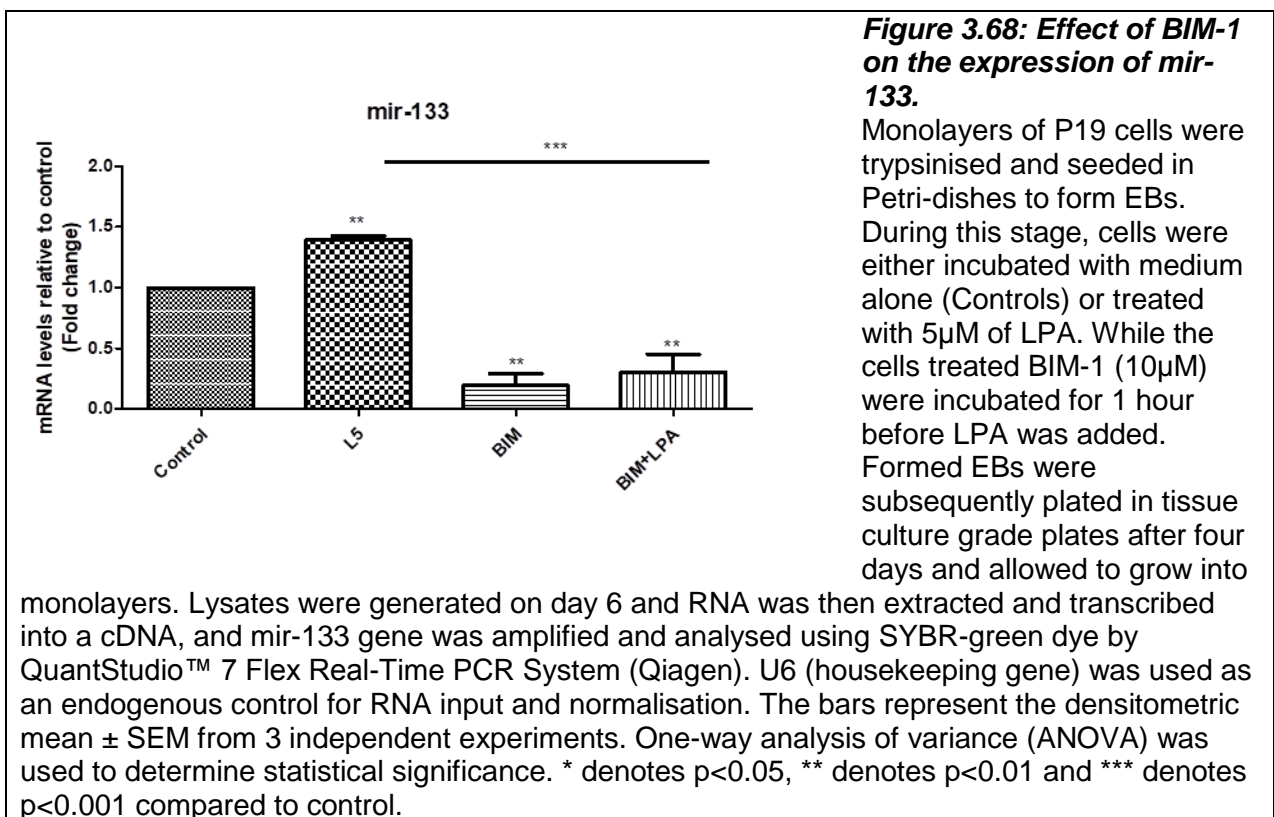
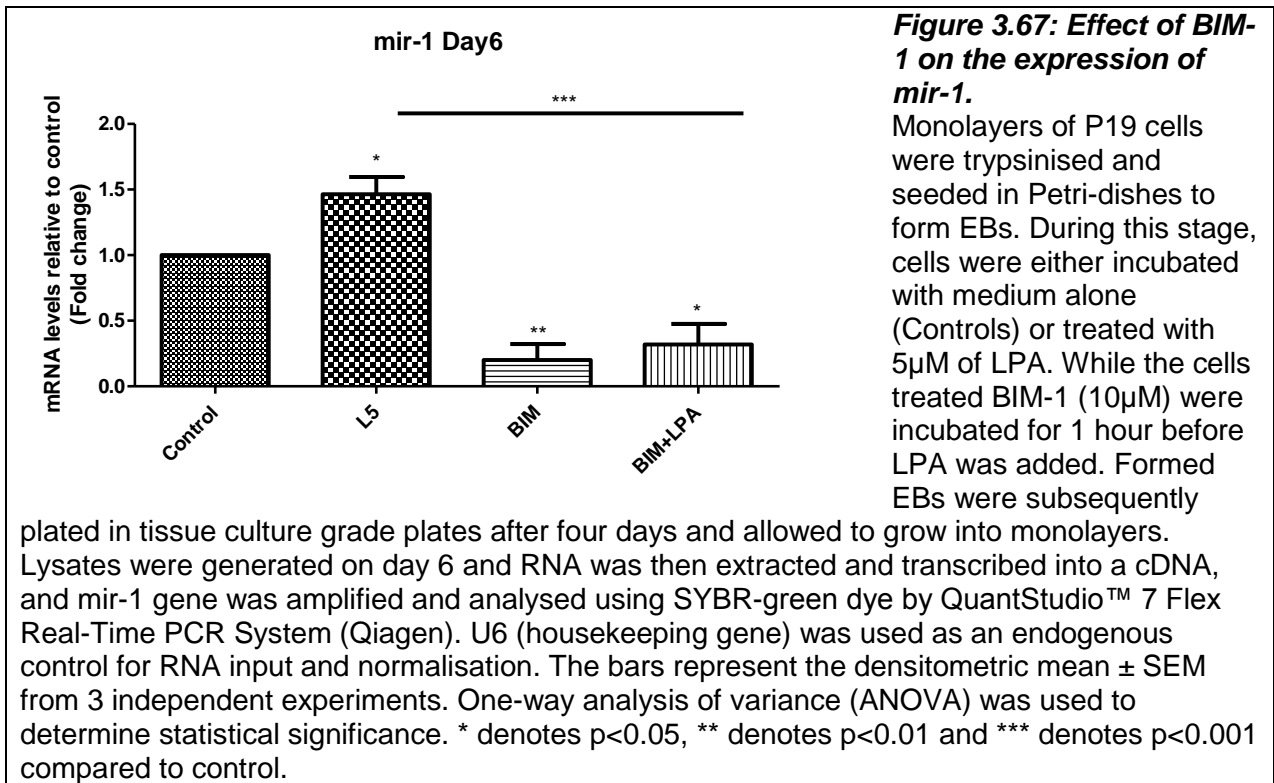


### 3.7.2 Effects of BIM-1 on mRNA/miRNA expression

The effects of BIM-1 were additionally investigated on expression of the various miRNAs and genes investigated previously. In these studies, LPA (5 $\mu$ M) enhanced mir-145 expression, which was still statistically significant when compared to control. More importantly, BIM-1 (10 $\mu$ M) significantly inhibited both basal and LPA-induced expression of mir-145 (Figure 3.66). Similarly, BIM-1 (10 $\mu$ M) also suppressed mir-1 (Figure 3.67) and mir-133 (Figure 3.68) expression in both controls and in LPA-treated cells where both miRNAs were significantly enhanced by LPA when compared to controls respectively.

In contrast to the miRNAs, expression of OCT4 mRNA was only marginally suppressed by LPA but this and indeed levels in controls were enhanced by BIM-1. The enhancements in both instances were significantly higher than levels in controls, and LPA treated cells for mir-133; and for BIM-1, respectively (Figure 3.69). NKX2.5, on the other hand, was enhanced by LPA and BIM-1 partially inhibited this although this response did not appear to be statistically significant due to large variabilities in the experiments which were limited to an n of 3 because of time constraints. BIM-1 did not significantly alter basal NKX2.5 expression (Figure 3.70). By comparison, BIM-1 significantly inhibited GATA4 expression in controls and LPA treated cells where GATA4 levels were markedly enhanced above controls by LPA, respectively (Figure 3.77).





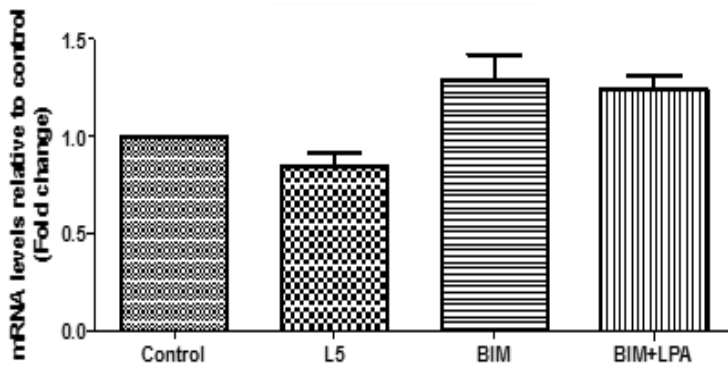


**Figure 3.69: Effect of BIM-1 on the expression of OCT4.**

Monolayers of P19 cells were trypsinised and seeded in Petri-dishes to form EBs. During this stage, cells were either incubated with medium alone (Controls) or treated with 5µM of LPA. While the cells treated BIM-1 (10µM) were incubated for 1 hour before LPA was added. Formed EBs

were subsequently plated in tissue culture grade plates after four days and allowed to grow into monolayers. Lysates were generated on day 6 and RNA was then extracted and transcribed into a cDNA, and OCT4 gene was amplified and analysed using SYBR-green dye by QuantStudio™ 7 Flex Real-Time PCR System (Qiagen). U6 (housekeeping gene) was used as an endogenous control for RNA input and normalisation. The bars represent the densitometric mean ± SEM from 3 independent experiments.

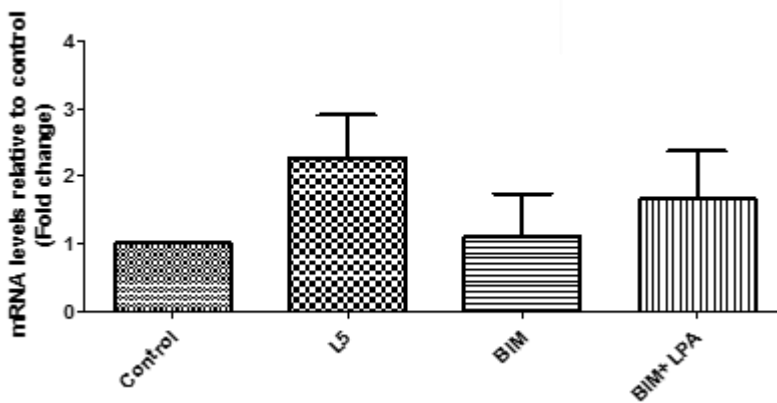


**Figure 3.70: Effect of BIM-1 on the expression of NKX2.5.**

Monolayers of P19 cells were trypsinised and seeded in Petri-dishes to form EBs. During this stage, cells were either incubated with medium alone (Controls) or treated with 5µM of LPA. While the cells treated BIM-1 (10µM) were incubated for 1 hour before LPA was added.

Formed EBs were

subsequently plated in tissue culture grade plates after four days and allowed to grow into monolayers. Lysates were generated on day 6 and RNA was then extracted and transcribed into a cDNA, and NKX2.5 gene was amplified and analysed using SYBR-green dye by QuantStudio™ 7 Flex Real-Time PCR System (Qiagen). U6 (housekeeping gene) was used as an endogenous control for RNA input and normalisation. The bars represent the densitometric mean ± SEM from 3 independent experiments.

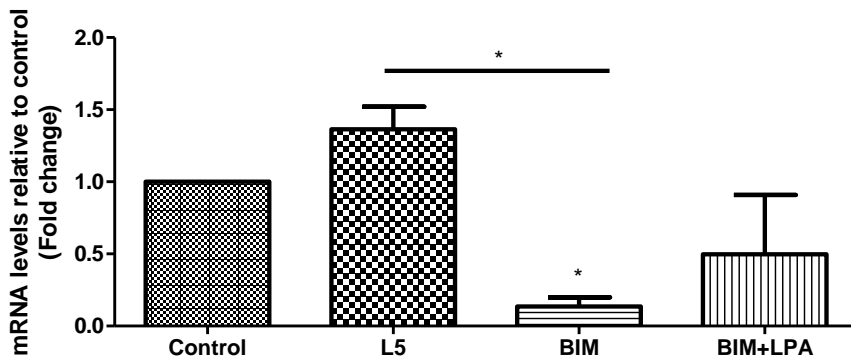


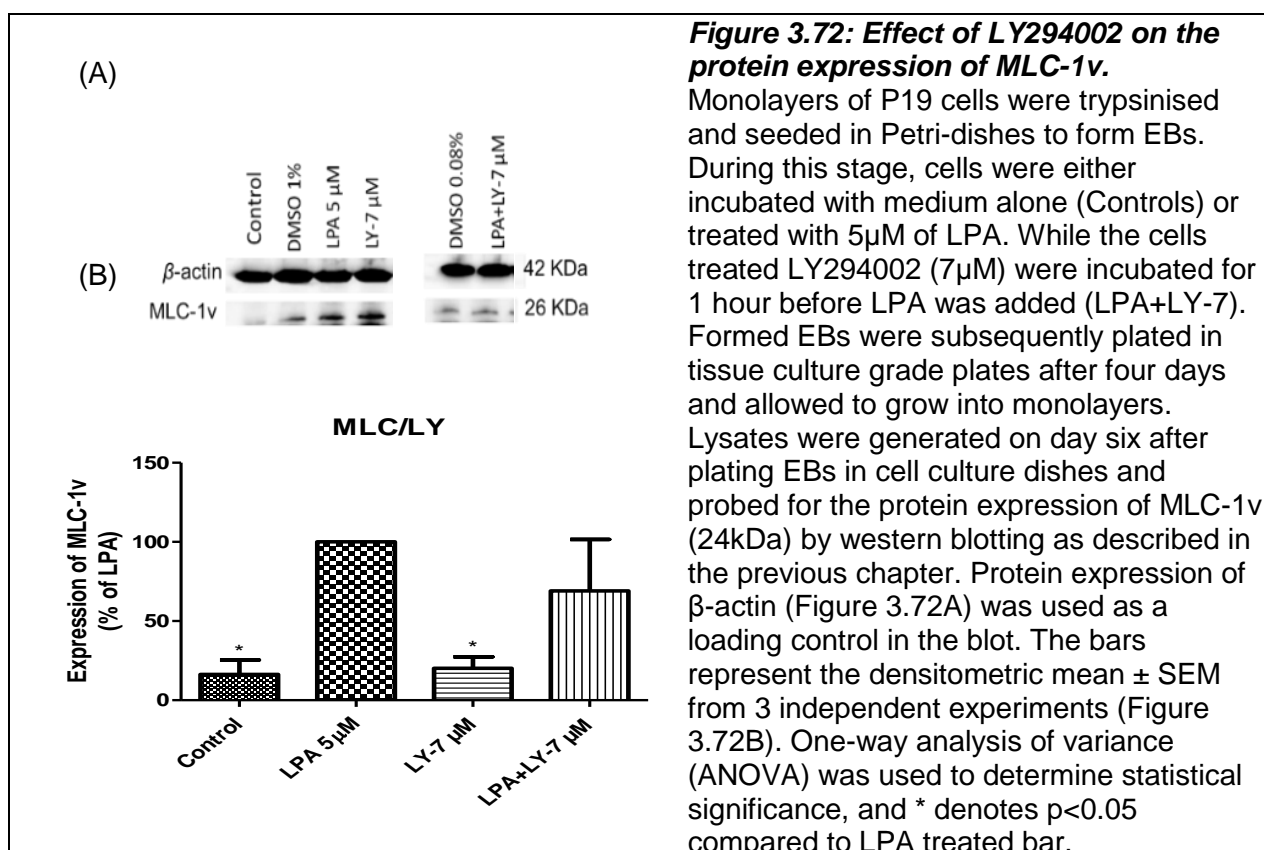
**Figure 3.71: Effect of BIM-1 on the expression of GATA4.**

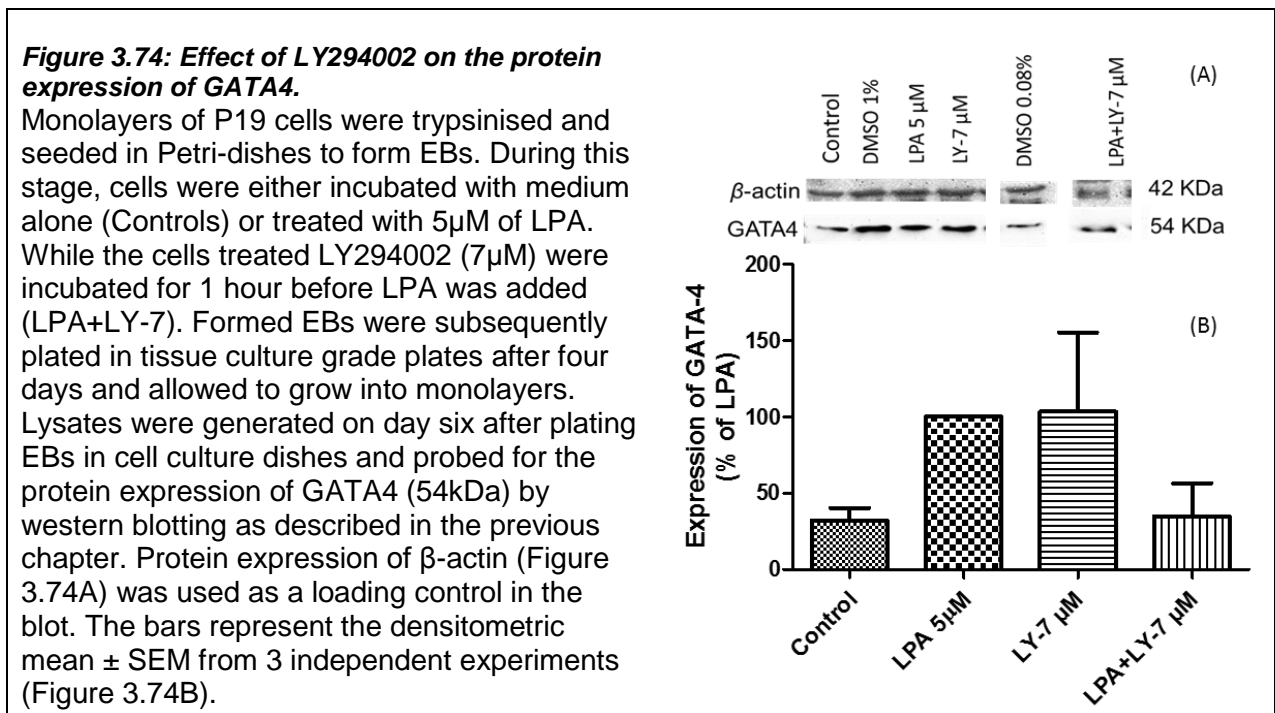
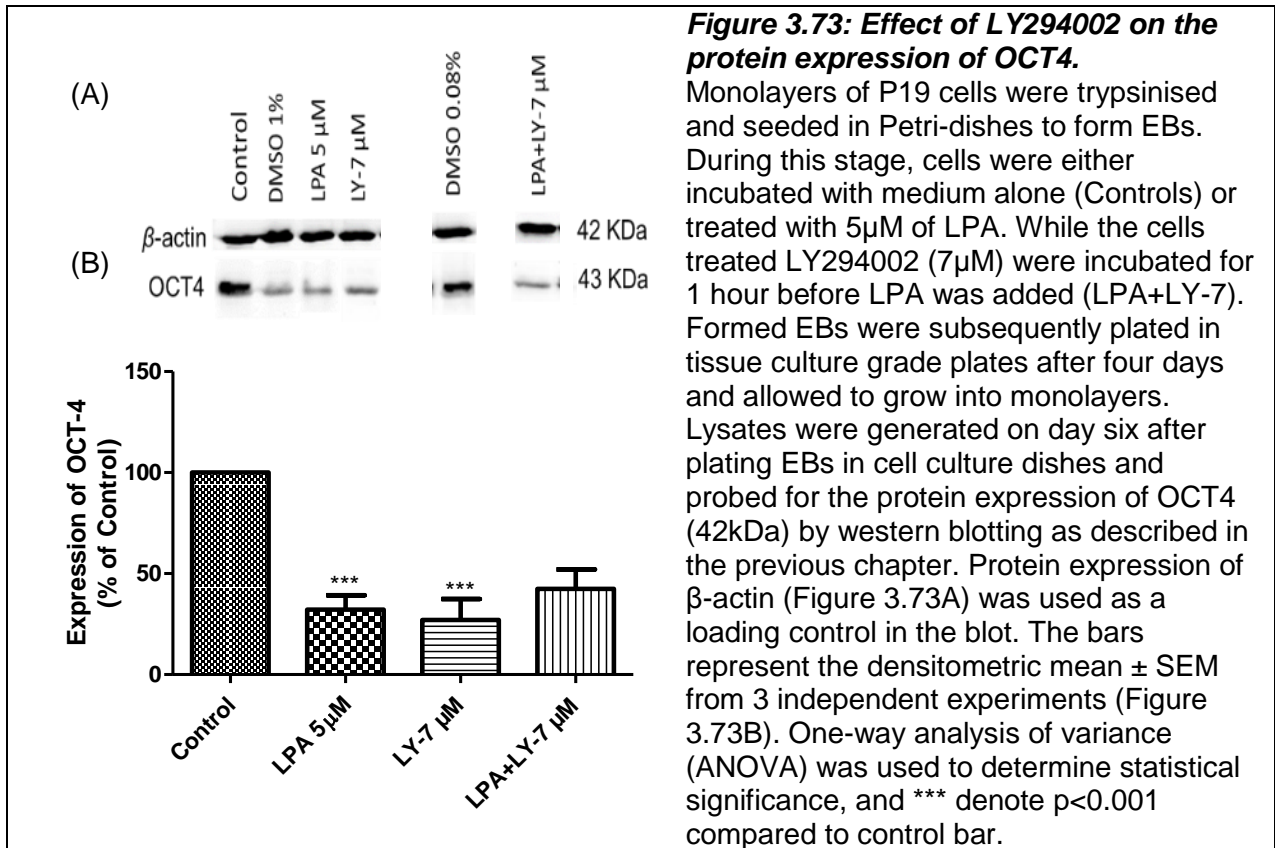
Monolayers of P19 cells were trypsinised and seeded in Petri-dishes to form EBs. During this stage, cells were either incubated with medium alone

(Controls) or treated with 5 $\mu$ M of LPA. While the cells treated BIM-1 (10 $\mu$ M) were incubated for 1 hour before LPA was added. Formed EBs were subsequently plated in tissue culture grade plates after four days and allowed to grow into monolayers. Lysates were generated on day 6 and RNA was then extracted and transcribed into a cDNA, and GATA4 gene was amplified and analysed using SYBR-green dye by QuantStudio™ 7 Flex Real-Time PCR System (Qiagen). U6 (housekeeping gene) was used as an endogenous control for RNA input and normalisation. The bars represent the densitometric mean  $\pm$  SEM from 3 independent experiments. One-way analysis of variance (ANOVA) was used to determine statistical significance. \* denotes  $p < 0.05$  compared to control and LPA treated cells.

### 3.7.3 Effects of LY294002 (PI3 kinase) inhibition on protein expression

The result of LY294002 antagonist (7 $\mu$ M) in this sub-section was examined on MLC (24kDa), OCT4 (43kDa) and GATA4 (54kDa) at the protein level using western blotting. Consistently, with the previously shown results on the development of the model, expression of MLC-1v in control was significantly lower following treatment of P19 cells with LPA (5 $\mu$ M). This induction was, however, inhibited back to control levels in cells pre-treated with LY294002 (7 $\mu$ M; Figure 3.72). While the expression of OCT4 was remarkably downregulated in all the conditions except in control (Figure 3.73). Cells incubated with LPA alone or LY294002 were both downregulated with a p-value of <0.001 compared to the basal levels. In contrast, the protein expression of GATA4 showed no evident impact when treated with either LPA or with LY294002 (Figure 3.74).





### 3.7.4 Effects of LY294002 (PI3 kinase) inhibition on mRNA expression

In the current sub-section, mir-145, mir-1, mir-133, OCT4 and NKX2.5 expressions are investigated in response to the inhibition by LY294002 (7 $\mu$ M). The expression of mir-145, mir-1, mir-133 and NKX2.5 (Figure 3.75-3.77 and 3.79), did not result in any significant enhancement or decrease. LY294002 was marginally significant in LPA-induced cells expression of mir-145 and mir-1. Interestingly, expression of mir-133 was not enhanced either affected by LPA or LY294002 (Figure 3.83).

In contrast to the miRNAs, the mRNA expression of OCT4 was significantly suppressed and even further inhibited by LY294002 in basal and LPA-induced expression (Figure 3.78). LY294002 pre-incubated LPA-induced cells were also significantly lower compared to LPA-induced cells. NKX2.5, on the other hand, was enhanced by LPA while the basal was also partially inhibited by LY294002 but, not significant. LY294002 likewise did not significantly alter the LPA-induced cells of the expression of NKX2.5 (Figure 3.79).

**Figure 3.75: Effect of LY294002 on the expression of mir-145.**

Monolayers of P19 cells were trypsinised and seeded in Petri-dishes to form EBs. During this stage, cells were either incubated with medium alone (Controls) or treated with 5 $\mu$ M of LPA. While the cells treated LY294002 (7 $\mu$ M) were incubated for 1 hour before LPA was added. Formed EBs were subsequently plated in tissue culture grade plates after four days and allowed to grow into monolayers. Lysates were generated on day 6 and RNA was then extracted and transcribed into a cDNA, and mir-145 gene was amplified and analysed using SYBR-green dye by QuantStudio™ 7 Flex Real-Time PCR System (Qiagen). U6 (housekeeping gene) was used as an endogenous control for RNA input and normalisation. The bars represent the densitometric mean  $\pm$  SEM from 3 independent experiments.

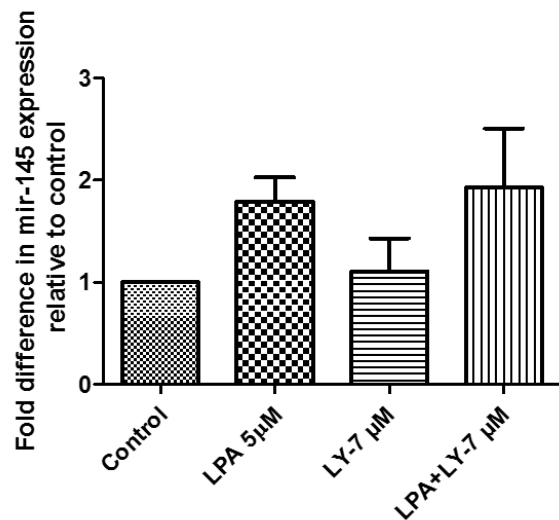


**Figure 3.76: Effect of LY294002 on the expression of mir-1.**

Monolayers of P19 cells were trypsinised and seeded in Petri-dishes to form EBs. During this stage, cells were either incubated with medium alone (Controls) or treated with 5 $\mu$ M of LPA. While the cells treated LY294002 (7 $\mu$ M) were incubated for 1 hour before LPA was added. Formed EBs were subsequently plated in tissue culture grade plates after four days and allowed to grow into monolayers. Lysates were generated on day 6 and RNA was then extracted and transcribed into a cDNA, and mir-1 gene was amplified and analysed using SYBR-green dye by QuantStudio™ 7 Flex Real-Time PCR System (Qiagen). U6 (housekeeping gene) was used as an endogenous control for RNA input and normalisation. The bars represent the densitometric mean  $\pm$  SEM from 3 independent experiments.

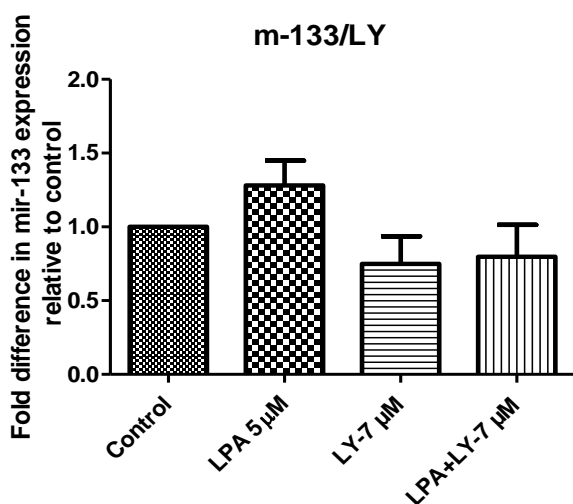
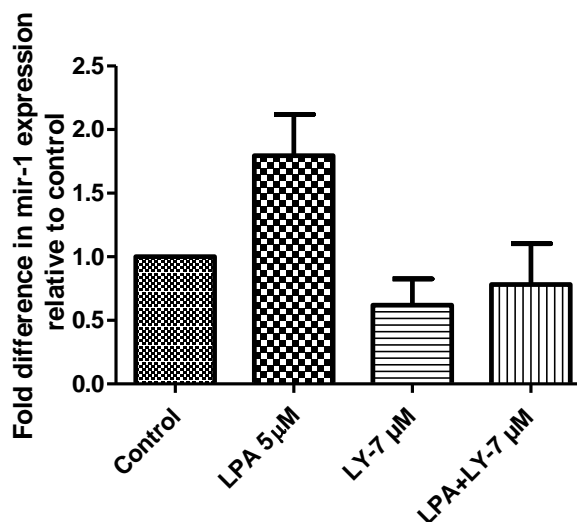


**Figure 3.77: Effect of LY294002 on the expression of mir-133.**

Monolayers of P19 cells were trypsinised and seeded in Petri-dishes to form EBs. During this stage, cells were either incubated with medium alone (Controls) or treated with 5 $\mu$ M of LPA. While the cells treated LY294002 (7 $\mu$ M) were incubated for 1 hour before LPA was added. Formed EBs were subsequently plated in tissue culture grade plates after four days and allowed to grow into monolayers. Lysates were generated on day 6 and RNA was then extracted and transcribed into a cDNA, and mir-133 gene was amplified and analysed using SYBR-green dye by QuantStudio™ 7 Flex Real-Time PCR System (Qiagen). U6 (housekeeping gene) was used as an endogenous control for RNA input and normalisation. The bars represent the densitometric mean  $\pm$  SEM from 3 independent experiments.

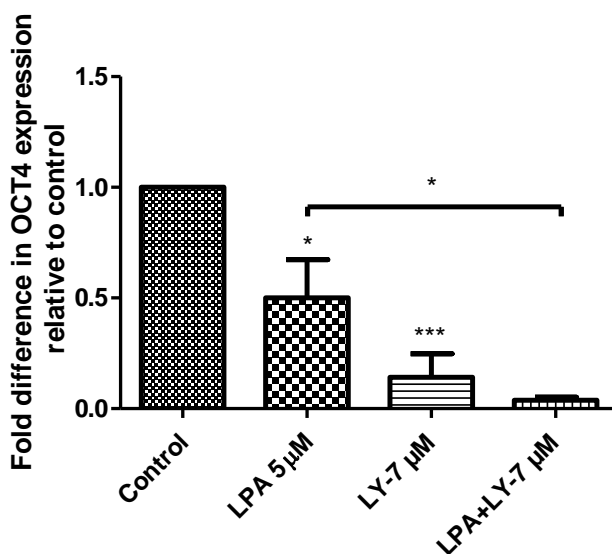


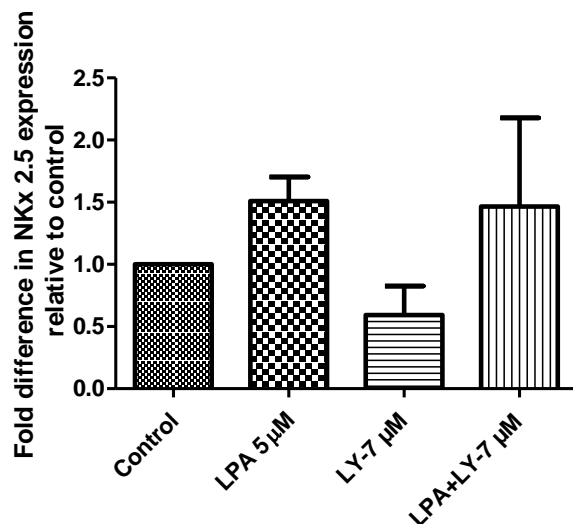
**Figure 3.78: Effect of LY294002 on the expression of OCT4.**

Monolayers of P19 cells were trypsinised and seeded in Petri-dishes to form EBs. During this stage, cells were either incubated with medium alone (Controls) or treated with 5µM of LPA. While the cells treated LY294002 (7µM) were incubated for 1 hour before LPA was added. Formed EBs were subsequently plated in tissue culture grade plates after four days and allowed to grow into monolayers. Lysates were generated on day 6 and RNA was then extracted and transcribed into a cDNA, and OCT4 gene was amplified and analysed using SYBR-green dye by QuantStudio™ 7 Flex Real-Time PCR System (Qiagen). U6 (housekeeping gene) was used as an endogenous control for

RNA input and normalisation. The bars represent the densitometric mean ± SEM from 3 independent experiments. The bars represent the densitometric mean ± SEM from 3 independent experiments. One-way analysis of variance (ANOVA) was used to determine statistical significance and \* denotes  $p < 0.05$  and \*\*\* denote  $p < 0.001$  compared to control.

**Figure 3.79: Effect of LY294002 on the expression of NKX2.5.**

Monolayers of P19 cells were trypsinised and seeded in Petri-dishes to form EBs. During this stage, cells were either incubated with medium alone (Controls) or treated with 5µM of LPA. While the cells treated LY294002 (7µM) were incubated for 1 hour before LPA was added. Formed EBs were subsequently plated in tissue culture grade plates after four days and allowed to grow into monolayers. Lysates were generated on day 6 and RNA was then extracted and transcribed into a cDNA, and NKX2.5 gene was amplified and analysed using SYBR-green dye by QuantStudio™ 7 Flex Real-Time PCR System (Qiagen). U6 (housekeeping gene) was used as an endogenous control for RNA input and normalisation. The bars represent the densitometric mean ± SEM from 3 independent experiments.



## **3.8 Effects of knockdown and overexpression of mir-145 and mir-1 on differentiation**

In the current section, cells were treated according to the protocol illustrated in chapter 2 to either knockdown or overexpress mir-145 and mir-1. These studies were carried out to determine whether depletion or overexpression of either mir-145 or mir-1 regulated differentiation of P19 SCs into cardiomyocytes. siRNA for the inhibitors and a mimic of each target were used categorically.

Additionally, a negative sample was used as a signal for the efficiency of the transfection process. Thus, changes in MLC-1v and OCT4 protein expression were investigated by western blot while expression of mir-145, mir-1, mir-133, OCT4, NKX2.5 and GATA4 by qPCR. Differentiation was also induced using 20 $\mu$ M of LPA to examine the maximum possible effect.

### **3.8.1 Effect of transfection on Protein expression**

#### **Effect of transfection on MLC-1v protein expression**

MLC-1v was first targeted to analyse any changes in differentiation that could occur as a result of the transfection, including when activated with LPA. This is to test the possible relationship between the actions of these miRNAs and LPA in the differentiation. The blot in Figure 3.80 is representative of the western blots generated with lysates from cells treated with LPA alone (20 $\mu$ M), cells with the master mix but no siRNA (negative/-ve), LPA- induced cells premixed with negative (-ve + LPA), cells treated with the inhibitor siRNA (inhib- mir-145/inhib-mir1), cells treated with overexpression siRNA (mim-mir-145/mim-mir-1) and cells with overexpressed or inhibited mir-145/mir-1 induced by LPA (inhib-mir145+LPA/inhib- mir-1+LPA and mim-mir145+LPA/mim-mir-1+LPA).  $\beta$ -actin was used as a loading control and a normaliser.

Although marginally high, cells treated with LPA (20 $\mu$ M) showed similar levels of protein expression of MLC-1v statistically when compared to control. This is also what is observed when cells treated with the mimic of mir-145 and LPA was activated also showed a marginally higher trend but non-significantly. It did not, however, alter the effects of LPA when

applied together (Figure 3.81).

Cells treated with mir-145 inhibitor alone did not show any statistically significant change even with the decrease in expression of up to 50% in MLC-1v levels when compared to LPA treated cells. Inducement of cells with LPA when applied together with a mir-145 inhibitor also did not increase the latter, suggesting a possible suppression of the LPA effect marginally (Figure 3.81).

Different trends as those described for mir-145 were seen when mir-1 was used compared to LPA treated cells. Inhibitor-1 did not significantly suppress the LPA responses, but the mimic mir-1 enhanced MLC-1v protein expression on its own and more with the inducement of LPA (Figure 3.82). Moreover, MLC-1v marker potentiated the response to LPA every time it was added to the negative cells and cells with mir-1 inhibitor but not statistically (Figure 3.82). Table 3.2 is a summary of the outcome from the statistical analysis for the MLC-1v protein expression, which shows the statistical difference to be between the different conditions.

*Table 3.2: One-way analysis of variance (ANOVA) table analysed for the antibodies MLC-1v and OCT4.*

ANOVA						
Variable	Source of variation	Sum of Square	Df	Mean Square	F	Sig.
WBMLC	Between Groups	181801.9	11	16527.448	2.435	0.033*
	Within Groups	162916.6	24	6788.193		
	Total	344718.556	35			
WBOCT4	Between Groups	141409.3	11	12855.394	2.782	0.017*
	Within Groups	110911.0	24	4621.291		
	Total	252320.3	35			
“*” is Significant (p < 0.05): “ns” is non-significant (p > 0.05)						

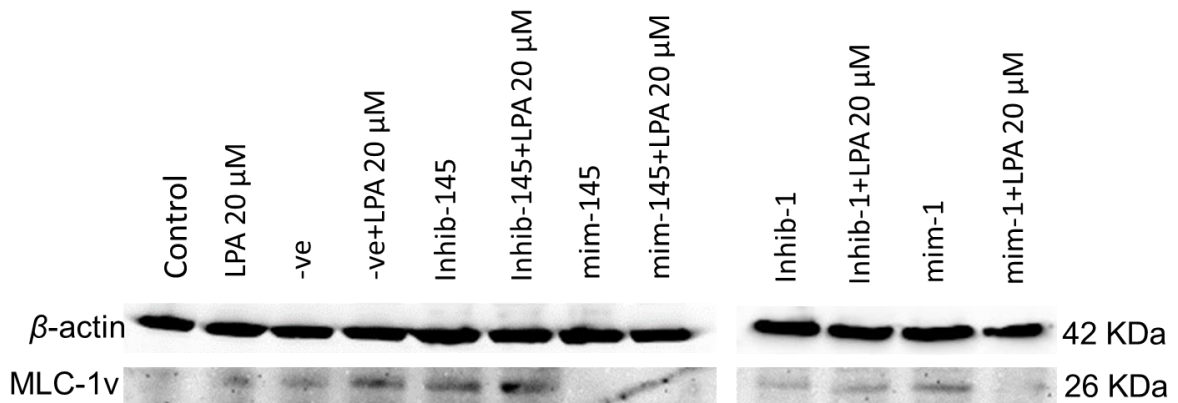


**Figure 3.80: Blots for the effect of knockdown and overexpression of mir-145 and mir-1 on MLC-1v.**

Monolayers of P19 cells were trypsinised and seeded in Petri-dishes to form EBs. Before forming EBs cells were transfected with either over-expression (mimic) or the inhibition mixture (siRNA) for 24 hours following the manufacturer's protocol (as detailed in chapter 2). During this stage, cells were either incubated with medium alone (Controls) or treated with 20 $\mu$ M of LPA. Formed EBs were subsequently plated in tissue culture grade plates after four days and allowed to grow into monolayers. Lysates were generated on day six after plating EBs in cell culture dishes and probed for the protein expression of MLC-1v (24kDa) by western blotting as described in the previous chapter. Protein expression of  $\beta$ -actin (43kDa) was used as a loading control in the blot.

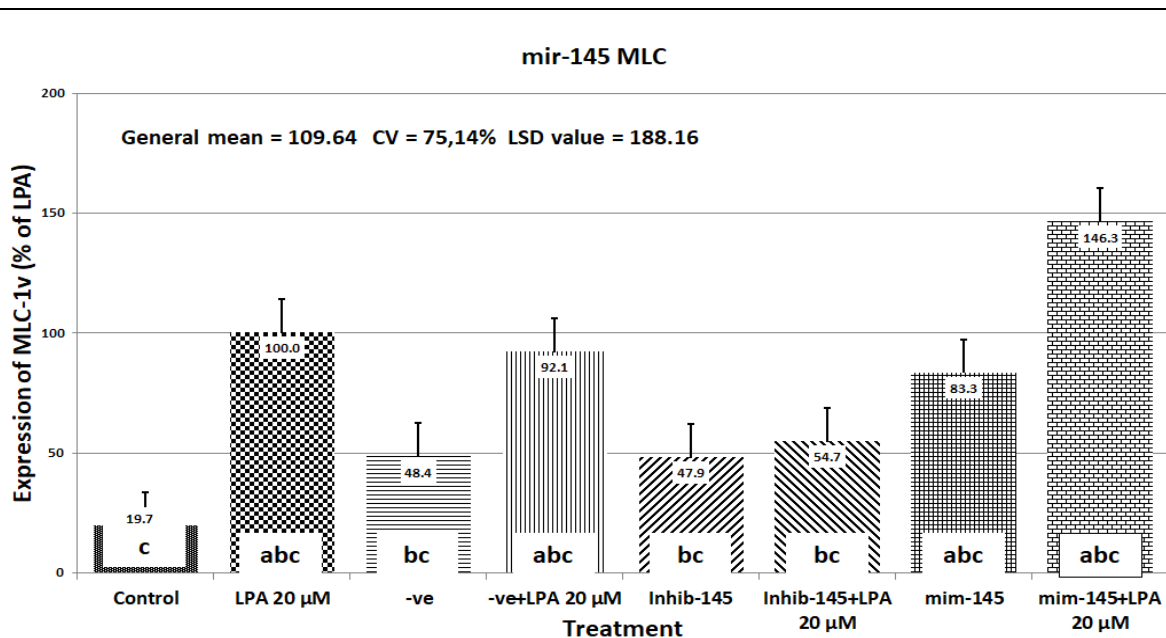


**Figure 3.81: Effect of knockdown and overexpression of mir-145 on MLC-1v.**

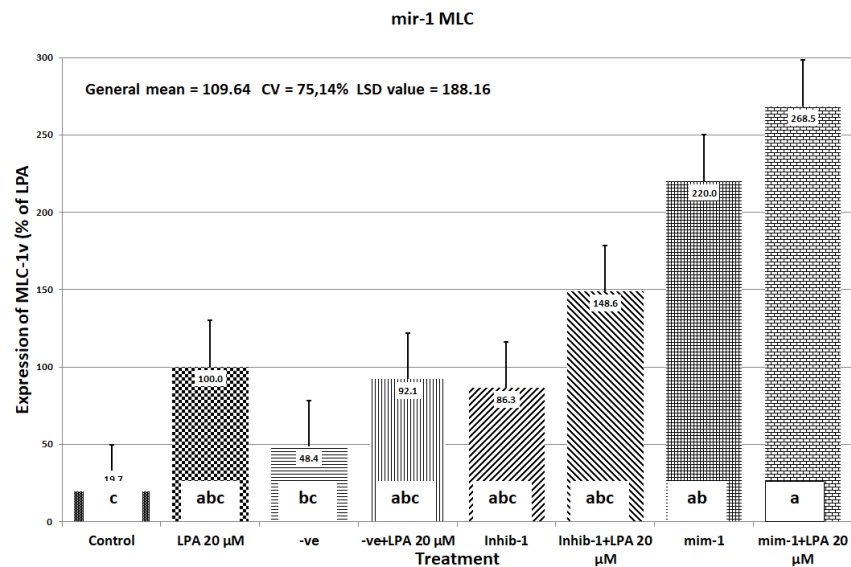
Monolayers of P19 cells were trypsinised and seeded in Petri-dishes to form EBs. Before forming EBs cells were transfected with either the mir-145 over-expression (mimic) or the inhibition mixture (siRNA) for 24 hours following the manufacturer's protocol (as detailed in chapter 2). During this stage, cells were either incubated with medium alone (Controls) or treated with 20 $\mu$ M of LPA. The negative bar represents cells with the master-mixture without the

siRNA or mimic. EBs were subsequently plated in tissue culture grade plates after four days and allowed to grow into monolayers. Lysates were generated on day six after plating EBs in cell culture dishes and probed for the protein expression of MLC-1v (24kDa) by western blotting as described in the previous chapter. Protein expression of  $\beta$ -actin (43kDa; figure 3.80) was used as a loading control in the blot. The bars represent the densitometric mean  $\pm$  SEM from 3 independent experiments. ANOVA and Least Significant Differences (LSD) test were used in statistical analysis to determine significant differences. Similar letters indicate similar means, according to LSD.

**Figure 3.82: Effect of knockdown and overexpression of mir-1 on MLC-1v.**

Monolayers of P19 cells were trypsinised and seeded in Petri-dishes to form EBs. Before forming EBs cells were transfected with either the mir-1 overexpression (mimic) or the inhibition mixture (siRNA) for 24 hours following the manufacturer's protocol (as detailed in chapter 2). During this stage, cells were either incubated with medium alone (Controls) or

treated with 20 $\mu$ M of LPA. The negative bar represents cells with the master-mixture without the siRNA or mimic. EBs were subsequently plated in tissue culture grade plates after four days and allowed to grow into monolayers. Lysates were generated on day six after plating EBs in cell culture dishes and probed for the protein expression of MLC-1v (24kDa) by western blotting as described in the previous chapter. Protein expression of  $\beta$ -actin (43kDa; figure 3.80) was used as a loading control in the blot. The bars represent the densitometric mean  $\pm$  SEM from 3 independent experiments. ANOVA and Least Significant Differences (LSD) test were used in statistical analysis to determine significant differences. Similar letters indicate similar means, according to LSD.



## **Effect of transfection on OCT4 protein expression**

Figure 3.83 is another representative of the western blots to investigate the impact on protein expression of OCT4 (43kDa). OCT4 was targeted as a marker for the pluripotency to test the response to the transfection of both mir-1 and mir-145. Generated lysates on day 6 are from cells treated with LPA alone (20 $\mu$ M), cells with the master mix but no siRNA (negative/-ve), LPA-induced cells premixed with negative (-ve + LPA), cells treated with the inhibitor siRNA (inhib-mir-145/inhib- mir1), cells treated with overexpression siRNA (mim-mir-145/mim-mir-1) and cells with overexpressed or inhibited mir-145/mir-1 induced by LPA (inhib-mir145+LPA/inhib-mir-1+LPA and mim-mir145+LPA/mim-mir-1+LPA).  $\beta$ -actin was used as a loading control and a normaliser.

Similar to the previous sub-section, the expression of OCT4 was as expected considerably low. However, that effect was not significant compared to Control. This was also the case with all the other conditions which did not show any influence by the overexpression or inhibition of mir-145 statistically (Figure 3.84). The expression of the protein OCT4 again is influenced by mir-1 transfection. Although not statistically significant, the % expression of LPA treated cells are visibly lower. Overall, LPA and mimic mir-1 showed a more evident responsibility in altering the latter in OCT4 (Figure 3.85). Cells transfected with a mir-1 inhibitor which treated with LPA showed another evident reaction on the marker of OCT4 compared to LPA only treated cells. Likewise, cells with mimic-mir-1 and mimic-mir-1 with LPA added (Figure 3.85). A very comparable reaction also was apparent compared to cells objected with the negative solution with LPA mixed.

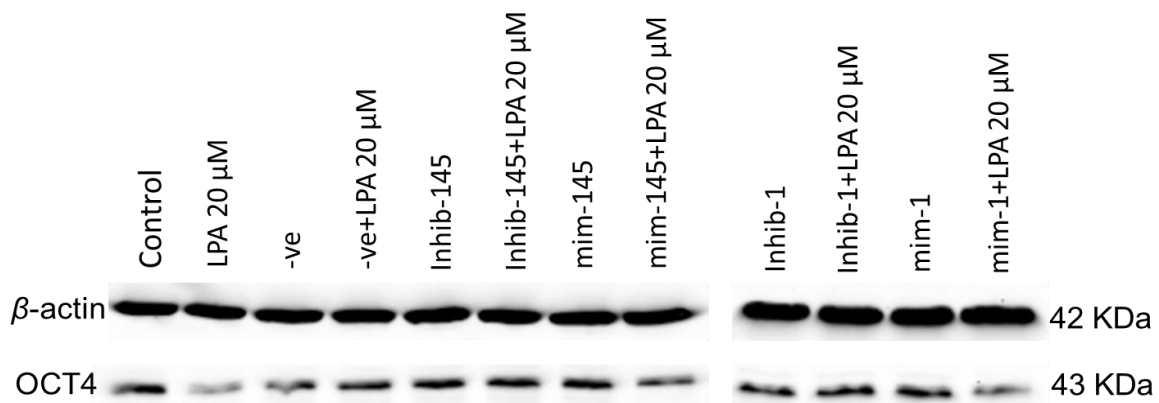
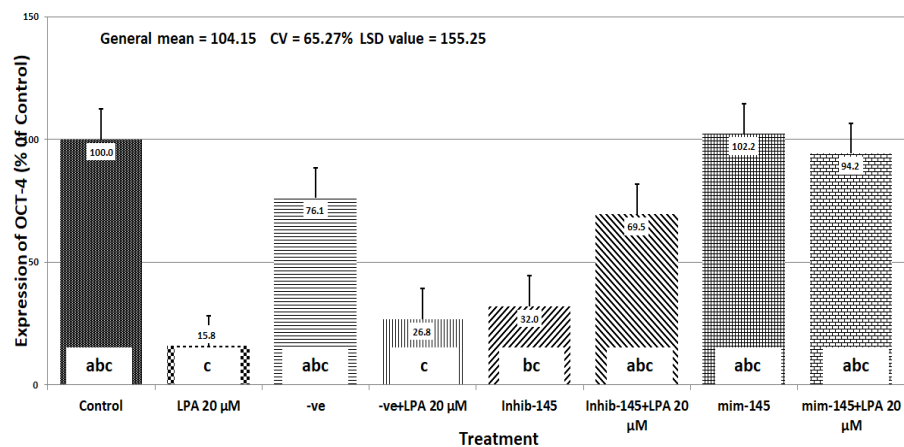


**Figure 3.83: Blot for the effect of knockdown and overexpression of mir-145 and mir-1 on OCT4.**

Monolayers of P19 cells were trypsinised and seeded in Petri-dishes to form EBs. Before forming EBs cells were transfected with either over-expression (mimic) or the inhibition mixture (siRNA) for 24 hours following the manufacturer's protocol (as detailed in chapter 2). During this stage, cells were either incubated with medium alone (Controls) or treated with 20μM of LPA. Formed EBs were subsequently plated in tissue culture grade plates after four days and allowed to grow into monolayers. Lysates were generated on day six after plating EBs in cell culture dishes and probed for the protein expression of OCT4 (43kDa) by western blotting as described in the previous chapter. Protein expression of β-actin (43kDa) was used as a loading control in the blot.

**Figure 3.84: Effect of knockdown and overexpression of mir-145 on OCT4.**

Monolayers of P19 cells were trypsinised and seeded in Petri-dishes to form EBs. Before forming EBs cells were transfected with either the mir-145 over-expression (mimic) or the inhibition mixture (siRNA) for 24 hours

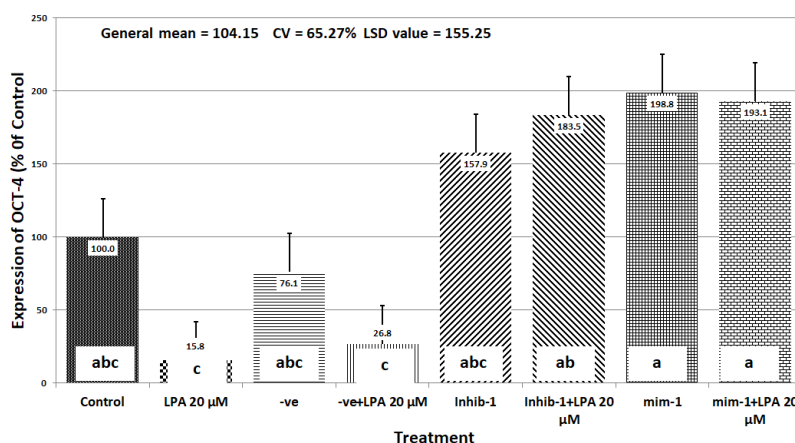


following the manufacturer's protocol (as detailed in chapter 2). During this stage, cells were either incubated with medium alone (Controls) or treated with 20μM of LPA. The negative bar represents cells with the master-mixture without the siRNA. EBs were subsequently plated in tissue culture grade plates after four days and allowed to grow into monolayers. Lysates were generated on day six after plating EBs in cell culture dishes and probed for the protein expression of OCT4 (43kDa) by western blotting as described in the previous chapter. Protein expression of β-actin (43kDa; figure 3.83) was used as a loading control in the blot. The bars represent the densitometric mean ± SEM from 3 independent experiments. ANOVA and Least Significant Differences (LSD) test were used in statistical analysis to determine significant differences. Similar letters indicate similar means, according to LSD.

**Figure 3.85: Effect of knockdown and overexpression of mir-1 on OCT4.**

Monolayers of P19 cells were trypsinised and seeded in Petri-dishes to form EBs. Prior to forming EBs cells were transfected with either the mir-1 over-expression (mimic) or the inhibition mixture (siRNA) for 24 hours following the manufacturer's protocol (as

detailed in chapter 2). During this stage, cells were either incubated with medium alone (Controls) or treated with 20 $\mu$ M of LPA. Negative bar represents cells with the master-mixture without the siRNA. EBs were subsequently plated in tissue culture grade plates after four days and allowed to grow into monolayers. Lysates were generated on day six after plating EBs in cell culture dishes and probed for the protein expression of OCT4 (43kDa) by western blotting as described in the previous chapter. Protein expression of  $\beta$ -actin (43kDa; figure 3.83) was used as a loading control in the blot. The bars represent the densitometric mean  $\pm$  SEM from 3 independent experiments. ANOVA and Least Significant Differences (LSD) test were used in statistical analysis to determine significant differences. Similar letters indicate similar means, according to LSD.



### 3.8.2 mRNA/miRNA expression

This sub-section highlights the results from the qPCR experiments which targeted mir-145, mir-1, mir-133, OCT4, NKX2.5 and GATA4 in response to the inhibition of mir-145/mir-1 and overexpression of mir-145/mir-1.

LPA-treated cells showed similar mir-145 and mir-1 expression compared to control. This was not affected by the negative, inhib-145 and not enhanced by mim-145. The latter also did not improve the basal expression of mir-145 and mir-1 when treated with inhib-1 and mim-1. The same was also true for, all the other targets examined including mir-133, OCT4, NKX2.5 and GATA4 which did not appear to be altered in any statistically significant manner under any of the conditions examined as summarised in table 3.3.

*Table 3.3: One-way analysis of variance (ANOVA) table analysed for the antibodies MLC-1v and OCT4.*

ANOVA						
Variable	Source of	Sum of	Df	Mean	F	Sig.
PCRmir145	Between Groups	0.865	11	0.079	1.336	0.265 ns
	Within Groups	1.412	24	0.059		
	Total	2.277	35			
PCRmir1	Between Groups	0.850	11	0.077	0.602	0.809 ns
	Within Groups	3.080	24	0.128		
	Total	3.930	35			
PCRmir133	Between Groups	0.225	11	0.020	0.776	0.660 ns
	Within Groups	0.633	24	0.026		
	Total	0.858	35			
PCROCT4	Between Groups	5.288	11	0.481	0.698	0.728 ns
	Within Groups	16.521	24	0.688		
	Total	21.809	35			
PCRNKY	Between Groups	16.829	11	1.530	0.484	0.895 ns
	Within Groups	75.861	24	3.161		
	Total	92.690	35			
PCRGATA4	Between Groups	1.989	11	0.181	0.902	0.553 ns
	Within Groups	4.813	24	0.201		
	Total	6.802	35			

“ns” is non-significant ( $p > 0.05$ )

# **CHAPTER 4**

# **DISCUSSION**

Many diseases of the heart are linked to the loss of cardiomyocytes (Chiong *et al.*, 2011; Nakano *et al.*, 2012; Kumar *et al.*, 2005). The cardiomyocytes could be lost through necrosis, apoptosis, or autophagy (Kumar *et al.*, 2005; Chiong *et al.*, 2011). Year by year, the mortality caused by this loss of cardiomyocytes increase and CVD remains the number one cause of death globally (American heart association update, 2014; World Health Organisation).

Despite considerable advances in understanding some of the mechanisms of CVD at the cellular level, and the early diagnosis, surgical and pharmacological interventions in these diseases, there is no robust consensus on the best approach for its management. Transplantation of mature cardiomyocytes is one approach that has been developed recently and although it has been shown to improve the structure and the function of the heart after a myocardial infarction (MI) in several clinical trials, it is limited by poor cellular survival (Smits *et al.*, 2009; Murry *et al.*, 2005; Beltrami *et al.*, 2001). The positive effect depends on the actual cell type transplanted (Hughes, 2002 & Hodgson *et al.*, 2004). Embryonic SCs and many other cell types were transplanted to the region of damage post-MI (Hodgson *et al.*, 2004 & Kumar *et al.*, 2005). However, the best efficient donor cell type and technique to perform this process are still not identified. Potential donor cells need to be studied thoroughly through differentiation *in vivo* or *in vitro*. Differentiation into cardiomyocyte using a clinically relevant differentiation inducer is a crucial requirement in understanding the different pathways involved in this process.

The involvement of endogenous non-coding small RNAs which affect protein production post-transcriptionally holds an ability to change gene expression and would advance our understanding of CVD in health and disease (Kumar *et al.*, 2005). To address this, an embryonic carcinoma stem cell line (P19) was used in this thesis. They are multipotent cells which may develop into all three germ layers (Hu *et al.*, 2011 & Van Der Heyden *et al.*, 2003B). P19 cells are an established cardiomyocyte model which are used to investigate the early transcription factors involved in the signalling pathways (Hu *et al.*, 2011). It is one of the first to be described as a successful cardiac muscle model (Van Der Heyden *et al.*, 2003A).

One of the main advantages of P19 cell line differentiation to cardiac cells over human SCs or other types of SCs is that P19 do not require a feeder layer or a differentiation inhibitor like LIF to maintain the growth and differentiation into different lineages (Hu *et al.*, 2011 &

Van Der Heyden *et al.*, 2003A). This use of P19 cells contributes to lowering the cost and the complications that occur when using other types of cells. These advantages, as well as being able to self-renew and grow indefinitely undifferentiated (Martin & Evans, 1975; Van Der Heyden *et al.*, 2003A), show that P19 stem cell line is the best choice to investigate cardiovascular cellular mechanisms over other types of SCs.

P19 cells were maintained to develop a cardiac lineage using a bio-phospholipid molecule (LPA) as an agent. LPA is present endogenously in the heart and circulates in the blood and is released from activated platelets (Moolenaar *et al.*, 1997). Although the role of LPA has not been fully established, however, it is known that it plays a role in proliferation, apoptosis inhibition, cell migration, and many other functions that are not fully elucidated (Ishii *et al.*, 2004). Recently, LPA has been found to play essential roles in wound healing, maintenance of vascular tone, vascular integrity and reproduction (Tyagi, 2014).

LPA is an important component in the pathophysiology of the cardiovascular system. This importance is shown by the increase in serum LPA levels in post-acute MI which increased two-fold (10.43 mg/L) within 48-72 h, as compared with the control level of LPA 1.66 mg/L after 7 days (Chen *et al.*, 2003). This outcome is consistent with LPA being antiapoptotic and protecting the myocytes from hypoxia, which requires an elevated level of LPA (Chen *et al.*, 2008). However, the antiapoptotic role was mainly seen at concentrations between 2 and 20 $\mu$ M (Chen *et al.*, 2006; 2008). This range is the physiological concentration in serum, but it could be elevated and released in plasma in response to injury or thrombosis and MI in the pathological conditions (Chen *et al.*, 2006). This correlates with other findings of how LPA plays a role in smooth muscle contraction, platelet aggregation and vasoactive effects to improve the myocytes in the heart (Gaits *et al.*, 1997). This suggests a critical role of LPA in regenerating new cardiac cells from SCs, thus inhibiting apoptosis. Yang *et al.* (2013) observed that LPA receptor 1 knock-out enhanced LPA- induced cardiac hypertrophy. While LPA receptor 3 when over-expressed, repressed the cardiac hypertrophy and silenced LPA receptor 1. Accordingly, it is suggested that LPA receptors could have opposing roles that need further clarification by investigating possible targets and pathways that might explain these events.

To investigate further, the signalling pathway and the potential role of other endogenous factors that may mediate and affect the regulation of P19 SCs differentiation into

cardiomyocytes induced by LPA; miRNAs were explored. These non-coding single-stranded RNA are known to be involved in cell proliferation, apoptosis, migration and differentiation (Crone *et al.*, 2012), and LPA independently shares some of these roles. Growing evidence is establishing the involvement of miRNA in differentiation into several lineages, the development of diseases and cancer progression (Crone *et al.*, 2012; Wilson KD *et al.*, 2010). Yang *et al.* (2013) recently suggested how mir-23a and 2 linked to the LPA receptors could reciprocally regulate each other. It has also been suggested that mir-146a could inhibit the G protein-coupled receptors (Crone *et al.*, 2012), which are mainly activated by LPA in several systems (Moolenaar *et al.*, 1997).

Additionally, mir-30c-2 is expressed in ovarian cancer cells, and down-regulated an oncogene called BCL9. It also suppressed growth factor-induced cell proliferation, a role that LPA plays in the ovarian tumour microenvironment (Jia *et al.*, 2011).

Another example is, mir-24, which targets LPA acyltransferase (LPAAT $\beta$ ), and inhibits cell proliferation in osteosarcoma, one of the most commonly found tumours in the bones of adolescents and children (Song *et al.*, 2013). Physiologically, LPA is converted into phosphatidic acid (PA) by LPAAT (Rastegar *et al.*, 2010). This association of LPA with several cellular pathways suggests that miRNA may be involved in the differentiation of cardiomyocytes. The specific miRNAs involved, and their effects are essential in understanding their modes of action on how this translates into pathology in the cardiovascular system.

Initially, this report looked at the effect of LPA on P19 SCs differentiation into cardiomyocytes, investigating the time and concentration-dependent actions. Also, as miRNAs are attracting increasing interest as a possible therapeutic target and as biomarkers, their role in LPA differentiation was investigated. The focus of this thesis, therefore, centred around two of the promising primary therapies, SCs and miRNA. This aim would significantly enhance the rationale in the treatment of cardiac hypertrophy and cardiac failure, as well as myocardial infarction and other heart problems. The induction of differentiation into cardiomyocytes by LPA, the endogenous phospholipid, would be of benefit as a biomarker, and as a potential advancement to the repair and regeneration of damaged hearts.

## 4.1. Primary cultures and model establishment

The primary cultures of P19 cells were demonstrated to be rapidly growing cells, reaching 70- 80% confluence within two days. We found that over-confluent cultures could cause unexpected and non-specific differentiation leading to inconsistent results in the protein level and elevated expression of cardiac biomarkers. This result observed in areas with dark plaques and growth of multiple layers of cells in the culture. Super-confluency of cells was avoided by continuous monitoring of cells and regular trypsinisation of cultures. Cultures were also maintained with media changes every second day and monitored daily under an inverted microscope for any unexpected changes.

## 4.2. Cardiac cells model and effects of LPA

Cells treated with LPA were examined using a confocal microscope and treated with either OCT4 or Troponin I. The pictures suggest a high expression of OCT4 in control unlike the cells treated with LPA and DMSO which shows diminished expression (Green). Troponin-I was also highly expressed in LPA, and DMSO treated cells (Figure 3.4). Velasquez-Mao *et al.* (2017) used amniotic fluid-derived SCs (AFSC) iPSC and differentiated cardiac myocytes and demonstrated the expression of a range of pluripotency markers, which indicated downregulation of OCT4 when differentiated into cardiac myocytes with functional cardiac genes. Czysz *et al.*, (2015) showed that DMSO also rapidly downregulated the expression of OCT4 and NANOG using, immunohistochemistry, flow cytometry and RT-PCR. Lian *et al.*, (2012) used GSK3 inhibitor to initiate the differentiation which did not result in the expression of OCT4 but expressed heart ISL1 and Nkx2.5 from human pluripotent SCs. Tasmin (2010), showed the role of the chemical induction into CM from P19 cells. They demonstrated the downregulation of OCT4 and the expression of Troponin I as explained in our data. All these confirm that downregulation of OCT4 is consistent with induction of differentiation into a cardiac lineage.

In terms of the cardiomyocyte development, LPA triggered significant signalling to induce differentiation of the P19 cells as assessed by the differential expression of key protein markers. Initial experiments were designed to look at whether exerted its effect in a

concentration and time-dependent manner and if so, which concentration exerted the maximal effect and at which time point. The endpoint target was to monitor the significant expression of cardiac markers like MLC-1v and Troponin I as well as looking for lower expression in pluripotency markers like OCT4 protein reciprocally. Cells were aggregated into EB (as explained in the methods section) in the presence of LPA at concentrations of 0, 0.5, 1, 5, 10, & 20 $\mu$ M. These cultures were lysed at day 6 after plating the aggregated EBs and western blot results were generated. MLC-1v expression was induced significantly at 5 ( $p < 0.05$ ), 10 ( $p < 0.05$ ) and 20 $\mu$ M ( $p < 0.01$ ) compared to control. While LPA 0.5 and 1 $\mu$ M concentration did not significantly induce MLC-1v, as shown in Figure 3.4. Correspondingly, beating clumps were observed at a 20 $\mu$ M concentration of LPA starting from day 3 until day 6. In addition to MLC-1v, troponin-I was also enhanced following LPA treatment further confirming the ability of LPA to induce the differentiation of P19 SCs to differentiate.

This data suggests that the regulation of differentiation by LPA is concentration dependent and the higher the concentration, the higher the expression of MLC-1v. This conclusion comes hand in hand with what our colleague Pramod (2017) found in her work. According to many reports on cardiac development, one of the main findings is observing beating clusters under the microscope (Van Der Heyden *et al.*, 2003B; Kehat *et al.*, 2001; Boheler *et al.*, 2002; Maltsev *et al.*, 1994; Kumar *et al.*, 2005). These beating cells were elongated and increased in size as well as forming cell-cell junctions (Figure 3.7). These beating cells that are discussed in the mentioned reports were shadowed in our case when cells were clustered with LPA. However, this was apparent and constant at 20 $\mu$ M of LPA compared to the lesser concentrations. Even though Pramod (2017) discussed this finding but, the difference and the relevance of the beating clusters between the different concentrations were not disclosed.

Other than LPA, oxytocin has also been reported to stimulate the production of beating cells by other researchers (Paquin *et al.*, 2002). This report suggested that oxytocin could be a serum-borne factor which might be activated by DMSO. Whether oxytocin mediates the effect of LPA in our model remains to be established. Others have suggested that LPA and oxytocin share a similar role which includes inducing stress-fiber formation which is vital for the maintenance and the initiation of contractions in smooth muscle cells (Gogarten *et al.*, 2001). However, LPA is found to upregulate oxytocin receptors in vitro in the myometrial

cells (uterine myocytes) (Jeng *et al.*, 2003). Clinically, labour in pregnancies is led by contractions, which are induced by oxytocin in the uterine (reviewed in Wocławek-Potocka *et al.*, 2014). Therefore, LPA possesses the ability to enhance the stress-fiber in the uterine for contraction (reviewed in Wocławek-Potocka *et al.*, 2014). LPA also could act similarly in regulating contraction of cardiomyocytes.

The pluripotency marker, OCT4, was investigated to establish whether differentiation coincided with the loss or decrease in stemness. The expression of OCT4 decreased significantly as the concentration of LPA increased. However, a significant difference was found starting from a concentration of 1  $\mu$ M of LPA in contrast with MLC-1v, which showed a significant difference starting from 5  $\mu$ M. This reaction could be because the differentiation of the P19 SCs depends on the decrease in the factors that moderate their self-repair and regeneration that keeps the cells in their undifferentiated state through different transcription factors that hold the responsibility of these roles. Thus, as soon as the cells lose these characteristics, the cells start to differentiate and respond to the differentiation inducers (Wilson *et al.*, 2010; Xu *et al.*, 2009). While at 5, 10 & 20  $\mu$ M LPA suppressed the expression of OCT4, the difference between these three concentrations was not significant. The main pluripotency transcription factors were silenced or were downregulated, from 5  $\mu$ M LPA. This suggests that at a 5  $\mu$ M concentration of LPA, the pluripotency markers reduced, and the cells are expressing markers of differentiation or committed to differentiation.

Having established our model showing that LPA regulates P19 stem cell differentiation in a concentration-dependent manner, the next step was to focus on determining the mechanism by which LPA establishes whether this differentiation is time-dependent. Long-time course and short-time course experiments were designed. In the long-time course experiment with 5  $\mu$ M of LPA was used because of the ability to regulate P19 into myocytes. This concentration is in the lower range of the physiological concentration. 5  $\mu$ M of LPA and untreated P19 cell (negative control) from the same batch were lysed on day 0 (before plating), day 3, day 6, day 9 and day 12. The results obtained showed an apparent increase in the expression of MLC-1v in LPA treated cells in a time-dependent manner, except for day 12. At day 12, the expression slightly decreased as compared to day 6 and day 9. This was only significant in cells from day 6 compared to the untreated cells ( $p < 0.01$ ). This could suggest that the numbers of cells in the culture could affect the constant monolayer

formation. This also indicates that commitment occurs even after three days and that it is a time-dependent process.

The second part of this time-course experiment was to investigate the expression of MLC-1v from 5 minutes up to 24 hours. In this experiment, 5 & 20 $\mu$ M of LPA were used, and lysates were collected at day 6 and day 12. The results revealed that LPAs effect was both concentration and time-dependent. In these experiments, cells were treated with LPA before forming EBs, unlike the previous experiment, to investigate the capability of LPA to induce differentiation when treating the cells on a monolayer.

The differences between cells treated with LPA 5 $\mu$ M for 4 days compared to cells incubated with the same concentration for shorter times (5 mins-24 hrs) were analysed and the least significance compared to LPA induced cells is shown in cells incubated for 24-hours ( $p < 0.05$ ), in contrast to all the other times which matched the basal levels ( $p < 0.001$ ). This suggests that 24 hours is the lowest time to show a difference in comparison to their peers.

Furthermore, at 20 $\mu$ M LPA shows a clear difference compared to 5 $\mu$ M. The current outcome clarifies the variance seen at 6 hours and higher, including the 30 minutes incubation. These data suggest that while commitment may be initiated at a much earlier time point, sustained induction of differentiation requires longer incubation times, which gave rise to an enhanced commitment into the cardiac lineage. The cell viability was assessed in response to increasing concentration of LPA of 1-80 $\mu$ M. The different concentrations did not induce any significant changes in cell viability except on cells treated with 40 $\mu$ M, a non-physiological concentration which ranges between 5-20 $\mu$ M.

In addition to LPA, DMSO was used as a positive control and was shown to regulate the differentiation showing high expression of MLC-1v. DMSO has been established as a differentiation inducer of P19 cells to cardiomyocytes (Abilez *et al.*, 2006; Angello *et al.*, 2006; Van der Heyden *et al.*, 2003A; Boheler *et al.*, 2002; Jasmin *et al.*, 2010; Edwards *et al.*, 1983; Arreola *et al.*, 1993; Skerjanc, 1994). The differentiation of the cardiac cells is associated with transcription factors which are highly expressed and upregulated in cardiac cells like Csx/NKx2.5, GATA4/6 and Mef2c (Kumar *et al.*, 2005). These are activated by some extracellular molecules such as WNT, BMP, DMSO, fibroblast growth factors (FGF), LPA and other chemicals (Bartunek *et al.*, 2007). These factors possibly play a role in

suppressing OCT4, SOX and NANOG and specific kinases would, as a result, activate and initiate some signalling events such as MAPK ERK, P38 MAPK, PKC, PI3K, TAK1 and other pathways known to be established in their activation in myogenesis (Van Der Heyden *et al.*, 2003B). MLC-1v, MLC-2v,  $\alpha$  and  $\beta$ - MHC, atrial natriuretic protein (ANP), cardiac Troponin C and other proteins are up-regulated and are expressed more in induced differentiated cardiac cells compared to the undifferentiated state (Van Der Heyden *et al.*, 2003B; Bartunek *et al.*, 2007; Kumar *et al.*, 2005). However, it is not entirely clear how DMSO and LPA induce this differentiation, and which pathway is involved.

### **4.3. Concentration-dependent expression of transcription factors and key miRNAs induced by LPA**

Having established and validated the regulation of P19 cells differentiation into cardiomyocytes, by exploring the expression of cardiac-specific proteins (MLC-1v & Troponin and pluripotent factors. Further studies carried out focused on miRNAs (mir-145 and mir-1) and transcription factors (OCT4, Nkx2.5). mir-145 and mir-1 were selected because mir-145 is found to be highly over-expressed when cells are committed to differentiation (Xu *et al.*, 2009). While mir-1 mainly linked to cardiomyocytes and CVDs (Roma-Rodrigues *et al.*, 2015). OCT4 and NKX2.5 were selected to reflect the transition from pluripotency to cardiomyocytes.

qRT-PCR is one the most appropriate methods for the identification of specific miRNA expression profiles (Tong & Nemunaitis, 2008; Hu *et al.*, 2011; Callis & Wang., 2008; Wang K. *et al.*, 2012). Multiple investigators looked at the miRNA's expression profile specifically during cardiogenesis. Some miRNAs play critical roles in some of the biological systems that have thoroughly identified. However, these findings are related to different stem cell lines such as mesenchymal, human embryonic and induced pluripotent SCs, or using different differentiation inducers like DMSO.

Similarly, isolated cardiomyocytes from animal models which do not need any external inducers also used for the same purpose. In our case, this project is unique in its idea because it is for the first time that the roles of miRNAs are to be investigated about the induction of cardiomyocytes differentiation by LPA in P19 cells.

qRT-PCR is one of the primary techniques for miRNA studies, especially in identifying critical roles for regulation (Hohjoh & Fukushima *et al.*, 2007; Wilson *et al.*, 2010). In our reviews, miRNAs chosen due to their close association with cardiogenesis and its up-regulation in the heart or its regulatory reciprocals with LPA receptors. mir-1, mir-133, mir-145 and U6 gene chosen and ordered from Qiagen for that purpose and RNA extraction is one of the most critical steps before running qPCR that is involved. For specific and reliable results in this project, the RNA quality intended was high, which containing no degraded RNA and no DNA contamination (Swift *et al.*, 2000; Pfaffl, 2004). RNA purity was measured at A260 and the ratio of A260/A280 in a spectrophotometer and used to determine the purity of the RNA isolated. Pure RNA ratio is between 1.8-2.1, while, less absorption means protein contaminants present (QIAGEN guidelines). The integrity and the size of the total RNA were further checked on a denaturing agarose gel stained by ethidium bromide. The ribosomal RNA (18s and 28s rRNA) should appear sharp, and with no smear; otherwise, it would indicate signs of degradation of RNA in the sample. In this report, the isolated RNA samples had sharp bands and clear 18s and 28s rRNAs, which assure no degradation of RNA. All RNA samples were transcribed into cDNA according to the method described above. This helps in preserving the samples as cDNAs are more stable, unlike RNAs.

Optimisation of assays and primers is an essential phase before running samples on qRT-PCR. An effective way of optimising the qPCR assay is by running serial dilutions, and the results used to generate a standard curve. An optimised linear standard curve should be close to  $R^2 > 0.980$  or  $r > | -0.990 |$ . While high amplification efficiency should be between 90 and 105% and consistency across replicates (Bio-Rad guidelines). In the optimisation steps, 2 house-keeping genes (U6 and mir-15a) and the primers evaluated in this research were optimised as illustrated in the results section.

All the required steps were achieved, and the qRT-PCR experiments for all conditions were performed and analysed under the optimised conditions. U6 (house-keeping gene) was used as a control gene. Samples were mixed with a carefully calculated SYBR green mixture (according to the protocol described in materials and methods).

The mRNA expression for OCT4 was tested initially as a pluripotent gene. It was analysed on 3 different days (Day 3, 6 and 12) with 5 different concentrations of LPA. However, there was no significant difference over the 3 days but, a decline in the latter, especially on day 6

and 12, was evident and marginally significant on day 6 for the 5 $\mu$ M of LPA. It was reported that LPA did not affect the expression of OCT4 (mRNA) in the blastocyst stage of a bovine embryo (Torres *et al.*, 2014), and was able to decrease or increase the effect of apoptotic agents and growth factors. This thesis focused on the context of cardiac cell progenitors. This suggests that the expression of OCT4 is dependent on the type of cells and the lineage. There is no published research on cardiomyocytes induced by LPA, which examines the expression of OCT4. Additionally, Gq and Gi proteins coupled receptors were able to affect the expression of OCT4 and NANOG in neuronal cells developed from P19 cells by retinoic acid (Heck *et al.*, 1997). This was also suggested by Cappuccio *et al.* (2005) in ES cells induced by MGLU5 metabotropic glutamate. Although the protein expression of OCT4 showed an evident increasing trend, the mRNA levels tested on day six was unexpected. This could be due to the post-transcriptional regulation and other factors like methylation or acetylation. This is because “overall low correspondence between mRNA and protein expression, implying strong contribution of post-transcriptional levels of regulation.” (Koussounadis *et al.*, 2015). In other similar experiments, there was also a significant decrease in OCT4 mRNA, which could also be related to the same reasons.

Similarly, NKX2.5 showed no significant change, but there was a clear increase in the expression on day 12 with 5, 10 and 20 $\mu$ M LPA.

mir-145 was shown to be up-regulated in cardiomyocyte generated by LPA on day six compared to the untreated SCs. This confirms the role of mir-145, which is widely understood and observed to be down-regulated in self-renewing embryonic SCs (Xu *et al.*, 2009). This specific miRNA is distinct in inducing pluripotency (iPSC) or re-programming the cells which are already specialised with different kinds of cells. This is because mir-145 down-regulates the main influential pluripotency-inducers and act to preserve the cells in the undifferentiated state, retains cells-renewal and cells-regeneration. Mir-145 regulates OCT4, KLF4 and SOX2, by repressing the un-translated 3' regions. According to XU and his colleagues (2009), they found that OCT4 binds and repress the promoters of mir-145. This suggests the reciprocal relationship between OCT4 and mir-145. In conclusion, it can be confirmed from the outcomes in this project that LPA up-regulates mir-145, which can explain the regulation of OCT4, specifically on day 6.

Mir-1 is overexpressed ( $p < 0.05$ ) when cells were treated with 2, 5 and 10 $\mu$ M of LPA on day

3 and at 5 $\mu$ M on day 6. While day 12, did not show any significant change in the expression. Unlike with mir-145, the effect on mir-1 seems to be happening earlier on day 3. mir-1 is widely known to be an anti-hypertrophic and one of the key players in heart failure (Da Costa Martins *et al.*, 2012; Hou *et al.*, 2012).  $\beta$ -adrenoreceptor ( $\beta$ -AR) induces contraction through Gs proteins and regulates the release of nitric oxide (NO) in the heart through Gi protein when the endothelial NO-synthase is activated (Hou *et al.*, 2012). According to Hou *et al.*, (2012), when  $\beta$ -AR is stimulated with Isoproterenol (ISO), mir-1 was found to be upregulated as NO was also released in accordance and this concluded the anti-hypertrophic role of mir-1 as well as its link with heart and cardiac cells. This was again proposed in vivo experiments and the ability of mir-1 in reversing induced cardiac hypertrophy by preventing maladaptive cardiac remodelling promised some possible therapeutic roles (Karakikes *et al.*, 2013).

In 2013, Lu and his colleagues overexpressed mir-1 in a human cardiovascular progenitor cell differentiated into cardiomyocytes. They concluded that this was done by suppressing roles of mir-1 that targets the WNT and FGF signalling pathways at a very early stage of the cardiac commitment. Recently, it was shown in P19 cells that mir-1 is significantly increased in differentiated cells and promotes cardiogenesis. They also showed that when over-expressed, it decreases apoptosis by downregulating caspase-3 and expressing Hand2 (Liu *et al.*, 2017). Our findings in this regard, confirms that mir-1 is upregulated in cells induced to differentiate into cardiomyocytes, supporting the conclusions above.

#### **4.4. Inhibition of LPA receptors**

These experiments aimed to investigate the effect of each LPA receptor when pre-treated with its specific antagonist. In some of the inhibitors, there were multiple IC<sub>50</sub>s, which means each has a different affinity for the various receptor (Table 4.1). These receptors also have different downstream pathways and as a result, different roles and activities. Nevertheless, some of the receptors share the same or multiple pathways (Figure 4.1)

**Table 4.1: Inhibitors and antagonists used and their targets.**

Antagonist	Conc./IC <sub>50</sub>	Target	Used conc.	Target (based on Conc.)
1 Suramin	43µM	GPCRs (EDG-3/S1P3), LPA receptor 4	50µg/ml	All
2 LY294002	0.31, 0.73, 1.06 and 6.60µM	PI3-kinase (PI3-Kβ, PI3-Kα, PI3-Kσ and PI3-Kγ)	7µM	All
3 H2L5765834	94, 463 and 752nM	LPA receptor 1, 5 and 3	0.5 & 0.8µM	LPA R1 & 5 LPA R1, 5 & 3
4 H2L5186303	8.9, 1230 and 27354nM	LPA receptor 2, 3 and 1	1.25µM	LPA R2 & 3
5 TC-LPA5-4	0.8µM	LPA receptor 5	1.6µM	LPA R5

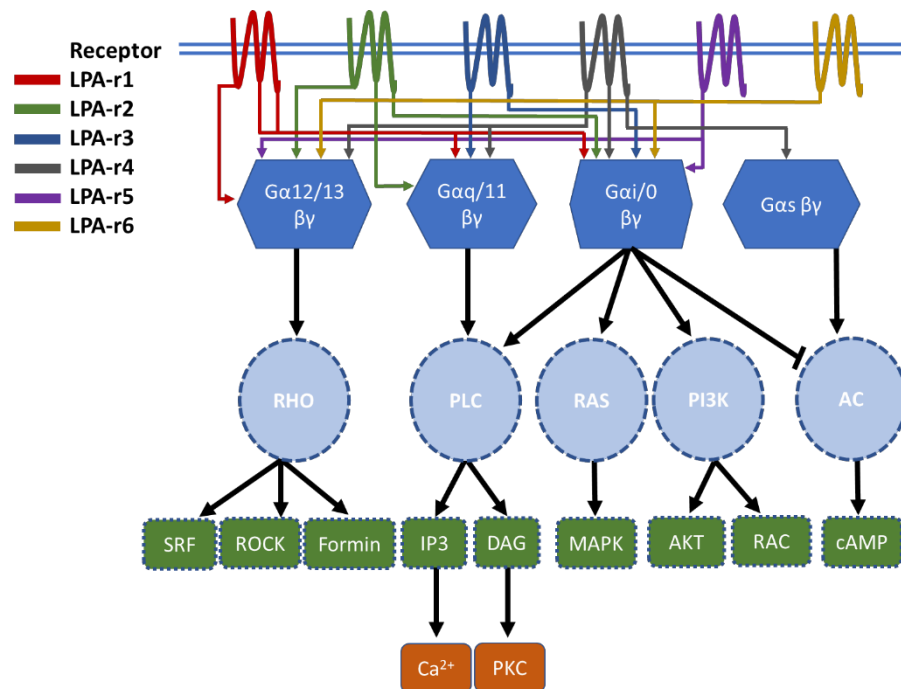


**Figure 4.1: LPA receptors and downstream signalling pathways.**

LPA receptors from LPA receptor 1 to 6 are labelled with different colours on the membrane. The blue hexagonal structures represent the G protein-coupled receptors. The other structures represent the downstream signalling pathways (González-Gil *et al.*, 2014; Riaz *et al.*, 2016; Kihara *et al.*, 2014; Gardell *et al.*, 2006). This is reproduced from Chapter 1, Figure 1.8.

## **LPAR4**

Suramin is a widely used inhibitor that targets the P2Y purinergic receptors, which are closely related to LPAR4, according to González-Gil *et al.* (2014). Cells were pre-treated with suramin and displayed effective antagonistic abilities on the expression of MLC-1v by significantly inhibiting the differentiation induced by LPA, which also suppressed the basal levels of MLC-1v. This exerted action could be linked with the block of LPAR4, which was consistently tested and discussed by Pramod (2017) in her work, by which similar impact was observed on MLC-1v in this thesis.

## **LPAR5**

Next, the protein expression of MLC-1v induced by LPA was again tested, but this time against LPAR5. Previously, Pramod (2017) suggested that due to the absence of LPAR5, which was undetected by qPCR and on gel electrophoresis contrary to LPA1-4, that it could be because it is not expressed in P19 cells. However, TC-LPA5-4 is a potent and specific inhibitor first discovered and identified by Kozian *et al.* (2012). They described TC-LPA5-4 as “the first non-lipid, small molecule inhibitor for LPA5/GPR92, specifically inhibiting LPA-mediated platelet activation in vitro.”. The LPA-mediated platelet activation role was tested by comparing the impact of this inhibitor against the other inhibitors which targeted selectively, LPAR1/3 and LPAR2 against LPAR5. In conclusion, their data showed that the antagonistic effect of LPAR5 interfered with 16:0 alkyl-LPA-mediated platelet activation (Kozian *et al.*, 2012).

Comparably, our results suggest an active role for LPAR5 and that it is indeed could be expressed in P19 cells induced by LPA. This comes from the significant enhancement in MLC-1v compared to the cells treated with the inhibitor only and a partial decrease of up to a mean of 30% compared to the LPA treated cells that occurred following the addition of LPA to the inhibited cells. Additionally, OCT4 at a protein and mRNA levels had also reversed the effect of LPA when cells were similarly pre-treated with LPAR5 inhibitor. Although, we established the crosslink between OCT4 and mir-145, however, the impact on the expression of mir-145 when LPAR5 was blocked seems to be minimal and does not reflect the expression of OCT4. This do not negate the involvement of mir-145 or the other miRNAs like mir-1 at least indirectly.

The possible reason for the loss or the non-detection of LPAR5 in Pramod's (2017) research could be due to a non-specific primer which was used which resulted in the lack of amplification of LPAR5 mRNA which further would mean the loss of the band in the gel electrophoresis. This finding proposes that the effect of LPA is at least in part mediated through LPAR5 and hence opens another door for more extensive research and re-evaluation which possibly can help in the prevention of the fatal consequences of atherosclerosis as Kozian *et al.* (2012) recommended.

## **LPAR2 and LPAR3**

In conjunction with the previous inhibitors that we used, H2L5186303 is another interesting inhibitor aimed to block LPAR2 and 3 (Table 4.1) selectively. LPAR2 was not investigated by Pramod (2017) at the time due to the lack of any commercial inhibitors. However, she identified the highest mRNA expression for LPAR2 in between the other receptors. She also tested LPAR1/3 using Ki16425 by which her results suggested that LPA induced differentiation is maintained through both LPAR 1/3, including LPAR4. To further our understanding of the matter, 1.25 $\mu$ M of H2L5186303, which is a concentration that covers the IC50 of 8.9nM for LPAR2 and 1,230nM LPAR3, respectively (Fells *et al.*, 2009). However, this concentration is more selective and potent to LPAR3 at the mentioned IC50 than LPAR2. The results generated were unexpected, as the impact of this inhibitor was not extended to MLC-1v or the other cardiac markers. OCT4 was the key factor identified in both protein level and mRNA. The LPA induced OCT4 protein expression has increased significantly in addition to the mRNA decrease of the basal levels when the inhibitor is added. This could be associated with the changes in the expression of mir-145, an OCT4 regulator, as it evidently increased when LPA was added to a similar level to LPA-induced P19 cells. This could mean that LPA was blocked and had no effect on the expression of OCT4 at the basal level in the presence of the inhibitor, and this reflects the expression of mir-145, which was low.

To conclude, inhibiting the dual LPAR (2&3) has partially blocked the differentiation through the regulation of OCT4 and mir-145 and did not affect protein expression of MLC-1v significantly. LPAR3 was shown by Pramod (2017) to be the least to express compared to LPAR2, which was the highest to express. As mentioned earlier, as the concentration used

was to target both receptors and seems to be more directed toward LPAR3 in terms of the IC50, this could be linked to the low expression of LPAR3 in P19 cells, which require further investigation and increase in the n values to reach to more conclusive answers.

In contrast, we attempted to investigate another inhibitor, H2L5765834 which did not show any antagonistic actions except on one occasion. The basal mRNA of OCT4 decreased when LPAR3 was encompassed using the concentration required. This reaction of OCT4 was not apparent when a lower concentration used. Initially to specifically target the dual LPAR1 & 5 to be assessed. This dual again, for some reason, didn't seem to cause any changes, suggesting further evaluation to affirm the possible link between LPAR3 and OCT4 and the actual role of LPAR1 and 5.

## **4.5. Suppression of protein kinase-C inhibit differentiation**

Bisindolylmaleimide 1 (BIM-1), is an established protein kinase inhibitor of PKC isoform and MLC kinase. BIM-1 was used to ascertain the possible effect on differentiation and expression of key factors involved in the process of differentiation. It has been shown that PKC is one of the critical regulators of the differentiation. The total reduction in the expression of myogenic markers induced by LPA is confirmed in this thesis supported by the decrease in miRNAs due to the impact of BIM-1. This is consistent with the conclusion others reached that PKC is critical in the differentiation of stem cells into cardiomyocytes (Xu *et al.*, 1991; Koyanagi *et al.*, 2009). Even though different isoforms of PKC showed to have a contrary role in the development of myocytes (Moblely *et al.*, 2010; Koyanagi *et al.*, 2009), however, the selective block to all the isoform by BIM-1 seems to be negatively affecting the cardio-myogenesis as also shown previously by my colleague Pramod (2017). Rawal *et al.* (2014) discussed the possible link between miRNAs and PKC signalling pathways specifically in the context of the protection of heart linked diseases (Liu *et al.*, 2018; Wang *et al.*, 2016A). In this case, the data strongly support their suggestions and further propose that the regulation of miRNAs by LPA are critically dependent on the activation of a mixture of PKC and MLC Kinase.

## 4.6. Role of PI3K in LPA-induced regulation of MLC-1v and OCT4

Next, cells treated with LY294002 were evaluated. The PI3 kinase is another downstream pathway which is activated by LPA through Gi GPCR (Figure 4.1). When activated, it is understood to play a role in cell proliferation, cancer, and cell cycle (Wang *et al.*, 2003). In cancer, the over-activation of PI3k increase the resistance to apoptosis via the PI3k/AKT/mTOR pathway (McKenzie & Kyprianou, 2006; Tørring *et al.*, 2003). It also plays a pro-apoptotic role, mediated by mir-210 in the development of atherosclerosis (Li *et al.*, 2017). miRNAs are evidently reported to be associated with atherosclerosis by developing the atherosclerotic plaques (Raitoharju *et al.*, 2011; Li *et al.*, 2017; Parahuleva *et al.*, 2018). Mir-92a, mir-99a, miR-21, miR-210, miR-34a, and miR-146 are all upregulated and known to be involved in atherosclerosis (Raitoharju *et al.*, 2011; Yu *et al.*, 2014; Li *et al.*, 2017; Parahuleva *et al.*, 2018). mir-210 specifically, which is also a pro-apoptotic regulator acts through targeting PDK1 towards forming the plaques (Li *et al.*, 2017. This is relevant to this thesis since miRNAs are shown to be one of the main regulators of diseases and cell development, which makes them a therapeutic target, as reviewed in Araldi & Suárez (2016).

The link between LPA and PI3K pathway seems to be related to NHE3 mobility (Cha *et al.*, 2010). NHE3 mobility is a Na<sup>+</sup>/H<sup>+</sup> exchange isoform found in the apical membrane, which also plays a role in the pH regulation (Alexander *et al.*, 2005; Cha *et al.*, 2010). Inhibition of PI3K leads to the induction of cell apoptosis in some cases, which correlates with the inhibition of in-vitro ovarian cancer models. In vivo, it can suppress tumour growth and induction of apoptosis (Semba *et al.*, 2002) and in-vitro it can significantly downregulate the formation and growth of carcinoma in the ovary. As such, OCT4 is widely understood to be an crucial antiapoptotic agent (Wang *et al.*, 2013; Wen *et al.*, 2013; Zhang *et al.*, 2016; Meng *et al.*, 2018) and an essential factor in maintaining stem cells in their undifferentiated state and exerts the ability to regain the pluripotency of the cells (Takahashi & Yamanaka, 2006; Yu *et al.*, 2007; Xu *et al.*, 2009). This could relate to how the antagonist of a PI3K seems to be affecting the basal level of OCT4 by just less than a mean of 50%. This was also consistent with the mRNA levels of OCT4 which was very low, not only that, the latter was further demolished when LPA was mixed with the inhibitor which caused something like a

double effect on the latter. Besides that, Rho, a downstream signalling pathway which is activated by several LPA receptors according to Alexander *et al.* (2005) showed that it exerts the ability to dictate the mobility of the Na<sup>+</sup>/H<sup>+</sup> exchange through the LPA G-protein Gα12/13 (Figure 4.1).

miRNAs are a regulating sequence to most of the genes like OCT4 by mir-145. However, the expression of mir-145 was not implicated, which suggest that there is no direct link to the PI3 kinase. This was also the case with mir-1, which was very marginal with at least 1-fold difference observed when LPA is blocked through the PI3k. The expression of mir-133 was similarly partially blocked. This implies that miRNAs have no significant effect on the abnormal inhibitory regulation of some kinases, in our case, post-PI3 kinase inhibition based on the results. Our observations showed that the latter was without effect on basal MLC-1v and GATA4 protein expression but appear to suppress the induction caused by LPA partially. This was, however, found not to be statistically significant due to the possibly considerable variation in the individual experimental data. This comes in contrary to what Pramod (2017) found in her produced data, although the concentration used by herself was less, starting from 5µM (p<0.001) to a total demolition at 10 and 20µM of the MLC-1v expression induced by LPA. The outcome of our result could be due to the low concentration compared to the successful inhibition of differentiation occurred by several researchers (Klinz *et al.*, 1999; Sauer *et al.*, 2000; Humphrey, 2009). By which all these mentioned, has used an excess of 20µM up to 50µM to induce and establish the effect of the inhibition of the PI3K pathway. The low concentration that we used in our experiments (7µM) could be a factor in the unexpected results. This will require an increase in the n value in future studies as well as the elevation of the concentration. It is also possible that responses to LPA are only partially mediated via PI3 kinase as part of a signalling cascade as concluded by D'amico and his group (2016). They suggest that IL6 induce cardiac differentiation of embryonic stem cells through a signalling cascade that includes PTEN, PKC as well as PI3K.

## 4.7. Effects of transfection of siRNA (inhibitors) and mimic (overexpression) with or without LPA

In this part of the research, the siRNA/mimic experiments with mir-145 and mir-1 following the successful previous link to the differentiation and MLC-1v was investigated. The analysis included testing protein expression and assessing the effect of the overexpression or inhibition at the translational level. qPCR experiments were also used to analyse the mRNA levels as a response to the transfection.

Although there were no direct binding sites between mir-145 and myosin light chain, mir-143 seems to have a binding site, as shown in figure 4.2. This was extracted from an online database tool called Target-Scan. mir-143 and mir-145 are found as clusters and shares various activities physiologically like switching the phenotype of vascular smooth muscle cells (Rangrez *et al.*, 2011). Previously, mir-145 was shown as a tumour suppressor (Zhang *et al.*, 2015B). According to Hong and his colleagues (2017), both modulate the synovial fibroblasts cells phenotype in samples of rheumatoid arthritis. Cell adhesion, proliferation and apoptosis, as well as the disruption of cervical epithelial barriers are activities that mir-145/143 actively involved in (Anton *et al.*, 2017). In addition, mir-145/143 function as tumour suppressors together as clusters, but this could be influenced by different factors (Johannessen *et al.*, 2017). Tumour suppression was also reported by Chivukula *et al.* (2014) as roles for the cluster together in the colon and the intestinal epithelial cells. They highlighted the importance of mir-145/143 in the regeneration of mouse intestinal epithelial cells.

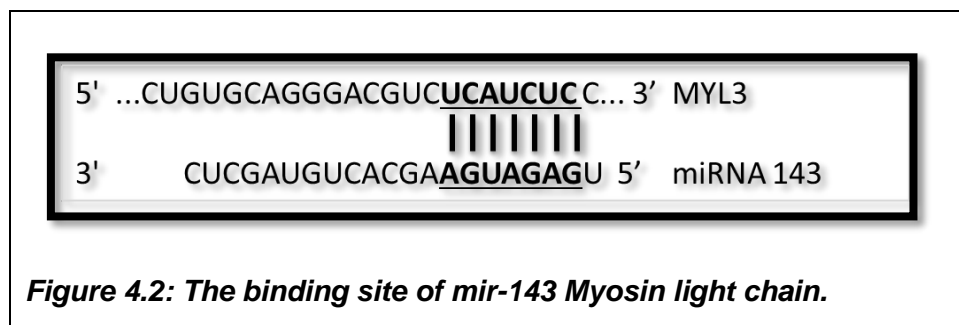
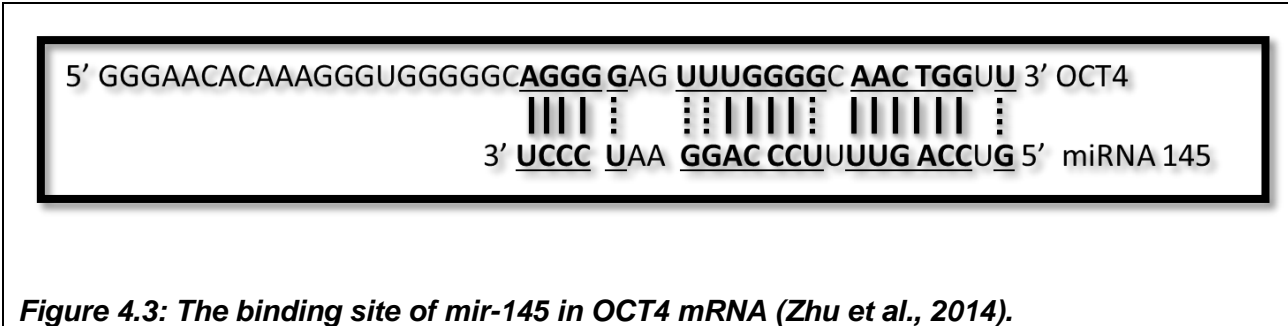


**Figure 4.2: The binding site of mir-143 Myosin light chain.**

mir-133 is shown in various researches to be a critical cardiology and differentiation inducer as well as a unique anti-hypertrophic factor (table 1.2) However; we were interested in finding if there is a relationship between mir-145 and mir-133. It is understood that mir-133

with mir-145 has been associated with some specific activities. Qui *et al.* (2014) concluded that both miRNAs regulate the expression of an MMP-9 and Cyclin D1 because of targeting SP1. They also concluded that both inhibit the cell cycle, cell proliferation invasion and migration, specifically in cancer cells. This regulation and activities were also predicted in Target-Scan and reported in several published papers in different cells and tissues (Chiyomaru *et al.*, 2010; Yoshino *et al.*, 2011; Akanuma *et al.*, 2014; Kano *et al.*, 2010; Guo *et al.*, 2013). As mentioned previously, mir-145 targets the main key pluripotency markers of stem cells, majorly OCT4 which we are in our work focusing on as it shares binding sites with mir-145 (Figure 4.3; Zhu *et al.*, 2014). For that reason, mir-145 was targeted to be inhibited and overexpressed using a transfection technique to assess the importance of this miRNAs in the differentiation, including understanding the molecular mechanism that regulates the LPA-induced cardiomyocytes.



In another very recent study, mir-145 and mir-133 were together associated closely in playing critical roles in regulating genes involved in atherosclerosis precisely in plasma (Klu *et al.*, 2018). This critical regulation, however, was a cross-reaction activity by which mir-133 was up-regulated, unlike mir-145, which was down-regulated. Another research on myogenesis in a rainbow trout has reported that mir-133 represented myogenic miRNAs (Koganti *et al.*, 2017). Moreover, Narickas *et al.* (2016) reviewed the established role of both miRNAs in the vascular smooth muscle cells differentiation concluding the importance of understanding the cross-activity between miRNAs as well as considering the specific purpose of these miRNAs. Mir-133 and mir-1 are normally transcribed together and located in the same chromosomal loci. Both are linked closely to cardiomyocytes and early embryogenesis, specifically cardiogenesis.

As per our results, mir-1 has shown an increase in expression in response to the differentiation induced by LPA. It was earlier (From day 3) compared to mir-145 (day 6) and more apparent compared to mir-133. For that reason, a choice was made to also beside mir-145 to target mir-1 as a cardiac marker to investigated with specific mir-1 siRNA inhibitor and another specific mimic for mir-1. Our results of transfection support this. The overexpression of mir-1 has given rise to an overly enhanced expression of MLC-1v. This enhancement went even further when LPA was added.

When mir-145 inhibited, LPA did not affect its expression, although we hypothesised that LPA might play a significant role in regulating miR-145 as shown previously. The addition of LPA minimally impacted overexpressed mir-145 using a mimic. All the other targeted proteins and mRNAs were also minimally affected by the addition of LPA when mir-1 was aimed (either inhibited or over-expressed), except that mir-1 when overexpressed showed a significant visible increase with and without LPA in OCT4 gene expression. This is unexpected as the increase in mir-1 should refer to the fact that the cells are committed to differentiate with the protein expression to decline rather than increase. Looking at the other results which were not implicated We can conclude that the inhibition and overexpression of mir-145 did not enhance or decrease any of the targets and this could be a failure in the technical experimental design. While mir-1 was similar except the effect observed on MLC-1v and OCT4 protein, furthermore, questions about the transfection efficiency rightly could be asked. Other reasons could be the cell state and the confluence, as suggested by some scientists to be critical for efficiency. Toxicity of the solutions is another possible factor in which can decrease expression of the target. Another set of advice includes using miR-negative control from a scramble mimic that is not like any other used sequences. Additionally, multiple sets of concentration of the target are to be used in conjunction with a similar concentration in the negative samples. This would attempt to identify the toxicity and effectiveness of each concentration in the future.

**CHAPTER 5**  
**CONCLUSION and FUTURE WORK**

## 5.1 Conclusion

A model has been validated in this thesis, confirming an ability of LPA to induce the generation of cardiomyocyte from the embryonic p19 SCs. This induction was concentration and time-dependent. Also, this regulation was shown to be achieved through the activation of specific signalling pathways linked to LPA receptors, PKC and partially PI3 kinase. While LPA receptors like LPAR4 and LPAR5 selectively shown to be critical in generating cardiomyocytes while LPAR2 and LPAR3 has a partial mediation activity of the LPA-induced differentiation. These were also supported by examining changes in cardiac-specific miRNAs expression, which were altered significantly. Our results show a clear involvement of miRNAs in the generation of cardiomyocytes from P19 SCs. Specifically, mir-145 and mir-1, by which the role of mir-145 was linked to the regulatory effect that it imposed on OCT4 the pluripotent factor. mir-1, on the other side, had shown a close relation with differentiation as enhancer and activator of expression of MLC-1v. As part of our results, we also confirm that miRNAs could regulate LPAR5, which was only predicted by Belleannée *et al.* (2012) and not shown practically.

## 5.2 Future work

The research conducted for this thesis has validated the in vitro model for generating cardiomyocytes from SCs and has further generated a novel data outlining the potential role of some key transcription factors and miRNAs in the differentiation process induced by the endogenous biolipid, LPA. The research has however raised further supplementary questions. The following bullet points have suggested a summary of future works:

- The n value for several of the studies needs to be increased to determine the statistical significance of trends observed. This was not possible during this thesis because of time constraints.
- Re-validation of the specific role each LPA receptor plays by using specific inhibitors with a range of concentrations exploring the molecular mechanism involved (miRNA).
- For a more profound understanding of the role miRNA play in the regulation of differentiation of P19 SCs into cardiac cells, the studies should be extended to other potential miRNAs to determine the most critical ones.
- Investigating the effect of the inhibition and overexpression of miRNA that could impact the differentiation using a properly designed experiment aiming a high efficiency and standardised negative control.
- Using alternative techniques to validate all the results for robust conclusions.
- A comparative study between P19 and embryonic human SCs in LPA induced differentiation of SCs into cardiomyocytes is also required to determine whether our observations are reflected in other SCs, preferably of human origin.

# References

- Abilez, O., Benharash, P., Miyamoto, E., Gale, A., Xu, C., & Zarins, C. K. (2006). P19 progenitor cells progress to organized contracting myocytes after chemical and electrical stimulation: implications for vascular tissue engineering. *Journal of Endovascular Therapy: An Official Journal of the International Society of Endovascular Specialists*, 13(3), 377–388. <https://doi.org/10.1583/06-1844.1>
- Agarwala, P., Pandey, S., & Maiti, S. (2015). Organic & Biomolecular Chemistry The tale of RNA G-quadruplex. *Organic & Biomolecular Chemistry*, 13. <https://doi.org/10.1039/c4ob02681k>
- Akanuma, N., Hoshino, I., Akutsu, Y., Murakami, K., Isozaki, Y., Maruyama, T., ... Matsubara, H. (2014). MicroRNA-133a regulates the mRNAs of two invadopodia-related proteins, FSCN1 and MMP14, in esophageal cancer. *British Journal of Cancer*, 110(1), 189–198. <https://doi.org/10.1038/bjc.2013.676>
- Alexander, R. T., Furuya, W., Szászi, K., Orłowski, J., & Grinstein, S. (2005). Rho GTPases dictate the mobility of the Na/H exchanger NHE3 in epithelia: role in apical retention and targeting. *Proceedings of the National Academy of Sciences of the United States of America*, 102(34), 12253–8. <https://doi.org/10.1073/pnas.0409197102>
- An, S., Bleu, T., Zheng, Y., & Goetzl, E. J. (1998). Recombinant Human G Protein-Coupled Lysophosphatidic Acid Receptors Mediate Intracellular Calcium Mobilization. *Molecular Pharmacology*, 54(5), 881–888. <https://doi.org/10.1124/mol.54.5.881>.
- Angello, J. C., Kaestner, S., Welikson, R. E., Buskin, J. N., & Hauschka, S. D. (2006). BMP induction of cardiogenesis in P19 cells requires prior cell-cell interaction(s). *Developmental Dynamics*, 235(8), 2122–2133. <https://doi.org/10.1002/dvdy.20863>
- Anton, L., DeVine, A., Sierra, L.-J., Brown, A. G., & Elovitz, M. A. (2017). miR-143 and miR-145 disrupt the cervical epithelial barrier through dysregulation of cell adhesion, apoptosis and proliferation. *Scientific Reports*, 7(1), 3020. <https://doi.org/10.1038/s41598-017-03217-7>
- Araldi, E., & Suárez, Y. (2016). MicroRNAs as regulators of endothelial cell functions in cardiometabolic diseases. *Biochimica et Biophysica Acta (BBA) - Molecular and Cell Biology of Lipids*, 1861(12), 2094–2103. <https://doi.org/10.1016/j.bbalip.2016.01.013>

- Arreola, J., Spires, S., & Begenisich, T. (1993). Na<sup>+</sup> channels in cardiac and neuronal cells derived from a mouse embryonal carcinoma cell line. *The Journal of Physiology*, 472(1), 289–303. <https://doi.org/10.1113/jphysiol.1993.sp019947>
- Auda-Boucher, G., Bernard, B., Fontaine-Pérus, J., Rouaud, T., Mericksay, M., & Gardahaut, M.-F. (2000). Staging of the Commitment of Murine Cardiac Cell Progenitors. *Developmental Biology*, 225(1), 214–225. <https://doi.org/10.1006/dbio.2000.9817>
- Ayatollahi, M. (2011). Hepatogenic differentiation of mesenchymal stem cells induced by insulin like growth factor-I. *World Journal of Stem Cells*, 3(12), 113. <https://doi.org/10.4252/wjsc.v3.i12.113>
- Bartel, D. P. (2004). MicroRNAs: genomics, biogenesis, mechanism, and function. *Cell*, 116(2), 281–97. Retrieved from <http://www.ncbi.nlm.nih.gov/pubmed/14744438>.
- Bartel, D. P. (2009). MicroRNAs: Target Recognition and Regulatory Functions. *Cell*, 136(2), 215–233. <https://doi.org/10.1016/j.cell.2009.01.002>.
- Bartunek, J., Croissant, J. D., Wijns, W., Gofflot, S., de Lavareille, A., Vanderheyden, M., ... Heyndrickx, G. R. (2007). Pretreatment of adult bone marrow mesenchymal stem cells with cardiomyogenic growth factors and repair of the chronically infarcted myocardium. *AJP: Heart and Circulatory Physiology*, 292(2), H1095–H1104. <https://doi.org/10.1152/ajpheart.01009.2005>
- Baudhuin, L. M., Cristina, K. L., Lu, J., & Xu, Y. (2002). Akt Activation Induced by Lysophosphatidic Acid and Sphingosine-1-phosphate Requires Both Mitogen-Activated Protein Kinase Kinase and p38 Mitogen-Activated Protein Kinase and Is Cell-Line Specific. *Molecular Pharmacology*, 62(3), 660. Retrieved from <http://molpharm.aspetjournals.org/content/62/3/660.abstract>
- Belleannée, C., Calvo, E., Thimon, V., Cyr, D. G., Légaré, C., Garneau, L., & Sullivan, R. (2012). Role of microRNAs in controlling gene expression in different segments of the human epididymis. *PLoS One*, 7(4), e34996. <https://doi.org/10.1371/journal.pone.0034996>
- Beltrami, A. P. A. P., Barlucchi, L. L., Torella, D. D., Baker, M. M., Limana, F. F., Chimenti, S. S., ... Anversa, P. P. (2003). Adult Cardiac Stem Cells Are Multipotent and Support Myocardial Regeneration. *Cell* ..., 114(6), 14. Retrieved from

[http://www.sciencedirect.com/science/article/pii/S0092867403006871%5Cnpapers3://publication/doi/10.1016/S0092-8674\(03\)00687-1](http://www.sciencedirect.com/science/article/pii/S0092867403006871%5Cnpapers3://publication/doi/10.1016/S0092-8674(03)00687-1)

Beltrami, A. P., Urbanek, K., Kajstura, J., Yan, S. M., Finato, N., Bussani, R., ... Anversa, P. (2001). Evidence that human cardiac myocytes divide after myocardial infarction. *The New England Journal of Medicine*, *344*(23), 1750–7. <https://doi.org/10.1056/NEJM200106073442303>

Bertero, A., Madrigal, P., Galli, A., Hubner, N. C., Moreno, I., Burks, D., ... Vallier, L. (2015). Activin/nodal signaling and NANOG orchestrate human embryonic stem cell fate decisions by controlling the H3K4me3 chromatin mark. *Genes & Development*, *29*(7), 702–17. <https://doi.org/10.1101/gad.255984.114>

Bian, D., Su, S., Mahanivong, C., Cheng, R. K., Han, Q., Pan, Z. K., ... Huang, S. (2004). Lysophosphatidic Acid Stimulates Ovarian Cancer Cell Migration via a Ras-MEK Kinase 1 Pathway. *Cancer Research*, *64*(12), 4209–4217. <https://doi.org/10.1158/0008-5472.CAN-04-0060>

Boheler, K. R., Czyz, J., Tweedie, D., Yang, H.-T. T., Anisimov, S. V., & Wobus, A. M. (2002). Differentiation of Pluripotent Embryonic Stem Cells Into Cardiomyocytes. *Circulation Research*, *91*(3), 189–201. <https://doi.org/10.1161/01.res.0000027865.61704.32>

Bragdon, B., Moseychuk, O., Saldanha, S., King, D., Julian, J., & Nohe, A. (2011). Bone Morphogenetic Proteins: A critical review. *Cellular Signalling*, *23*(4), 609–620. <https://doi.org/10.1016/j.cellsig.2010.10.003>

Brand, T. (2003). Heart development: molecular insights into cardiac specification and early morphogenesis. *Developmental Biology*, *258*(1), 1–19. [https://doi.org/10.1016/S0012-1606\(03\)00112-X](https://doi.org/10.1016/S0012-1606(03)00112-X)

Broderick, J., & Zamore, P. (2011). MicroRNA therapeutics. *Gene Therapy*, *18*, 1104–1110. <https://doi.org/10.1038/gt.2011.50>

Callis, T. E., & Wang, D. Z. (2008). Taking microRNAs to heart. *Trends in Molecular Medicine*, *14*(6), 254–260. <https://doi.org/10.1016/j.molmed.2008.03.006>

- Cammas, A., & Millevoi, S. (2017). SURVEY AND SUMMARY RNA G-quadruplexes: emerging mechanisms in disease. *Nucleic Acids Research*, 45(4), 1584–1595. <https://doi.org/10.1093/nar/gkw1280>
- Cappuccio, I., Spinsanti, P., Porcellini, A., Desiderati, F., De Vita, T., Storto, M., ... Melchiorri, D. (2005). Endogenous activation of mGlu5 metabotropic glutamate receptors supports self-renewal of cultured mouse embryonic stem cells. *Neuropharmacology*, 49, 196–205. <https://doi.org/10.1016/J.NEUROPHARM.2005.05.014>
- Carè, A., Catalucci, D., Felicetti, F., Bonci, D., Addario, A., Gallo, P., ... Condorelli, G. (2007). MicroRNA-133 controls cardiac hypertrophy. *Nature Medicine*, 13(5), 613–618. <https://doi.org/10.1038/nm1582>
- Carninci, P., Kasukawa, T., Katayama, S., Gough, J., Frith, M. C., Maeda, N., ... RIKEN Genome Exploration Research Group and Genome Science Group (Genome Network Project Core Group). (2005). The Transcriptional Landscape of the Mammalian Genome. *Science*, 309(5740), 1559–1563. <https://doi.org/10.1126/science.1112014>
- Cha, B., Zhu, X. C., Chen, W., Jones, M., Ryoo, S., Zachos, N. C., ... Donowitz, M. (2010). NHE3 mobility in brush borders increases upon NHERF2-dependent stimulation by lyophosphatidic acid. *Journal of Cell Science*, 123. <https://doi.org/10.1242/jcs.056713>
- Chen, J. F., Mandel, E. M., Thomson, J. M., Wu, Q., Callis, T. E., Hammond, S. M., ... Wang, D. Z. (2006). The role of microRNA-1 and microRNA-133 in skeletal muscle proliferation and differentiation. *Nature Genetics*, 38(2), 228–233. <https://doi.org/10.1038/ng1725>
- Chen, J., Baydoun, A. R., Xu, R., Deng, L., Liu, X., Zhu, W., ... Chen, X. (2008). Lysophosphatidic Acid Protects Mesenchymal Stem Cells Against Hypoxia and Serum Deprivation-Induced Apoptosis. *Stem Cells*, 26(1), 135–145. <https://doi.org/10.1634/stemcells.2007-0098>.
- Chen, J., Cui, L., Yuan, J., Zhang, Y., & Sang, H. (2017). Circular RNA WDR77 target FGF-2 to regulate vascular smooth muscle cells proliferation and migration by sponging miR-124. *Biochemical and Biophysical Research Communications*, 494(1–2), 126–132. <https://doi.org/10.1016/j.bbrc.2017.10.068>

- Chen, J., Han, Y., Zhu, W., Ma, R., Han, B., Cong, X., ... Chen, X. (2006). Specific receptor subtype mediation of LPA-induced dual effects in cardiac fibroblasts. *FEBS Letters*, *580*(19), 4737–4745. <https://doi.org/10.1016/J.FEBSLET.2006.07.061>.
- Chen, X., Yang, X. Y., Wang, N. D., Ding, C., Yang, Y. J., You, Z. J., ... Chen, J. H. (2003). Serum lysophosphatidic acid concentrations measured by dot immunogold filtration assay in patients with acute myocardial infarction. *Scandinavian Journal of Clinical and Laboratory Investigation*, *63*(7–8), 497–503. <https://doi.org/10.1080/00365510310003265>
- Cheng, X., & Joe, B. (2017). Circular RNAs in rat models of cardiovascular and renal diseases. *Physiological Genomics*, *49*(9), 484–490. <https://doi.org/10.1152/physiolgenomics.00064.2017>
- Chiong, M., Wang, Z. V., Pedrozo, Z., Cao, D. J., Troncoso, R., Ibacache, M., ... Lavandero, S. (2011). Cardiomyocyte death: Mechanisms and translational implications. *Cell Death and Disease*, *2*(12). <https://doi.org/10.1038/cddis.2011.130>
- Chivukula, R. R., Shi, G., Acharya, A., Mills, E. W., Zeitels, L. R., Anandam, J. L., ... Mendell, J. T. (2014). An Essential Mesenchymal Function for miR-143/145 in Intestinal Epithelial Regeneration. *Cell*, *157*(5), 1104–1116. <https://doi.org/10.1016/J.CELL.2014.03.055>
- Chiyomaru, T., Enokida, H., Tatarano, S., Kawahara, K., Uchida, Y., Nishiyama, K., ... Nakagawa, M. (2010). miR-145 and miR-133a function as tumour suppressors and directly regulate FSCN1 expression in bladder cancer. *British Journal of Cancer*, *102*(5), 883–891. <https://doi.org/10.1038/sj.bjc.6605570>
- Cho, Y.-D., Yoon, W.-J., Woo, K.-M., Baek, J.-H., Park, J.-C., & Ryoo, H.-M. (2010). The canonical BMP signaling pathway plays a crucial part in stimulation of dentin sialophosphoprotein expression by BMP-2. *The Journal of Biological Chemistry*, *285*(47), 36369–76. <https://doi.org/10.1074/jbc.M110.103093>
- Choi, S.-C., Yoon, J., Shim, W.-J., Ro, Y.-M., & Lim, D.-S. (2004). 5-azacytidine induces cardiac differentiation of P19 embryonic stem cells. *Experimental & Molecular Medicine*, *36*(6), 515–523. <https://doi.org/10.1038/emm.2004.66>.
- Choong, O. K., Lee, D. S., Chen, C.-Y., & Hsieh, P. C. H. (2017). The roles of non-coding RNAs in cardiac regenerative medicine. *Non-Coding RNA Research*, *2*(2), 100–110. <https://doi.org/10.1016/J.NCRNA.2017.06.001>.

- Cissell, K. A., & Deo, S. K. (2009). Trends in microRNA detection. *Analytical and Bioanalytical Chemistry*, 394(4), 1109–1116. <https://doi.org/10.1007/s00216-009-2744-6>
- Contos, J. J., Fukushima, N., Weiner, J. A., Kaushal, D., & Chun, J. (2000). Requirement for the IpA1 lysophosphatidic acid receptor gene in normal suckling behavior. *Proceedings of the National Academy of Sciences of the United States of America*, 97(24), 13384–9. <https://doi.org/10.1073/pnas.97.24.13384>.
- Crone, S. G., Jacobsen, A., Federspiel, B., Bardram, L., Krogh, A., Lund, A. H., & Friis-Hansen, L. (2012). MicroRNA-146a inhibits G protein-coupled receptor-mediated activation of NF- $\kappa$ B by targeting CARD10 and COPS8 in gastric cancer. *Molecular Cancer*, 11. <https://doi.org/10.1186/1476-4598-11-71>
- Czysz, K., Minger, S., & Thomas, N. (2015). DMSO efficiently down regulates pluripotency genes in human embryonic stem cells during definitive endoderm derivation and increases the proficiency of hepatic differentiation. *PloS One*, 10(2), e0117689. <https://doi.org/10.1371/journal.pone.0117689>
- Da Costa Martins, P. A., & De Windt, L. J. (2012). MicroRNAs in control of cardiac hypertrophy. *Cardiovascular Research*, 93(4), 563–572. <https://doi.org/10.1093/cvr/cvs013>
- De Backer, G., Ambrosioni, E., Borch-Johnsen, K., Brotons, C., Cifkova, R., Dallongeville, J., ... Zanchetti, A. (2003). European guidelines on cardiovascular disease prevention in clinical practice Third Joint Task Force of European and other Societies on Cardiovascular Disease Prevention in Clinical Practice (constituted by representatives of eight societies and by invited experts). *European Heart Journal*, 24(17), 1601–1610. [https://doi.org/10.1016/S0195-668X\(03\)00347-6](https://doi.org/10.1016/S0195-668X(03)00347-6)
- Decorsière, A., Cayrel, A., Vagner, S., & Millevoi, S. (2011). Essential role for the interaction between hnRNP H/F and a G quadruplex in maintaining p53 pre-mRNA 3'-end processing and function during DNA damage. *Genes & Development*, 25(3), 220–225. <https://doi.org/10.1101/gad.607011>
- Derrien, T., Johnson, R., Bussotti, G., Tanzer, A., Djebali, S., Tilgner, H., ... Guigó, R. (2012). The GENCODE v7 catalog of human long noncoding RNAs: analysis of their gene structure, evolution, and expression. *Genome Research*, 22(9), 1775–89. <https://doi.org/10.1101/gr.132159.111>

- Derynck, R., & Zhang, Y. E. (2003). Smad-dependent and Smad-independent pathways in TGF- $\beta$  family signalling. *Nature*, *425*(6958), 577–584. <https://doi.org/10.1038/nature02006>
- Deshwar, A. R., Chng, S. C., Ho, L., Reversade, B., & Scott, I. C. (2016). The Apelin receptor enhances Nodal/TGF $\beta$  signaling to ensure proper cardiac development. *ELife*, *5*. <https://doi.org/10.7554/eLife.13758>
- DeWood, M. A., Spores, J., Notske, R., Mouser, L. T., Burroughs, R., Golden, M. S., & Lang, H. T. (1980). Prevalence of Total Coronary Occlusion during the Early Hours of Transmural Myocardial Infarction. *New England Journal of Medicine*, *303*(16), 897–902. <https://doi.org/10.1056/NEJM198010163031601>
- Donovan, P. J., & Gearhart, J. (2001). The end of the beginning for pluripotent stem cells. *Nature*, *414*(6859), 92–97. <https://doi.org/10.1038/35102154>.
- Dubin, A. E., Herr, D. R., & Chun, J. (2010). Diversity of LPA receptor-mediated intracellular calcium signaling in early cortical neurogenesis. *The Journal of Neuroscience : The Official Journal of the Society for Neuroscience*, *30*(21), 7300. <https://doi.org/10.1523/JNEUROSCI.6151-09.2010>.
- Duelen, R., & Sampaolesi, M. (2017). Stem Cell Technology in Cardiac Regeneration: A Pluripotent Stem Cell Promise. *EBioMedicine*, *16*, 30–40. <https://doi.org/10.1016/j.ebiom.2017.01.029>
- Eddy, J., & Maizels, N. (2008). Conserved elements with potential to form polymorphic G-quadruplex structures in the first intron of human genes. *Nucleic Acids Research*, *36*(4), 1321–1333. <https://doi.org/10.1093/nar/gkm1138>
- Edwards, M. K., Harris, J. F., & McBurney, M. W. (1983). Induced muscle differentiation in an embryonal carcinoma cell line. *Molecular and Cellular Biology*, *3*(12), 2280–6. Retrieved from <http://www.ncbi.nlm.nih.gov/pubmed/6656767>
- Eichholtz, T., Jalink, K., Fahrenfort, I., & Moolenaar, W. H. (1993). The bioactive phospholipid lysophosphatidic acid is released from activated platelets. *The Biochemical Journal*, *291* ( Pt 3(3), 677–680. <https://doi.org/10.1042/bj2910677>
- Evans, M. & Kaufman, M (1981). Establishment in culture of pluripotent cells from mouse embryos. *Nature*, *292*:154-156.

- Fells, J. I., Tsukahara, R., Liu, J., Tigyi, G., & Parrill, A. L. (2009). Structure-based drug design identifies novel LPA3 antagonists. *Bioorganic & Medicinal Chemistry*, *17*(21), 7457. <https://doi.org/10.1016/J.BMC.2009.09.022>.
- Fernández-Ruiz, I. (2016). Stem cells: A step closer to cardiac repair therapies. *Nature Reviews Cardiology*, *13*(12), 695–695. <https://doi.org/10.1038/nrcardio.2016.178>
- Forouzanfar, M. H., Liu, P., Roth, G. A., Ng, M., Biryukov, S., Marczak, L., ... Murray, C. J. L. (2017). Global Burden of Hypertension and Systolic Blood Pressure of at Least 110 to 115 mm Hg, 1990-2015. *JAMA*, *317*(2), 165. <https://doi.org/10.1001/jama.2016.19043>
- Frangogiannis, N. G. (2015). Pathophysiology of Myocardial Infarction. In *Comprehensive Physiology* (pp. 1841–1875). Hoboken, NJ, USA: John Wiley & Sons, Inc. <https://doi.org/10.1002/cphy.c150006>
- Friedman, R. C., Farh, K. K. H., Burge, C. B., & Bartel, D. P. (2009). Most mammalian mRNAs are conserved targets of microRNAs. *Genome Research*, *19*(1), 92–105. <https://doi.org/10.1101/gr.082701.108>
- Gadue, P., Huber, T., Nostro, M., Kattman, S., & Keller, G. (2005). Germ layer induction from embryonic stem cells. *Experimental Hematology*, *33*(9), 955–964. <https://doi.org/10.1016/j.exphem.2005.06.009>
- Gahr, S. A., Weber, G. M., & Rexroad, C. E. (2012). Identification and expression of Smads associated with TGF- $\beta$ /activin/nodal signaling pathways in the rainbow trout (*Oncorhynchus mykiss*). *Fish Physiology and Biochemistry*, *38*(5), 1233–1244. <https://doi.org/10.1007/s10695-012-9611-7>
- Gaits, F., Fourcade, O., Le Balle, F., Gueguen, G., Gaigé, B., Gassama-Diagne, A., ... Chap, H. (1997). Lysophosphatidic acid as a phospholipid mediator: Pathways of synthesis. *FEBS Letters*, *410*(1), 54–58. [https://doi.org/10.1016/S0014-5793\(97\)00411-0](https://doi.org/10.1016/S0014-5793(97)00411-0)
- Gangaraju, V. K., & Lin, H. (2009). MicroRNAs: Key regulators of stem cells. *Nature Reviews Molecular Cell Biology*, *10*(2), 116–125. <https://doi.org/10.1038/nrm2621>
- Gardell, S. E., Dubin, A. E., & Chun, J. (2006). Emerging medicinal roles for lysophospholipid signaling. *Trends in Molecular Medicine*, *12*(2), 65–75. <https://doi.org/10.1016/j.molmed.2005.12.001>

- Gay, A., & Towler, D. A. (2017). Wnt signaling in cardiovascular disease. *Current Opinion in Lipidology*, 28(5), 387–396. <https://doi.org/10.1097/MOL.0000000000000445>
- Gó Mez-Orte, E., Sá Enz-Narciso, B., Moreno, S., & Cabello, J. (2013). Multiple functions of the noncanonical Wnt pathway. *Trends in Genetics*, 29, 545–553. <https://doi.org/10.1016/j.tig.2013.06.003>
- Gogarten, W., Emala, C. W., Lindeman, K. S., & Hirshman, C. a. (2001). Oxytocin and lysophosphatidic acid induce stress fiber formation in human myometrial cells via a pathway involving Rho-kinase. *Biology of Reproduction*, 65(2), 401–6. <https://doi.org/10.1095/biolreprod65.2.401>
- González-Gil, I., Zian, D., Vázquez-Villa, H., Ortega-Gutiérrez, S., & López-Rodríguez, M. L. (2015). The status of the lysophosphatidic acid receptor type 1 (LPA 1 R). *MedChemComm*, 6(1), 13–23. <https://doi.org/10.1039/C4MD00333K>
- Grépin, C., Nemer, G., & Nemer, M. (1997). Enhanced cardiogenesis in embryonic stem cells overexpressing the GATA-4 transcription factor. *Development (Cambridge, England)*, 124(12), 2387–2395.
- Grote, P., Wittler, L., Hendrix, D., Koch, F., Währisch, S., Beisaw, A., ... Herrmann, B. G. (2013). The tissue-specific lncRNA Fendrr is an essential regulator of heart and body wall development in the mouse. *Developmental Cell*, 24(2), 206–14. <https://doi.org/10.1016/j.devcel.2012.12.012>
- Guttman, M., Amit, I., Garber, M., French, C., Lin, M. F., Feldser, D., ... Lander, E. S. (2009). Chromatin signature reveals over a thousand highly conserved large non-coding RNAs in mammals. *Nature*, 458(7235), 223–7. <https://doi.org/10.1038/nature07672>
- Hansen, T. B., Jensen, T. I., Clausen, B. H., Bramsen, J. B., Finsen, B., Damgaard, C. K., & Kjems, J. (2013). Natural RNA circles function as efficient microRNA sponges. *Nature*, 495(7441), 384–388. <https://doi.org/10.1038/nature11993>
- Heck, S., Enz, R., Richter-Landsberg, C., & Blohm, D. H. (1997). Expression of eight metabotropic glutamate receptor subtypes during neuronal differentiation of P19 embryocarcinoma cells: a study by RT-PCR and in situ hybridization. *Developmental Brain Research*, 101(1–2), 85–91. [https://doi.org/10.1016/S0165-3806\(97\)00048-5](https://doi.org/10.1016/S0165-3806(97)00048-5)

- Hentze, M. W., & Preiss, T. (2013). Circular RNAs: Splicing's enigma variations. *EMBO Journal*, 32(7), 923–925. <https://doi.org/10.1038/emboj.2013.53>
- Hong, B.-K., You, S., Yoo, S.-A., Park, D., Hwang, D., Cho, C.-S., & Kim, W.-U. (2017). MicroRNA-143 and -145 modulate the phenotype of synovial fibroblasts in rheumatoid arthritis. *Experimental & Molecular Medicine*, 49(8), e363. <https://doi.org/10.1038/emm.2017.108>
- Hou, Y., Sun, Y., Shan, H., Li, X., Zhang, M., Zhou, X., ... Lu, Y. (2012).  $\beta$ -adrenoceptor regulates miRNA expression in rat heart. *Medical Science Monitor: International Medical Journal of Experimental and Clinical Research*, 18(8), BR309-314. <https://doi.org/10.12659/MSM.883263>
- Hsiao, K.-Y., Sun, H. S., & Tsai, S.-J. (2017). Circular RNA – New member of noncoding RNA with novel functions. *Experimental Biology and Medicine*, 242(11), 1136–1141. <https://doi.org/10.1177/1535370217708978>
- Huang, L., Lin, J.-X., Yu, Y.-H., Zhang, M.-Y., Wang, H.-Y., & Zheng, M. (2012). Downregulation of Six MicroRNAs Is Associated with Advanced Stage, Lymph Node Metastasis and Poor Prognosis in Small Cell Carcinoma of the Cervix. *PLoS ONE*, 7(3), e33762. <https://doi.org/10.1371/journal.pone.0033762>
- Huang, P., Gong, Y. Z., Peng, X. L., Li, S. J., Yang, Y., & Feng, Y. P. (2010). Cloning, identification, and expression analysis at the stage of gonadal sex differentiation of chicken miR-363 and 363\*. *Acta Biochimica Et Biophysica Sinica*, 42(8), 522–529. <https://doi.org/10.1093/abbs/gmq061>
- Humphrey, P. S. (2009). *Signal Transduction Mechanisms for Stem Cell Differentiation Into Cardiomyocytes*. Retrieved from <https://uhra.herts.ac.uk/handle/2299/3760>.
- Hunter, J. J., & Chien, K. R. (1999). Signaling Pathways for Cardiac Hypertrophy and Failure. *New England Journal of Medicine*, 341(17), 1276–1283. <https://doi.org/10.1056/NEJM199910213411706>.
- Huppert, J. L., Bugaut, A., Kumari, S., & Balasubramanian, S. (2008). G-quadruplexes: the beginning and end of UTRs. *Nucleic Acids Research*, 36(19), 6260–8. <https://doi.org/10.1093/nar/gkn511>

- Inoue, M., Rashid, M. H., Fujita, R., Contos, J. J. A., Chun, J., & Ueda, H. (2004). Initiation of neuropathic pain requires lysophosphatidic acid receptor signaling. *Nature Medicine*, *10*(7), 712–718. <https://doi.org/10.1038/nm1060>
- Ishii, I., Fukushima, N., Ye, X., & Chun, J. (2004). Lysophospholipid Receptors: Signaling and Biology. *Annual Review of Biochemistry*, *73*(1), 321–354. <https://doi.org/10.1146/annurev.biochem.73.011303.073731>
- Ivey, K. N. K. N. K., Muth, A., Arnold, J., King, F. W. F. F. W., Yeh, R. R. R. F., Jason, E., ... others. (2008). MicroRNA regulation of cell lineages in mouse and human embryonic stem cells. *Cell Stem Cell*, *2*(3), 219–229. Retrieved from <http://www.sciencedirect.com/science/article/pii/S193459090800057X>
- Jasmin, Spray, D. C., Campos de Carvalho, A. C., & Mendez-Otero, R. (2010). Chemical Induction of Cardiac Differentiation in P19 Embryonal Carcinoma Stem Cells. *Stem Cells and Development*, *19*(3), 403–412. <https://doi.org/10.1089/scd.2009.0234>
- Jayaraj, G. G., Pandey, S., Scaria, V., & Maiti, S. (2012). Potential G-quadruplexes in the human long non-coding transcriptome. *RNA Biology*, *9*(1), 81–89. <https://doi.org/10.4161/rna.9.1.18047>
- Jeng, Y.-J., Soloff, S. L., Anderson, G. D., & Soloff, M. S. (2003). Regulation of Oxytocin Receptor Expression in Cultured Human Myometrial Cells by Fetal Bovine Serum and Lysophospholipids. *Endocrinology*, *144*(1), 61–68. <https://doi.org/10.1210/en.2002-220636>
- Jia, W., Eneh, J. O., Ratnaparkhe, S., Altman, M. K., & Murph, M. M. (2011). MicroRNA-30c-2\* Expressed in Ovarian Cancer Cells Suppresses Growth Factor-Induced Cellular Proliferation and Downregulates the Oncogene BCL9. *Molecular Cancer Research*, *9*(12), 1732–1745. <https://doi.org/10.1158/1541-7786.MCR-11-0245>
- Jiang, Q., Wang, Y., Hao, Y., Juan, L., Teng, M., Zhang, X., ... Liu, Y. (2009). miR2Disease: A manually curated database for microRNA deregulation in human disease. *Nucleic Acids Research*, *37*(SUPPL. 1). <https://doi.org/10.1093/nar/gkn714>
- Johannessen, C., Moi, L., Kiselev, Y., Pedersen, M. I., Dalen, S. M., Braaten, T., & Busund, L.-T. (2017). Expression and function of the miR-143/145 cluster in vitro and in vivo in human breast cancer. *PLOS ONE*, *12*(10), e0186658. <https://doi.org/10.1371/journal.pone.0186658>

- Karakikes, I., Chaanine, A. H., Kang, S., Mukete, B. N., Jeong, D., Zhang, S., ... Lebeche, D. (2013). Therapeutic cardiac-targeted delivery of miR-1 reverses pressure overload-induced cardiac hypertrophy and attenuates pathological remodeling. *Journal of the American Heart Association*, 2(2), e000078. <https://doi.org/10.1161/JAHA.113.000078>
- Katz, M. G., Fargnoli, A. S., Kendle, A. P., Hajjar, R. J., & Bridges, C. R. (2016). The role of microRNAs in cardiac development and regenerative capacity. *American Journal of Physiology. Heart and Circulatory Physiology*, 310(5), H528-41. <https://doi.org/10.1152/ajpheart.00181.2015>
- Kehat, I., Kenyagin-Karsenti, D., Snir, M., Segev, H., Amit, M., Gepstein, A., ... Gepstein, L. (2001). Human embryonic stem cells can differentiate into myocytes with structural and functional properties of cardiomyocytes. *Journal of Clinical Investigation*, 108(3), 407–414. <https://doi.org/10.1172/JCI200112131>
- Keller, G. (2005). Embryonic stem cell differentiation: Emergence of a new era in biology and medicine. *Genes and Development*, 19(10), 1129–1155. <https://doi.org/10.1101/gad.1303605>
- Kihara, Y., Maceyka, M., Spiegel, S., & Chun, J. (2014). Lysophospholipid receptor nomenclature review: IUPHAR Review 8. *British Journal of Pharmacology*, 171(15), 3575–3594. <https://doi.org/10.1111/bph.12678>
- Klattenhoff, C. A., Scheuermann, J. C., Surface, L. E., Bradley, R. K., Fields, P. A., Steinhauser, M. L., ... Boyer, L. A. (2013). Braveheart, a long noncoding RNA required for cardiovascular lineage commitment. *Cell*, 152(3), 570–83. <https://doi.org/10.1016/j.cell.2013.01.003>
- Kobayashi, T., Lyons, K. M., McMahon, A. P., & Kronenberg, H. M. (2005). BMP signaling stimulates cellular differentiation at multiple steps during cartilage development. *Proceedings of the National Academy of Sciences*, 102(50), 18023–18027. <https://doi.org/10.1073/pnas.0503617102>
- Koganti, P. P., Wang, J., Cleveland, B., Ma, H., Weber, G. M., & Yao, J. (2017). Estradiol regulates expression of miRNAs associated with myogenesis in rainbow trout. *Molecular and Cellular Endocrinology*, 443, 1–14. <https://doi.org/10.1016/j.mce.2016.12.014>

- Kohn, A. D., & Moon, R. T. (2005). Wnt and calcium signaling:  $\beta$ -Catenin-independent pathways. *Cell Calcium*, 38(3–4), 439–446. <https://doi.org/10.1016/j.ceca.2005.06.022>
- Kostic, I., Fidalgo-Carvalho, I., Aday, S., Vazão, H., Carvalheiro, T., Grãos, M., ... Ferreira, L. (2015). Lysophosphatidic acid enhances survival of human CD34+ cells in ischemic conditions. *Scientific Reports*, 5(1), 16406. <https://doi.org/10.1038/srep16406>
- Kotarsky, K. (2006). Lysophosphatidic Acid Binds to and Activates GPR92, a G Protein-Coupled Receptor Highly Expressed in Gastrointestinal Lymphocytes. *Journal of Pharmacology and Experimental Therapeutics*, 318(2), 619–628. <https://doi.org/10.1124/jpet.105.098848>
- Koyanagi, M., Iwasaki, M., Haendeler, J., Leitges, M., Zeiher, A. M., & Dimmeler, S. (2009). Wnt5a Increases Cardiac Gene Expressions of Cultured Human Circulating Progenitor Cells via a PKC Delta Activation. *PLoS ONE*, 4(6), e5765. <https://doi.org/10.1371/journal.pone.0005765>.
- Kozian, D. H., Evers, A., Florian, P., Wonerow, P., Joho, S., & Nazare, M. (2012). Selective non-lipid modulator of LPA5 activity in human platelets. *Bioorganic & Medicinal Chemistry Letters*, 22(16), 5239–5243. <https://doi.org/10.1016/j.bmcl.2012.06.057>.
- Kue, P. F., Taub, J. S., Harrington, L. B., Polakiewicz, R. D., Ullrich, A., & Daaka, Y. (2002). Lysophosphatidic acid-regulated mitogenic ERK signaling in androgen-insensitive prostate cancer PC-3 cells. *International Journal of Cancer*, 102(6), 572–579. <https://doi.org/10.1002/ijc.10734>
- Kumar, D., Kamp, T. J., & LeWinter, M. M. (2005). Embryonic stem cells: differentiation into cardiomyocytes and potential for heart repair and regeneration. *Coronary Artery Disease*, 16(2), 111–6. Retrieved from <http://www.ncbi.nlm.nih.gov/pubmed/15735404>.
- Li Y, Qiu C, Tu J, Geng B, Yang J, Jiang T, and C. Q. (2013). HMDD v2.0: a database for experimentally supported human microRNA and disease associations. *Nucl. Acids Res.* <https://doi.org/10.1093/nar/gkt1023>.
- Li, Y., Yang, C., Zhang, L., & Yang, P. (2017). MicroRNA-210 induces endothelial cell apoptosis by directly targeting PDK1 in the setting of atherosclerosis. *Cellular & Molecular Biology Letters*, 22, 3. <https://doi.org/10.1186/s11658-017-0033-5>

- Lian, X., Hsiao, C., Wilson, G., Zhu, K., Hazeltine, L. B., Azarin, S. M., ... Palecek, S. P. (2012). Cozzarelli Prize Winner: Robust cardiomyocyte differentiation from human pluripotent stem cells via temporal modulation of canonical Wnt signaling. *Proceedings of the National Academy of Sciences*, *109*(27), E1848–E1857. <https://doi.org/10.1073/pnas.1200250109>
- Lim, S. S., Vos, T., Flaxman, A. D., Danaei, G., Shibuya, K., Adair-Rohani, H., ... Ezzati, M. (2012). A comparative risk assessment of burden of disease and injury attributable to 67 risk factors and risk factor clusters in 21 regions, 1990–2010: a systematic analysis for the Global Burden of Disease Study 2010. *The Lancet*, *380*(9859), 2224–2260. [https://doi.org/10.1016/S0140-6736\(12\)61766-8](https://doi.org/10.1016/S0140-6736(12)61766-8)
- Lin, M. E., Herr, D. R., & Chun, J. (2010). Lysophosphatidic acid (LPA) receptors: Signaling properties and disease relevance. *Prostaglandins and Other Lipid Mediators*, *91*(3–4), 130–138. <https://doi.org/10.1016/j.prostaglandins.2009.02.002>
- Liu, G. S., Cohen, M. V., Mochly-Rosen, D., & Downey, J. M. (1999). Protein Kinase C-  $\xi$  is Responsible for the Protection of Preconditioning in Rabbit Cardiomyocytes. *Journal of Molecular and Cellular Cardiology*, *31*(10), 1937–1948. <https://doi.org/10.1006/jmcc.1999.1026>.
- Liu, J. T. (2015). Arsenic Inhibits P19 Stem Cell Differentiation By Altering MicroRNA Expression and Repressing the Sonic Hedgehog. Clemson University.
- Liu, K., Xuekelati, S., Zhou, K., Yan, Z., Yang, X., Inayat, A., ... Guo, X. (2018). Expression Profiles of Six Atherosclerosis-Associated microRNAs That Cluster in Patients with Hyperhomocysteinemia: A Clinical Study. *DNA and Cell Biology*, *37*(3), 189–198. <https://doi.org/10.1089/dna.2017.3845>
- Liu, L., Yuan, Y., He, X., Xia, X., & Mo, X. (2017). MicroRNA-1 upregulation promotes myocardiocyte proliferation and suppresses apoptosis during heart development. *Molecular Medicine Reports*, *15*(5), 2837–2842. <https://doi.org/10.3892/mmr.2017.6282>
- Lu, T.-Y., Lin, B., Li, Y., Arora, A., Han, L., Cui, C., ... Yang, L. (2013). Overexpression of microRNA-1 promotes cardiomyocyte commitment from human cardiovascular progenitors via suppressing WNT and FGF signaling pathways. *Journal of Molecular and Cellular Cardiology*, *63*, 146–54. <https://doi.org/10.1016/j.yjmcc.2013.07.019>

- Malliaras, K., & Marban, E. (2011). Cardiac cell therapy: where we've been, where we are, and where we should be headed. *British Medical Bulletin*, 98(1), 161–185. <https://doi.org/10.1093/bmb/ldr018>
- Maltsev, V. A., Wobus, A. M., Rohwedel, J., Bader, M., & Hescheler, J. (1994). Cardiomyocytes differentiated in vitro from embryonic stem cells developmentally express cardiac-specific genes and ionic currents. *Circulation Research*, 75(2), 233–244. <https://doi.org/10.1161/01.RES.75.2.233>
- Martin, G. R. (1981). Isolation of a pluripotent cell line from early mouse embryos cultured in medium conditioned by teratocarcinoma stem cells. *Proceedings of the National Academy of Sciences*, 78(12), 7634–7638. <https://doi.org/10.1073/pnas.78.12.7634>
- Martin, G. R., & Evans, M. J. (1975). Differentiation of clonal lines of teratocarcinoma cells: formation of embryoid bodies in vitro. *Proceedings of the National Academy of Sciences*, 72(4), 1441–1445. <https://doi.org/10.1073/pnas.72.4.1441>
- McBurney, M. W. (1993). P19 embryonal carcinoma cells. *The International Journal of Developmental Biology*, 37(1), 135–40. Retrieved from <http://www.ncbi.nlm.nih.gov/pubmed/8507558>.
- McIntyre, T. M., Pontsler, A. V., Silva, A. R., St. Hilaire, A., Xu, Y., Hinshaw, J. C., ... Prestwich, G. D. (2003). Identification of an intracellular receptor for lysophosphatidic acid (LPA): LPA is a transcellular PPAR agonist. *Proceedings of the National Academy of Sciences*, 100(1), 131–136. <https://doi.org/10.1073/pnas.0135855100>
- McKenzie, S., & Kyprianou, N. (2006). Apoptosis evasion: the role of survival pathways in prostate cancer progression and therapeutic resistance. *Journal of Cellular Biochemistry*, 97(1), 18–32. <https://doi.org/10.1002/jcb.20634>
- Meng, L., Hu, H., Zhi, H., Liu, Y., Shi, F., Zhang, L., ... Lin, A. (2018). OCT4B regulates p53 and p16 pathway genes to prevent apoptosis of breast cancer cells. *Oncology Letters*, 16(1), 522–528. <https://doi.org/10.3892/ol.2018.8607>.
- Meyer, I. S., Jungmann, A., Dieterich, C., Zhang, M., Lasitschka, F., Werkmeister, S., ... Leuschner, F. (2017). The cardiac microenvironment uses non-canonical WNT signaling to activate monocytes after myocardial infarction. *EMBO Molecular Medicine*, 9(9), 1279–1293. <https://doi.org/10.15252/emmm.201707565>

- Mobley, S., Shookhof, J. M., Foshay, K., Park, M., & Gallicano, G. I. (2010). PKG and PKC Are Down-Regulated during Cardiomyocyte Differentiation from Embryonic Stem Cells: Manipulation of These Pathways Enhances Cardiomyocyte Production. *Stem Cells International*, 2010, 701212. <https://doi.org/10.4061/2010/701212>.
- Monzen, K., Shiojima, I., Hiroi, Y., Kudoh, S., Oka, T., Takimoto, E., ... Komuro, I. (1999). Bone morphogenetic proteins induce cardiomyocyte differentiation through the mitogen-activated protein kinase kinase kinase TAK1 and cardiac transcription factors Csx/Nkx-2.5 and GATA-4. *Molecular and Cellular Biology*, 19(10), 7096–105. <https://doi.org/10.1128/MCB.19.10.7096>
- Moolenaar, W. H., Kranenburg, O., Postma, F. R., & Zondag, G. C. M. (1997). Lysophosphatidic acid: G-protein signalling and cellular responses. *Current Opinion in Cell Biology*, 9(2), 168–173. [https://doi.org/10.1016/S0955-0674\(97\)80059-2](https://doi.org/10.1016/S0955-0674(97)80059-2)
- Murry, C. E., Field, L. J., & Menasché, P. (2005). Cell-based cardiac repair reflections at the 10-year point. *Circulation*, 112(20), 3174–3183. <https://doi.org/10.1161/CIRCULATIONAHA.105.546218>
- Naito, A. T., Shiojima, I., Akazawa, H., Hidaka, K., Morisaki, T., Kikuchi, A., & Komuro, I. (2006). Developmental stage-specific biphasic roles of Wnt/beta-catenin signaling in cardiomyogenesis and hematopoiesis. *Proceedings of the National Academy of Sciences of the United States of America*, 103(52), 19812–7. <https://doi.org/10.1073/pnas.0605768103>
- Nakagawa, M., Koyanagi, M., Tanabe, K., Takahashi, K., Ichisaka, T., Aoi, T., Okita, K., Mochiduki, Y., Takizawa, N., and Yamanaka, S. (2008). Generation of induced pluripotent stem cells without Myc from mouse and human fibroblasts. *Nature Biotechnol.*, 26, 101–106. Retrieved from <http://dx.doi.org/10.1038/nbt1374>
- Nakagawa, S. (2016). Lessons from reverse-genetic studies of lncRNAs. *Biochimica et Biophysica Acta (BBA) - Gene Regulatory Mechanisms*, 1859(1), 177–183. <https://doi.org/10.1016/J.BBAGRM.2015.06.011>.
- Nie, J., Jiang, M., Zhang, X., Tang, H., Jin, H., Huang, X., ... Yang, Z. (2015). Post-transcriptional Regulation of Nkx2-5 by RHAU in Heart Development. *Cell Reports*, 13(4), 723–732. <https://doi.org/10.1016/j.celrep.2015.09.043>

- Noguchi, K., Ishii, S., & Shimizu, T. (2003). Identification of p2y9/GPR23 as a novel G protein-coupled receptor for lysophosphatidic acid, structurally distant from the Edg family. *Journal of Biological Chemistry*, 278(28), 25600–25606. <https://doi.org/10.1074/jbc.M302648200>
- Ohuchi, H., Hamada, A., Matsuda, H., Takagi, A., Tanaka, M., Aoki, J., ... Noji, S. (2008). Expression patterns of the lysophospholipid receptor genes during mouse early development. *Developmental Dynamics*, 237(11), 3280–3294. <https://doi.org/10.1002/dvdy.21736>.
- Ooi, B., Goh, B., & Yap, W. (2017). Oxidative Stress in Cardiovascular Diseases: Involvement of Nrf2 Antioxidant Redox Signaling in Macrophage Foam Cells Formation. *International Journal of Molecular Sciences*, 18(11), 2336. <https://doi.org/10.3390/ijms18112336>
- Ottaviani, L., & da Costa Martins, P. A. (2017). Non-coding RNAs in cardiac hypertrophy. *The Journal of Physiology*, 595(12), 4037–4050. <https://doi.org/10.1113/JP273129>
- Padmanabhan, S., Caulfield, M., & Dominiczak, A. F. (2015). Genetic and molecular aspects of hypertension. *Circulation Research*, 116(6), 937–59. <https://doi.org/10.1161/CIRCRESAHA.116.303647>
- Paquin, J., Danalache, B. A., Jankowski, M., McCann, S. M., & Gutkowska, J. (2002). Oxytocin induces differentiation of P19 embryonic stem cells to cardiomyocytes. *Proceedings of the National Academy of Sciences of the United States of America*, 99(14), 9550–5. <https://doi.org/10.1073/pnas.152302499>.
- Parahuleva, M. S., Lipps, C., Parviz, B., Hölschermann, H., Schieffer, B., Schulz, R., & Euler, G. (2018). MicroRNA expression profile of human advanced coronary atherosclerotic plaques. *Scientific Reports*, 8(1), 7823. <https://doi.org/10.1038/s41598-018-25690-4>
- Pasternack, S. M., Von Kügelgen, I., Aboud, K. Al, Lee, Y. A., Rüschenhoff, F., Voss, K., ... Betz, R. C. (2008). G protein-coupled receptor P2Y5 and its ligand LPA are involved in maintenance of human hair growth. *Nature Genetics*, 40(3), 329–334. <https://doi.org/10.1038/ng.84>
- Pauklin, S., & Vallier, L. (2015). Activin/Nodal signalling in stem cells. *Development*, 142(4), 607–619. <https://doi.org/10.1242/dev.091769>

- Perrakis, A., & Moolenaar, W. H. (2014). Autotaxin: structure-function and signaling. *Journal of Lipid Research*, 55(6), 1010–1018. <https://doi.org/10.1194/jlr.R046391>
- Potten, C. S., & Loeffler, M. (1990). Stem cells: attributes, cycles, spirals, pitfalls and uncertainties. Lessons for and from the crypt. *Development*, 110(4), 1001–1020. Retrieved from <http://www.ncbi.nlm.nih.gov/pubmed/2100251>
- Qiu, T., Zhou, X., Wang, J., Du, Y., Xu, J., Huang, Z., ... Liu, P. (2014). MiR-145, miR-133a and miR-133b inhibit proliferation, migration, invasion and cell cycle progression via targeting transcription factor Sp1 in gastric cancer. *FEBS Letters*, 588(7), 1168–1177. <https://doi.org/10.1016/J.FEBSLET.2014.02.054>
- Qu, S., Yang, X., Li, X., Wang, J., Gao, Y., Shang, R., ... Li, H. (2015). Circular RNA: A new star of noncoding RNAs. *Cancer Letters*, 365(2), 141–148. <https://doi.org/10.1016/j.canlet.2015.06.003>
- Raitoharju, E., Lyytikäinen, L.-P., Levula, M., Oksala, N., Mennander, A., Tarkka, M., ... Lehtimäki, T. (2011). miR-21, miR-210, miR-34a, and miR-146a/b are up-regulated in human atherosclerotic plaques in the Tampere Vascular Study. *Atherosclerosis*, 219(1), 211–217. <https://doi.org/10.1016/j.atherosclerosis.2011.07.020>
- Rajala K, Pekkanen-Mattila M, Aalto-Setälä K. (2011). Cardiac differentiation of pluripotent stem cells. *Stem Cells International*, 2011.
- Rangrez, A. Y., Massy, Z. A., Meuth, V. M. Le, & Metzinger, L. (2011). MiR-143 and miR-145 molecular keys to switch the phenotype of vascular smooth muscle cells. *Circulation: Cardiovascular Genetics*, 4(2), 197–205. <https://doi.org/10.1161/CIRCGENETICS.110.958702>
- Rastegar, F., Gao, J.-L., Shenaq, D., Luo, Q., Shi, Q., Kim, S. H., ... He, T.-C. (2010). Lysophosphatidic Acid Acyltransferase  $\beta$  (LPAAT $\beta$ ) Promotes the Tumor Growth of Human Osteosarcoma. *PLoS ONE*, 5(12), e14182. <https://doi.org/10.1371/journal.pone.0014182>
- Rawal, S., Manning, P., & Katare, R. (2014). Cardiovascular microRNAs: as modulators and diagnostic biomarkers of diabetic heart disease. *Cardiovascular Diabetology*, 13, 44. <https://doi.org/10.1186/1475-2840-13-44>.

- Reinhart, B. J., Slack, F. J., Basson, M., Pasquienelli, A. E., Bettlinger, J. C., Rougvie, A. E., ... Ruvkun, G. (2000). The 21-nucleotide let-7 RNA regulates developmental timing in *Caenorhabditis elegans*. *Nature*, *403*(6772), 901–906. <https://doi.org/10.1038/35002607>
- Riaz, A., Huang, Y., & Johansson, S. (2016). G-Protein-Coupled Lysophosphatidic Acid Receptors and Their Regulation of AKT Signaling. *International Journal of Molecular Sciences*, *17*(12), 215. <https://doi.org/10.3390/ijms17020215>
- Roma-Rodrigues, C., Raposo, L. R., & Fernandes, A. R. (2015). MicroRNAs Based Therapy of Hypertrophic Cardiomyopathy: The Road Traveled So Far. *BioMed Research International*, *2015*, 1–8. <https://doi.org/10.1155/2015/983290>
- Rongbing Chen, Jessica Roman, Jia Guo, Erin West, John Mcdyer, M. A. W. and S. N. G. (2006). Lysophosphatidic Acid Modulates the Activation of Human Monocyte-Derived Dendritic Cells. *Stem Cells and Development*, *86*, 79–86. <https://doi.org/10.1089/scd.2006.0013>
- Rosen, H., & Goetzl, E. J. (2005). Sphingosine 1-phosphate and its receptors: An autocrine and paracrine network. *Nature Reviews Immunology*, *5*(7), 560–570. <https://doi.org/10.1038/nri1650>
- Rougvie, A. E. (2001). Control of developmental timing in animals. *Nature Reviews Genetics*, *2*(9), 690–701. <https://doi.org/10.1038/35088566>
- Sauer, H., Rahimi, G., Hescheler, J., & Wartenberg, M. (2000). Role of reactive oxygen species and phosphatidylinositol 3-kinase in cardiomyocyte differentiation of embryonic stem cells. *FEBS Letters*, *476*(3), 218–223. [https://doi.org/10.1016/S0014-5793\(00\)01747-6](https://doi.org/10.1016/S0014-5793(00)01747-6)
- Schier, A. F. (2003). Nodal Signaling in Vertebrate Development. *Annual Review of Cell and Developmental Biology*, *19*(1), 589–621. <https://doi.org/10.1146/annurev.cellbio.19.041603.094522>
- Schuldiner, M., Yanuka, O., Itskovitz-Eldor, J., Melton, D. A., & Benvenisty, N. (2000). Effects of eight growth factors on the differentiation of cells derived from human embryonic stem cells. *Proceedings of the National Academy of Sciences*, *97*(21), 11307–11312. <https://doi.org/10.1073/pnas.97.21.11307>

- Sengupta, S., Wang, Z., Tipps, R., & Xu, Y. (2004). Biology of LPA in health and disease. *Seminars in Cell & Developmental Biology*, 15(5), 503–512. <https://doi.org/10.1016/j.semcdb.2004.05.003>
- Shiba, Y., Gomibuchi, T., Seto, T., Wada, Y., Ichimura, H., Tanaka, Y., ... Ikeda, U. (2016). Allogeneic transplantation of iPS cell-derived cardiomyocytes regenerates primate hearts. *Nature*, 538(7625), 388–391. <https://doi.org/10.1038/nature19815>
- Shimizu, I., & Minamino, T. (2016). Physiological and pathological cardiac hypertrophy. *Journal of Molecular and Cellular Cardiology*. Academic Press. <https://doi.org/10.1016/j.yjmcc.2016.06.001>
- Siede, D., Rapti, K., Gorska, A. A., Katus, H. A., Altmüller, J., Boeckel, J. N., ... Dieterich, C. (2017). Identification of circular RNAs with host gene-independent expression in human model systems for cardiac differentiation and disease. *Journal of Molecular and Cellular Cardiology*, 109, 48–56. <https://doi.org/10.1016/j.yjmcc.2017.06.015>
- Sinicato, N. A., da Silva Cardoso, P. A., & Appenzeller, S. (2013). Risk factors in cardiovascular disease in systemic lupus erythematosus. *Current Cardiology Reviews*, 9(1), 15–9. <https://doi.org/10.2174/157340313805076304>
- Skerjanc, I. S. (1999). Cardiac and skeletal muscle development in P19 embryonal carcinoma cells. *Trends in Cardiovascular Medicine*, 9(5), 139–43. Retrieved from <http://www.ncbi.nlm.nih.gov/pubmed/10639728>.
- Skerjanc, I. S., Slack, R. S., & McBurney, M. W. (1994). Cellular aggregation enhances MyoD-directed skeletal myogenesis in embryonal carcinoma cells. *Molecular and Cellular Biology*, 14(12), 8451–9. <https://doi.org/10.1128/MCB.14.12.8451>. Updated
- Sluijter, J. P. G., van Mil, A., van Vliet, P., Metz, C. H. G., Liu, J., Doevendans, P. A., & Goumans, M. J. (2010). MicroRNA-1 and -499 Regulate Differentiation and Proliferation in Human-Derived Cardiomyocyte Progenitor Cells. *Arteriosclerosis, Thrombosis, and Vascular Biology*, 30(4), 859–868. <https://doi.org/10.1161/ATVBAHA.109.197434>
- Slusarski, D. C., Corces, V. G., & Moon, R. T. (1997). Interaction of Wnt and a Frizzled homologue triggers G-protein-linked phosphatidylinositol signalling. *Nature*, 390(6658), 410–413. <https://doi.org/10.1038/37138>

Smith, A. G. (2001). Embryo-derived stem cells: of mice and men. *Annual Review of Cell & Developmental Biology*, 17(1), 435. Retrieved from <http://search.ebscohost.com/login.aspx?direct=true&db=aph&AN=6262729&site=ehost-live>

Song, L., Yang, J., Duan, P., Xu, J., Luo, X., Luo, F., ... Zhou, Q. (2013). MicroRNA-24 inhibits osteosarcoma cell proliferation both in vitro and in vivo by targeting LPAAT $\beta$ . *Archives of Biochemistry and Biophysics*, 535(2), 128–135. <https://doi.org/10.1016/j.abb.2013.04.001>

Srivastava, D., & Olson, E. N. (2000). A genetic blueprint for cardiac development. *Nature*, 407(6801), 221–226. <https://doi.org/10.1038/35025190>.

Swift, G. H., Peyton, M. J., & MacDonald, R. J. (2000). Assessment of RNA quality by semi-quantitative RT-PCR of multiple regions of a long ubiquitous mRNA. *BioTechniques*, 28(3), 524–531.

Taha, M. F., & Valojerdi, M. R. (2008). Effect of bone morphogenetic protein-4 on cardiac differentiation from mouse embryonic stem cells in serum-free and low-serum media. *International Journal of Cardiology*, 127(1), 78–87. <https://doi.org/10.1016/j.ijcard.2007.04.173>

Takahashi, K., & Yamanaka, S. (2016). Induction of Pluripotent Stem Cells from Mouse Embryonic and Adult Fibroblast Cultures by Defined Factors. *Cell*, 126(4), 663–676. <https://doi.org/10.1016/j.cell.2006.07.024>

Teo, S. T., Yung, Y. C., Herr, D. R., & Chun, J. (n.d.). Critical Review Lysophosphatidic Acid in Vascular Development and Disease. <https://doi.org/10.1002/iub.220>.

Tham, Y. K., Bernardo, B. C., Ooi, J. Y. Y., Weeks, K. L., & McMullen, J. R. (2015). Pathophysiology of cardiac hypertrophy and heart failure: signaling pathways and novel therapeutic targets. *Archives of Toxicology*, 89(9), 1401–1438. <https://doi.org/10.1007/s00204-015-1477-x>

Thum, T., Galuppo, P., Wolf, C., Fiedler, J., Kneitz, S., Van Laake, L. W., ... Bauersachs, J. (2007). MicroRNAs in the human heart: A clue to fetal gene reprogramming in heart failure. *Circulation*, 116(3), 258–267. <https://doi.org/10.1161/CIRCULATIONAHA.107.687947>

- Tigyi, G. (2001). Physiological responses to lysophosphatidic acid and related glycerophospholipids. *Prostaglandins & Other Lipid Mediators*, 64(1–4), 47–62. [https://doi.org/10.1016/S0090-6980\(01\)00107-1](https://doi.org/10.1016/S0090-6980(01)00107-1)
- Tong, A. W., & Nemunaitis, J. (2008). Modulation of miRNA activity in human cancer: A new paradigm for cancer gene therapy? *Cancer Gene Therapy*, 15(6), 341–355. <https://doi.org/10.1038/cgt.2008.8>
- Torres, A. C., Boruszewska, D., Batista, M., Kowalczyk-Zieba, I., Diniz, P., Sinderewicz, E., ... Lopes-da-Costa, L. (2014). Lysophosphatidic acid signaling in late cleavage and blastocyst stage bovine embryos. *Mediators of Inflammation*, 2014, 678968. <https://doi.org/10.1155/2014/678968>
- Tørring, N., Dagnaes-Hansen, F., Sørensen, B. S., Nexø, E., & Hynes, N. E. (2003). ErbB1 and prostate cancer: ErbB1 activity is essential for androgen-induced proliferation and protection from the apoptotic effects of LY294002. *The Prostate*, 56(2), 142–149. <https://doi.org/10.1002/pros.10245>
- Tyagi, M. G. (2014). Evaluation of the signalling mechanisms of lysophosphatidic acid and its role in the central nervous system. *Journal of Biomedical and Pharmaceutical Research*, 3(3). Retrieved from <http://jbpr.in/index.php/jbpr/article/view/279>
- Van Der Heyden, M. A. G., & Defize, L. H. K. (2003). Twenty one years of P19 cells: What an embryonal carcinoma cell line taught us about cardiomyocyte differentiation. *Cardiovascular Research*, 58(2), 292–302. [https://doi.org/10.1016/S0008-6363\(02\)00771-X](https://doi.org/10.1016/S0008-6363(02)00771-X)
- Van Der Heyden, M. A. G., Van Kempen, M. J. A., Tsuji, Y., Rook, M. B., Jongsma, H. J., & Opthof, T. (2003). P19 embryonal carcinoma cells: A suitable model system for cardiac electrophysiological differentiation at the molecular and functional level. *Cardiovascular Research*, 58(2), 410–422. [https://doi.org/10.1016/S0008-6363\(03\)00247-5](https://doi.org/10.1016/S0008-6363(03)00247-5)
- van Dijk, M. C., Postma, F., Hilkmann, H., Jalink, K., van Blitterswijk, W. J., & Moolenaar, W. H. (1998). Exogenous phospholipase D generates lysophosphatidic acid and activates Ras, Rho and Ca<sup>2+</sup> signaling pathways. *Current Biology: CB*, 8(7), 386–92. [https://doi.org/10.1016/S0960-9822\(98\)70157-5](https://doi.org/10.1016/S0960-9822(98)70157-5)

- Van Vliet, P., Wu, S. M., Zaffran, S., & Puc at, M. (2012). Early cardiac development: A view from stem cells to embryos. *Cardiovascular Research*. <https://doi.org/10.1093/cvr/cvs270>
- Veerkamp, J., Rudolph, F., Cseresnyes, Z., Priller, F., Otten, C., Renz, M., ... Abdelilah-Seyfried, S. (2013). Unilateral Dampening of Bmp Activity by Nodal Generates Cardiac Left-Right Asymmetry. *Developmental Cell*, *24*(6), 660–667. <https://doi.org/10.1016/j.devcel.2013.01.026>
- Velasco, M., O’Sullivan, C., & Sheridan, G. K. (2017). Lysophosphatidic acid receptors (LPARs): Potential targets for the treatment of neuropathic pain. *Neuropharmacology*, *113*, 608–617. <https://doi.org/10.1016/J.NEUROPHARM.2016.04.002>
- Velasquez-Mao, A. J., Tsao, C. J. M., Monroe, M. N., Legras, X., Bissig-Choisat, B., Bissig, K. D., ... Jacot, J. G. (2017). Differentiation of spontaneously contracting cardiomyocytes from non-virally reprogrammed human amniotic fluid stem cells. *PLoS ONE*, *12*(5). <https://doi.org/10.1371/journal.pone.0177824>
- Vincent, S. D., & Buckingham, M. E. (2010). How to Make a Heart (pp. 1–41). [https://doi.org/10.1016/S0070-2153\(10\)90001-X](https://doi.org/10.1016/S0070-2153(10)90001-X)
- Wang, J., Liew, O., Richards, A., & Chen, Y.-T. (2016). Overview of MicroRNAs in Cardiac Hypertrophy, Fibrosis, and Apoptosis. *International Journal of Molecular Sciences*, *17*(5), 749. <https://doi.org/10.3390/ijms17050749>
- Wang, K., Lin, Z.-Q., Long, B., Li, J.-H., Zhou, J., & Li, P.-F. (2012). Cardiac hypertrophy is positively regulated by MicroRNA miR-23a. *The Journal of Biological Chemistry*, *287*(1), 589–99. <https://doi.org/10.1074/jbc.M111.266940>.
- Wang, K., Long, B., Liu, F., Wang, J.-X., Liu, C.-Y., Zhao, B., ... Li, P.-F. (2016). A circular RNA protects the heart from pathological hypertrophy and heart failure by targeting miR-223. *European Heart Journal*, *37*(33), 2602–2611. <https://doi.org/10.1093/eurheartj/ehv713>
- Wang, R. N., Green, J., Wang, Z., Deng, Y., Qiao, M., Peabody, M., ... Shi, L. L. (2014). Bone Morphogenetic Protein (BMP) signaling in development and human diseases. *Genes and Diseases*. Elsevier. <https://doi.org/10.1016/j.gendis.2014.07.005>

Wang, S., Gao, J., Lei, Q., Rozengurt, N., Pritchard, C., Jiao, J., ... Wu, H. (2003). Prostate-specific deletion of the murine Pten tumor suppressor gene leads to metastatic prostate cancer. *Cancer Cell*, 4(3), 209–21. Retrieved from <http://www.ncbi.nlm.nih.gov/pubmed/14522255>

Wang, Y.-D., Cai, N., Wu, X.-L., Cao, H.-Z., Xie, L.-L., & Zheng, P.-S. (2013). OCT4 promotes tumorigenesis and inhibits apoptosis of cervical cancer cells by miR-125b/BAK1 pathway. *Cell Death & Disease*, 4(8), e760–e760. <https://doi.org/10.1038/cddis.2013.272>.

Wanrooij, P. H., Uhler, J. P., Simonsson, T., Falkenberg, M., & Gustafsson, C. M. (2010). G-quadruplex structures in RNA stimulate mitochondrial transcription termination and primer formation. *Proceedings of the National Academy of Sciences*, 107(37), 16072–16077. <https://doi.org/10.1073/pnas.1006026107>

Wen, K., Fu, Z., Wu, X., Feng, J., Chen, W., & Qian, J. (2013). Oct-4 is required for an antiapoptotic behavior of chemoresistant colorectal cancer cells enriched for cancer stem cells: Effects associated with STAT3/Survivin. *Cancer Letters*, 333(1), 56–65. <https://doi.org/10.1016/J.CANLET.2013.01.009>.

Wocławek-Potocka, I., Rawińska, P., Kowalczyk-Zieba, I., Boruszewska, D., Sinderewicz, E., Waśniewski, T., & Skarzynski, D. J. (2014). Lysophosphatidic acid (LPA) signaling in human and ruminant reproductive tract. *Mediators of Inflammation*, 2014. <https://doi.org/10.1155/2014/649702>

Wu, S. M., Fujiwara, Y., Cibulsky, S. M., Clapham, D. E., Lien, C., Schultheiss, T. M., & Orkin, S. H. (2006). Developmental Origin of a Bipotential Myocardial and Smooth Muscle Cell Precursor in the Mammalian Heart. *Cell*, 127(6), 1137–1150. <https://doi.org/10.1016/j.cell.2006.10.028>

Wu, X., Ding, S., Ding, Q., Gray, N. S., & Schultz, P. G. (2004). Small Molecules that Induce Cardiomyogenesis in Embryonic Stem Cells. *Journal of the American Chemical Society*, 126(6), 1590–1591. <https://doi.org/10.1021/ja038950i>.

Xie Y, Gibbs TC, M. Y. and M. K. (2002). Role for 18:1 lysophosphatidic acid as an autocrine mediator in prostate cancer cells. *J. Biol. Chem*, 32516–32526.

Xu, F. Y., Fandrich, R. R., Nemer, M., Kardami, E., & Hatch, G. M. (1999). The Subcellular Distribution of Protein Kinase C $\alpha$ , - $\epsilon$ , and - $\zeta$  Isoforms during Cardiac Cell Differentiation.

*Archives of Biochemistry and Biophysics*, 367(1), 17–25.  
<https://doi.org/10.1006/ABBI.1999.1229>.

Xu, N., Papagiannakopoulos, T., Pan, G., Thomson, J. A., & Kosik, K. S. (2009). MicroRNA-145 Regulates OCT4, SOX2, and KLF4 and Represses Pluripotency in Human Embryonic Stem Cells. *Cell*, 137(4), 647–658. <https://doi.org/10.1016/j.cell.2009.02.038>

Xu, Y., Fang, X. J., Casey, G., & Mills, G. B. (1995). Lysophospholipids activate ovarian and breast cancer cells. *The Biochemical Journal*, 309 ( Pt 3)(3), 933–40. <https://doi.org/10.1042/BJ3090933>

Xu, Y., Shen, Z., Wiper, D. W., Wu, M., Morton, R. E., Elson, P., ... Casey, G. (1998). Lysophosphatidic acid as a potential biomarker for ovarian and other gynecologic cancers. *JAMA*, 280(8), 719–23. Retrieved from <http://www.ncbi.nlm.nih.gov/pubmed/9728644>

Xu, Y., Xiao, Y. J., Baudhuin, L. M., & Schwartz, B. M. (2001). The role and clinical applications of bioactive lysolipids in ovarian cancer. *J Soc Gynecol Investig*, 8(1), 1–13. <https://doi.org/S1071557600000927> [pii]

Yamaguchi, T. P. (2001). Heads or tails: Wnts and anterior-posterior patterning. *Current Biology*: CB, 11(17), R713-24. Retrieved from <http://www.ncbi.nlm.nih.gov/pubmed/11553348>

Yang, J., Nie, Y., Wang, F., Hou, J., Cong, X., Hu, S., & Chen, X. (2013). Reciprocal regulation of miR-23a and lysophosphatidic acid receptor signaling in cardiomyocyte hypertrophy. *Biochimica et Biophysica Acta (BBA) - Molecular and Cell Biology of Lipids*, 1831(8), 1386–1394. <https://doi.org/10.1016/j.bbalip.2013.05.005>

Yang, L., Froberg, J. E., & Lee, J. T. (2014). Long noncoding RNAs: fresh perspectives into the RNA world. *Trends in Biochemical Sciences*, 39(1), 35–43. <https://doi.org/10.1016/j.tibs.2013.10.002>

Yang, Ping Zhu, Jintao Guo, Xiang Liu, Sheng Wang, Guoxin Wang, Wen Liu, Shupeng Wang, N. G. (2017). Circular RNAs in thoracic diseases. *Journal of Thoracic Disease*. Retrieved from <http://jtd.amegroups.com/article/view/16958>

- Ye, X., Hama, K., Contos, J. J. A., Anliker, B., Inoue, A., Skinner, M. K., ... Chun, J. (2005). LPA3-mediated lysophosphatidic acid signalling in embryo implantation and spacing. *Nature*, *435*(7038), 104–108. <https://doi.org/10.1038/nature03505>
- Ye, X., Skinner, M. K., Kennedy, G., & Chun, J. (2008). Age-dependent loss of sperm production in mice via impaired lysophosphatidic acid signaling. *Biology of Reproduction*, *79*(2), 328–36. <https://doi.org/10.1095/biolreprod.108.068783>.
- Ying, S.-Y., Chang, D. C., & Lin, S.-L. (2013). *The MicroRNA. Methods in molecular biology (Clifton, N.J.)* (Vol. 936). [https://doi.org/10.1007/978-1-62703-083-0\\_1](https://doi.org/10.1007/978-1-62703-083-0_1)
- Yoshino, H., Chiyomaru, T., Enokida, H., Kawakami, K., Tatarano, S., Nishiyama, K., ... Nakagawa, M. (2011). The tumour-suppressive function of miR-1 and miR-133a targeting TAGLN2 in bladder cancer. *British Journal of Cancer*, *104*(5), 808–818. <https://doi.org/10.1038/bjc.2011.23>
- Yu, J., Vodyanik, M. A., Smuga-Otto, K., Antosiewicz-Bourget, J., Frane, J. L., Tian, S., ... Thomson, J. A. (2007). Induced Pluripotent Stem Cell Lines Derived from Human Somatic Cells. *Science*, *318*(5858), 1917–1920. <https://doi.org/10.1126/science.1151526>.
- Yu, X., Zhang, Y., & Chen, H. (2016). LPA receptor 1 mediates LPA-induced ovarian cancer metastasis: an in vitro and in vivo study. *BMC Cancer*, *16*(1), 846. <https://doi.org/10.1186/s12885-016-2865-1>
- Yu, Xiaotian. (2014). *Functional impact of microRNA-34a on stem cell differentiation towards smooth muscle cell. Queen Mary University of London*. Queen Mary University of London. Retrieved from <https://qmro.qmul.ac.uk/xmlui/handle/123456789/9121?show=full>
- Yuan, G., Yang, G., Zheng, Y., Zhu, X., Chen, Z., Zhang, Z., & Chen, Y. (2015). The non-canonical BMP and Wnt/ $\beta$ -catenin signaling pathways orchestrate early tooth development. *Development (Cambridge, England)*, *142*(1), 128–39. <https://doi.org/10.1242/dev.117887>
- Yung, Y. C., Stoddard, N. C., & Chun, J. (2014). LPA receptor signaling: pharmacology, physiology, and pathophysiology. *Journal of Lipid Research*, *55*(7), 1192–1214. <https://doi.org/10.1194/jlr.R046458>

- Zhang, H., & Bradley, A. (1996). Mice deficient for BMP2 are nonviable and have defects in amnion/chorion and cardiac development. *Development (Cambridge, England)*, 122(10), 2977–86. Retrieved from <http://www.ncbi.nlm.nih.gov/pubmed/8898212>.
- Zhang, H., Xu, C., Yang, R., Chen, H., Kong, X., Qian, L., ... Sun, W. (2015). Silencing of nodal modulator 1 inhibits the differentiation of P19 cells into cardiomyocytes. *Experimental Cell Research*, 331(2), 369–376. <https://doi.org/10.1016/j.yexcr.2014.12.016>
- ZHANG, Q., YAN, W., BAI, Y., XU, H., FU, C., ZHENG, W., ... MA, J. (2015). Synthetic miR-145 mimic inhibits multiple myeloma cell growth in vitro and in vivo. *Oncology Reports*, 33(1), 448–456. <https://doi.org/10.3892/or.2014.3591>
- Zhang, S.-C., Wernig, M., Duncan, I. D., Brüstle, O., & Thomson, J. A. (2001). In vitro differentiation of transplantable neural precursors from human embryonic stem cells. *Nature Biotechnology*, 19(12), 1129–1133. <https://doi.org/10.1038/nbt1201-1129>.
- Zhang, X., Yang, Y., & Li, L. (2016). *Original Article OCT4 expression maintained cancer stem-like properties in hepatoma cell line. Int J Clin Exp Pathol (Vol. 9)*. Retrieved from [www.ijcep.com/](http://www.ijcep.com/).
- Zhang, Y. E. (2009). Non-Smad pathways in TGF- $\beta$  signaling. *Cell Research*. Nature Publishing Group. <https://doi.org/10.1038/cr.2008.328>
- Zhu, Z., Xu, T., Wang, L., Wang, X., Zhong, S., Xu, C., & Shen, Z. (2014). MicroRNA-145 directly targets the insulin-like growth factor receptor I in human bladder cancer cells. *FEBS Letters*, 588(17), 3180–3185. <https://doi.org/10.1016/J.FEBSLET.2014.06.059>